AD-A191 464 ADVANCED IN GUIDANCE AND CONTROL SYSTEMS AND TECHNOLOGY 1/2
(U) ADVISORY GROUP FOR AEROSPACE RESEARCH AND
DEVELOPMENT NEUILLY-SUR-SEINE (FRAN CE) JUL 87
UNCLASSIFIED AGARD-CP-411 F/G 17/11 NL

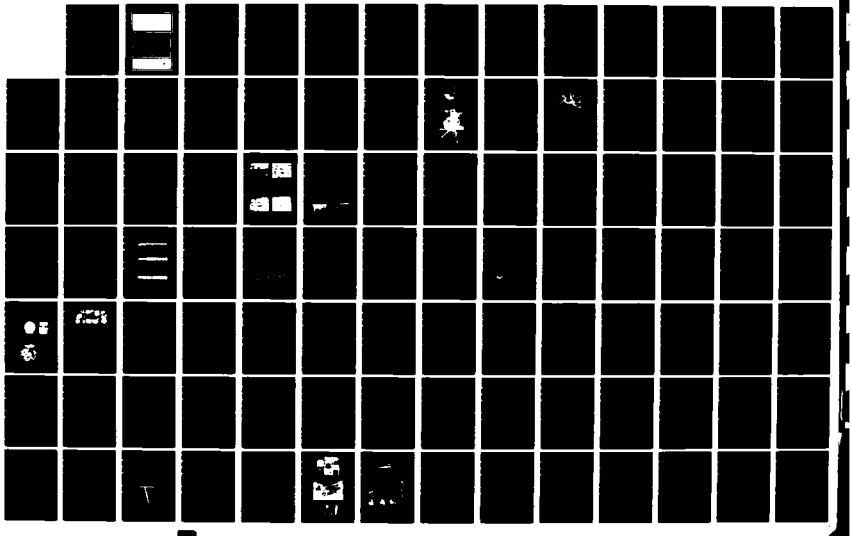

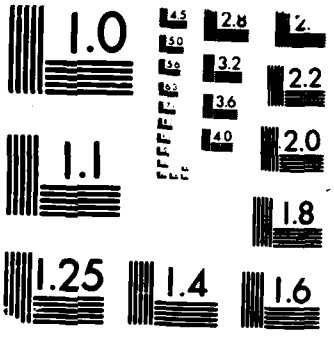

AGARD-CP-411

AGARD-CP-411

AGARD

ADVISORY GROUP FOR AEROSPACE RESEARCH & DEVELOPMENT

7 RUE ANCELLE 92200 NEUILLY SUR SEINE FRANCE

AGARD CONFERENCE PROCEEDINGS No.411

Advances in Guidance and Control Systems and Technology

*Original contains color plates: All DTIC reproductions will be in black and white.

NORTH ATLANTIC TREATY ORGANIZATION

DISTRIBUTION AND AVAILABILITY
ON BACK COVER

AGARD-CP-411

NORTH ATLANTIC TREATY ORGANIZATION

ADVISORY GROUP FOR AEROSPACE RESEARCH AND DEVELOPMENT

(ORGANISATION DU TRAITE DE L'ATLANTIQUE NORD)

AGARD Conference Proceedings No.411

ADVANCES IN GUIDANCE AND CONTROL SYSTEMS AND TECHNOLOGY

Papers presented at the Guidance and Control Panel 43rd Symposium held in London, United Kingdom from 7 to 10 October 1986.

THE MISSION OF AGARD

The mission of AGARD is to bring together the leading personalities of the NATO nations in the fields of science and technology relating to aerospace for the following purposes:

- Exchanging of scientific and technical information;
- Continuously stimulating advances in the aerospace sciences relevant to strengthening the common defence posture;
- Improving the co-operation among member nations in aerospace research and development;
- Providing scientific and technical advice and assistance to the Military Committee in the field of aerospace research and development (with particular regard to its military application);
- Rendering scientific and technical assistance, as requested, to other NATO bodies and to member nations in connection with research and development problems in the aerospace field;
- Providing assistance to member nations for the purpose of increasing their scientific and technical potential;
- Recommending effective ways for the member nations to use their research and development capabilities for the common benefit of the NATO community.

The highest authority within AGARD is the National Delegates Board consisting of officially appointed senior representatives from each member nation. The mission of AGARD is carried out through the Panels which are composed of experts appointed by the National Delegates, the Consultant and Exchange Programme and the Aerospace Applications Studies Programme. The results of AGARD work are reported to the member nations and the NATO Authorities through the AGARD series of publications of which this is one.

Participation in AGARD activities is by invitation only and is normally limited to citizens of the NATO nations.

Published July 1987

ISBN 92-835-0421-6

Printed by Specialised Printing Services Limited
40 Chigwell Lane, Loughton, Essex IG10 3TZ

PREFACE

Sensors and seekers are essential to guidance and control of weapon systems and of aircraft. At the opposite end of the guidance and control problem, force and moment generators are required to effect actual control. The efficiency of a sensor system or an actuating system is greatly increased by estimation. The technologies of these systems were last addressed by a Guidance and Control Panel Symposium in 1972. In view of the advancements in these technologies it was considered timely to discuss these issues in a symposium in 1986.

The theme of this meeting covers a broad area of sensor and seeker techniques, such as active and passive target seekers, inertial, air data and airflow sensors, and force and moment generation techniques, complemented by associated estimation methods, all of which are an integral part of guidance and control technology.

***

Les senseurs et les autodirecteurs sont essentiels au guidage et au pilotage des systèmes d'armes et des avions. En plus des problèmes de guidage et de pilotage, des générateurs de force et de moment sont nécéssaires pour effecteur les manoeuvres des commandes. L'efficacité d'un système capteur ou système temps réel est fortement amplifiée par les techniques d'estimation. Les technologies de ces systèmes ont été examinées lors du symposium de la Commission Guidage et Pilotage de 1972. En vue des progrès réalisés dans ces technologies, il nous a paru opportun d'examiner les résultats obtenus au cours d'un symposium en 1986.

Le thème de cette reunion embrasse le large domaine des techniques des capteurs et des autodirecteurs, tels que les autodirecteurs de cibles, actifs ou passifs, inertiels, les capteurs de données aériennes et de flux, les techniques de génération de force et de moment, augmentées par les méthodes d'estimation associées, qui toutes sont une partie integrante de la technologie du guidage et du pilotage.

GUIDANCE AND CONTROL PANEL OFFICERS

Chairman: Mr Kenneth A Peebles
Director, Electro-Optics Division
Defence Research Establishment
Valcartier
PO Box 8800
Courcelette, P.Q. G0A 1R0
Canada

Deputy Chairman: Ir P Ph van den Broek
Department of Aerospace Engineering
Delft University of Technology
Kluyverweg 1
2629 HS Delft
Netherlands

TECHNICAL PROGRAMME COMMITTEE

Chairman:	Mr R.S.Vaughn	US
Members:	Mr J.B.Senneville	FR
	Mr U.K.Krogmann	GE
	Dr B.Mazzetti	IT
	Ir P.P.van den Broek	NE
	PR J.T.Shepherd	UK
	Mr J.K.Ramage	US

PANEL EXECUTIVE

From Europe:
Lt Colonel A.Rocher, FAF
AGARD-OTAN
7 Rue Ancelle
92200 Neuilly-sur-Seine, France
Telephone: (1) 4738 5780 — Telex: 610176 F

From USA and Canada only:
AGARD-NATO
APO New York 09777

HOST PANEL COORDINATOR

Mr R.W.Jones
Head, Flight Systems Department (F)
Building R.177
Royal Aircraft Establishment
Farnborough, Hants GU14 6TD
UK

HOST NATION COORDINATOR

Group Captain R.D.Hillary
Ministry of Defence (PE)
Room 9/145, St Christopher House
Southwark Street
London SE1 0TD
UK

ACKNOWLEDGEMENTS/REMERCIEMENTS

The Panel wishes to express its thanks to the United Kingdom National Delegates to AGARD for the invitation to hold this meeting in their country and for the facilities and personnel which made the meeting possible.

Le Panel tient à remercier les Délégués Nationaux du Royaume Uni près l'AGARD de leur invitation à tenir cette réunion dans leur pays et de la mise à disposition de personnel et des installations nécéssaires.

CONTENTS

*Printed in classified publication CP 411 (Supplement)

*Printed in classified publication CP 411 (Supplement)
†Not available at time of printing

KEYNOTE ADDRESS FOR AGARD SYMPOSIUM ON ADVANCES IN GUIDANCE AND CONTROL SYSTEMS AND TECHNOLOGY

by

Mr J.Barnes
DCER
Ministry of Defence
London SW1A 2HB, UK

Introduction

It is a pleasure to be invited to deliver this Keynote Address. As you will have gathered from the information published before this Symposium, it is fourteen years since the technologies of guidance and control were last addressed within the Advisory Group for Aeronautical Research and Development at a meeting organised by this Panel. Moreover that particular Symposium was devoted to Inertial Navigation Components and Systems. A glance through the papers presented at that time reveals that several items of established technology today were little more than bright ideas in 1972.

Much of what I have to say this morning is intended to provide an introduction to the six main sessions which follow over the next three days. However it would be out of place simply to move straight to what I have to say on today's and tomorrow's technology without any historical perspective.

In the earliest aircraft guidance and control depended in large measure on the skill and strength of the pilot. The aerodynamic forces acting upon an aircraft were known to be powerful but were imperfectly understood. Experience was bought dearly in terms of human life.

It was not until 1914 that Sperry produced the first practical auto pilot based on gyroscopes. He used to demonstrate his invention by climbing out of the cockpit of his biplane and standing upon the wing. In doing so, he demonstrated that the aircraft could continue to fly stably with no human at the controls. He also showed that the aircraft could cope with the relatively large rolling movement applied by the weight of his body.

In the years leading up to World War II something more than the ability to keep an aircraft flying stably was needed. To relieve crew fatigue on long flights an autopilot was needed to keep an aircraft on a predetermined course. The system developed here in the United Kingdom at the Royal Aircraft Establishment came to be known as "George". It enabled the tedious portion of long haul flights to be accomplished with the flight crew in no more than a monitoring role. "George" went through several stages of evolution and came to be fitted to both military and civil aircraft. In parallel there were developments by Sperry and others, in the United States and also in Germany. The second World War saw the first practical applications of guided flight in the German VI and V2 weapons and also the first attempt to produce anti-aircraft guided weapons. The pace accelerated after the war. The Firebird air-to-air weapon in the United States and the Fireflash in the United Kingdom used command-to-line-of-sight guidance. Infra-red homing followed quickly in the United States Sidewinder and the British Firestreak. Evolutionary descendants of these missiles are still in service.

The rate of advance in guidance and control, as always, has been limited by the available technology. Until well after World War II, reliability and safety required that aircraft autopilots should be based on pneumatic and magnetic amplifiers: early guided weapons used vacuum tubes but power and mass constraints set severe limits to what could be achieved.

Solid state electronics have transformed this picture and have caused automatic guidance and control to become a major force in aviation.

In the following sections I shall aim to give a brief description of current capabilities in each of the following:

a. Inertial Navigation Systems for Aircraft;

b. Flight Control Systems, including active control technology, fly-by-wire and fly-by-light;

c. Mission systems with special emphasis on weapon aiming;

d. Missile guidance and navigation and missile seekers;

e. Space craft guidance and control.

Almost all of what I have to say has been contributed by members of the staff of the Royal Aircraft Establishment. To them I extend my thanks.

Inertial Navigation Systems for Aircraft

For military use the ideal navigation system should be fully autonomous, undetectable, unjammable, usable world wide in all weathers, and of vanishingly low weight and infinitesimal cost. These aims have driven development for the past thirty years. Systems are now sufficiently reliable and accurate for virtually all modern fixed wing military aircraft to be equipped with an inertial navigator.

Most applications require an accuracy of about one nautical mile per hour of flight. However, some phases, for example ground attack, require much higher accuracy, sometimes of the order of a few metres. To achieve this standard of accuracy the INS has to be updated from an external reference. In the past this process relied on visual or radar identification of known ground features. Now, with modern computers and advances in signal processing, new systems have become possible. Two of them are the Terrain Reference System and the Satellite Global Positioning System, NAVSTAR.

Terrain Reference Systems compare measured features of the terrain below with a map of the same features stored in the navigation system. Terrain height is the most commonly used. High density digital storage permits large quantities of data to be stored. Modern microprocessors allow the comparison to be done sufficiently quickly.

NAVSTAR measures range to a set of four satellites in 12 hour orbits, by timing the arrival of radio signals transmitted from the satellites at precisely known times. Theoretically a minimum of only three satellites would allow a fix to be obtained but since three satellites may not always be in suitable positions and because timing errors in the receiving system have to be eliminated, a fourth satellite is necessary.

Both systems suffer because they are not continuously available under all conditions. Terrain reference is of no use over large areas of water and GPS satellites may be shielded by terrain or jammed by enemy action. Inertial Navigation Systems therefore remain necessary. Moreover, by using modern mathematical techniques (Kalman Filtering) it is possible to combine all three systems into an integrated system which is more accurate than any of its individual components; and which is capable of degrading gracefully if any sub-system is lost.

Inertial navigation has itself been improved by the development of high speed computers and optical technology. Computers have made it possible to fix accelerometers and gyroscopes to the aircraft and to compute their orientation relative to the earth's axis, thereby eliminating complex mechanical gymbals. This reduced cost and improved reliability and maintainability. Optical technology allowed mechanical devices to be replaced by lasers and fibre optics.

The Ring Laser Gyroscope and the Fibre Optic Gyroscope need no description here. The former is already in airline service and lends itself to other applications, including missiles. The latter offers the prospect of devices which are both rugged and cheap, with very long shelf life and virtually instantaneous start-up - making it eminently suitable for missiles.

Flight Control Systems for Aircraft

Advanced fixed wing military aircraft now almost exclusively embody Active Control Technology (ACT). The pilot's control demands pass to the control surfaces through a digital Flight Control Computer having full authority over control surface movement. The control laws programmed into the computer shape the pilot's demands to ensure that the aircraft handles in the desired manner. More importantly, ACT has permitted many of the traditional constraints on aircraft configuration to be removed. It is no longer essential for an aircraft to be statically stable; for example a tail surface is not essential but may generate lift provided that the ACT system has the capability automatically to correct the tendency of the aircraft to depart from controlled flight. Agile aircraft dramatic improvements in manoeuvrability are possible and as a bonus smaller control surfaces are needed. For a given mission the airframe can be smaller.

There is a price to be paid; this comes in achieving adequate integrity of the control system with no mechanical connection between the pilot and the control surfaces. The failure rate of current electronics is inherently many times that of mechanical control rods. Moreover the problems of validating both the mathematical model of the aircraft on which the control laws are designed and of validating the control software itself still remain to be fully solved. For the foreseeable future ACT systems will employ redundant architecture with, typically, quadruplex "black boxes" and there will be a requirement for comprehensive ground tests prior to flight. The acceptability of this approach is confirmed by the entry of ACT into the civil field on aircraft such as the Airbus A320. Here safety is paramount.

In the United Kingdom, acceptance of ACT has evolved through flight research at the Royal Aircraft Establishment on a converted Hunter aircraft; through engineering demonstration sponsored by the Ministry of Defence and the "fly-by-wire" Jaguar aircraft at British Aerospace, Warton; through application on a modern combat aircraft configuration in the Experimental Aircraft Programme (EAP); and now to proposed service use in the European Fighter Aircraft (EFA). En route valuable experience was gained from Concorde and Tornado, both of which have electrically signalled primary control systems but with back-up mechanical control systems.

Looking ahead, RAE has recently taken delivery of a modified Harrier, the variable thrust Aircraft Advanced Flight Control (VAAC) Harrier fitted with ACT. The aim of the research using this aircraft is to investigate concepts appropriate to future advanced Short Take-off Vertical Landing (ASTOVL) aircraft; and in particular to establish the degree of integration necessary between the flight control system and the engine control system.

On the civil side, automatic flight control systems (not ACT) of high performance and reliability have been in service for almost thirty years to meet the requirements of fully automatic landing in poor weather. RAE has also worked on Direct Lift Control to increase safety in windshear and on energy based control laws to reduce cyclic variations in engine power and thereby to improve fuel economy. None of this research regards flight controls as isolated systems. They are integrated into the total aircraft and in particular into the cockpit. The aims are to reduce pilot workload and to achieve improved mission performance for both military and civil aircraft.

A further application is to programme the aircraft control system to alleviate gust-induced structural loads. The experience gained by British Aerospace on a BAC 1-11 aircraft will be applied to the A320.

So far in this section I have concentrated on fixed wing aircraft. In several respects the scope for active control on rotary wing aircraft is even greater. A conventional helicopter has considerable coupling between the pitch, roll and yaw modes. Moreover, because the lifting power of a helicopter is provided directly by the engine through the main rotor, propulsion and flight control are more closely interdependent than on fixed wing aircraft. We foresee major benefits to the handling qualities of helicopters both through the reduction and removal of couplings and by integration of engine and flight control. There is also the prospect of reducing high vibration levels by passing appropriate feedback demands to the control surfaces to reduce structural response. This technique is known as Higher Harmonic Control. An alternative approach is Advanced Gearbox Interface Control where "anti-vibration" compensating demands are fed to actuators which separate the transmission from the airframe.

There is much to be done on helicopters, both by RAE and by Westland Helicopters. Moreover "Fly by Light" is likely to supersede "Fly by Wire", with optical fibres rather than cables carrying the signals. The advantages here will be relative immunity to electromagnetic hazards as well as further weight savings and a potentially wider bandwidth of signal.

Mission Systems

An exhaustive treatment is not possible within the time available. Therefore I shall concentrate on ground attack.

The major factor influencing developments since World War II has been the emphasis on low level flight, in order to minimise exposure of the aircraft to ground based radar and, until a development of "look down" Doppler radars, to reduce the ability of defensive fighter aircraft to detect an incoming raid. Low level attack makes the task of target acquisition more difficult and the total time of an attack pass may be only a few seconds. In that short time the pilot of an attacking aircraft armed with unguided weapons has to maneouvre on to an attack heading, stabilise the aircraft path and release the weapon. To be successful an attack requires precise navigation, so that target acquisition is as early as possible, and accurate calculation of weapon release to minimise delivery error.

Inertial platforms and moving map displays have together fulfilled the requirements for precise navigation with an acceptable workload, even at high speed and low levels. They have eased the task of acquiring early pre-planned targets in fixed positions. Acquisition of targets of opportunity, remains a problem.

Accurate calculation of weapon release has been met by the combination of data on aircraft altitude, heading and speed from the inertial platform with range to target from a ranging system processed digitally in the aircraft.

So far we have considered only attacks which can be conducted under visual conditions. Further developments have extended the ability to carry out high speed low level attacks at night and in poor visibility. Ground mapping radar represented the first development in this direction. It became possible to attack targets giving discrete radar returns and targets whose position was known relative to some observable and recognisable feature on the radar screen. However the aircraft was forced to increase its altitude and hence its vulnerability.

The advent of Terrain Following Radar allowed aircraft to fly at reduced clearance heights and to use the terrain profile to gain some measure of screening from the enemy defences. Nonetheless the aircraft is confined to relatively gentle manoeuvres because of the limited sector over which the radar scans. Moreover, Terrain Following Radar is an active system; and its complexity and cost tend to make it unsuitable for several categories of ground attack aircraft. Therefore there has been a search for alternatives which are both passive and less expensive.

Recent work has shown that two electro-optical devices, Forward Looking Infra Red (FLIR) and Night Vision Goggles (NVG) can be used in combination to provide a cheap and effective alternative to TFR in all except the worst visibility. The technique is to use the FLIR to enhance the pilot's ability to look forward, particularly when flying under cloud with little or no moonlight, and to have the NVG attached directly to the pilot's helmet to give the wide look around capability essential for vigorous manoeuvring at low level. The FLIR is also of value by day in penetrating smoke, haze and mist but is limited by thick fogs and rain. The output of the FLIR may also be used to identify "hot spots" having characteristics similar to those of a tank. The technology is still evolving.

In the earlier section on navigation I have already mentioned terrain data bases. When used with precise knowledge of the aircraft's position they comprise another passive flying aid capable of being used under visibility conditions which are so bad that FLIR becomes degraded. Moreover it will soon be possible to synthesise an image of the scene ahead which can be displayed in perspective on a Head Up Display and overlaid on the image from the FLIR.

Map information can also be stored with the terrain data base so that it is now practical to present to the pilot an optimised mission display depicting (for example) missile threat zones. Such an integrated mission system is now being assembled jointly by RAE and British Industry for evaluation in flight.

With increasing on-board computing capacity, it is now becoming possible to exploit Intelligent Knowledge-Based Systems, with the prospect of assessing data from several different sensors mounted on the aircraft, together with sensors in a cooperating aircraft or a ground based system, to generate information and to take decisions which are beyond the capacity of a single man who has at the same time to fly and manage his aircraft.

Missile Guidance and Navigation and Missile Seekers

I propose to consider long range missiles and short range missiles separately. Furthermore I shall sub-divide the long range category into those intended to attack high value fixed targets on land and those intended to attack ships.

To attack targets such as airfields located well behind the Forward Edge of the Battle Area, large payloads are required and the weapons must be delivered with high accuracy. Our current capability requires over-flight of the target by the manned aircraft. As air defences continue to improve in the Central Region of Europe, stand off weapon systems provide the only means of protecting the attacking aircraft, to the extent that missiles will have to have sufficiently long range to allow them to be launched from friendly airspace.

The accuracy required for missiles to cut a runway, for example, in a number of places to prevent its subsequent use without time consuming repairs cannot be achieved over ranges of 200 kilometres or more by inertial systems alone. Improved navigation systems, which must also be covert, are needed. One possibility would be to make position fixes from a satellite base GPS. However, if an autonomous missile navigation system is required alternatives must be sought. In the United Kingdom terrain matching techniques have been under examination. As with aircraft, the terrain based navigation system is only possible because small fast microprocessors and techniques for compact data storage are now available. The aim of future work will be to achieve delivery accuracies of the order of one to five metres Circular Error Probable so that targets such as bridges may be attacked. This will require autonomous detection and recognition of targets. A similar problem, which may arise first, is the remote attack of armour by missiles delivering terminally guided submunitions.

The attack of maritime targets prsents some similarities and some differences. Sea-skimming techniques have reduced the time available for the ship to take defensive action. Improved night and poor weather capability were also required, together with improved resistance of the missile guidance system to electronic countermeasures. Nonetheless, saturation tactics are still required to ensure successful penetration of shipborne defences. This means that the attacking aircraft have each to launch more than one missile. Moreover, because ships move a significant distance from the time of initial detection to the time of missile impact, the guidance system of each missile must be autonomous. Further, because high value targets such as capital ships are usually surrounded by escorts, the missile must incorporate autonomous target discrimination capabilities.

Radar seekers remain the preferred choice, capable of covering a sea area sufficiently large to ensure that in spite of any errors in target position fed to the missile by the aircraft at the time of launch, target detection is still achieved. As defences improve, stand-off range will have to increase, thereby making the navigation and guidance problems more difficult. Dual mode sensors, for example combined infra-red and passive radar, may be required.

For shorter range weapons, there are also exciting developments in prospect. Irrespective of whether the task is surface-to-air, air-to-air or air-to-ground, the prevailing trend is towards increased autonomy and greater intelligence built into the weapon to guide it precisely onto the target.

In the infra-red field the big development in the United Kingdom has been the efficient volume production of staring array detectors using Cadmium Mercury Telluride. In parallel there has been a great deal of research on image processing, leading now to the use of Intelligent Knowledge Based Systems techniques to identify the most vulnerable part of the target. Given the right approach to software, it has been possible to implement this capability on processors suitable for small and even low cost missiles.

With radar seekers, the trend is towards active guidance with both the radar transmitter and receiver within the missile. Coupled with this are enhanced capabilities for signal processing of target returns. The more we examine the fine structure of these returns, the more we discover that there is useful information to be extracted. One prospect is the ability to distinguish targets from non-targets using techniques which do not require an image to be formed.

There are two possible ways by which missiles might become less expensive. One is to build smaller missiles incorporating seekers which function with no moving parts. The key to solving this problem lies in the enhanced computing power it is possible to have on board a missile. The second way is to remove the need for a proximity fuze and a warhead, in other words to turn a 'missile' into a 'hittile' as exemplified by the highly successful Rapier System.

Spacecraft Guidance and Control

I want now to move away from aircraft and missile systems to say a few words about spacecraft guidance and control. The problems to be tackled are important but, for the most part, quite distinct from those discussed previously.

During launch a spacecraft is dormant. The launch vehicle provides guidance and control. The transition of the spacecraft to operational orbit is achieved by a short burn of comparatively short duration. Until now all propellant has generally been used; spin stabilisation has been employed to control thrust direction and duration has been determined by the size of the charge. The resulting inaccuracies in attitude and orbit become the initial conditions for spacecraft orbital operation. Liquid motor technology to put spacecraft more accurately into orbit is still under development: the problems are similar to those of missiles.

Once in orbit a spacecraft remains in a state of free fall, with only minor changes to the orbit, either caused by naturally occurring forces such as non-uniformities in the earth's gravity field, or brought about by controlled low thrust jets operated in response to commands sent from the ground. Automatic 'station keeping' is in the early stages.

The principal control problem experienced with spacecraft is maintaining attitude. Communication dishes may have to be pointed towards ground receivers with an accuracy of a fraction of a degree, scientific instruments may have to be pointed at celestial objects with great precision and solar panels must face the sun.

To achieve attitude control, reliance has to be placed on one or more of the following: the use of external radiation sources such as light from the earth, sun or stars, ground based RF beacons; inertial sensing of attitude motion using gyroscopes; artificially produced versions of the commands given to on-board actuators.

Once attitude has been measured, commands may have to be sent to the actuators which control the dynamic system. Traditional, mission-specific, hard-wired systems are being replaced by microprocessor-based modular systems, interconnected by data buses. The incorporation of microcomputers at the heart of the control system has led to quite complex modelling of the spacecraft dynamics, the sensing devices and the actuators to be incorporated within the control loop. However a problem attracting much attention is the achievement of better resistance to incident radiation, both natural and artificially induced. Other topics of current importance are the control of spacecraft with significant structural flexibility, and the achievement of greater spacecraft autonomy of control.

Concluding Remarks

The pace of change at the present time is clear. New capabilities are feasible and 'hittiles' soon be within our grasp. Most striking are those that lead to greater speed of response and either to less reliance on human intervention or to the elimination of human intervention. The dominant common factor in all of these changes is the use of Information Technology. There is no indication yet that the pace of change will slacken and so long as change occurs there will be new possibilities for improved guidance and control of aircraft, missiles and spacecraft.

It is arguable that our ability to exploit these new opportunities will be limited more by our lack of imagination and inventiveness than by the capabilities of the enabling technology. This is something you may wish to consider during the next three days.

EYE SAFE RAMAN LASER RANGE FINDER FOR GROUND AND AIRBORNE APPLICATION

by

Dr.J.Ruger
ELTRO GmbH
Kurpfalzring 1o6
69oo Heidelberg
West-Germany

SUMMARY

The need for an eye safe laser for military fire control systems especially in the function as a range finder is described. The performance achieved with a Raman shifted Neodymium-YAG-laser with a resulting wavelength of 1.54 micrometers is given in detail and compared to that of a 1.o64 micrometer and a 1o.6 micrometer laser range finder under various atmospheric conditions. The use of the Raman range finder in prototype equipment contracted by the German MOD is described showing the advantages of eye safety and superior ranging performance as compared to the Neodymium-YAG-laser range finder.

PREFACE

Lasers have become an indispenable part of modern fire control, target designation and weapon guidance systems. Especially Neodymium-YAG-lasers operating at a wavelength of 1.o64 µm are being widely used in proven military applications requiring laser pulses of approximately 1o nanosecond duration with peak pulse power in the megawatt region.

The effectiveness of a weapon system during combat conditions can only be assured by intensive prior training of the operating personnel with the system. However the silent and invisible 1.o64 µm laser pulse is an extreme Hazard to the human eye since practically all the laser energy arriving at the cornea is focussed at the retina causing high energy desities resulting in permanent blind spots at the retina. The safe distance to an observer - Nominal Optical Hazard Distance - for a typical Nd:YAG range finder as used in a tank fire control system is, for example, larger than 1 km and is several kilometers when observing with binoculars. For this reason extensive safety precautionary measures must be taken and must be supervised by the authorized security officer as spelled out in the STANAG 36o6 before such training exercises can commence. Therefore such training exercises are not conducted as frequently as would be required to assure most effective combat readiness.

In order to eliminate this problem in the future the German MOD has placed the eye safe requirement for development projects using lasers, meaning that at least class III A - NOHD = 0 meters without use of optical magnification - must be achieved. Fig. 1 shows the derivation of the NOHD as a function of system parameters, atmospheric extinction and the protection standard at the cornea.

Fig. 2 shows the protection standard in J/cm² per pulse as a function of the pulse repetition rate for the wavelengths 1.o6 µm, 1.54 µm and 1o.6 µm. Since 1.54 µm is transmitted through the cornea and lens but is completely absorbed by the vitreous body of the eye and thus cannot reach the retina, this wavelength is the least hazardous - 1 J/cm² per pulse for single shot lasers for example - of all IR-lasers. The 1.o6 µm wavelength - Nd:YAG-laser - with only 5 µJ/cm² per pulse belongs to the most hazardous IR-laser group.

The 1o.6 µm wavelength - CO_2-laser - with 1o mJ/cm² per pulse also belongs to the eye safe laser group since the cornea absorbing all the energy can withstand up to 1o mJ/cm² per pulse for 1 Hz pulse repetition rate before the damage threshold is exceeded. The NOHD values for typical 1.o6 µm, 1.54 µm and 1o.6 µm laser transmitters suitable for tank, anti aircraft and airborne applications are shown in fig. 3 and 4.

As can be seen the 1.54 µm laser having an NOHD value of zero in all the exemples is the least hazardous laser.

The most efficient method of producing a 1.54 µm laser radiation is the Raman shift of the Nd:YAG-laser. This laser is referred to as Raman laser hereafter. The conversion efficiency defined as the ratio of 1.54 µm energy output to the 1.o6 µm pump energy input well exceeds 4o%.

The basic principle of the Raman laser is shown in fig. 5. This transmitter consisting of a miniaturized hard sealed passive Raman cell which is pumped by a small military proven Nd:YAG laser has been incorporated into prototype target acquisition systems and into a test prototype for the fire control system of the main battle tanks Leopard 1 and 2. A closed cycle miniature liquid cooled transmitter having a pulse repetition frequency of greater than 8 Hz is being developed as a prototype for the fire control system of the P75L anti aircraft gun and for the target designation/navigation update system of the Alpha Jet aircraft.

In order to determine the performance of the Raman laser range finder as compared to that of a Nd:YAG or CO_2 range finder all three were simultaneously tested on a Leopard 2 main battle tank. The optical axis of the CO_2 and Raman laser were harmonized to that of the Nd:YAG laser and thermal image of the Leopard 2 fire control system and the laser firings were simultaneous. These tests were conducted at the German military proving grounds in Meppen in 1984. Although the sensitivity of this prototype Raman laser range finder had a system sensitivity which was a factor 2o (13 dB) less than the Nd:YAG system it matched or out performed the Nd:YAG range finder. Since the target Albedo for 1.54 µm is about the same as for 1.o64 µm it is obvious that the superior atmospheric transmission at 1.54 µm is the reason for the better range data at this wavelength.

The Raman laser used in these tests was a prototype of the one shown in fig. 6 which now has the dimensions 24 cm x 13 cm x 7.5 cm, weight 3 kg and is used in the target acquisition system ZOG shown in fig. 7. Field and logistics testing will be completed by the German army end 1986 with the ZOG unit and a production contract is anticipated early 1987.

Fig. 8 shows the calculated range performance as a function of the standard visibility for the present receiver (lower curve) and for the newly developed receiver (upper curve).

Below the curves of fig. 8 some measured data is given showing that the actual ranging performance is better than the calculated values.

Fig. 9 shows the P75L anti aircraft gun system and fig. 1o shows a block diagram of the system function. With the addition of the laser range finder and fire control computer into the system the hit probability has been improved so drastically that this older anti aircraft system when retrofitted accordingly becomes a very effective low cost weapon against low flying aircraft.

In the combat efficiency improvement program for the German Alpha Jet aircraft a Raman laser is being proposed for navigation up dating which will considerably improve navigation accuracy during combat missions to distant targets in that range and direction data to known objects during the mission is used to update the position data predicted by the navigation system. The same laser can be used for target designation and rangig purposes. Such a system using a Nd:YAG laser has been proven in the French Alpha Jet.

The Raman laser has a good potential for use in military systems when considering its excellent characteristics in respect to eye safety, good atmospheric transmission, good efficiency, and the uncooled highly sensitive receiver being developed.

CALCULATION OF THE NOMINAL OPTICAL HAZARD DISTANCE

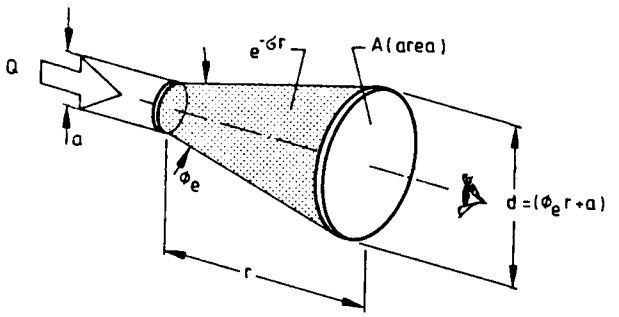

Q = radiant energy (J)
a = emergent beam diameter (cm) at 1/e radiant intensity points
ϕ_e = natural beam divergence (rad) at 1/e radiant intensity points
r = range (cm)
σ = atmospheric extinction coefficient at laser wavelength
G = hazard magnification factor of an optical instrument
H = radiant exposure (J cm^{-2})

$$H = \frac{Q \cdot e^{-\sigma r} \cdot G}{A} = \frac{4Q \cdot e^{-\sigma r} \cdot G}{\pi d^2} = \frac{1.27Q \cdot e^{-\sigma r} \cdot G}{(a+\phi_e r)^2}$$

if H_m is the maximum permissible exposure then solving for r yields:

$$r = \frac{\frac{1.27Q \cdot e^{-\sigma r} \cdot G}{H_m} - a}{\phi_e}$$

Fig. 1

PROTECTICN STANDARD AT CORNEA FOR 1.06 µm, 1.54 µm and 10.6 µm LASERS VERSUS PULSE REPETITION RATE

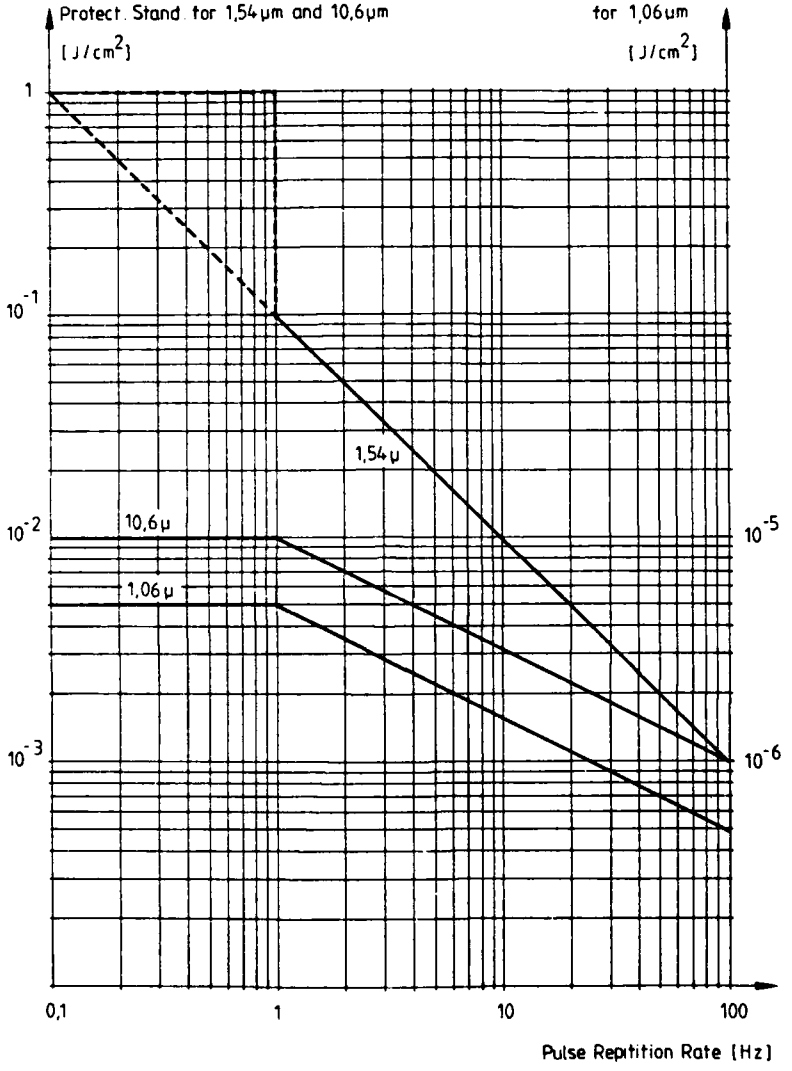

Fig. 2

EYE SAFETY CHARACTERISTICS OF TYPICAL GROUND-GROUND LRF

Protection Standard of STANAG 3606

PRR	H_m [J/cm²] per pulse		
	Nd:YAG	RAMAN	CO_2
1 Hz	$5(10)^{-6}$	1	$1(10)^{-2}$
10 Hz	$1,6(10)^{-6}$	$1(10)^{-2}$	$3,16(10)^{-3}$
20 Hz	$1,1(10)^{-6}$	$5(10)^{-3}$	$2,23(10)^{-3}$

typical values for a, $\emptyset_e$ a and Q:

a = 4 cm for Nd:YAG; RAMAN; a = 7 cm for CO_2

$\emptyset_e$ = $5(10)^{-4}$ Rad.(ground-ground); $2,5(10)^{-3}$ Rad.(ground-air)

Q = $25(10)^{-3}$ J for Nd:YAG G = 80

$15(10)^{-3}$ J for RAMAN G = 60

$100(10)^{-3}$ J for CO_2 G = 0

σ = $0.27(10)^{-5}$ cm^{-1} for 1.064 µm

$0.22(10)^{-5}$ cm^{-1} for 1.54 µm

$0.19(10)^{-5}$ cm^{-1} for 10.6 µm

equivalent to V_s = 10 km

Eye Safety Characteristics of typical Ground-Ground LRF

$\emptyset_e$	type	PRR	NOHD	(10x50)	class
0.5 mrad	Nd:YAG	1 Hz	1262 m	6141 m	III
		10 Hz	2055 m	8223 m	III
		20 Hz	2383 m	8972 m	III
0.5 mrad	RAMAN	1 Hz	0	0	III A
		10 Hz	0	131 m	III A
		20 Hz	0	215 m	III A
0.5 mrad	CO_2	1 Hz	0	0*	I*
		10 Hz	11 m	0*	I*
		20 Hz	11 m	0*	III

*assumes glass optics in the magnification device.

Fig. 3

EYE SAFETY CHARACTERISTICS OF TYPICAL AIR-AIR LRF

ϕ_e	type	PRR	NOHD	(1ox5o)	class
2.5 mrad	Nd:YAG	1 Hz 1o Hz 2o Hz	29o m 51o m	2124 m 3239 m	III III
2.5 mrad	RAMAN	1 Hz 1o Hz 2o Hz	O O O	O 27 m 45 m	III A III A III A
2.5 mrad	CO_2	1 Hz 1o Hz 2o Hz	O O 2.2 m	O* O* O*	I* I* III

+ assumes glass optics in the magnification device

Fig. 4

R A M A N - L A S E R

RAMAN TRANSMITTER

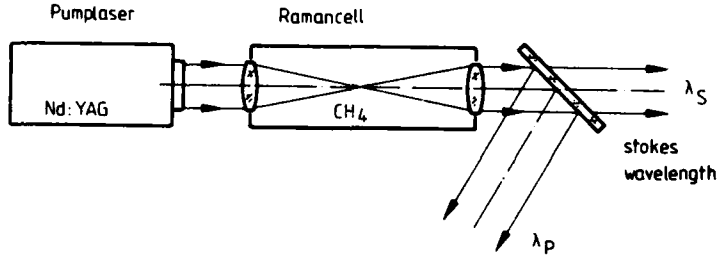

METHANE GAS AS RAMAN MEDIUM

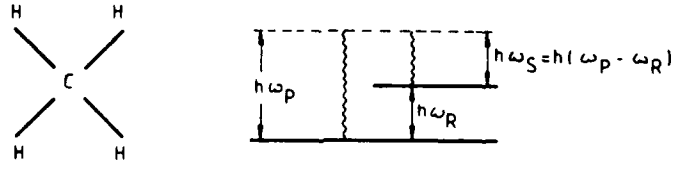

$$\lambda_S = \frac{\lambda_P \cdot \lambda_R}{\lambda_R - \lambda_P} \qquad \omega_S = \omega_P - \omega_R$$

ω_P = Pumplaser-Frequency

ω_R = Raman shift frequency

ω_S = Stockes-Frequency

Fig. 5

EYE SAFE RAMAN LASER RANGE FINDER CE 634

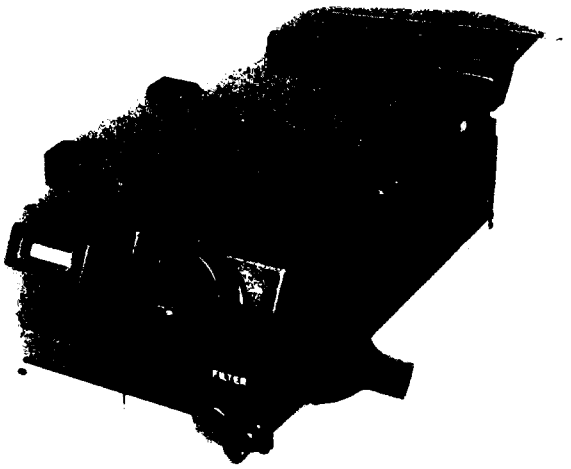

Fig. 6

TARGET ACQUISITION SYSTEM ZOG T/N

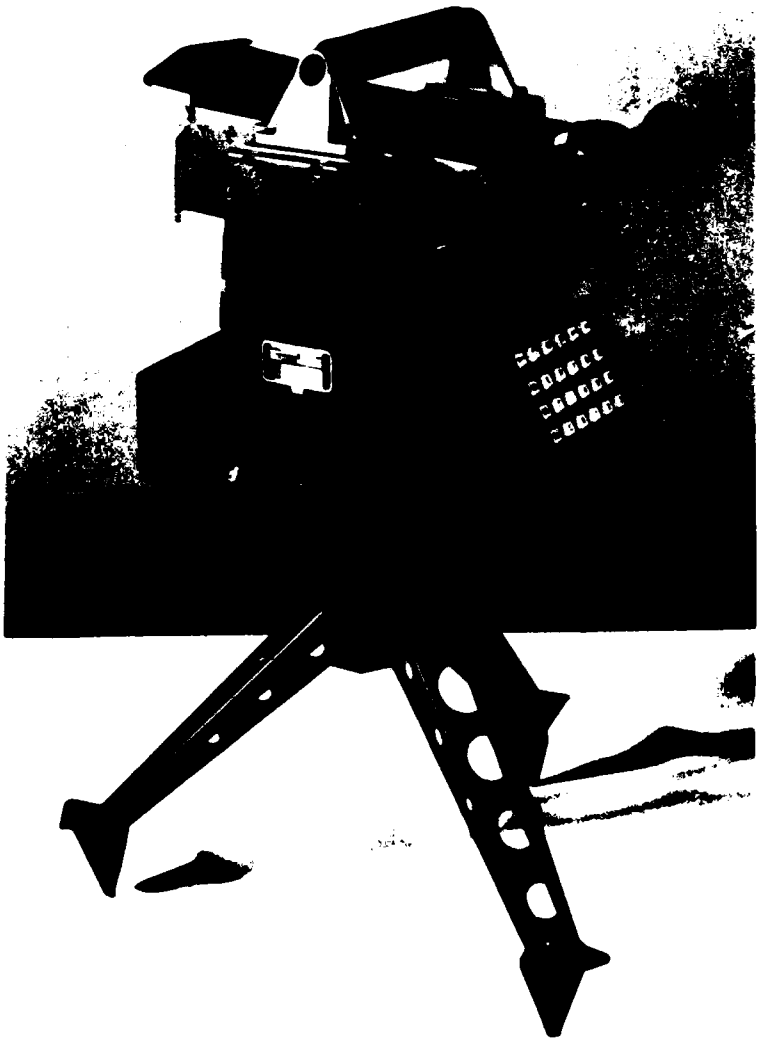

Fig. 7

TAS RANGE VERSUS ATMOS.EXT.COEFFICIENT AND STANDARD VISIBILITY

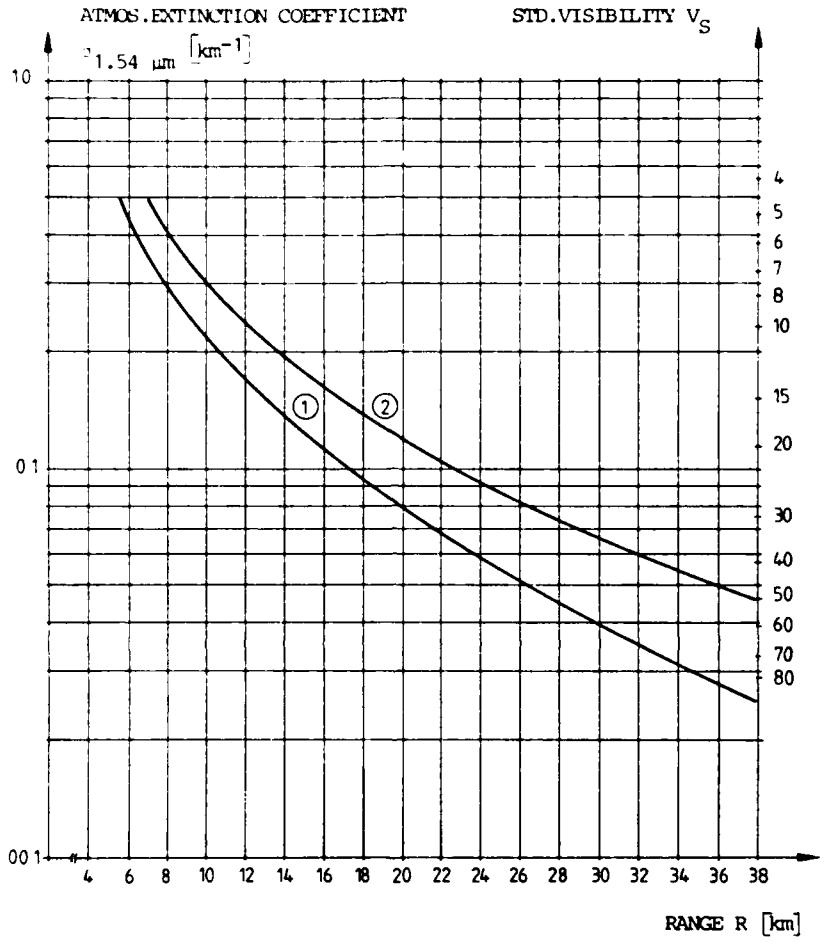

Practical Results:

Königstuhl ⟶ Bad Dürkheim (Apartment Building)
V_S = 80 km R = 39,4 km

HD-Pfgrd. ⟶ Neckartal (single trees)
V_S = 11 km R = 11 km

HD-Pfgrd. ⟶ Mannheim (Television Transmitting Tower)
V_S = 19 km R = 19 km

Fig. 8

P75L ANTIAIRCRAFT GUN REAR VIEW

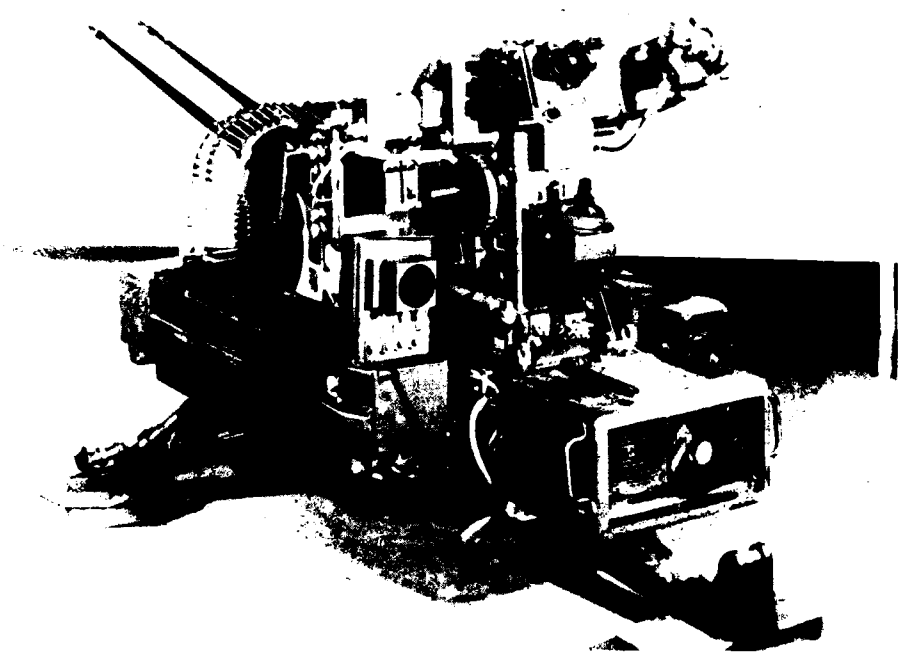

Fig. 9

P75L ANTIAIRCRAFT GUN BLOCK DIAGRAM

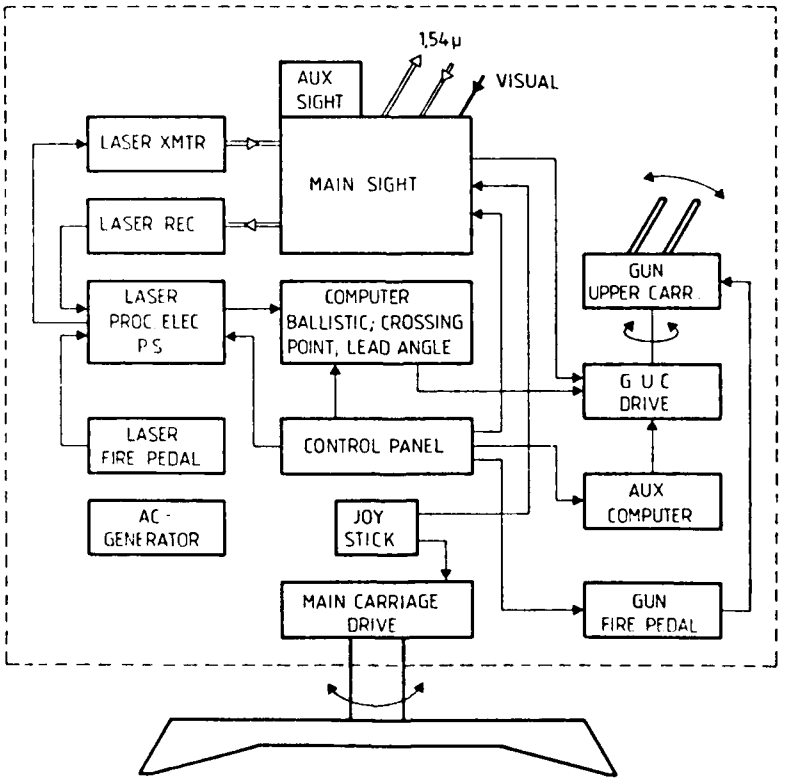

Fig. 10

THE BAe (BRACKNELL) AUTOMATIC DETECTION, TRACKING AND CLASSIFICATION SYSTEM

C.J. Samwell and G.A. Cain
British Aerospace PLC, Electronic Systems and Equipment Division,
Downshire Way, Bracknell, Berkshire, England, RG12 1QL

SUMMARY

BAe Bracknell has been designing and building real-time electro-optical digital tracking systems for 8 years. Tracking systems have been purchased by the MOD and evaluated on MOD missile and target tracking trials.

The BAe detection and tracking system uses images from infra-red and TV sensors, mounted on a 2-axis platform, to detect and determine the angular position of an object with respect to the sensor boresight (boresight errors). These boresight errors are used to control the position of the platform such that the sensor tracks the object.

The first and second generation centroid and correlation tracking systems have undergone several revisions. This paper describes a third-generation system which provides the following facilities:

- Image enhancement and segmentation.
- Automatic detection of multiple objects.
- Tracking of multiple objects.
- Automatic acquisition of detected objects.
- Automatic decoy/obscuration avoidance.
- Classification of objects.

INTRODUCTION

In recent years there has been a great deal of interest shown in the development of real-time electro-optical tracking systems that have the facilities to detect, track and classify objects. These systems have both military and industrial applications.

This paper discusses a BAe electro-optical digital tracking system that is used for detecting, tracking and classifying military targets. The technology also has equivalent applications in robotic vision systems.

A typical BAe real-time electro-optical tracking system consists of raster scan imaging sensors (infra-red (IR) and TV) mounted on a 2-axis platform whose angular position is controlled by an automatic digital tracking unit and closed loop control system. This tracking unit processes video images of an object in real-time to ascertain the object's angular position with respect to the sensor boresight (boresight errors). These boresight errors are used to control the position of the platform so that the sensor tracks the object.

As well as the basic single-object tracking facility, several additional facilities have been included:

- Image enhancement and segmentation to improve the signal-to-noise ratio of the object.
- Automatic detection of multiple objects.
- Tracking of multiple objects.
- Automatic acquisition of detected objects.

- Automatic decoy/obscuration avoidance.
- Classification of objects.

During extensive field trials and simulations, these additional facilities were found to improve the performance of the unit in realistic operational scenarios. The ability to add additional features to the basic tracking unit was an initial design aim; this has been achieved by using a modular and flexible architecture based on high speed logic, in which modules communicate via a common bus and have access to raw and processed video data via a number of common data buses. The architecture described takes advantage of both serial and parallel processing techniques. Typically, modules are implemented using dedicated line processors and microprogrammed algorithm processors.

More recent research and development has concentrated on producing tracking units using 2-micron semi-custom VLSI technology. A design feasibility study has shown that it is possible to achieve a 10:1 size reduction on the present tracking unit to produce a sophisticated tracking system on one double Eurocard.

SYSTEM DESCRIPTION

A functional block diagram of the BAe tracking system is shown in Figure 1. It consists of two tracking systems: the multiple target tracking functions (shown in dark shading) which can track up to 30 objects within the sensor field of view (FOV), and the high performance tracker (shown in light shading) which can track one selected object with high precision.

High Performance Tracking System

The object to be tracked using the high performance tracker is initially detected and acquired either manually by the operator placing an overlay (tracking window) around the object, or automatically by the automatic detection and acquisition processors.

Video data from the sensor, for the full field-of-view, is digitised at 10 MHz into 128 levels of grey. The digitised grey data is then preprocessed using both detrending (local mean removal) and Sobel edge enhancement operators before being distributed on separate data buses.

In parallel, the image data is segmented into objects of potential interest and background pixels using two-dimensional (2D) histogram segmentation (Mitchell (1) and Cussons (2)). The 2D histogram segmentation processor uses detrended grey level and Sobel edge magnitude features to produce an image in which objects exhibiting unusual grey level and edge magnitude features are illuminated. Three-dimensional histogram segmentation has also been investigated (Samwell et al (3)) using grey level, Sobel edge magnitude and texture. The use of texture, however, was not shown to give any significant performance improvement in the scenarios considered.

High performance tracking of objects is performed by the centroid and correlation processors which operate in parallel. As can be seen from Figure 1, it is optional whether or not 2D histogram data or Sobel edge magnitude data is used in the centroid and correlation processors. 2D histogram segmented data is used when tracking objects exhibiting poor contrast, and Sobel edge magnitude data is used when tracking objects exhibiting detailed structure.

The centroid and correlation algorithms determine the movement of the object being tracked relative to the centre of the tracking window (tracking errors). These tracking errors are used to determine the movement of the tracked object relative to the sensor boresight.

The centroid algorithm is a contrast-based technique that is best utilised for tracking bounded objects with little detailed structure (such as point source objects). It provides low jitter at reasonable contrast levels and can easily be modified to provide an edge tracking facility with much less jitter at lower contrast levels than a true edge tracker. The centroid tracker is complemented by the area correlation tracker which is best employed for tracking unbounded targets in difficult clutter conditions.

The correlation algorithm determines the relative movement of an object from image-to-image by mathematically correlating a filtered reference image of the object with a search area containing the object to form a 2D correlation surface. The angular movement of the object is then determined from this surface in one field time. The size of the search and reference areas are chosen so that objects exhibiting high dynamics can be tracked.

The reference image is initially formed by taking a 'snapshot' of the search area and subsequently exponentially filtering previous search areas in time. The exponential smoothing time-constant is adjusted automatically to suit the dynamics of the object. For example, if the object is changing its aspect rapidly or a decoy situation looks imminent, reference smoothing will not occur. The shape of the correlation surface and the object's trajectory history are used in determining the time constant.

The tracking error combination process (Figure 1) forms a weighted sum of the centroid and correlation tracking errors. The weighting factors are adapted automatically to give an optimal estimate of the tracking errors.

An automatic adaptive window algorithm is used to estimate the width and height of the object or part of the object within the tracking window, and adaptively adjust the tracking window size to encompass the object detail. A facility for manually adjusting the window size is also provided.

A moving window algorithm is used to reduce the effects of dynamic lag on the servo system, when tracking an object that is exhibiting high angular acceleration, by allowing the tracking window to move with the object. Since the displacement between the tracking window and boresight is known, the object's angular position relative to the boresight can be determined.

Multiple Object Detection, Acquisition and Tracking

The automatic detection system uses the 2D histogram segmented data in which objects exhibiting unusual grey and edge magnitude features are illuminated. A moving object detection system that will detect all objects moving within the sensor FOV and estimate their position is currently being developed. This will be complementary to the 2D histogram segmentation technique in that it will be especially effective in detecting small objects of low contrast that do not necessarily exhibit unusual features within the image.

Each of the objects detected by the above techniques are boundary traced using a boundary detection routine, and several geometric properties of the objects are determined. An object is accepted as being of interest if its geometric properties are within predetermined threshold limits. If it is accepted as being an object of interest its central coordinates are estimated. An example of this automatic detection technique is given in Figures 2, 3, 4, and 5. Figure 2 illustrates an IR image of Landrovers, and Figures 3 and 4 show the corresponding Sobel enhanced and 2D histogram segmented images respectively. The final image, Figure 5, shows the ability of the detection technique to reject false alarms and highlight the objects of interest

The measured and predicted central coordinates and the geometric and statistical features of the objects of interest are used in a track association algorithm, which associates each object of interest with one of several established tracks. Using this process, track trajectories for each object of interest in the sensor FOV are established. Each track is maintained by a filter which determines a quality of track measure. Should the track-measure quality fall below a predetermined level, the track is dropped and a new track is initiated. In this manner, up to 30 objects can be tracked in the sensor FOV.

Each of the tracked objects is assigned a priority indicating the degree of similarity between the observed object and a pre-defined object of interest. The priority of each object is indicated by a number on the video tracker display. The operator can assign a particular object to the high performance tracker by entering its number into the system. This object will then be automatically acquired and subsequently tracked. In the automatic mode, the high performance tracker is automatically placed on the target with the highest priority.

Object Classification System

The classification system that is being developed is used to give each object (being tracked by the multiple object tracker) a priority number based on the object's likeness to a particular pre-defined object. In the military application it would be used for example to distinguish between military vehicles and trees or bushes, and to assign the highest priority to the vehicle that represented the largest threat. The system also reduces the false alarm probability of the detection system.

The classification technique is based on extracting statistical features of objects of interest and then forming a discriminant function from combinations of these features. Using this discriminant function, objects are assigned probabilities of belonging to a particular class. These probabilities are then used to reject false alarms and to assign threat priorities.

Automatic Decoy/Obscuration Avoidance

A major operational problem with many electro-optical automatic tracking systems is their tendency to be disrupted by a decoy/obscuration entering the tracking window.

Using the multiple object detection and tracking output, the Guard Band system (Figure 1) detects decoys/obscurations in an area of pixels surrounding the tracking window. From the trajectory it can be predicted whether or not a decoy/obscuration is likely to enter the tracking window and disrupt the tracking of the prime tracked object. If disruption is likely, the decoy evasion routine is alerted. The evasion routine can take a number of avoidance actions depending on how serious the disruption is likely to be. These avoidance actions range from adjusting the tracking window size and position, thus excluding the decoy/obscuration, to using an intelligent correlation reference updating scheme.

REAL TIME IMPLEMENTATION

The implementation of most real-time systems is an iterative process between system algorithm perfection and practical realisation. This is particularly true in image processing. The loading in terms of digital programmable processing can approach the order of 200 million instructions per second (MIPS). This is at present difficult to achieve within a system aimed at being cost-effective in the military market. The packaging volume and portability of the requirements are also dominant parameters in the overall system approach.

Providing the algorithms have been well proven, the use of hard-wired elements can be of considerable benefit in meeting the processing throughput.

The architectural arrangement of this system has been designed to give a flexible and expandable system which can:

- Incorporate new technology as it becomes available
- Allow expansion as new functions are required.

Although many architectural designs that are optimised for high speed digital processing have been investigated in various establishments, most are research projects only. This paper describes a unit which is intended as a production item in a military system.

System Architecture

Figure 6 is a schematic diagram of the individual tracking boards and shows the data control paths between them. The classification board is being developed at the time of writing.

The electronic design follows an integrated philosophy such that the digital video data, in raw and processed forms, is capable of being distributed throughout the system so that the multiple object tracker and high performance tracker share the same data buses and dedicated processing electronics. In this scheme, a number of secondary data buses are implemented along with the standard high bandwidth command bus.

Modules that allow data to be passed in and out are usually designed with an interface capability for a number of input selections and a number of output selections; the particular buses are set up by the command bus. Control and timing information such as field, frame and line sync pulses are also bused. This bus structure allows a module to pick up the data and timing signals that it requires to perform its own functions. With this arrangement, a system can be designed which takes maximum benefit from previously designed modules, and allows the design of new modules to be well specified in terms of interface requirements.

A description of the boards shown in Figure 6 is given in the following sections. To illustrate the technology being used and the packing density of these boards, a picture of the correlator board is shown in Figure 7. Figure 8 is a picture of a typical automatic tracking unit showing the electronics contained in a 19-inch rack 6U high.

Z8000 Single Board Computer

There are three Z8000 Single Board Computers (SBC) in the tracking unit. The Tracker SBC controls the centroid tracking, adaptive window and moving window algorithms. The multiple detection and tracking SBC performs part of the multiple detection function, the multiple object trajectory formation and Guard Band processing. On the closed loop SBC, the overall platform closed loop control system is implemented.

The Z8000 SBC is a single board 16-bit computer. The design is based on the Zilog Z8000 family of components and incorporates the Z8001 or Z8002 (either can be fitted), one Z8036 counter-timer I/O device, and either one or two Z8030 dual-channel serial communication controllers.

On-board memory is user-definable in that currently 16 IC positions are provided for static byte-wide memory products. Each position can accomodate RAM, EPROM or fuse link PROM in CMOS, NMOS or bi-polar technology, and with sizes varying from 2K x 8 bits to 16 K x 8 bits. In this application CMOS EPROM is used. The design includes a Multibus interface complete with arbitration logic for a multi-master environment. This interface is configurable by firmware to master only, slave only or master/-slave.

The memory map for the Z8000 processor is defined by fuse link programmable devices. These devices allocate the physical memory locations to the address space and also define the Multibus address space for both master and slave modes.

Data Acquisition Board

The data acquisition board strips synchronizing pulses from the incoming target video and bandwidth limits the video prior to digitizing it at 10 MHz. The digitized data is then distributed throughout the system via one of the high speed data buses. The data acquisition board also provides the main synchronizing signals for the system control signals defining the areas of the video to be processed. This board also has multiple input and automatic gain control facilities.

Edge Enhancement Board

The edge enhanced image is generated at 10 MHz using 2D matrix convolution with the Sobel operators. The operators operate on image data that is either sourced directly from the digital data lines or from these lines via four look-up tables. To perform Sobel enhancement directly requires the addition of 12 pixel elements (6 per mask) in the time of a 100 ns. This rate is equivalent to 120 MIPS which is performed by a high speed dedicated line processor.

All the data channels on the Sobel board are controlled by the Multibus. Using this facility, any combination of input and output lines can be brought into use as required, with internal board data routing also directed by this means.

Histogram Board

The histogram board uses detrended grey level and Sobel edge enhanced data obtained from two of the data buses. This data is then processed to form a 2D histogram for a full frame of data in 40 ms.

During each frame, the histogram data is smoothed using an exponential filter and the contents of the addressed bin are read and presented to the histogram output latch to be transmitted to the segmentation boards.

Segmentation Board

The purpose of these boards is to segment the histogram data into either object pixels (white) or background pixels (black) by thresholding the input data. Object pixels are stored as a 512 x 512 x 1 bit map or as an address string in main memory. After formation of the segmented data, a high speed 32-bit processor analyses the bit map for bounded objects using a boundary detection algorithm.

The multiple detection and tracking SBC controls the data in the memories by use of Multibus commands.

Video Store Board

The video store board consists of two banks of memory, each 32K x 8 bits. When not storing video data, this memory may be accessed from the Multibus as one continuous memory, 64K x 8 bits (or 32K x 16 bit words). Data may be accessed direct from the Multibus or via the high speed data buses (this function being software selectable) to enable post-storage processing of data.

Video information, converted to a digital data stream at 10 MHz by the data acquisition board, may be stored in either or both the 32K x 8 bit memory banks, again under software control. During this time the memory being used is not accessible by the processors.

The video store board can also be used to provide full field storage if required (512 x 256 pixels).

Correlation Board

This board is a microprogrammed state machine. It performs the basic correlation process of shifting 2D arrays with respect to one another and determining the degree of match between the two images at all the shift positions. In addition it has an algorithm which rejects the gross mis-match positions extremely rapidly. In this way, only those shifts that are candidates for producing the correct registration position in the correlation surface output are selected for completion. The processor can achieve a high speed image match rate.

This module is equivalent to a processor of some 20 MIPS. It also performs the most time-intensive centroid algorithm functions.

The correlation module works as an independent processor in the system, operating independently of other tracking functions.

Video Symbology Board

This board performs the essential task of providing a man-machine visual feedback. It overlays the image data with alpha-numeric or graphic information in selected areas to display such symbols as tracking windows and status information.

Moving Object Detection Boards

The moving object detection system uses the difference of two consecutive fields of data, where the previous field is shifted to account for background motion, to identify objects that have moved relative to the background.

The moving object detection system is implemented on two boards, which are essentially video stores. These stores process the previous field and current field and compute the current difference between these two fields in real time. These boards form a part of the automatic detection system.

Object Classification Board

The classification software will be implemented on the Programmable Pixel Processor (P3) board which is currently being developed.

This board consists of two blocks of 256 x 128 bytes of memory and a high speed 32-bit microprocessor with 64 K bytes of RAM, 32 K bytes of PROM and 1 K byte of global memory that can be accessed via the Multibus. It is a programmable device in which the program is initiated via the Multibus. Since the video store memory is contained on the same board as the processor, data transfer times are kept to a minimum.

CONCLUSION

A typical BAe electro-optical automatic tracking system has been presented.

The architecture used for the tracking unit has proved to be flexible and efficient enough to accommodate new algorithms and new technology when required. This is an important consideration, since in a relatively short time, increased sophistication and throughput of high speed memory, arithmetic and logical elements have become available.

Several tracking systems have been evaluated extensively on field trials, during which the tracker electronics unit has proved to be very reliable in a variety of environmental conditions. At these field trials, the multiple object tracking system and the high performance tracking system have been shown to perform very effectively in a variety of scenarios. The Guard Band and decoy evasion system increases the reliability of the high performance tracking system when decoys and obscurations are present.

In conclusion, the electronic modules developed have proved to be effective in cost, size, power and computational throughput, and the performance of the tracking system has been impressive.

REFERENCES

1. Mitchell, D.R., and Luton, S.M., "Segmentation and Classification of Targets in FLIR", SPIE VOL 155, 1978

2. Cussons, S., "A Real-Time Operator for the Segmentation of Blobs in Imaging Sensors", IEE Electronic Image Processing Conference PROC, 214, 1982, 51-57

3. Samwell, C.J., Luke, P.D., and Davies, M.K., "Automatic Detection of Military Vehicles in Cluttered Background Using Multivariate Histogram Segmentation and Boundary Detection" RSRE Proc, Image Processing Symposium, 1983, 2.6.1 - 2.6.14

ACKNOWLEDGEMENTS

The work presented in this paper has been funded by the Ministry of Defence and British Aerospace. The authors wish to thank Dr. P.D. Luke and Mr. E.H. Davies for their comments in the preparation of this paper.

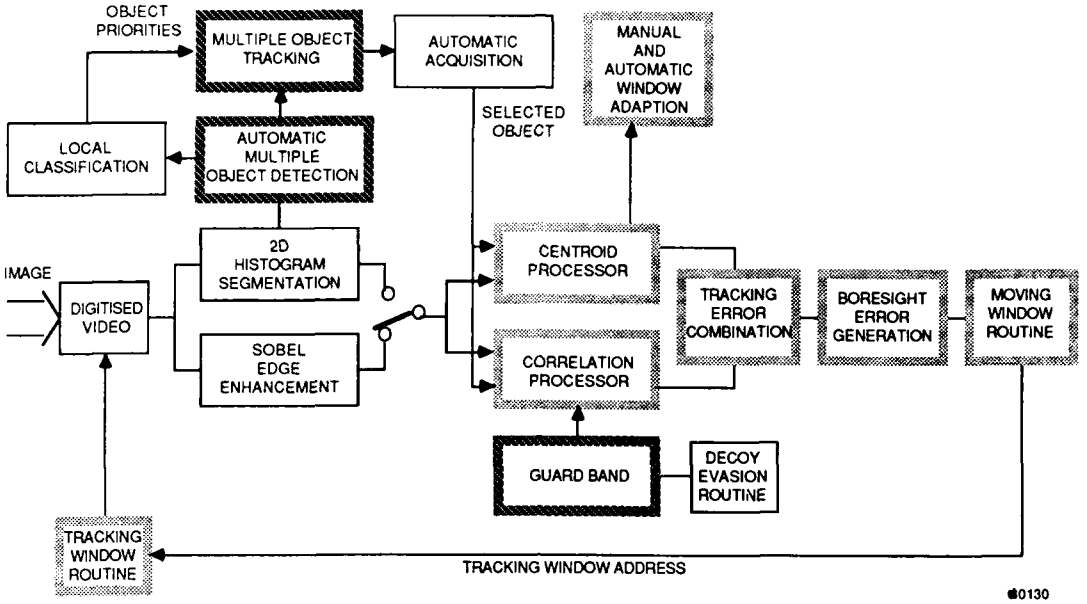

Figure 1 BAe Automatic Detection, Tracking and Classification System

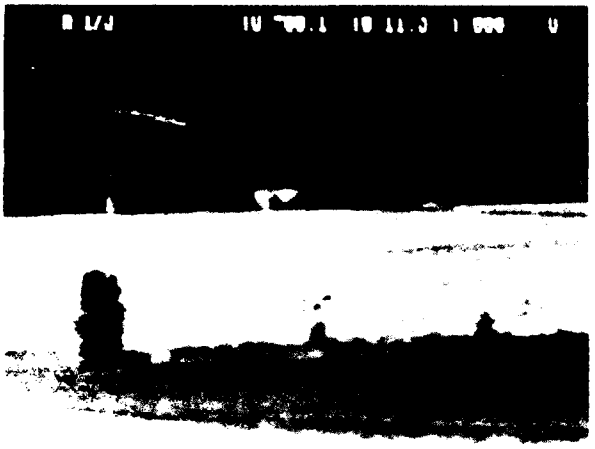

Figure 2 [illegible] of Landrovers

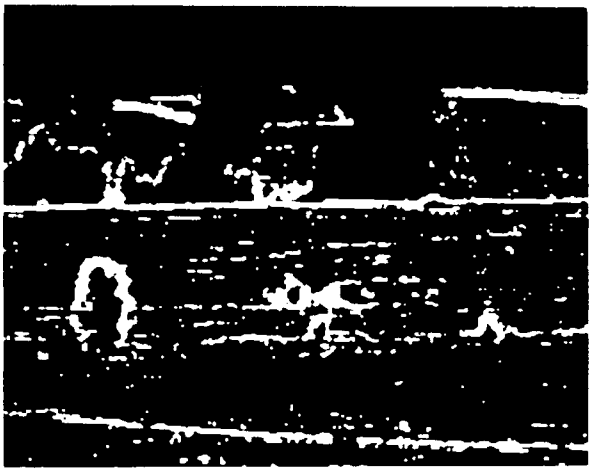

Figure 3 Sobel Enhanced Image

Figure 4 [illegible] Segmented Image

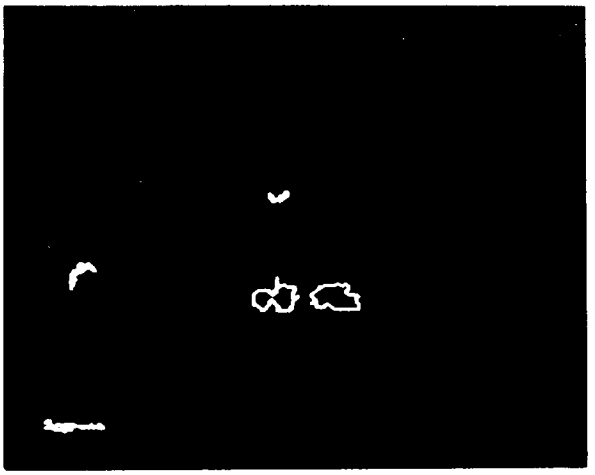

Figure 5 Boundary Traced After Clutter Rejection

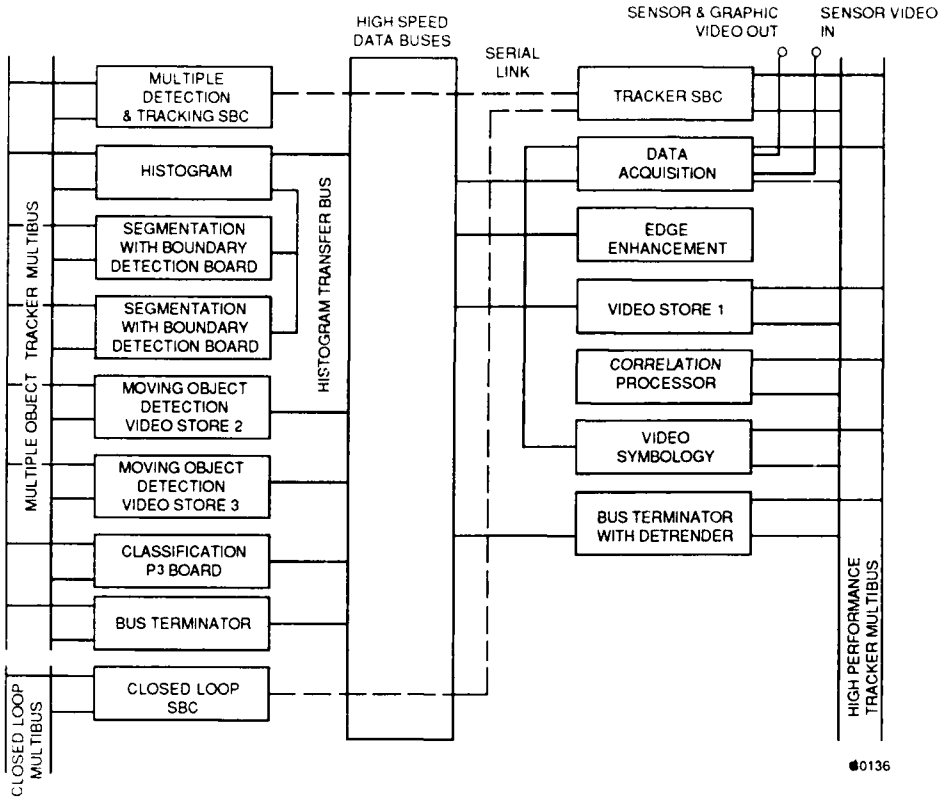

Figure 6 BAe Automatic Tracking System PCB Schematic Diagram

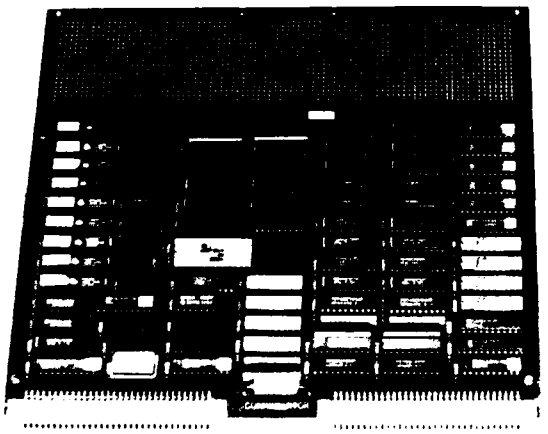

Figure 7 Correlator Board

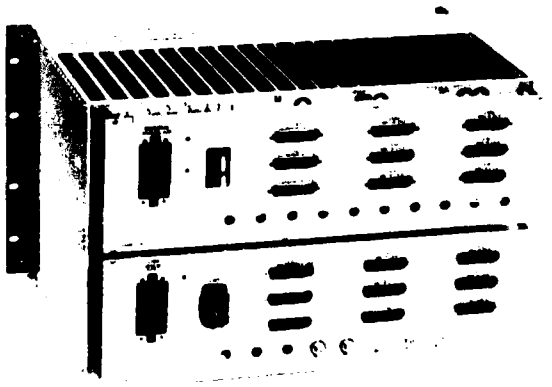

Figure 8 Automatic Tracking Electronics Unit

VELOCITY ACCURACY MEASUREMENT OF GPS USER EQUIPMENT

Joseph McGowan
U.S. Army Aviation Systems Command
Avionics Research & Development Activity
ATTN: SAVAA-N
Fort Monmouth, NJ 07703-5401

This paper describes a test program conducted by the U.S. Army Avionics Research and Development Activity (AVRADA) to determine the level of velocity accuracy achievable with GPS. The precision of the reference instrumentation and the availability of the GPS receiver measurement data were exploited to characterize the errors in GPS observables. An investigation into the performance benefits of GPS and inertial integration is described.

APTS	-	Aerial Profiling of Terrain System
CDU	-	Control Display Unit
C/No	-	Carrier to Noise Ratio
DOP	-	Dilution of Precision
GPS	-	Global Positioning System
IMU	-	Inertial Measurement Unit
LOS	-	Line of Sight
NAVSTAR	-	Navigation Signal Time and Range
PDR	-	Psuedo Delta Range
PPS	-	Precise Positioning Service
PR	-	Pseudo-Range
PRN	-	Pseudo-Random Noise
RPU	-	Receiver Processor Unit
SPS	-	Standard Positioning Service
TEC	-	Total Electron Content

I. INTRODUCTION

The Navigation Signal Time and Range Global Positioning System (NAVSTAR GPS) has been in development for more than a decade and has been the subject of numerous performance tests, by both government and industry. The volumes of test reports generated in these efforts indicate that GPS readily meets its claim to 15 (SEP) meter positioning accuracy, often performing better. It has also shown tremendous potential for wide range time synchronization applications.

GPS has the potential to provide extremely accurate velocity information. It has been specified to perform at 0.1 m/s (RMS per axis). However, very little of the extensive data base previously developed is useful in evaluating GPS velocity performance. Prior efforts have focused on comparison to differentiated reference position data. The noise enhancement inherent in this process degrades the resolution in the resulting velocity reference, making it unsuitable for determining performance at the 0.1 m/sec level. This paper describes a test program conducted by the U.S. Army where a precise reference system has enabled a detailed analysis of GPS velocity accuracy. The quality of the GPS measurements (i.e. range and range rate) are also analyzed and characterized.

II. GPS OVERVIEW

GPS is a space based radionavigation system. It is functionally divided into the Space, Control, and User segments.

The Space segment consists of a constellation of NAVSTAR satellites. A full constellation will have 18 satellites plus 3 active spares. They will be uniformly distributed in six orbit planes, providing 4 - 7 visible satellites at any time anywhere on earth. The planes are inclined 55 degrees with respect to the equitorial plane. The orbital altitude is 10,890 nautical miles, making the orbital period approximately 12 hours. Each satellite transmits specially coded signals that allow individual satellites to be distinguished, and the range and rate of range change to the user to be measured. The signals are pseudo-random binary noise codes (PRN). Two different codes are transmitted in phase quadrature, providing a Standard Positioning Service (SPS) and a Precise Positioning Service (PPS). A low rate data message is also transmitted.

The Control segment has five monitor stations that track all satellites in view of their antennas. Data is transmitted to a Master Control Station where processing takes place to determine orbital and clock modeling parameters for each satellite. The information is then uploaded to the satellites by one of three upload stations. The satellites incorporate this information into the data message.

The User segment consists of equipment designed to receive and process the satellite signals. The unique codes transmitted by each satellite allow the use of common RF carrier frequencies throughout the constellation, a process known as Code Division

Multiplexing. Measurements from four satellites are required in the general case. The DOD has developed two classes of receiver, continuous tracking and sequential tracking. The continuous tracking receiver provides a dedicated channel for each satellite being tracked and a fifth channel that performs ancillary functions (e.g. time correction, interchannel bias measurement). The sequential receiver has 1 or 2 channels, for low and medium dynamic applications, respectively. In these receivers the channels are time shared among satellites and housekeeping chores.

The PRN code in each satellite is reset to its initial state precisely at midnight, Saturday (Universal Coordinated Time). The codes have sufficient period so that no state will be repeated between the weekly resets. The receivers generate a replica of the code and phaselock on it using correlation techniques. The received code phase provides a direct indication of the time of transmission of the code and allows the transit time of the signal to be calculated against a local clock. Scaling this measurement by the speed of light (c) determines the range between the user and satellite antennas. This quantity is known as pseudo-range (PR) because it contains errors. Two dominant error sources are the error in the local clock (its quality is at least an order of magnitude worse than the satellite clock) and atmospheric delays suffered by the signal.

The atmospheric effects are composed of separate tropospheric and ionospheric components. The tropospheric delay can be estimated to within 4% using a simple elevation model. The results of this test indicate that the performance of this model does not appreciably degrade with elevation. Ionospheric delay can be modeled, however, the dynamic nature of the ionosphere limits the achievable accuracy to about 50%. A method of measuring it has been designed into the system. The amount of delay depends on the frequency of the signal and on the density of free electrons in the ionosphere, a quantity known as the Total Electron Content (TEC). By ranging to the same satellite on the two frequencies, a delay difference can be formed in which TEC is constant and can therefore be estimated.

[illegible]	[illegible]	[illegible] (Meters)
	Clock Stability	2.7
[illegible]	Clock Perturbations	1.3
[illegible]	Other	1.5
	Segment RSS	3.4
	Ephemeris Prediction	2.6
[illegible]	and Model Adj	
[illegible]	Other	1.5
	Segment RSS	2.9
	Ionospheric Delay	2.3
	Tropospheric Delay	2.3
[illegible]	Receiver Noise/Resolution	1.5
[illegible]	Multipath Interference	1.2
	Other	1.5
	Segment RSS	3.0
	System RSS	5.3

TABLE 1. GPS PSUEDORANGE ERROR BUDGET

The measurement of transit time by the receiver contains the bias between the satellite and user clocks. Since it affects all measurements equally, it can be estimated as part of the solution. Where three measurements are needed to determine three position coordinates, a fourth allows clock bias to be determined. Table 1 shows the error budget for the PR measurement, assuming that the dual frequency ionospheric compensation technique is used. As shown, a measurement error of 5 meters is predicted. The test results indicate that the high frequency fluctuation of the error is less than 1 meter. The error was dominated by a bias component that ranged from 2 - 10 meters.

During periods of sufficient received signal quality (C/No >29 dB Hz), the receiver can phaselock onto the carrier. The doppler shift observed is used to determine the line of sight (LOS) velocity between the satellite and user. This measurement is implemented as an integrated doppler known as the pseudo delta-range (PDR), which is a measure of the range change during the integration interval. Major sources of error in this observable are the frequency offset between the two clocks, the short term stability of the receiver clock, and the performance of the receiver tracking loop in the presence of noise. In a manner completely analogous to the estimation of clock bias, four LOS velocity measurements allow frequency bias to be determined. The test results indicated that the PDR measurement is extremely precise, being zero mean with an RMS value of about 0.8 centimeters (corresponding to a velocity error of 1 cm/s).

For the purpose of performance prediction and analysis, it is necessary to quantitatively describe the manner in which errors from four measurements combine in the navigation solution.

This combination of errors is directly affected by the geometric relationship between the satellites and user, and is expressed in terms of a Geometric Dilution of Precision (GDOP) factor. GDOP is comprised of terms which describe the degradation of

accuracy in the East, North, Vertical, and Time coordinates (EDOP, NDOP,VDOP, and TDOP respectively). These four components are combined in root-sum-square fashion to obtain GDOP. Simple performance prediction is obtained by multiplying the appropriate DOP by the expected measurement error. The specified accuracy of GPS will be available when GDOP $\leq$ 3.56.

The theory of operation of GPS is well described in the literature (Reference 1).

III. REFERENCE SYSTEM

Using traditional reasoning, a reference system was sought which would provide 1cm/s of velocity accuracy in order to properly evaluate the specified GPS accuracy of 10cm/s. The Aerial Profiling of Terrain System (APTS) was chosen.

APTS is an airborne surveying platform developed by the Charles Stark Draper Laboratories under the sponsorship of the U.S. Geological Survey. Its primary role is to provide the capability of generating elevation maps by overflight of the area of interest. The current APTS configuration is carried in a DeHavilland Twin Otter aircraft. Its essential components are a high quality Inertial Measurement Unit (IMU), a laser altimeter, a gimballed laser/tracker, and a series of ground-based retroflectors. The retroflectors are precisely located using manual survey techniques. The relative locations of the retroflectors are accurate to within 1 part in 100,000.

The APTS operating concept is shown in Figure 1. The aircraft flies a nominally straight and level path. The gimballed IMU measures aircraft acceleration and attitude, while the laser/tracker measures range, azimuth, and elevation to an illuminated retroflector. These latter measurements are sufficient to locate the aircraft in three dimensions relative to the retroflector's position. The laser altimeter measures height above terrain for surveying missions. The raw data from these sensors is simultaneously processed in real time to provide platform navigation, and recorded for post processing to obtain the survey solution.

In real time, laser/tracker position solutions are used to bound the inertial errors in a simple reset mechanization, providing accuracies of 60 meters and 20 cm/s in position and velocity, respectively. This level of accuracy is sufficient for aircraft navigation and retroflector acquisition, but does not satisfy the high accuracy requirements of the surveying problem.

The recorded raw sensor data is processed in a post-flight filter/smoother that embodies the extensive error models developed for the APTS. The position and velocity accuracies achieved are 60cm and 3-5 mm/sec between retroflector locks. During locks, performance is significantly better. This level of position accuracy has been demonstrated by direct comparison of APTS and manually generated elevation map data (Reference 2). From this, the stated 3 - 5 mm/sec velocity accuracy can be concluded. As a further check on APTS velocity accuracy, the diagonal elements of the post processing filter covariance matrix were examined. The peak velocity error estimated by the filter was 2.4 mm/sec.

A more thorough description of APTS can be found in Reference 3 and Reference 5.

IV. TEST DESCRIPTION

The GPS equipment utilized in this test was borrowed from the Test Directorate of the Armament Systems Division at Eglin AFB, Florida. These assets consisted of a 5 channel receiver/processor unit (RPU), a control display unit (CDU), and instrumentation providing data recording capability. Table 2 lists the GPS data blocks that were available. Of primary interest in the analysis were the navigation solutions available in message blocks 3 and 1028, the satellite ephemerides in block 5, and the receiver raw measurements and correction terms in blocks 1031 and 1100.

[illegible]	[illegible]CONTENTS
3	[illegible]AND [illegible] AT [illegible] AT TIME MARK
5	[illegible]SATELLITE EPHEMERIS DATA
1025	[illegible]SATELLITE TRACKING MEASURE
1026	[illegible]KALMAN FILTER DATA (E,N, RESIDUALS)
1027	[illegible]KALMAN FILTER DATA (E,N, RESIDUALS)
1028	[illegible]LINE OF SIGHT VECTORS TO SATELLITES
1029	[illegible]LINE OF SIGHT VECTORS TO SATELLITES
1029	[illegible]NAVIGATION STATE VECTOR COVARIANCE DIAGONAL
1031	[illegible]RAW RECEIVER MEASUREMENTS
1100	[illegible]DETERMINISTIC MEASUREMENT CORRECTIONS

TABLE 2. GPS RECORDED DATE BLOCKS

GPS and APTS were operated independently. Each system had its own time source and produced its own data tape. The only interface between them was a method of calibrating the clocks to provide post flight data tape synchronization capability. This was achieved by feeding a 1 Hz timing pulse, generated and time tagged by the GPS, to the APTS. Specially designed test hardware allowed APTS to receive these pulses and tag them in APTS time, providing synchronization to within 80 usec.

Four data collection flights were flown, yielding about 6

hours of simultaneous GPS and APTS data. The flight path, shown in Figure 2 was selected to utilize existing APTS retroflector sites. These sites were used during the APTS shakedown and system performance tests. A substantial data base documenting APTS performance using them exists.

At the time of the test there were 6 operational GPS satellites on orbit. The flights were scheduled to begin as soon as four were visible in the test area. The first 20 minutes of each flight was characterized by poor but rapidly improving GPS system geometry. The GDOP during this period generally varied from >25 to less than 4. During the remainder of the flight the geometry was more stable, with GDOP remaining in the range of 3 - 5. Plots of GDOP, EDOP, NDOP, VDOP, and TDOP are shown in Figures 3 and 4.

V. RESULTS

Figure 5 shows the difference between APTS and GPS navigated velocity for one of the flights. It is readily apparent that the GPS velocity error is predominantly random in nature. During periods of good constellation geometry (t > 4100 sec on the figure), the error appears to have zero mean.

CATEGORY	MESSAGE BLOCK	NORTH	EAST	VERTICAL	RSS	SEP
WHOLE FLIGHT	3	0.128	0.163	0.042	0.211	0.151
WHOLE FLIGHT	1028	0.076	0.096	0.024	0.125	0.089
STR & LEVEL	3	0.119	0.149	0.041	0.195	0.139
TURNING	3	0.152	0.196	0.045	0.252	0.180
CONSTELLATION:						
6,8,9,13	3	0.102	0.155	0.044	0.191	0.136
6,8,11,13	3	0.136	0.170	0.042	0.222	0.158
6,8,11,12	3	0.135	0.139	0.034	0.197	0.141

TABLE 3. FLIGHT #1 RMS VELOCITY ERROR (M/S)

CATEGORY	MESSAGE BLOCK	NORTH	EAST	VERTICAL	RSS	SEP
WHOLE FLIGHT	3	0.132	0.144	0.050	0.202	0.154
WHOLE FLIGHT	1028	0.078	0.085	0.031	0.119	0.091
STR & LEVEL	3	0.124	0.137	0.050	0.191	0.148
TURNING	3	0.152	0.165	0.051	0.230	0.176
CONSTELLATION						
6, 8, 9, 11	3	0.123	0.103	0.059	0.171	0.1309
6, 8, 9, 13	3	0.123	0.172	0.045	0.216	0.1656
6, 8, 11, 13	3	0.136	0.159	0.047	0.214	0.1642
6, 8, 11, 12	3	0.146	0.136	0.041	0.204	0.156

TABLE 4. FLIGHT #2 GPS RMS VELOCITY ERROR (M/S)

CATEGORY	MESSAGE BLOCK	NORTH	EAST	VERTICAL	RSS	SEP
WHOLE FLIGHT	3	0.173	0.150	0.164	0.282	0.222
WHOLE FLIGHT	1028	0.101	0.088	0.095	0.164	0.127
STR & LEVEL	3	0.161	0.140	0.159	0.266	0.214
TURNING	3	0.205	0.179	0.179	0.326	0.240

TABLE 5. FLIGHT #3 GPS RMS VELOCITY ERROR (M/S)
NOTE: ONLY ONE CONSTELLATION TRACKED (6, 8, 11, 12)

CATEGORY	MESSAGE BLOCK	NORTH	EAST	VERTICAL	RSS	SEP
WHOLE FLIGHT	3	0.159	0.146	0.061	0.224	0.175
WHOLE FLIGHT	1028	0.095	0.086	0.037	0.133	0.104
STR & LEVEL	3	0.147	0.136	0.060	0.209	0.166
TURNING	3	0.193	0.172	0.065	0.267	0.211
CONSTELLATION						
6, 8, 11, 12	3	0.166	0.150	0.037	0.227	0.178
8, 9, 11, 12	3	0.147	0.144	0.078	0.220	0.173
9,11, 12, 13	3	0.160	0.137	0.088	0.228	0.180

TABLE 6. FLIGHT #4 RMS VELOCITY ERROR (M/S)

Statistical analysis of the velocity difference time history was conducted for all of the flights. The data was grouped in several categories for this analysis. Whole flight statistics were calculated, the conditions of straight and level and turning (where roll > 5 degrees) were separated, and the statistics for each constellation tracked were evaluated. The results are tabulated in Tables 3 through 6. The whole flight statistics for both the block 3 and block 1028 solutions were calculated. As shown in the tables, the velocity solution available in message block 1028 was in spec in all coordinates, while the block 3 solution generally was not.

The block 1028 error is smaller than the block 3 solution by a nearly constant factor of 1.7 for all coordinates over all flights. The only apparent difference between these two solutions that could account for the performance discrepancy is in their times of validity. The block 1028 solution is valid 160 msec earlier than the block 3 solution, relative to the same measurement epoch. Velocity is propagated as the integral of the best estimate of acceleration at the time of a measurement epoch. The degradation between the two solutions, in the North coordinate for example, could be accounted for by an acceleration bias error as small as $_2$0.33 meters per second^2. Therefore, for high precision in unaided operation, solutions should be extracted as close to a measurement epoch as possible.

As shown in Tables 3 through 6, the results indicate that GPS can meet 0.1 m/s RMS velocity accuracy. For applications where the solution must be extrapolated from a measurement epoch, the need for proper Kalman Filter tuning to maximize acceleration estimate accuracy has been shown.

Subsequent analysis focused on the quality of the GPS measurements. The measurement errors are usually modeled as clock error plus noise.

The analysis was accomplished by forming predictions of the measurements based on the GPS ephemeris data, receiver clock estimates, and deterministic correction terms, and on the APTS navigation solution. The residual between this and the recorded measurements represent the GPS measurement errors. Figures 6 and 7 show the PR residuals for one of the flights. Generally, they consist of a small bias term (2 - 10 meters), a slowly varying systematic term of $\pm$ 3 to $\pm$ 5 meters, and a random fluctuation at about the 0.5 to 1.0 meter level.

Figures 8 and 9 show the PDR residual, divided by the integration interval to convert them to LOS velocity errors. During the first 20 minutes of the flight the geometry is poor, and the residuals consist of a bias-like component and a random component. At t = 4100 sec, the acquisition of a new satellite dramatically improves the geometry, and the residuals become more nearly zero mean and random in nature, at about a 5 to 10 mm/sec level. The bias-like behavior of the residuals during the early part of the flight has been attributed to the receiver's estimate of its clock frequency offset (the model on which the predictions were based depends on this estimate). A plot of this estimate is shown in Figure 10. At t = 4100 sec, a step-like refinement in the estimate is apparent. Another interesting feature of this plot is the reduction in the randomness of the estimate. Both of these artifacts are consistent with the step-like improvement in TDOP at this time.

The results from the other flights were consistent with these. The GPS measurement errors, during periods of good geometry, are summarized in Table 7.

MEASUREMENT	BIAS	SYSTEMATIC	RANDOM
PR	2 - 10 METERS	3 - 5 METERS ($\pm$)	.5 - 1 METERS (RMS)
PDR	INSIGNIFICANT	INSIGNIFICANT	1 CM/SEC (RMS)

TABLE 7. SUMMARY OF GPS MEASUREMENT ERRORS

PR PSUEDO-RANGE
PDR PSUEDO-DELTA RANGE

It is interesting to contrast the PDR measurement to the velocity solution. The randomness in the solution is 10 - 20 times as great as in the measurements. The DOPs were 1 - 2 during this time, which leads to an expected velocity error of 1 - 2 cm/s (DOP X measurement error). The velocity error that results from forming an unfiltered solution is shown in Figure 11. The performance closely matches the simple prediction model. It is reasonable to expect that a filterred solution valid at the measurement times would be as good.

GPS RECEIVER	FILTER
5 CHANNEL	17 STATE
2 CHANNEL	17 STATE
2 CHANNEL	11 STATE

TABLE 8. POST PROCESSING ITERATIONS

Having established the high precision of the GPS observables, the next phase of the analysis investigated the benefits of GPS/IMU integration. The APTS raw IMU data and the recorded GPS measurements were combined in several Kalman filters, and the resulting velocity performance statistically analyzed. This process was iterated three times, with filter complexity and/or receiver class varied in each. Table 8 summarizes the various iterations. The filter states are summarized in Table 9. Two channel GPS observables were simulated by adding noise to the actual 5 channel measurements.

PARAMETER	11 STATE	17 STATE
POSITION (3)	YES	YES
VELOCITY (3)	YES	YES
CLOCK BIAS	YES	YES
CLOCK DRIFT	YES	YES
PLATFORM TILT (3)	YES	YES
TILT DRIFT (3)	NO	YES
ACCELEROMETER BIAS (3)	NO	YES

TABLE 9. KALMAN FILTER STATES

The resulting velocity errors are summarized in Table 10, where the receiver's solution and the point solution are included for comparison. In the simulated results velocity errors are on the order of mm/sec. Clearly, the combination of GPS and IMU holds great promise for high accuracy aircraft state sensing problems.

This is especially true in high dynamic environments and situations where data rates exceeding the GPS measurement rate are needed.

VI. CONCLUSION

GPS velocity performance has been evaluated against the most precise reference system used for this purpose to date. The results show that the claimed 0.1 m/sec (RMS) error can be met at points near the measurement time. The block 1028 solution was always within this specification. The block 3 solution, a further extrapolation of the 1028 solution, had only its vertical component always within specification.

GPS VELOCITY ERRORS (RSS) WITH RESPECT TO THE REFERENCE SYSTEM SOLUTION (a)

NAVIGATION FILTER	VELOCITY (m/s) EAST	NORTH	UP
1. 5-Channel Set	0.130	0.100	0.050
2. 5-Channel; Point Solution	0.008	0.009	0.01
3. 5-Channel; 17-state Kalman filter	0.002	0.003	0.004
4. 2-Channel; 17-state Kalman filter (c)	0.005	0.008	0.018
5. 2-Channel; 11-state Kalman filter (c)	0.006	0.016	0.016

(a) Data from flight #1 during periods of good GDOP

(b) Aiding simulated by propagating state updates at 12 Hz rate, using accelerometer data

(c) Random noise is added to the deltaranges to simulate the effect of increased carrier tracking-loop bandwidth for 2-channel receivers relative to 5-channel receivers

TABLE 10.

Data has been presented which indicates that the GPS measurement process is very precise.

Post test analysis results were shown indicating the level of performance enhancement that can be achieved with the integration of GPS and inertial systems. The extreme accuracy of these results indicate that this combination will satisfy a host of platform state sensing problems.

Complete details of this test and the results can be found in Reference 4.

REFERENCES

1. "Global Positioning System", A collection of GPS papers published in Navigation Journal of the ION, Summer 1980.

2. "Aerial Profiling of Terrain System Performance Evaluation Flight Test Report", CSDL-R-1703, March 1984.

3. Soltz, J.A., G. Mamon, W. Chapman, "Aerial Profiling of Terrain System Implementation", presented at Second International Symposium on Inertial Technology for Surveying and Geodesy, Baniff Alberta Canada, June 1981.

4. Greenspan, R. L., Donna, J. I., "APTS/GPS Measurement Task Final Technical Report", CSDL-R-1845, February 1986.

5. Hursh, John W., "Aerial Profiling of Terrain System (Apts), Journal of the Institute of Navigation, Volume 32, No. 3, Fall 1985.

ACKNOWLEDGEMENTS

The author would like to thank the following organizations for their contributions to this program.

The Armament Systems Directorate at Eglin Air Force Base which loaned their GPS assets and reconfigured them onto a pallet compatible with the APTS aircraft.

Collins Government Avionics Division of Rockwell International, especially Merv Dosh who provided invaluable guidance in evaluating and interpreting the GPS data blocks and insight into the receiver navigation processing.

The Charles Stark Draper Laboratories, particularly Richard Greenspan and James Donna, whose creative analysis provided for program success that exceeded initial expectations.

APT — SYSTEM CONCEPT

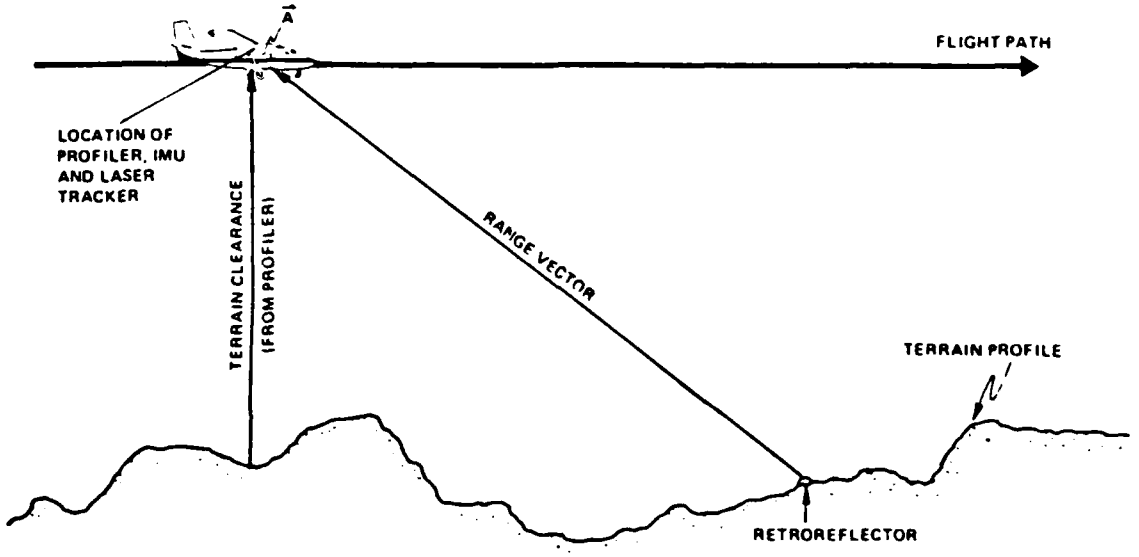

FIGURE 1

FLIGHT PATH ON MAY 30, 1985

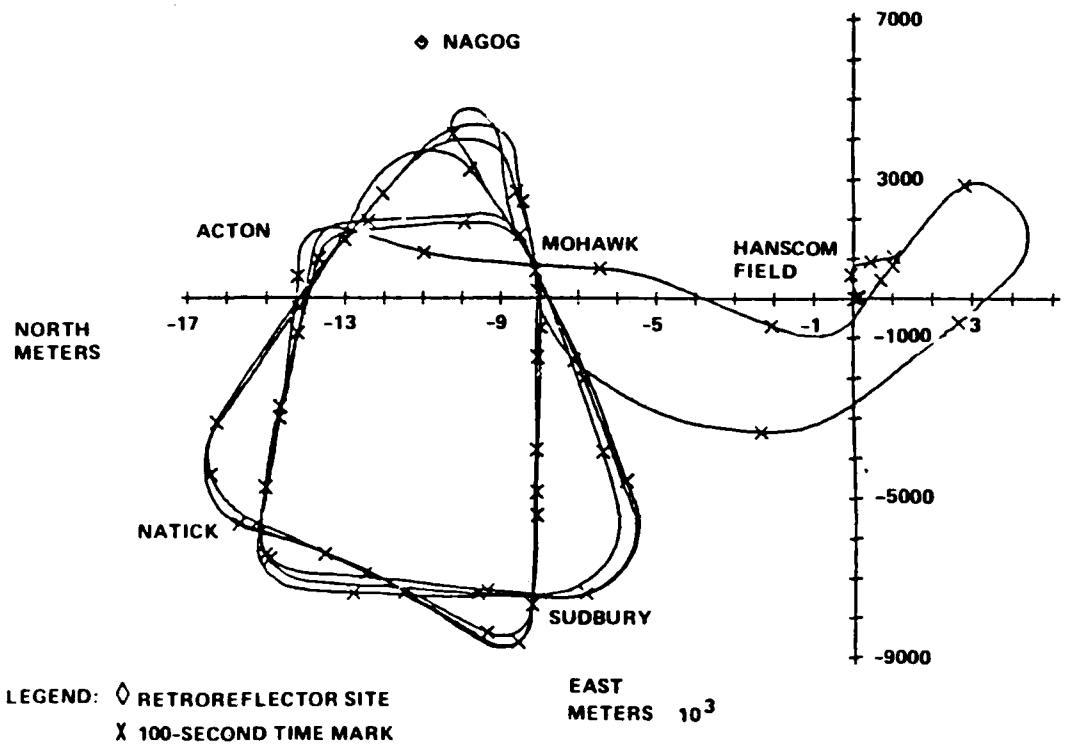

FIGURE 2

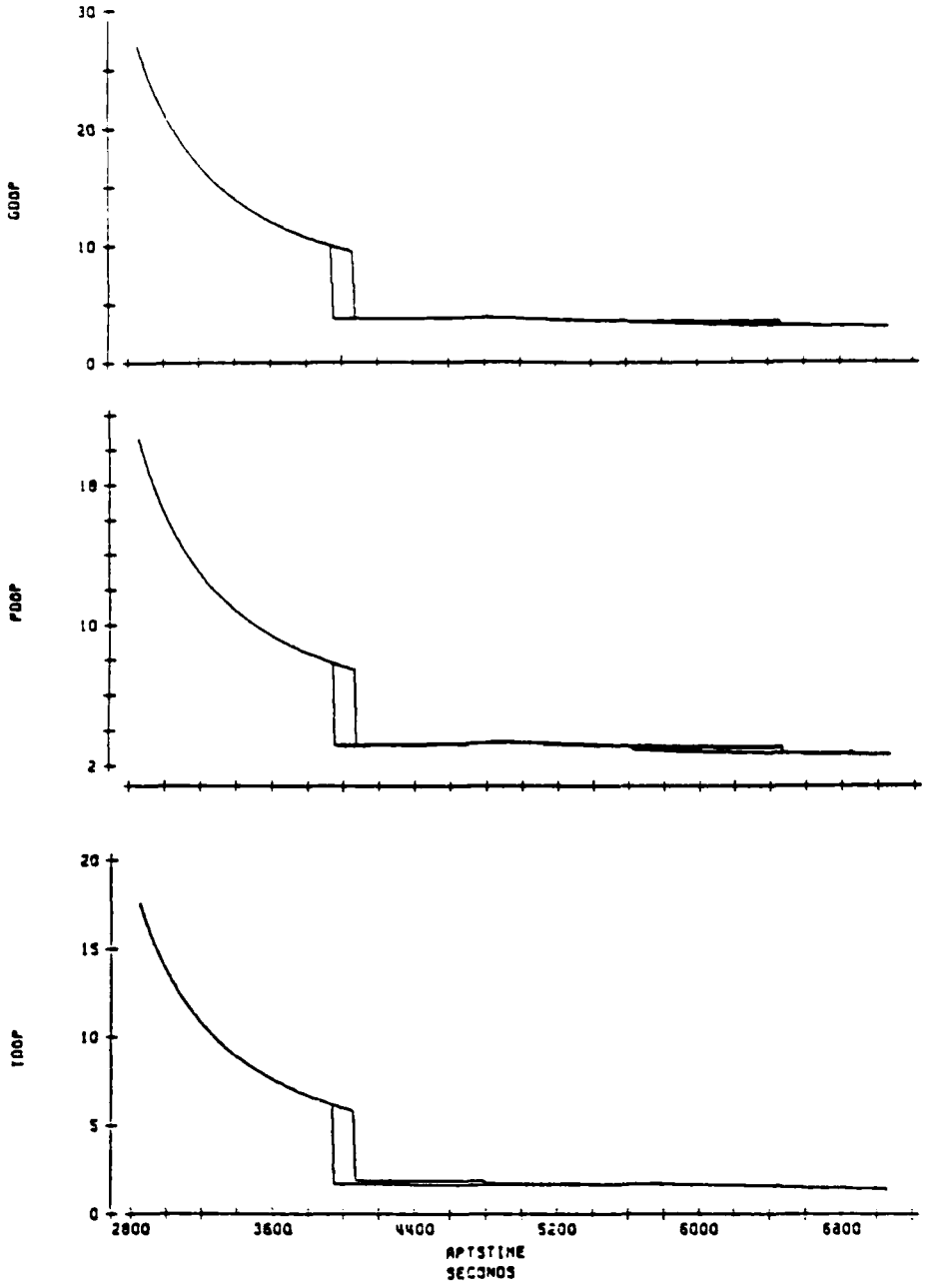

FIGURE 3. TDOP, PDOP, AND GDOP ON MAY 30.

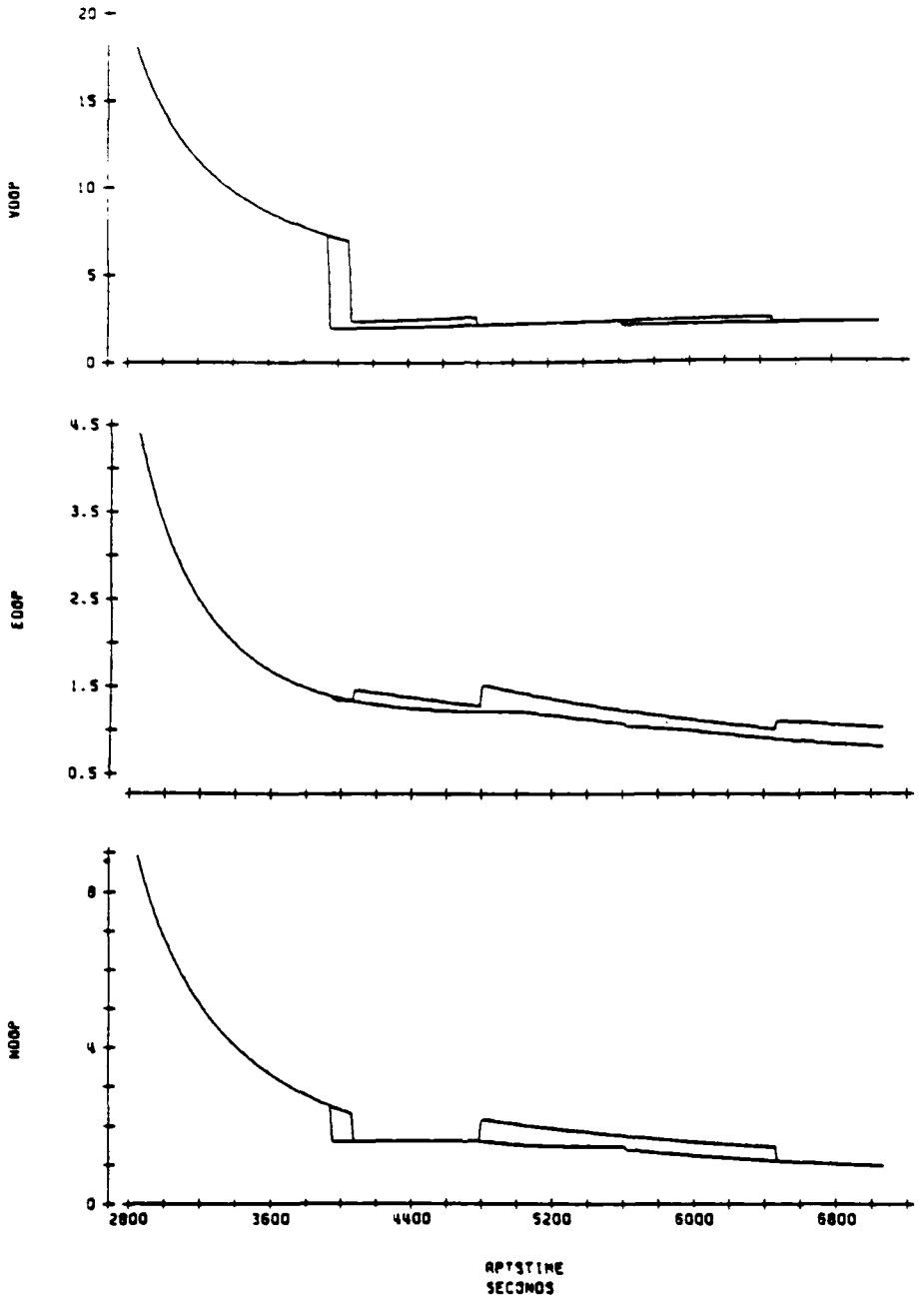

FIGURE 4. NDOP, EDOP, AND VDOP ON MAY 30.

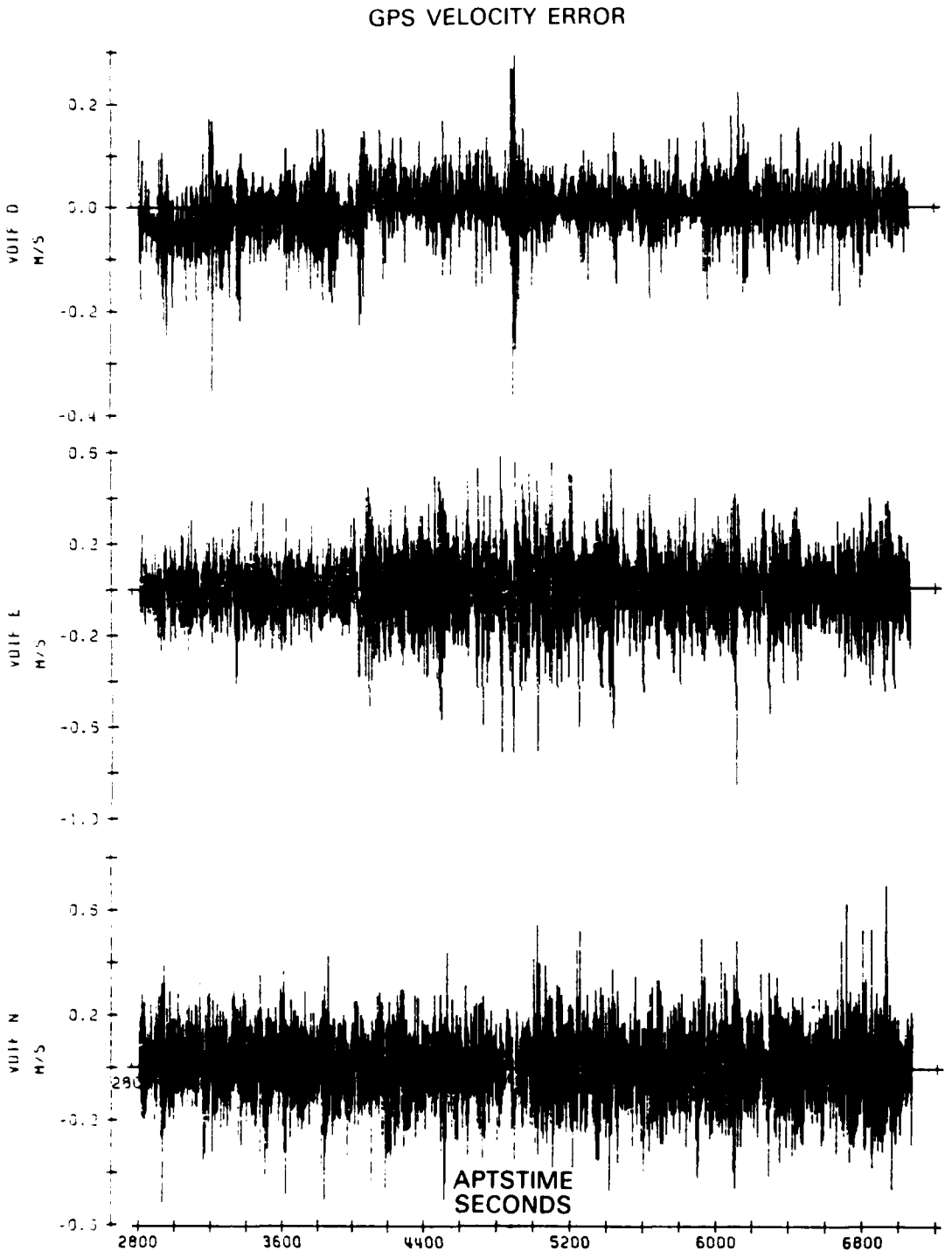
GPS VELOCITY ERROR
VDIF D
M/S
0.2
0.0
-0.2
-0.4
VDIF E
M/S
0.5
0.2
-0.2
-0.5
VDIF N
M/S
0.5
0.2
APTSTIME
SECONDS
2800
3600
4400
5200
6000
6800

FIGURE 5

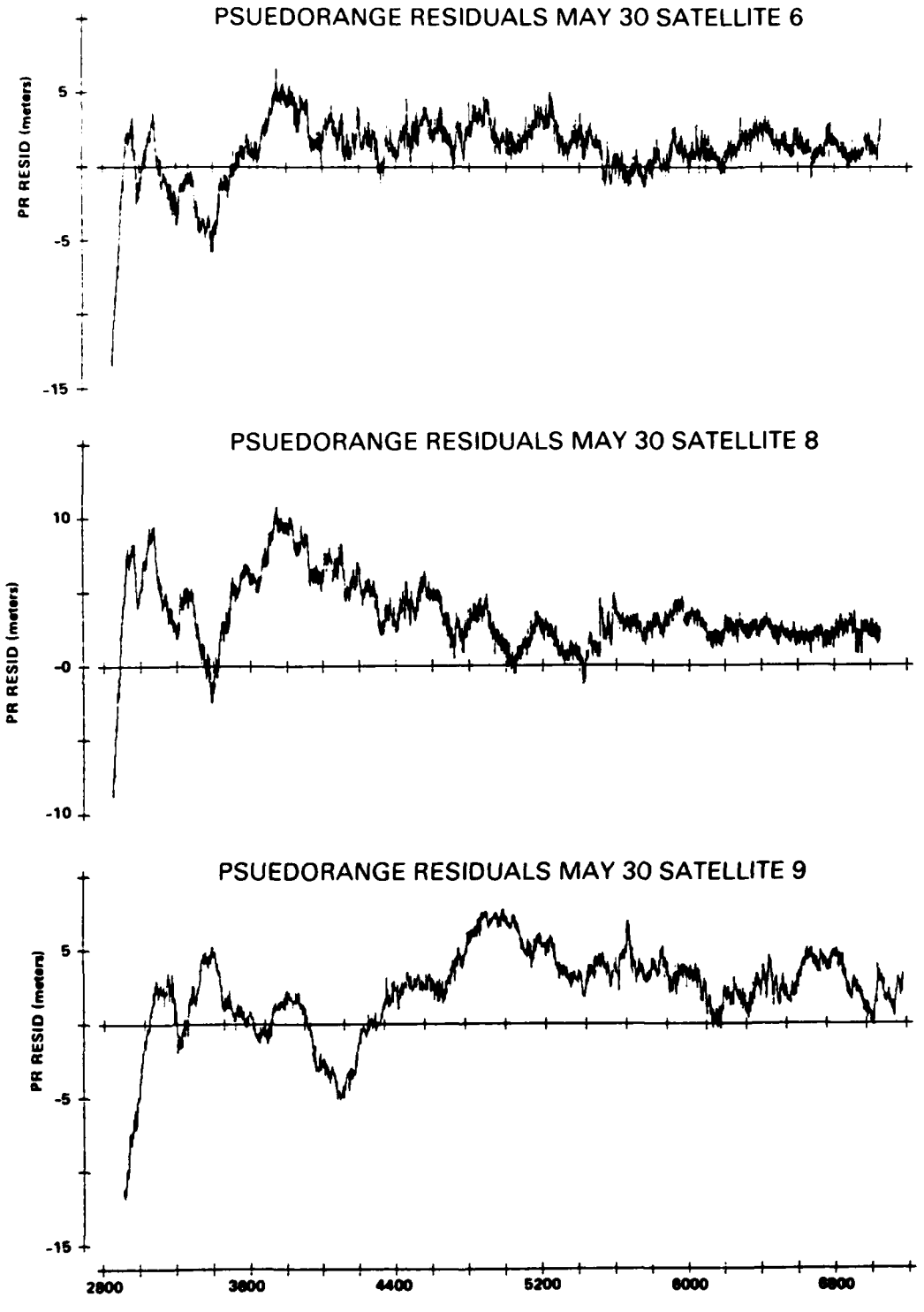
PSUEDORANGE RESIDUALS MAY 30 SATELLITE 6
PR RESID (meters)
5
-5
-15
PSUEDORANGE RESIDUALS MAY 30 SATELLITE 8
PR RESID (meters)
10
-0
-10
PSUEDORANGE RESIDUALS MAY 30 SATELLITE 9
PR RESID (meters)
5
-5
-15
2800
3600
4400
5200
6000
6800

FIGURE 6

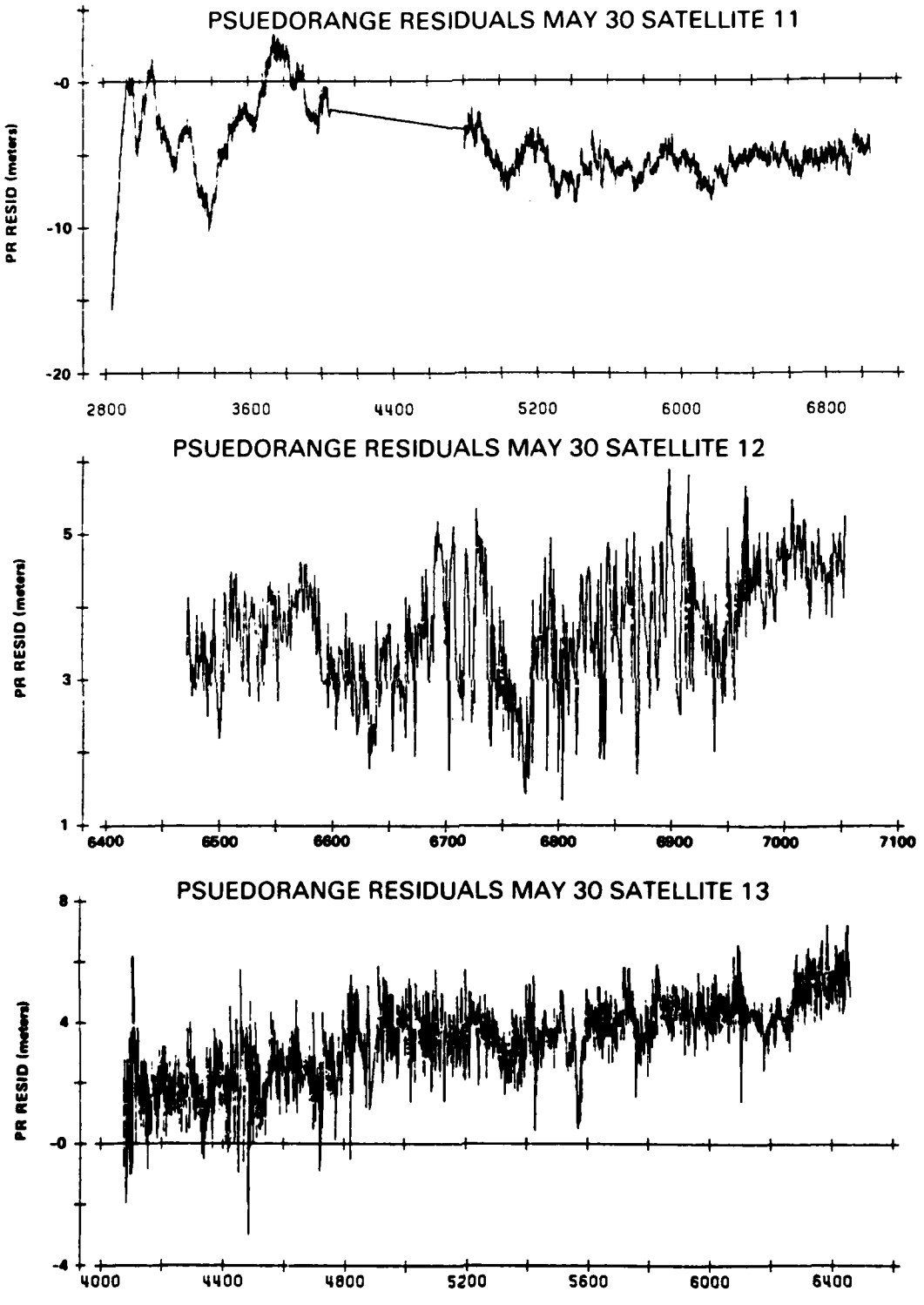
PSUEDORANGE RESIDUALS MAY 30 SATELLITE 11
PR RESID (meters)
-0
-10
-20
2800
3600
4400
5200
6000
6800
PSUEDORANGE RESIDUALS MAY 30 SATELLITE 12
PR RESID (meters)
5
3
1
6400
6500
6600
6700
6800
6900
7000
7100
PSUEDORANGE RESIDUALS MAY 30 SATELLITE 13
PR RESID (meters)
8
4
-0
-4
4000
4400
4800
5200
5600
6000
6400

FIGURE 7

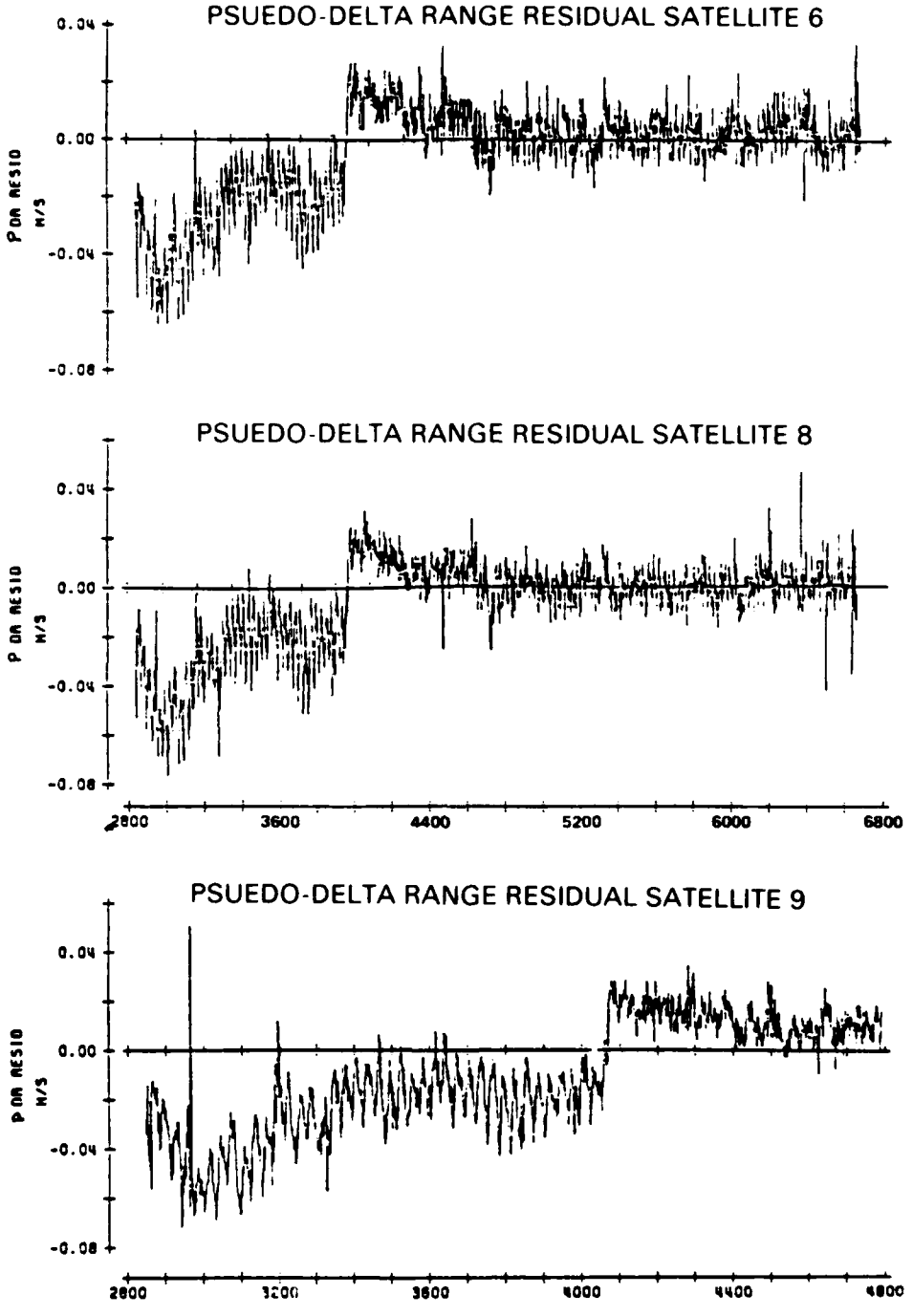
PSUEDO-DELTA RANGE RESIDUAL SATELLITE 6
0.04
0.00
-0.04
-0.08
P DR RESID
M/S
PSUEDO-DELTA RANGE RESIDUAL SATELLITE 8
0.04
0.00
-0.04
-0.08
P DR RESID
M/S
2800
3600
4400
5200
6000
6800
PSUEDO-DELTA RANGE RESIDUAL SATELLITE 9
0.04
0.00
-0.04
-0.08
P DR RESID
M/S
2800
3200
3600
4000
4400
4800

FIGURE 8

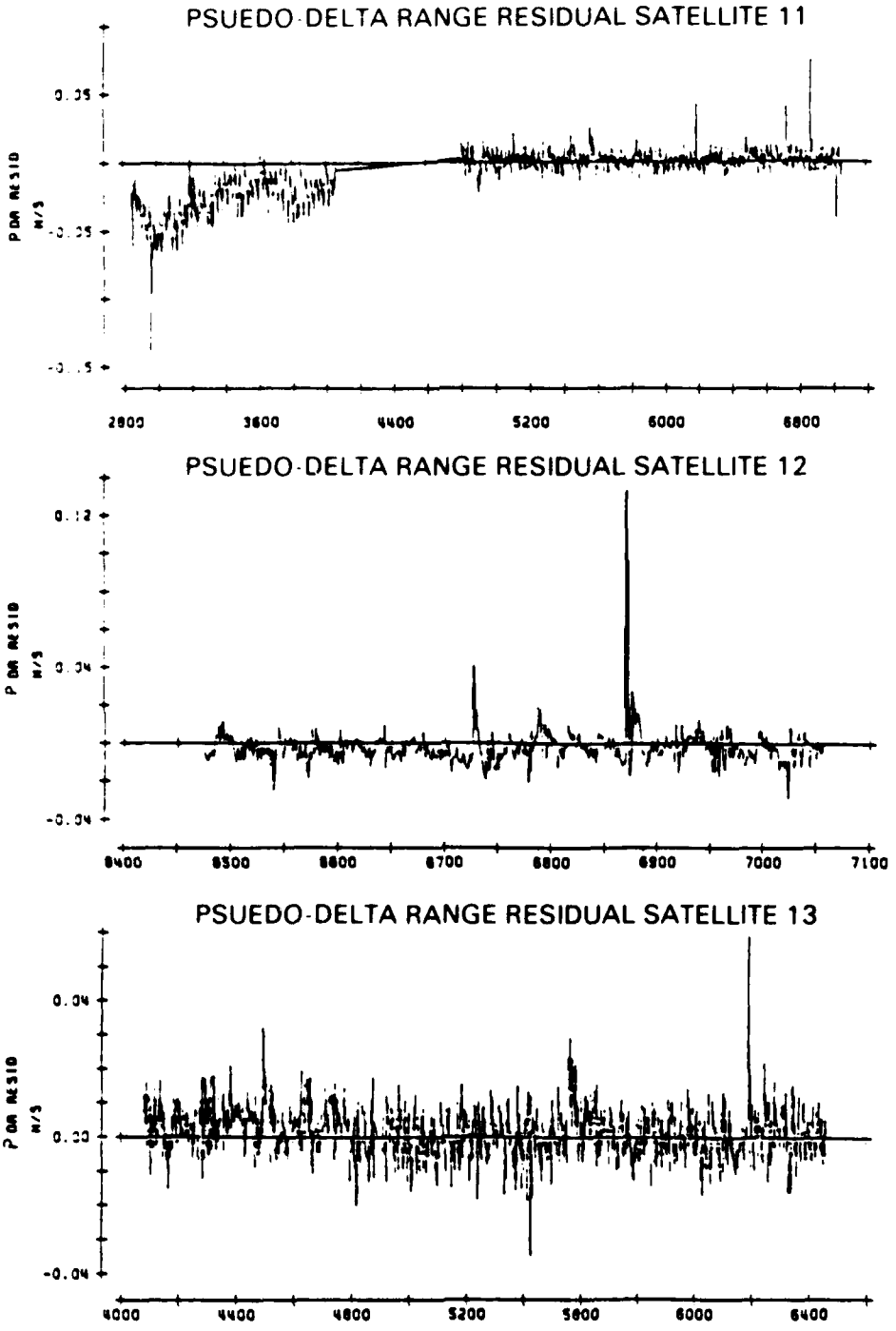
PSUEDO-DELTA RANGE RESIDUAL SATELLITE 11
PDR RESID M/S
0.05
-0.05
-0.15
2800
3600
4400
5200
6000
6800
PSUEDO-DELTA RANGE RESIDUAL SATELLITE 12
PDR RESID M/S
0.12
0.04
-0.04
6400
6500
6600
6700
6800
6900
7000
7100
PSUEDO-DELTA RANGE RESIDUAL SATELLITE 13
PDR RESID M/S
0.04
0.00
-0.04
4000
4400
4800
5200
5600
6000
6400

FIGURE 9

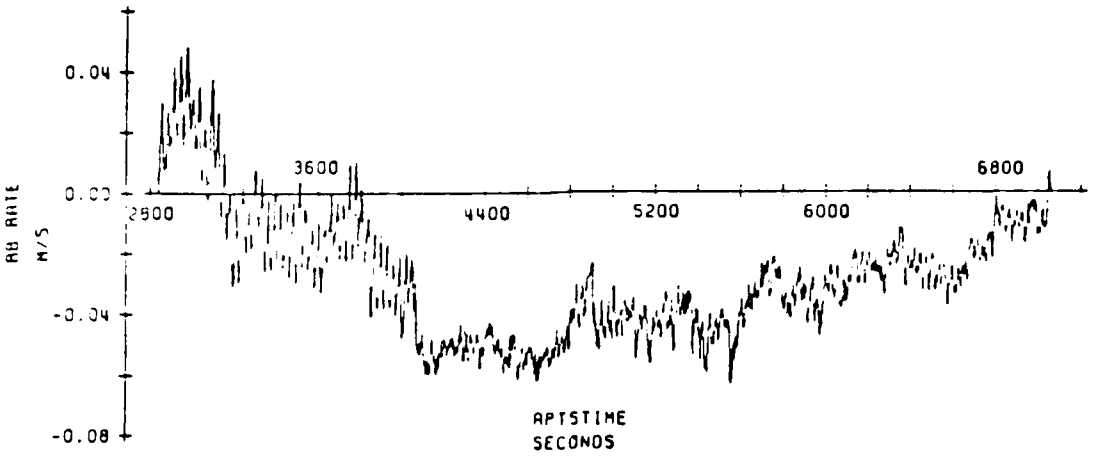

FIGURE 10. 8 RECEIVER ESTIMATE OF USER'S CLOCK DRIFT RATE.

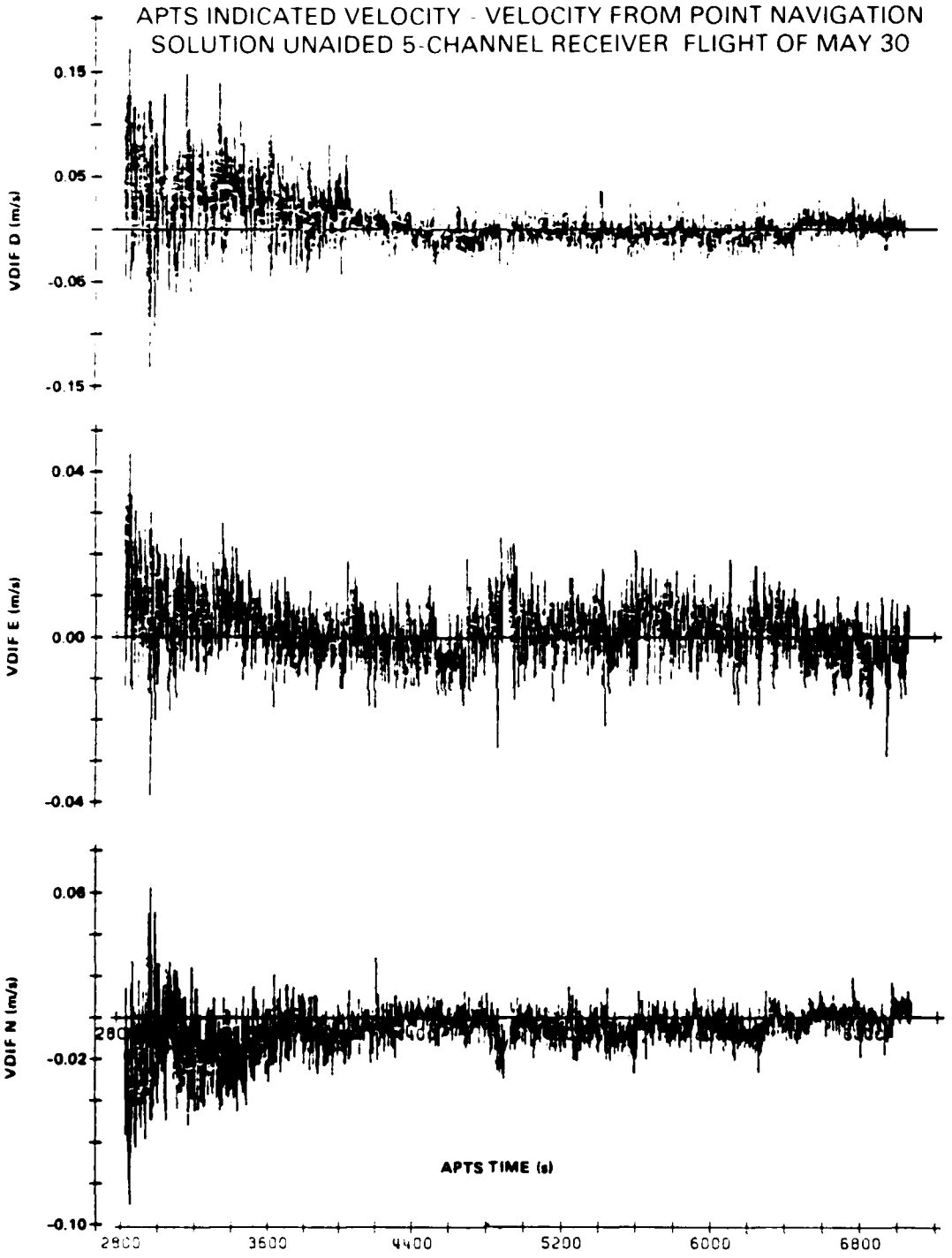
APTS INDICATED VELOCITY - VELOCITY FROM POINT NAVIGATION SOLUTION UNAIDED 5-CHANNEL RECEIVER FLIGHT OF MAY 30
VDIF D (m/s)
0.15
0.05
-0.05
-0.15
VDIF E (m/s)
0.04
0.00
-0.04
VDIF N (m/s)
0.06
-0.02
-0.10
APTS TIME (s)
2800
3600
4400
5200
6000
6800

FIGURE 11

A LOW COST GYROSCOPE FOR GUIDANCE AND STABILISATION UNITS

Author D G Harris - Technical Executive
Guidance Systems Division
GEC Avionics Ltd.,
Airport Works,
Rochester, Kent. ME1 2XX

SUMMARY

The potential requirements for a rugged moderate accuracy low cost gyro are very large, especially in 'smartening' simpler weapons. The paper begins by identifying suitable candidate weapons and deriving a composite specification for gyroscopes that would satisfy the guidance and stabilisation requirements. It then goes on to describe a development programme which is aimed at producing a suitable gyro by the combination of a well established principle for angular rate measurement and the latest materials and electronic techniques. A considerable effort was expended on basic experimental work before prototype batches of gyros were made. Results from test of the later designs show that this approach is very promising, especially in providing gyros which can survive cannon firing without performance degradation. This has been demonstrated by informal tests with potential customers.

The discipline of regular estimates of unit production cost has been firmly maintained to avoid a major pitfall of sub-inertial quality gyro design. However, there are many past projects which bear witness to the fact that this is an unforgiving art and the necessity for continuous attention to detail must be maintained if the START design is to be successfully taken through to mass production.

1. INTRODUCTION

Free flight ballistic or rocket propelled weapons are the most widely procured types because of their comparative simplicity and reliability, and the resultant low cost. The statistical spread in the impact pattern of such weapons is an accepted part of their tactical use. However, for air-to-ground weapons the launching aircraft is required to approach so close to the target using a gently maneouvring trajectory that the vulnerability to ground defences becomes disturbingly high. Hence the demand for 'Smart' weapons which can find and recognise a target, after launch from a comparatively safe range. Weapons of this type that are currently in service are sophisticated and expensive and their application is against high value or strategically crucial targets. If this technique is to be extended to the more numerous weapons for use in an opportunity or low-value target attack, the cost of the guidance and control sub-system must be very low, but this must not be achieved by sacrificing reliability.

A requirement for practically all envisaged weapons is the need to measure or control the attitude during transit and homing. In addition, there may be a need to stabilise a seeker head during search and homing phases. These functions require some form of gyroscope, but the combination of characteristics needed to survive the environment together with the need for very low cost makes the classical spinning mass gyro a very doubtful candidate.

This paper attempts to identify the potential weapon types requiring very low cost guidance and control and derive a performance envelope for the gyroscopes. A candidate which satisfies part of this envelope is currently under development and the principle of operation is described together with test results to date.

2. WEAPON TYPES CONSIDERED

An important factor in reducing the unit cost of sensors is to have a steady high rate of production so that best use can be made of the expensive capital equipment needed. To achieve this it is sensible to look at as wide a range of applications as possible that may have some commonality of requirements to see if a single sensor or small family of sensors can satisfy the range. The primary gyro parameters on which to base commonality of requirements are as follows:

(a) Maximum angular rate to be measured.

(b) Tolerable variation of zero offset from all causes.

(c) Minimum angular rate to be resolved.

(d) Linearity of rate measurement.

The general conditions of use are those associated with military applications but particular attention to the acceleration/shock regime is necessary as this can considerably modify the performance of some gyroscopes.

All gyroscopes take a finite time from power-on to being ready to measure rate and in weapon applications this can be a crucial factor.

In the following paragraphs, various weapon types are considered for their requirements against the parameters listed above, so that a requirement specification with the highest commonality factor can be derived.

2.1 Air-To-Air Short Range Weapons

The main gyro requirement is for seeker head stabilisation and weapon attitude control. The readiness time is less than 1 second and it is likely that the gyro must function throughout the launch acceleration phase. The peak acceleration is unlikely to exceed 50 'g'.

In this application the gyro is essentially an error correcting device and the requirements on linearity and scale factor accuracy are therefore not demanding; a combined effect of 5% is tolerable.

A maximum angular rate capability of 150°/sec will cope with in-flight transients and seeker head slewing needs.

The most important parameters are gyro drift rate and the threshold of angular rate detection. The tolerable gyro offset or drift rate is dependant on flight time and on the basis of a 10 sec duration, the gyro drift rate should be in the range of 0.5 to 1°/sec; A threshold of 0.05°/sec will satisfy a large majority of the air-to-air seeker stabilisation requirements. In this type of application the gyroscope natural frequency is important and for modern small weapons and seekers it is prudent to allow for at least 80Hz capability in the sensor.

In the case of short range air launched dispensers of sub-munitions the above stated requirements generally still apply but with natural frequency and maximum rate requirements reduced by a factor of 3. However, if some degree of guidance into a pre-determined 'basket' is needed, the scale factor and zero offset tolerances are much tighter by a factor of 30 times, at least. Effectively this a different class of gyro.

2.2 Terminally-Guided Sub-munitions (TGSM)

The gyro requirements for TGSM may be for sensor head stabilisation only or also include the need to control and guide the vehicle. The main differences in requirement from 2.1 are shorter start-up time (around 0.1 sec) and greater emphasis on small size and low power consumption. The TGSM electronics is unlikely to be accessible from the carrier vehicle, so that need for routine maintenance of the sensors is very undesirable.

The shorter active flight time of the TGSM allows the requirement for gyro drift to be relaxed to around 3°/sec.

2.3 Artillery-Launched Weapons

On the surface, the requirements for gyros to be used in guided artillery fired weapons appear very different from those for air-to-air or TGSM applications. But many of the performance requirements are similar; rapid start-up, stabilisation accuracies leading to gyro drift rates in the 0.5°/sec region; linear measurement of angular rate in the range up to 500°/sec and low cost, weight and power consumption.

For inputs well outside the linear range the gyro saturation characteristics must be predictable, for use in de-spinning the weapon.

The additional requirements for the guidance components of artillery weapons are the ability to withstand very high acceleration during launch, (up to 20,000 g) possibly combined with angular rates considerably greater than those that the gyro must measure during the guided phase of the trajectory. This applies to spin-stabilised projectiles and the guidance unit is required to survive this initial phase so that it will function normally in the subsequent homing operation.

2.4 Ground-Launched Rocket Propelled Weapons

Many potential weapons in this category have flight time and stabilisation accuracy similar to those for artillery-launched weapons but without the severe environmental regime associated with the artillery launch phase. The gyro which satisfies the needs for artillery weapons is therefore very likely to be usable in rocket propelled guidance and seeker units.

2.5 Longer Flight Duration Weapons

If the flight duration of a weapon is of the order of minutes it is likely to require a comparatively sophisticated navigation and guidance system to enable the positioning accuracy to be good enough for the seeker to acquire the target. The gyro drift tolerance in inertial navigation systems of this accuracy are in the 10 to 100°/hr range; this is a different category from that considered in the weapon types considered so far. There may be a need with the longer range weapons for separate seeker stabilisation which requires less accurate gyros, but even on optimistic estimates this is likely to be a small part of the overall demand for the lower grade of weapon gyro.

3. SPECIFICATION FOR WIDE APPLICATION GYRO

Some of the applications considered in section 2 will materialise only if gyros in the $250 to $500 price range are available. This level of price will be attained only if the gyros are made in large quantities with a high throughput. It is therefore necessary to seek the widest market that can be open to a gyro or closely related family of gyros if the benefit of mass production is to be realised.

If the widest common factors are extracted from the stabilisation and short term guidance requirements for the weapon types covered in section 2 the following requirements specification is obtained.

3.1 Reaction Time

This value is governed by the shortest time requirement. Essentially this time should be so short that it does not noticeably delay the launch of a weapon fired on an opportunity basis. A practical range for this is 0.1 to 0.25 seconds. The particular parameter which must be either stable or predictable after this time is the gyro rate offset or drift.

3.2 Power Consumption

A small power consumption is necessary for two reasons. First, high power dissipation in a small gyro rapidly leads to thermal gradients which produce variable performance. Second, small weapons carry small capacity power sources, to maximise payload; therefore the consumption of all electronic components must be strictly controlled to a low value.

The choice of this value for a gyro is a little arbitrary but to show an improvement on currently available devices a value of 1 watt maximum, including control electronics, is chosen.

3.3 Linearity and Stability of Scale Factor

In many applications a closely controlled input/output ratio is not a vital requirement and a value of 1% of full scale covers the large majority. It is possible that this parameter could be used to select gyros from a common production line, into wide and narrow tolerance groups, as the wide tolerance applications are likely to predominate.

This performance must be maintained over a minimum range of $\pm$ 500°/sec. It is desirable that the range can be extended to $\pm$ 1000°/sec for use in de-spinning operation.

3.4 Gyro Output Offset or Drift Rate

This is one of more important parameters and is notoriously variable in most low-cost gyros. Values measured during production test may change radically with temperature, acceleration and shelf life. A drift uncertainty of 0.5°/sec 1 sigma from all causes is needed for many of the applications of section 2. A practical approach to achieving this value is to reduce the effects of acceleration and shelf life on drift variation and aim for a predictable temperature coefficient of drift. The inclusion of a means for measuring the sensor temperature then makes electronic compensation possible, with little effect on cost.

3.5 Rate Threshold

For applications involving short flight time high speed projectiles, the occasions when a gyro is required to detect a sustained period of very low rotation rate are rare. In these circumstances it is sensible to relate the threshold rate that the gyro will detect to the drift uncertainty. A threshold of 0.1°/sec will contribute an angular error of 20% of that due to drift offset and this is an achievable compromise.

3.6 Natural Frequency of Gyro

It is desirable in some applications to be able to limit the natural frequency of the guidance sensors to prevent them responding to an unavoidable vibration. But for seeker stabilisation purposes a frequency up to 80Hz is desirable especially for the smaller low inertia units. To cater for the widest range of applications it is necessary to have a basic sensor with a high (80Hz) capability which can be easily reduced, preferably by electronic means.

3.7 Summary of Specification

The preceding parts of section 3 have outlined the reasons for the choice of the various gyro parameters. These are summarised in the following table.

The gyro must be capable of surviving the normal environmental conditions for military equipment and in particular the design must survive acceleration of at least 10,000 g and preferably 20,000 g if this does not involve a cost penalty.

PARAMETER	VALUE
Price	$250 to $500
Reaction Time	Less than 0.1 secs
Power Consumption	Less than 1 watt
Linearity and Scale Factor	1% to 5% (by selection)
Drift Offset	Less than 0.5°/sec
Threshold	Less than 0.1°/sec
Natural Frequency	Variable; 10Hz to 80Hz
Measurement Range	> 500°/sec

4. THE 'START' GYRO

There are many techniques available for measuring angular rate and these were considered at GEC Avionics as ways of meeting all of the above requirements in a single sensor. The most promising method is that based on sensing the shift in the nodal pattern of a vibrating structure, when it is rotated.

The principle is not new and the objective is to use modern materials technology to make a low cost moderately stable mechanical sensor and use electronic methods to compensate for parameter variations which are costly to avoid in the mechanics. The requirements for ruggedness, low power and rapid readiness are principal drivers in the choice of technique.

As the gyro does not use rotating parts and all the electronics including vibration drivers use semi-conductor material the acronym START (Solid sTate Angular Rate Transducer) is used to identify it.

4.1 Principle of Operation

Fig. 1 shows the schematic arrangement for START. The vibrating element is a cylinder, chosen for its symmetry about the axis of measurement. The vibration pattern is established using piezo electric transducers AA and BB in a phase locked loop. The full circle is the cylinder outline when at rest. The two dotted outlines show the limits of the vibration pattern. The choice of high efficiency transducers and low loss material for the cylinder results in a very small power requirement to sustain the oscillation, approx 10 mW. Positioned mid-way between the A and B transducers are piezo electric crystals CC which are ideally on the vibration nodes of the cylinder when it is not rotating. The oscillatory strain in the cylinder at the C transducers is measured by phase sensitively detecting their outputs with respect to the oscillation at AA. When the cylinder rotates about its principal axis, the nodes tend to rotate away from the 'C' positions by an angle related to the angular rate. The oscillatory strain in the cylinder at points C is therefore a measure of the angular rate about the cylinder axis and this is directly indicated by the output of the phase sensitive detector.

This basic scheme works satisfactorily for steady angular rates but has a very narrow bandwidth when varying rates are applied and the response is poorly damped. The function of the DD driver transducers is to feedback an amplified, frequency dependent version of the envelope of the signal at the points C. The frequency response of the electronics in this feed-back loop determines the natural frequency and damping of the gyro response and the gain in the pass-band is sufficiently high that the signal level at the C transducers is limited to the linear region of operation. Therefore the natural frequency and damping can be controlled entirely electronically, one of the desirable characteristics identified in section 3.

In such an arrangement the maximum linearly detected angular rate is determined by the physical dimensions of the cylinder and the sensitivity of the transducers. The maximum linearly indicated output is determined by the amplification applied to the output of the phase sensitively detected form of the D transducer drive. Therefore the gyro scale factor in degrees/sec per volt can be varied widely without changing any cylinder characteristics.

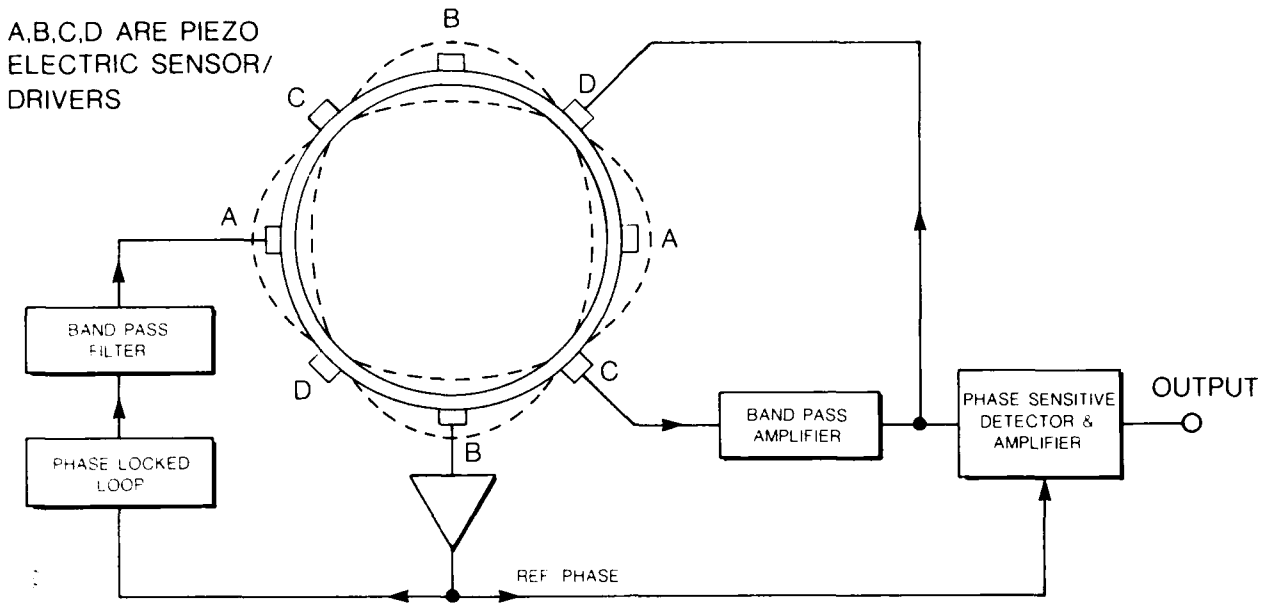

Fig. 1 'START' Gyro Scheme of Operation

The detection threshold is theoretically very low but in practice it is determined by the signal/noise ratio at the C transducers.

Gyro offset and offset stability is a more complex problem dependent on geometric accuracy of the cylinder/transducer assembly, the thermal characteristics of the materials and the stability of the electronic circuit parameters.

A detailed treatment of the theory of operation of the 'START' gyro is given in reference 1.

5 DEVELOPMENT PROGRAMME

Research and development for START has been continuous since early 1980 and the main features of the programme are outlined in this section.

5.1 Conceptual Work

The principle of the vibrating element angular rate sensor was well established when the START project began. The initial theoretical work at GEC Avionics was aimed at choosing a shape which is robust, easily made yet low in spurious output induced by linear acceleration. Calculations indicated that a cylinder supported at one end would satisfy these requirements and the size, weight and power consumption of a gyro to detect angular rates up to 1000°/sec were assessed. The results were sufficiently encouraging to proceed to the stage of experimental models to verify the study results. This work was carried out by the Avionics Research Laboratories of GEC Avionics. Interest in continuing this work was shown by potential users of the gyro and support for further development was provided by the Royal Aircraft Establishment (RAE) during 1983 and 84. In addition to continuing the work on design and performance analysis, experimental gyros were made using different materials for the cylinder and various techniques for aligning and affixing the piezo electric transducers. A major objective of this phase was the reduction of the inevitable variation of gyro offset and scale factor with temperature, to an acceptable level of predictability.

In early 1984 GEC decided to begin detailed engineering development of START aimed at the type of applications described in section 3. This resulted in the prime responsibility for START being transferred to the gyro manufacturing division of GEC Avionics, now Guidance Systems Division, with continuing close support from the Research Labs.

5.2 Development Phase

Low cost of manufacture was a requirement for START from the outset and it is a feature of the development programme that all changes of methods or materials are considered first for their impact in the cost of mass production.

The earlier work showed that it is preferable to use metallic materials for the cylinder. This can give rise to a sensitivity to temperature variation when the transducer/cylinder temperature coefficients of expansion differ markedly. Various combinations of materials and bonding techniques have been tried and 80 experimental

cylinders have been made, in batches of ten. In this way an initial assessment of the variation of the main characteristics is obtained, for each design variant.

The control electronics was initially designed using discrete components, ruggedly mounted on a printed circuit board. The final version will be a single hybrid, which could be integral with the sensing cylinder, and the design of this hybrid is now underway.

Photographs of the prototype gyros and typical discrete component electronic unit are shown in Figs. 2, 3 and 4.

Fig. 2 'START' Gyro Sensor Unit and Cover

Fig. 3 'START' Gyro Triad

Fig. 4 'START' Gyro Electronics Development Unit using Discrete Components

6 ACHIEVEMENT TO-DATE

The technical requirements for the electronics did not call for real innovation, and emphasis has concentrated on economy of power consumption and selection of techniques for ease of eventual hybrid packaging.

Most of the effort has been directed to selecting the best design for the sensing unit. The earlier batches had a modest yield of fully usable gyros and the experience gained enabled a high yield to be obtained from the later batches. The results summarised here are for the latest design.

6.1 Dimensions and Weight

The maximum rate capability is determined by the cylinder design and a unit with overall dimensions of 24mm diameter by 28mm length has demonstrated linear performance to a minimum rate of 1000°/sec. The weight of the mechanical part is 25gm; with a hybrid weight estimated as 20gm the estimate for the complete gyro weight is 45gm.

6.2 Power Consumption

Power consumption for the discrete component version is 0.5 watts. The hybrid version will be less than this.

6.3 Rate Threshold

The threshold of rate measurement is determined by the particular cylinder/transducer combination and the power applied to the excitation transducers. A value of 0.03°/sec is currently achieved. As the output of the gyro is a d.c. analogue voltage, detection of the threshold output needs careful attention to electrical noise reduction if the amplification is chosen for 10V (maximum output) at 1000°/sec.

6.4 Linearity

Throughout the development of START all of the designs have shown good linearity for this grade of gyro. The inherent linearity of the technique has been shown to be better than 0.5%, but variation of offset and scale factor with temperature make measurements below this value rather uncertain, so that 0.5% is a practical value to use in system design. A typical input/output result is shown in Fig. 5.

6.5 Scale Factor

The output of the pick-off (C) transducers is determined by the cylinder geometry, the transducer sensitivity and the level of oscillatory drive applied at the 'A' transducers. The intention is to fix these factors for a wide range of applications and use electronic amplification to vary the scale factor in volts/degree/sec. This can be achieved by changing the value of a single resistor in the electronic hybrid. The maximum linear output is 10V d.c. and the corresponding angular rate can be chosen to lie between 100°/sec and 1000°/sec by suitable choice of amplification. For increases in rate beyond the electronic saturation value of 12V, the output voltage remains constant.

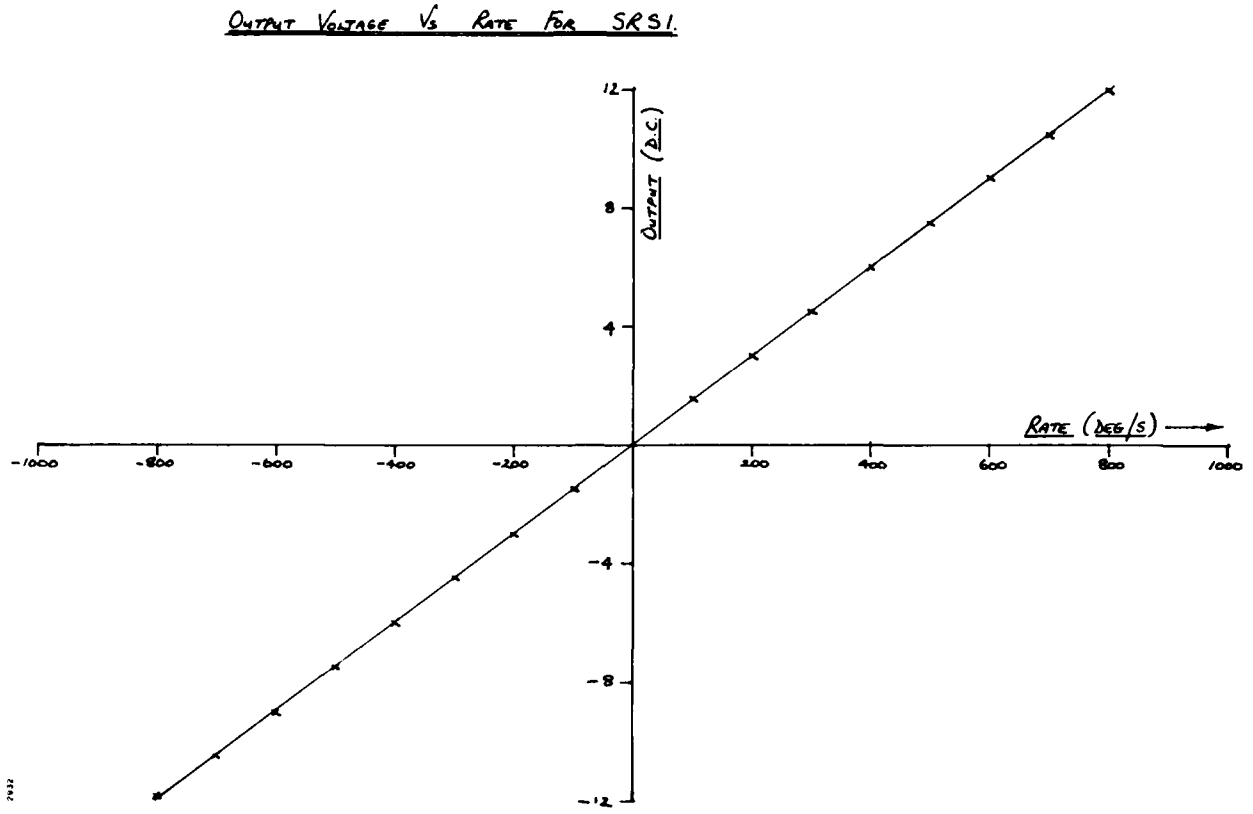

Fig. 5 Input/Output Characteristic

Large variation of scale factor with temperature is a potential problem with this type of gyro. The dominant source of this variation lies in any mismatch of the thermal and mechanical characteristics of the materials of the cylinder and piezo-electric transducers. Considerable effort has gone into surveying the range of materials available and choosing pairs to minimise mismatch. The remaining variation of scale factor with temperature can be, at least partially, compensated by use of a simple temperature sensor, in the gyro. Currently achieved performance is a variation of 5% over the temperature range -40°C to +80°C.

6.6 Natural Frequency and Damping Factor

The characteristics of the bandpass amplifier between the 'C' and 'D' transducers govern the bandwidth and damping of a gyro. As high natural frequency is often needed in missile use, experiments were made to discover the maximum practical bandwidth for the present design. A value of 90Hz was obtained stably, with a damping factor of around the critical norm of 0.7. Both natural frequency and degree of damping can be changed in a batch of gyros, by modifying the hybrid design, without changing the basic sensor.

6.7 Zero-Offset or Bias

Two aspects of the bias need to be controlled by choice of materials in the sensor unit. These are actual bias at a nominated temperature and variation of the bias as the temperature changes. Each gyro can be trimmed to bring the nominal bias within a specified range but this operation must be minimised as it adds to the cost of manufacture. Trimming to a value within the range $\pm 2°$/sec has been achieved regularly and a means has been designed for doing this automatically as part of the manufacturing process.

The variation of bias with temperature is dependent on the choice of materials and manufacturing tolerances. The later designs have a total variation of 10°/sec over the range -40°C to +80°C. For weapons launched from a stable (non-rotating) platform this offset variation can be simply backed-off at launch and the gyro performs linearly about the new zero.

For use where the launch platform is moving during gyro start-up it is desirable to reduce this total variation to a value around 1 to 2°/sec, either by compensating the variation in the electronics or reducing the basic temperature sensitivity. A combination of the two methods is being pursued.

6.8 Start-Up Time

With the present discrete electronics the time for the output voltage to stabilise after switch-on is approx 0.5 secs. However much of this is taken up for stabilisation of the circuit values. The cylinder vibration pattern can be established in less than 100m secs and the design of the hybrid circuit allows the complete gyro to stabilise in this time.

6.9 Sensitivity to Acceleration

Two aspects of g sensitivity have been investigated. The first is the effect of linear acceleration on the gyro output or g sensitive drift. The second aspect is the acceleration survival level, of interest in cannon launched weapons.

The g-sensitive drift is very small so that high speed centrifuge tests were necessary to produce measurable outputs. Because of uncertainty of coupling in of angular rates from the table it is possible to estimate the maximum of g sensitive drift value only. This is 0.05°/sec/g. This is along an axis perpendicular to the rate sensing axis. Acceleration survival tests were carried out on the gyro sensor element at increasing nominal levels of 5000, 8000 and 20,000g. In each case two sensors were used, mounted so that the acceleration effects along and perpendicular to the sensing axis were tested. The units were recovered after the tests and tested for damage or change in characteristics. All gyros survived the tests and changes in performance before and after the shock tests were within the normal spread of measurements. In a recent test, the START gyro survived 25,000 g.

Vibration tests were carried out using a 10g peak level up to 9kHz. No measurable change of output was caused by this environment.

REFERENCES

1 The Vibrating Cylinder Gyro
Dr R LANGDON
Marconi Review 1982
Vol 45 pp 231-249

JOINT DEVELOPMENT OF THE MULTI-FUNCTION INTEGRATED INERTIAL SENSOR ASSEMBLY (MIISA)

Jack Jankovitz
NAVAIRDEVCEN Code 4011
Warminster, PA 18974

David Krasnjanski
NAVAIRDEVCEN Code 4011
Warminster, PA 18974

Andrew S. Glista, Jr.
NAVAIRSYSCOM - AIR-933E
Washington, D.C. 20361

ABSTRACT

The U.S. Navy, Air Force and Army are in the process of formalizing the joint service development and flight evaluation of the Multi-Function Integrated Inertial Sensor Assembly (MIISA). The MIISA concept will provide a reliable, standardized, fault-tolerant, system which will serve as a common source of inertial data. MIISA will provide data for flight control, navigation, weapon delivery, automatic terrain following/terrain avoidance, sensor/tracker stabilization, flight instruments, and displays. A primary goal of this joint service activity is to resolve all technical issues and make this capability available for the next generation fighter and attack aircraft and for advanced helicopters.

The MIISA program is based on the coordination of current independent exploratory and advanced development projects. The principal efforts are the Navy's IISA (Integrated Inertial Sensor Assembly) program, the IIRA (Integrated Inertial Reference Assembly) program conducted by the Air Force, and the Hi-Rel IRU (High Reliabilty Inertial Reference Unit) program of the Army.

The Navy program to design, build, and evaluate an IISA Advanced Development Model was begun in FY80, and delivery of the equipment for Government DT&E is scheduled for Oct 1986. The IISA development uses high reliability laser gyro and accelerometer sensors packaged in a strapdown system configuration to provide a common, efficient source of aircraft body rates, attitude, and accelerations. These measurements provide the essential inertial data inputs for all core and mission avionic functions including stability and control augmentation, precision weapon delivery/fire control, and sensor stabilization for precision pointing and tracking.

Various design aspects in IISA using six ring-laser gyros and six inertial-grade accelerometers in two, separated clusters are described. The redundancy management mechanization and system design features for flight safety are given. Navigation performance limits of strapdown INS, including the effects of skewed sensors, are presented.

To insure that IISA is suitable for installation and flight test in an Air-Force F-15, extensive laboratory testing will be undertaken at the NAVAIRDEVCEN Strapdown Navigation Laboratory. These tests involve the examination of IISA system performance for navigation and flight control. These tests are discussed in the paper.

INTRODUCTION

Military aircraft require inertial sensor data for navigation, flight control, weapon delivery and targeting, sensor/tracker stabilization and cockpit display. Currently, these data are obtained from a multiplicity of independent onboard reference systems which provide the necessary data but contribute significantly to the size, weight and cost of the aircraft.

It is desirable, therefore, to eliminate these duplicative inertial sensors by consolidating their functions into one integrated inertial system. Furthermore, it is desirable that this one integrated inertial system produce all the inertial data parameters required by the aircraft with equal or better accuracy, increased functional reliability and survivability, and lower life cycle costs compared to conventional avionics system implementations.

The multiplicity of independent onboard reference system is a problem faced by all services. For example, the Navy's F-14 and F-18 aircraft each possess in excess of sixteen gyros and accelerometers installed in various locations on the aircraft. Similarly, the Air Force's F-15 and F-16 aircraft contain many gyros and accelerometers to provide various data required for their missions.

In order to eliminate the proliferation of these inertial sensors for the next generation aircraft and helicopters it was in the interest of the services to establish a joint program to develop and produce standardized fault tolerant, reliable hardware to provide all the data requirements for these advanced aircraft and helicopters. This joint program is known as the Multi-Function Integrated Inertial Sensor Assembly (MIISA) Program. (1)

The MIISA program is based on the coordination of current independent exploratory and advanced development projects. The principal efforts are the Navy's IISA (Integrated Inertial Sensor Assembly) program, the IIRA (Integrated Inertial Reference Assembly) program conducted by the Air Force, and the Hi-Rel IRU (High Reliability Inertial Reference Unit) Program of the Army.

The Navy program to design, build and evaluate an IISA Advanced Development Model (ADM) was begun in FY80, and delivery of the equipment to the Government is scheduled for Oct. 1986. An extensive test and evaluation program will then commence.

The IISA test and evaluation has become part of the MIISA program, the latter comprising four phases.

The first phase of the program, the IISA/ABICS (Ada Based Integrated Control System) Flight Control Evaluation, is underway. It will accomplish a flight control proof-of-concept demonstration of the IISA-configured sensors for fault tolerant flight control and facilitate completion of the ABICS program goals for Ada implementation in advanced integrated flight control systems.

The IISA/ABICS Flight Control Evaluation involves the installation of IISA into the F-15 aircraft and its integration with the F-15's Digital Electronics Flight Control System (DEFCS) by using the Ada High Order Language (HOL). The objectives of the flight test are to verify IISA air worthiness, to compare and evaluate IISA flying qualities with the flying qualities of the basic F-15, to verify proper redundancy management operation, to verify that the IISA sensors are of navigation quality and last but not least, to verify the efficiency and adequacy of Ada HOL. The IISA/ABICS Flight Control Evaluation

Phase will be preceded by laboratory test of IISA at the Naval Air Development Center's (NADC's) Strapdown System Evaluation Laboratory (SSEL). The laboratory tests of IISA to prove both navigation and flight control are discussed in detail below.

The second phase of the MIISA program is known as the Integrated Inertial Reference Development and Flight Evaluation. Conducted in parallel with the IISA/ABICS integration and flight trials, this effort will investigate and evaluate alternative system integration/implementation mechanization for MIISA. The objective of this joint phase is to develop an Integrated Inertial Reference System (IIRS) for the 1990's incorporating an IIRS with other sensors. Other sensors to be incorporated include Integrated Communications, Navigation, Identification Avionics (ICNIA), Global Positioning System (GPS) and relative navigation function of Joint Tactical Information Distribution System (JTIDS RELNAV), Ultra Reliable Radar (URR), Synthetic Aperture Radar function (SAR), Forward Looking Infra Red (FLIR), Integrated Terrain Access/Retrieval System (ITARS), radar/laser altimeters, and air data sensors.

Since Phase I will address most of the flight control integration issues, the second phase effort will concentrate mostly on navigation reference functions. Flight control functions will be treated as integration issues. Special concerns in the second phase will be fast reaction time, high-accuracy ground/ship and in-air alignment, close coupling between the inertial system and Global Positioning System receiver for jam resistance, accurate velocity/angular referencing for Synthetic Aperture Radar operation and Terrain Following/ Terrain Avoidance (TF/TA) operation.

The second phase will demonstrate the feasibility of interfacing an Integrated Inertial Reference System with an advanced avionics system of the 1990's. The resulting design criteria will provide a basis for joint service decisions relating to a standardized sytem, namely MIISA.

The 3rd phase of the MIISA program will address inertial sensing requirements for helicopters. Inertial sensing requirements for the next generation of tactical helicopters dictate a highly reliable, low cost, light weight sensor and processing suite that will provide aircraft data for navigation, flight control and weapon direction. Accuracy, ballistic vulnerability, size, weight and power constraints are different for the tactical helicopter as compared to the fixed-wing fighter. However, these dissimilarities should not preclude significant technology transfer in the areas of sensor technology and redundancy management software. This phase will assure that the technology transfer is maximized.

Based on the evaluation results from prior phases, an Engineering Prototype Model will be generated in the final phase. The hardware/software configuration is to have the widest possible application span across aircraft of the three services. Operational performance and logistic supportability characteristics will be tested and verified. Results will generate performance specification requirements for use by the services.

IISA SYSTEM DESCRIPTION

The Advanced Development Model (ADM) version of IISA has been designed by Litton under contract with NADC for concept evaluation in the laboratory and in high performance fighter/attack aircraft. The IISA-ADM (Figure 1) consists of five assemblies: two identical Inertial Navigation Assemblies (INA's) containing the inertial sensors and navigation computers; two identical Digital Computer Assemblies (DCA's) each containing dual redundant flight control redundancy management and sensor selection logic computers; and a Collins multi-function Control Display Unit (CDU) for displaying IISA data and providing the operator interface for initialization, mode selection, insertion of simulated failure data and execution of simulated failures. The IISA-ADM also includes a set of Ground Support Equipment (GSE) that allows all IISA outputs to be monitored. The GSE contains a Hewlett-Packard 9836 (HP 9836) desk top computer with software for IISA signal interrogation and display. The GSE also includes a bank of six digital to analog (D/A) converters to convert selected IISA flight control outputs to analog form for analog display purposes. A DMA (Direct Memory Access) capability is provided for any INA or DCA computer/processor for special signal monitoring via the HP 9836.

Within an INA, sensor axes are orthogonal but skewed relative to the aircraft yaw axis (see Figure 2). One accelerometer and one ring laser gyro in an INA are oriented along each skewed axis. Figure 2 depicts the orientation of axes when the INAs are installed into the equipment bays of the aircraft. When one INA is installed into the right equipment bay, with 180° rotation about yaw relative to the identical left INA, the six sensor axes are then distributed uniformly about a 54.7° half-angle cone. No two axes are coincident, nor are three in the same plane. Thus, any three sensors may be used to derive three-axis outputs in aircraft axes after suitable computer transformation.

An INA is divided into three, largely independent channels as shown in Figure 3. Each channel contains data form one gyro and one accelerometer plus related electronics, a preprocessor, provisions for output of data to the FCS and to the navigation computer, and independent power supplies. The navigation processor and its MIL-STD-1553B I/O are on the same power supply with one of the three sensor pair channels.

The three channels of electronics are physically separated to eliminate common failure modes. Wiring from the sensors to the sensor electronics is also kept physically separated to avoid short-circuit, EMI, etc., failure modes common to two channels.

NAVIGATION PERFORMANCE REQUIREMENTS

The navigation performance requirements for IISA are similar to general, medium accuracy systems currently in inventory. Requirements are:

Radial position error rate	1 nmi/hr (1.852 km/hr) (CEP)
Velocity errors, per axis	3 ft/sec (91.44 cm/sec) (rms)
Reaction time	5 minutes

Errors of strapdown inertial sensor systems using ring laser gyros become strongly dependent upon gyro scale factor and axis alignment errors (2). Ring laser gyros can maintain excellent scale factor stability. Achieving the 1-2 arc second axis alignment stability needed, if a significant portion of flights is to contain terrain avoidance and evasive maneuvering, requires very careful design. On IISA, material selection and structural rigidity between gyros has been determined primarily to meet this difficult requirement.

Skewing of accelerometer axes requires that accelerometer scale factor stability be significantly better than for a nonskewed configuration. An accuracy requirement of 35 ppm scale factor tracking between the three accelerometers is within the state-of-the-art and the requirement for IISA.

Performance during vibration is essentially the same for skewed and unskewed sensors. As described in (2), gyro input axis bending is the major error source for strapdown navigators in a vibration environment. Vibration levels at the INS mounting points are usually not known. Environmental test levels tend to be very unrealistic, over-conservative in the high-frequency region where the aircraft mounting shelf cannot transmit much energy, and possibly insufficient in the vicinity of the high-Q shelf

resonances. In the low-frequency region (under 50 Hz), traditional sine-sweep levels (0.036 inch (.914 mm) DA, for example) are totally unrealistic. Once real environmental data is obtained, the strapdown INS navigation accuracy can be projected. IISA has been designed for the most rigid gyro-to-gyro structure obtainable to attain accuracy goals during vibration.

FLIGHT CONTROL REQUIREMENTS

Inertial navigation gyros and accelerometers are orders of magnitude more accurate than those commonly used for flight control. Part of the accuracy is achieved by software modeling of residual errors and much of this benefit also applies to angular rate and acceleration outputs for flight control.

Software axis alignment correction, however, is more complex for a redundant system since it involves mixing of data between sensors. Flight control accuracy requirements are limited, however, and misalignment due to physical separation and vibration isolators cannot easily be compensated. Therefore, full inertial-grade axis alignment accuracy is not provided for flight control sensor outputs.

The specified accuracy of outputs to the flight control system is shown below. Actual accuracy will be significantly better since the outputs are derived from inertial navigation grade sensors.

	Angular Rate	Acceleration
Scale factor	0.1%	0.1%
Bias	1.5 deg/hr	4 mg
Alignment	1 milliradian	7 milliradians
Resolution	0.02 deg/sec	2 mg
Range	400 deg/sec	20 g

Important considerations for flight control are the time delays and synchronization of data from the IISA when used as part of a digital flight control system controlling the states of an aircraft in real time. Data sampling and processing time delays in the sensor element cause a destabilizing effect in an aircraft control system and must be carefully selected.

Gyro and accelerometer outputs consist essentially of pulse streams which are counted over some time interval to obtain an estimate of angular rate or acceleration. If this count interval is too long, excessive time delays are introduced into the FCS. Selection of count interval and subsequent digital filtering to reduce noise and quantization effects must be balanced against FCS time delay and phase lag constraints.

Since the IISA sensor subsystem is implemented as six separate skewed gyro and accelerometer pairs, the data sampling intervals may begin at different times for each sensor, unless some form of cross-channel synchronization is employed. The primary effect of such a time-skew between sensors is to contaminate redundancy management sensor comparisons during very high angular acceleration or rate of linear acceleration. (3)

To eliminate the complexities and risks of synchronized data sampling, the six IISA sensor outputs can run completely unsynchronized. Angular velocity and acceleration are computed and output at 1 kHz to minimize time delay, cross-coupling effects and redundancy management contamination.

Data sampling is initially derived from a single clock in order to achieve required navigation accuracy. Each sensor pair separately monitors the accuracy of this clock, relative to its own. If an error is detected the sensor pair's clock is used. This leads to the asynchronous operation discussed above.

Other important considerations for flight control are IISA's anti-aliasing filters and the other noise produced by the gyros. Modern flight control systems are digital and sensor data is sampled at some fixed frequency, e.g., 80 Hz for modern fighter aircraft. Sensor noise or vibration inputs at high frequencies can be aliased by the sampling process to a frequency within the flight-control bandwidth, causing control surface flutter or pilot discomfort. Therefore, it is necessary to filter gyro and accelerometer outputs to remove high-frequency noise. For digital sensors such as those used in IISA, filters must be digital in nature and the sampling frequency must be greater than twice the highest noise or vibration frequency. Since IISA sensors are attached to vibration isolators, limiting sensed vibration bandwidth, digital filters iterated at 1 kHz produce the required noise rejection.

It is desirable to reject noise in sensor outputs within 10 Hz of the FCS data sampling frequency and its harmonics. These are the frequencies which can potentially alias to the 0-10 Hz region, the maximum bandwidth of the FCS. This can be achieved, for example, by a low-pass filter. There is a trade-off between filter noise rejection capability and time delays and lags which could potentially destabilize FCS loops. Time delays or phase lags in angular rate measurements tend to be more destabilizing to FCS loops than acceleration phase lag. In IISA, angular rate anti-aliasing filters introduce a time delay of 8 milliseconds and consist of a gyro dither filter at 424Hz plus a notch filter at 80Hz. The latter filter not only provides filtering of structural or mount resonance effects which might alias to the FCS response, but also greatly attenuates the effect of gyro output quantization noise (0.5 arc second). Rate noise under static conditions has proven to be less than 0.01°/sec.

Accelerometer anti-aliasing filters are low-pass (21 Hz bandwidth) with 20 milliseconds of effective time delay. Dithered ring laser gyros produce measurable amounts of vibration and angular motion. The anti-aliasing filters filter these effects without the presence of low beat frequencies in acceleration outputs. Residual acceleration noise has been measured to be 0.05 ft/sec^2 (1.5 cm/sec^2) (2 milli-g) rms, and is due primarily to accelerometer quantization.

REDUNDANCY MANAGEMENT

Since the two groups of inertial sensors in the INAs are on separate vibration isolation systems and are physically separated, accurate navigation cannot be achieved after a second failure of the same sensor type (one failure per group). Therefore, redundancy management is directed exclusively toward flight control requirements. The redundancy management, described below, will be inserted within the F-15's Digital Electronics Flight Control System (DEFCS). The software will be rewritten by using the DOD High Order Language of Ada. Thus, with the incorporation of this function within the DEFCS, IISA will closely resemble a production system.

The sequence of operations performed in the redundancy management is illustrated in Figure 4. Sensor data is first reviewed for hard failures, detectable by normal self-test methods. The sensors themselves give an indication of failures through loop closure tests, loss-of-signal indications, etc. I/O tests assure that data has been correctly transmitted, and dynamic reasonableness tests detect spurious outputs inconsistent with the vehicle capability.

Due to the physical separation of the two sets of accelerometers, angular rotations and angular accelerations of the vehicle cause different accelerations to be sensed by each set. To allow direct comparison between acceleration measurements under dynamic conditions, each sensor output is related to a common point on the aircraft using the current best estimate of vehicle angular rate and angular acce-

leration along with known lever arm displacements from that point.

The six skewed gyro axes and six skewed accelerometers are spaced evenly on a 109.5° cone whose axis is vertical. Since no two axes are coincident and no three are in the same plane, full three-axis outputs can be provided with three failures of a sensor type.

Detection of up to three failures is assured by comparison of redundant sensor data in what are termed parity equations. These equations cancel vehicle angular rate, or acceleration in the case of accelerometers, and expose sensor errors. Because of information limitations, a third sensor failure of the same type can only be detected. Isolation of which of the four sensors active at that point has failed cannot be achieved except for hard failures which are detected by conventional self-test methods. For this reason IISA is termed fail-operational/fail-operational/fail-safe.

Six-gyro (similarly for accelerometers) parity equations can be formed by comparing each gyro output to a least-squares estimate of its output derived from the remaining sensors. Since there are always two sensors orthogonal to each axis, this results in six equations which are linear combinations of four sensor outputs. The orthogonal sensors cannot contribute to error detection. After sensor failures, a different set of parity equations is required. Again, fifteen linear equations involving four sensors can be formed, five equations after the first failure and only one after the second.

While the occurrence of two simultaneous failures appears extremely improbable from the standpoint of component reliability, sensors within a unit are under similar stresses (for example, local heating or shocks due to battle damage). Solution of all 15 potential parity equations during zero failure conditions, each derived from four sensors, allows detection and isolation of most soft dual-failure conditions, and this is the approach taken on IISA.

Under ideal conditions, parity equation outputs should be zero under any aircraft dynamic or vibration condition. However, because sensors are in separate, isolated units, shelf motion, isolator rocking and unit-to-unit misalignments cause parity equation outputs to appear when no sensor failures are present. For this reason, both filtered and unfiltered equation outputs are used for failure detection, the former for detection of small, soft failures in some short time interval and the latter for very rapid detection of larger soft failures. The parity equation output level which trips gyro error detection logic is also varied as a function of angular rates and angular acceleration to avoid false alarms during maneuvers. A similar approach is used for acceleration trip levels.

The 15 parity equation outputs are scaled to be equal in their response to white noise from sensors. In general, however, all equations involving a sensor may not fail simultaneously. The parity equation coefficient for a given sensor, which is derived from the geometry, varies from equation to equation.

To fail one sensor, 10 parity equations must fail. For a slowly degrading sensor, 10 equations will fail gradually rather than all at once. A sensor performance index (SPI) is formed for each sensor, equal to the number of parity equations it involves which have failed (0-10). The three sensors with the smallest SPI may be used for derivation of outputs. This is valid since in general three good sensors can be found easier than one bad one.

With inertial navigation quality sensors, there is little value in combining data from all six sensors in a least-squares solution to derive outputs, rather than selecting a triad from a single unit, when available. Combining sensors simply adds another source of noise, namely, the rocking motion of the second unit within the isolators. Therefore, whenever available, IISA outputs are derived from the three sensors in one unit. When there is one failed sensor in each unit, all four remaining sensors are used. For the condition where three failures are detected and failed sensors are known, the remaining three sensors are used. For the rare ambiguous case where all parity equations are failed and self-test cannot isolate the failure, warnings are issued to the pilot.

The equations which use selected sensor data to derive standard, orthogonal outputs to the flight control system are termed design equations. There will be 29 sets of equations stored in the DEFCS computer, 20 for all the combinations of three sensors-at-a-time, and 9 for the least-squares estimates for four sensors-at-a-time, one failure in each unit. Only one set of design equations is used at a time.

The quality of the redundancy management process rests on:

1. Noise level of parity equations
2. Thresholds that are used to detect failures
3. Transients that may occur in outputs when failures occur or when different sensors are selected due to normal noise conditions.

IISA LABORATORY TEST AND EVALUATION PLANS

The IISA will be tested in the NADC Strapdown Systems Evaluation Laboratory using special laboratory equipment. The two INA's will be mounted on a Carco three-axis, electrically controlled motion table. The table has a large mounting area sufficient to accommodate and drive both INAs simultaneously. A Control Console for the Carco table allows several modes of operator control of table motion (either rate or position) through a dedicated microprocesor/display/keyboard. A built-in Scorsby motion mode is one of the command options. The table can also be commanded through its Control Console by an external computer. (4)

A dedicated PDP-11/44 Computer with 1553B bus interface capability will provide the means for recording the 1553B data outputs from each INA. Because of the low data rate on the 1553B, it is difficult to measure high frequency characteristics of the flight control signals provided by the IISA on the 1553B bus. Consequently, a Digital to Analog (D/A) Converter will be available, as part of Ground Support Equipment (GSE), and can be used to convert the dedicated flight control digital outputs to analog form for strip chart recording and signal analysis. Signal analysis will be done with a Hewlett-Packard (HP) Dynamic Signal Analyzer to perform noise spectrum analysis and determine frequency response (gain/phase) characteristics.

A sweep oscillator will provide a sinusoidal input to the rate table (each axis separately) for frequency response testing. The input frequency will be incremented from 0 to 25 Hz. At each increment chart recordings will be made of the respective flight control output along side the rate table tachometer output. Phase and gain measurements will be made on these outputs. In addition, analysis of the flight control output noise spectrum to determine frequency components of the noise will be done with the HP Signal Analyzer. The sweep oscillator and the signal analyzer will be run simultaneously while data is sampled in the signal analyzer. The resulting transfer function plot (gain and/or phase) will be displayed and plotted on an HP Plotter. The IISA test configuration is shown in Figure 5.

FLIGHT CONTROL TESTS IN THE LABORATORY

Dither Noise - The dither frequency of the IISA RLG's is near 424 Hz. Due to aliasing the sampled dither signal may appear in the flight control frequency band. The dither magnitude is large enough that

it must be filtered before the sensed rate is used for flight control compensation. The IISA laboratory tests will determine the effectiveness of these filters in attenuating noise and determine the signal lags introduced by the filter. A spectrum analysis of the dither signals before and after the INA dither filter and at the DCA output will determine the effectiveness of the filter and identify the predominant signal components which may affect flight control performance. Test results will be compared with analytical results.

Structural Mode Interaction - Sensed structural body motion can be a problem in high performance aircraft unless the sensors are located near the points of minimum structural motion (bending nodes or anti-nodes). If not suppressed, the structural motion may be reinforced through the Control Augmentation System (CAS), possibly creating a limit cycle motion on the control surfaces. The filter's gain and phase characteristics and the flight control compensation will be verified in the IISA laboratory tests using rate table frequency response tests and comparing test results with analytical results.

System Time Delay - A key performance measure of an integrated sensor/flight control system is total system time delay. Sources of delay in the IISA include dither and structural filtering, and processor computational delay. Closed loop system analyses will be used to determine the effects of varying time delay on aircraft performance. Open loop analysis will be used to determine the effects on system stability. The results of these studies will be used as IISA goals which will be verified in the laboratory.

Fault Detection and Isolation - Sensor faults and INA/DCA interface failures will be isolated by the redundancy management algorithms in the DCAs. Redundancy management will provide fail-operate/fail-operate/fail-safe operation through the use of parity equations which linearly combine the sensor outputs to determine the residual errors. The residuals are compared to trip levels and the results are used to select the best performing sensors. The redundancy management algorithm's sensor trip levels have been determined and evaluated using an offline simulation. Lab testing to verify these trip levels will be accomplished by simulating sensor faults in software. By way of the CDU various sensor faults can be simulated, such as hardover failures, failures to zero, bias failures and ramp induced failures.

Switching Transients - During the redundancy management process, transients in the flight control command signals are possible due to dynamic axis misalignment between the two sensor packages and noise. The redundancy management algorithm is designed to minimize sensor switching. However, the laboratory setup will be used to evaluate the switching effects between the sensor output combinations. The test will cycle through all combinations of the rate and acceleration output sensors and determine the amplitude of the variation in the control surfaces commands due to the sensor switching. The resulting control surface command will be converted into equivalent aircraft motion to determine if the commanded aircraft motion is below the pilot's perception level (0.05g acceleration and 0.1 deg/sec rate).

Bending Mode Conditions - The effect of relative bending motion between the two INAs will be simulated in the laboratory. This will be done by placing one INA and a dummy INA on the Carco table. The dummy will act as a mass simulator and operate with the real INA on the table. The real INA will be mounted on a stationary fixture. By driving the table at selected frequencies using the function generator input, the effect of relative bending motion between the INAs can be simulated. A special offset mount fixture will be used to adjust the accelerometer location to simulate linear bending mode effects.

Lever Arm Compensation - Rate table tests are useful in determining how well the system identifies predetermined failures and failure types (hardover, bias, nulls, etc.) A significant factor in the acceleration parity equation computations is the lever arm compensation which makes the accelerometers in both INA's appear to be at a common location. An approach to verify the lever arm computations will be developed in the laboratory. Appropriate adjustments will be made in these tests to account for differences in the sensor separation distances on the rate table as opposed to those existing on the host aircraft.

NAVIGATION TESTS IN THE LABORATORY

Alignment Repeatability Tests - Forty-eight 15-minute alignment runs will be performed in six groups of eight runs. The six groups correspond to headings of 0°, 45°, 135°, 225°, 270°, and 315°. From these tests, the level axis fixed bias, the random walk value, the overall system alignment accuracy, and the sensitivity of the system to alignment heading will be determined. The results also will be used to predict system performance as a function of reaction time.

Alignment/Navigation Tests for Cold and Warm System - These tests will consist of four combination alignment/navigation runs at headings of 0°, 45°, and 90°. Each combination will consist of an alignment and 60 minute navigation run with the system starting at ambient temperature followed immediately by another alignment and 60-minute navigation run. These tests will be used to determine system position and velocity accuracy as a function of alignment heading and initial system temperature.

Static Pitch, Roll, and Heading Tests - The system pitch, roll, and heading accuracy will be determined as each axis is stepped through 360° in 10° increments. The tests will be performed at headings of 0°, 45°, and 90°. These tests will be used to verify system attitude output accuracy and to determine whether the output accuracy varies as a function of heading.

Accelerometer Bias Test - The system will be aligned on a particular heading, then rotated in azimuth 180 degrees immediately after going to navigate. The system will then be allowed to navigate for 90 minutes. The 180 degree rotation normally doubles the effect of the accelerometer bias and east gyro drift errors. The test will be performed six times at heading of 0°, 45°, and 90° at both cold and warm temperatures. This has been found to be one of the most useful tests in determining error sources affecting navigation performance.

Rate Output Tests - These tests will be performed in order to get a measure of the system angular rate outputs. The system pitch, roll and yaw rate outputs will be recorded as the system is subjected, one axis at a time, to rates of $\pm$10, $\pm$30, and $\pm$45, degrees per second. In addition, pitch will be tested at $\pm$60 degress per second and roll and heading at $\pm$100 and $\pm$300 degrees per second.

Linearity/Symmetry Tests - A 60-minute navigation run will be performed with a sinusoidal single axis motion of 2 degree peak amplitude and 0.5 hz. frequency applied to the system. The test will be performed twice with the motion put in about the pitch axis, and twice with the motion about the roll axis. During this test any scale factor asymmetry problems will look like an equivalent level axis gyro drift.

Schuler Pump Test - This test will consist of rotating the system 180 degrees in azimuth immediately after going to navigate, and rotating 180 degrees every 42 minutes until 150 minutes of navigate time have been accumulated. This test will be executed twice. The purpose will be to accentuate errors due to aligning a strapdown system in one heading and then navigating on a different heading.

Scorsby Test - During this test the system will be subjected to a 12 degree peak-to-peak, six cycles-per-minute Scorsby motion while performing a 90-minute navigation run. Two runs with a clockwise Scorsby motion and two with a counter-clockwise Scorsby motion will be performed at headings of 0 degrees and 90 degrees for a total of eight runs. This test will uncover any coning compensation, gyro scale factor asymmetry, and gyro axis misalignment errors that may be present in the system.

Coning Test - This test will consist of applying two sine wave inputs with a phase difference of 90 degrees to the heading and roll axis of the three-axis table to produce a coning motion about the pitch axis. The test will be performed twice. The inputs will then be applied about heading and pitch to give coning about roll and the test will be performed twice in this configuration for 60 minutes each.

Profile Sensitivity Tests - Flight profiles will be executed to duplicate mission profile angular rate and attitude histories. The tests will be performed on the computer controlled, three-axis attitude and rate table. Four standard flight profiles will be performed. Each profile will have a duration of approximately 3-4 hours. The profile sensitivity tests will exercise the system to give a very good indication of performance that can be expected during actual flight.

SUMMARY

IISA has been designed to meet the flight safety needs of flight control inertial sensors while simultaneously operating as a medium accuracy inertial navigator. Key portions of the system have been built and shortly will be undergoing test.

Results of the IISA test and evaluation will be used for the joint service development and flight evaluation of MIISA. Given the trends of the design of high performance aircraft, an integrated system design such as MIISA is essential for minimum avionics cost.

REFERENCES

1. Memorandum of argreement between the Naval Air Systems Command and the Air Force Aeronautical Systems Division and the Army Aviation Systems Command for joint development and production of the Multi-Function Integrated Inertial Sensor Assembly (MIISA), (signed 21 Nov 1985 by Navy and Air Force)

2. J. G. Mark, R. E. Ebner, and A. K. Brown, "Design of RLG Systems for High Vibration," PLANS '82 Symposium pp. 379-385.

3. D. Krasnjanski U.S. Naval Air Development Center and R. E. Ebner Litton System Inc. "Design of the Integrated Inertial Sensor Assembly (IISA) Advanced Development Model" IEEE/AIAA Guidance Symposium, Seattle, Washington 30 Oct 2-Nov 1983.

4. J. Jankovitz, U.S. Naval Air Development Center, "Performance Evaluation Test Plan for the Advanced Development Model (ADM) Integrated Inertial Sensor Assembly (IISA)," 12 Sep 1983.

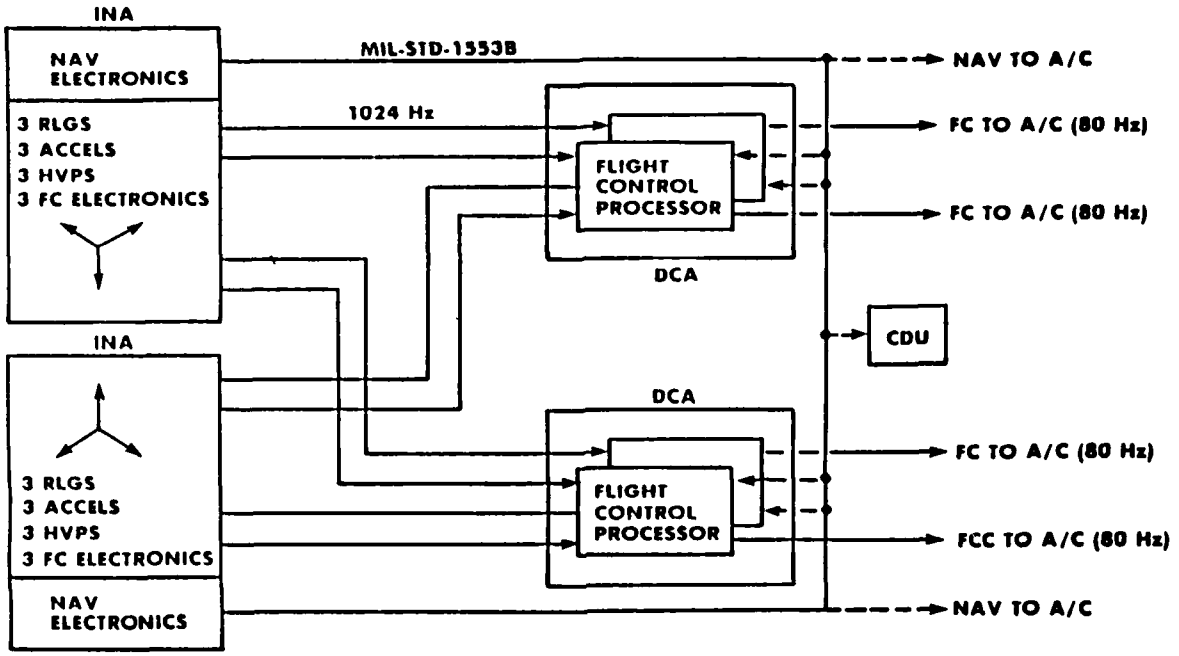

FIGURE 1 - IISA FUNCTIONAL BLOCK DIAGRAM

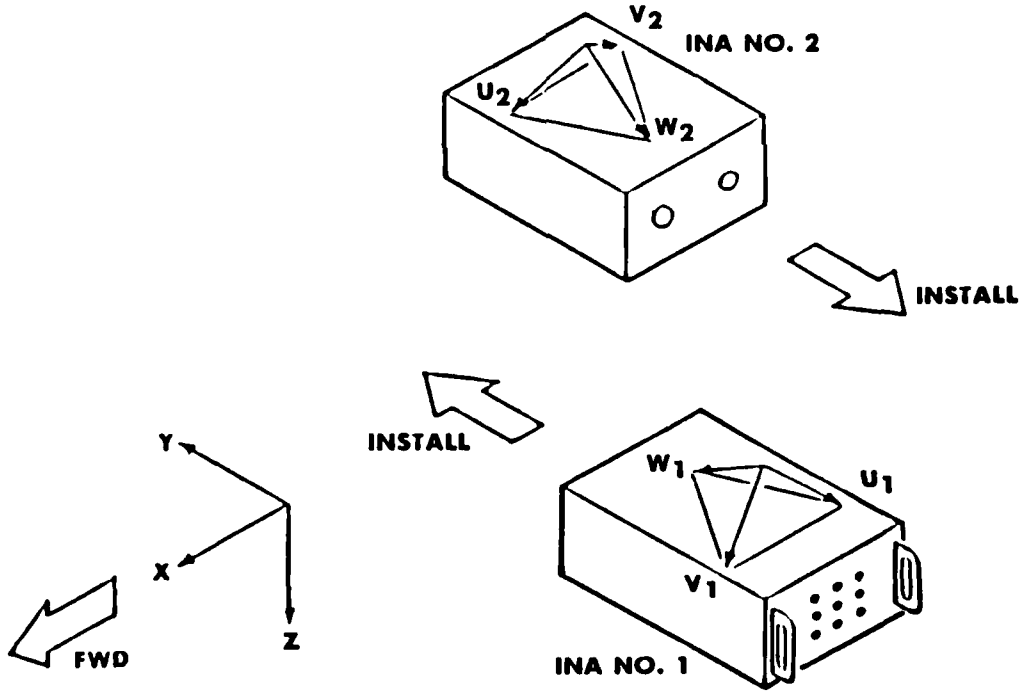

FIGURE 2 - INA INSTALLATION CONFIGURATION

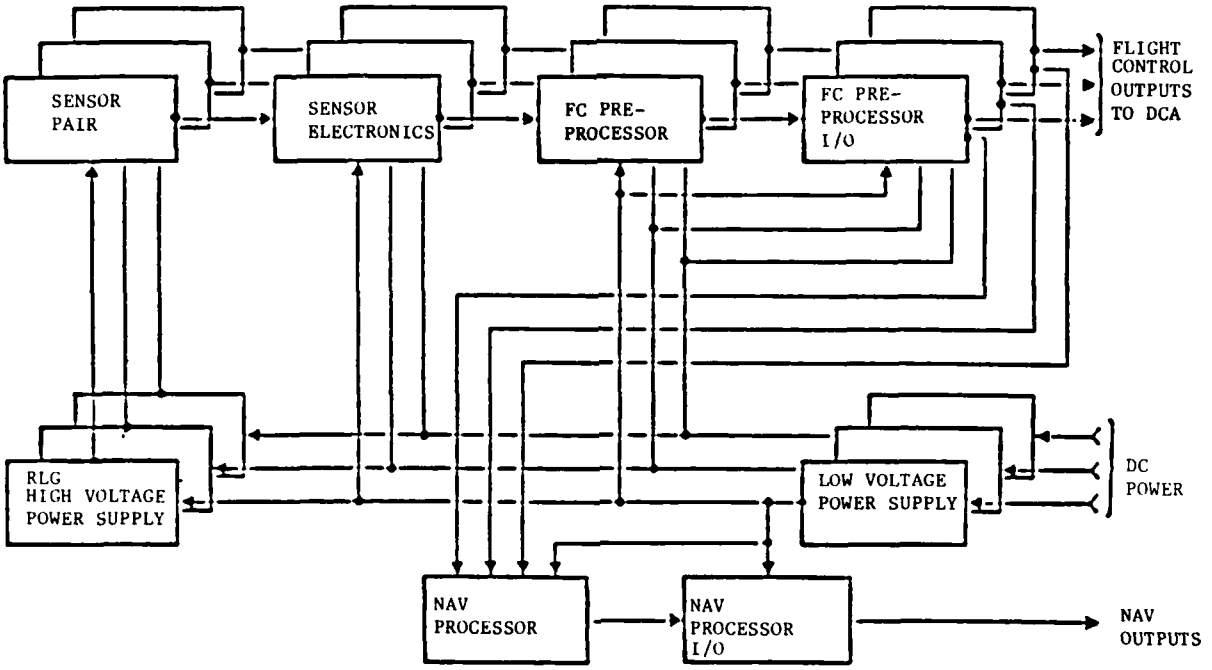

FIGURE 3 - INA FUNCTIONAL BLOCK DIAGRAM

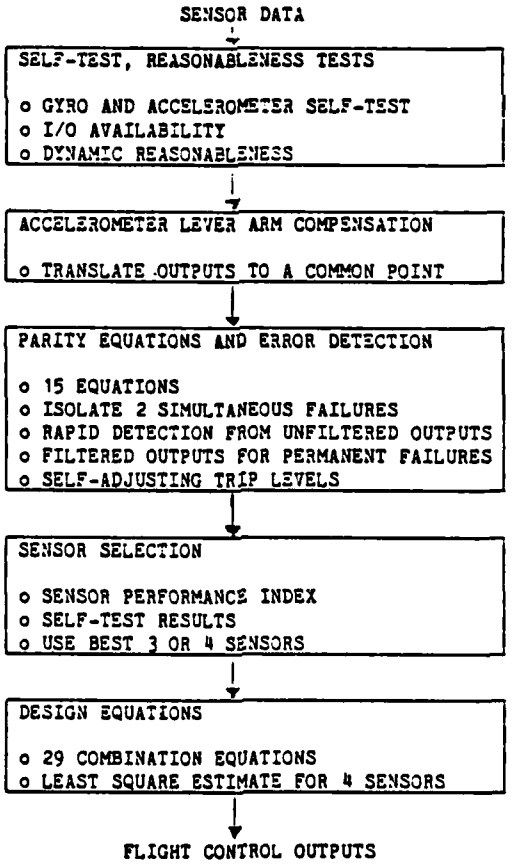

FIGURE 4 - REDUNDANCY MANAGEMENT OPERATION

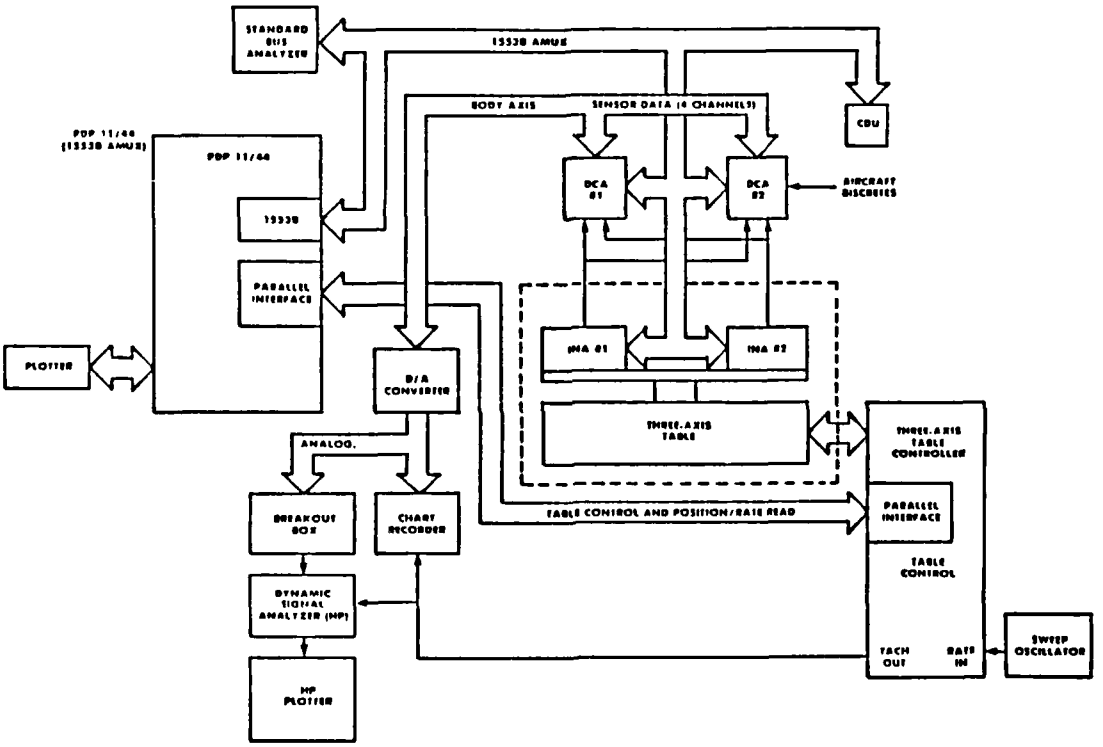

FIGURE 5 - IISA TEST CONFIGURATIONS

Configuration Design

of a Helicopter Integrated Navigation System

S.I. Fingerote, D.B. Reid
Honeywell Advanced Technology Centre
Honeywell Ltd.
155 Gordon Baker Road
North York, Ontario
CA

D.F. Liang
Defence Research Establishment Ottawa
Ottawa, Ontario
CA

L. Vallot, C. Greene, J. Mahesh
Honeywell Systems and Research Center
Honeywell Inc.
Minneapolis, MN
US

Abstract

Results are presented from configuration performance study phase of the Helicopter Integrated Navigation System project sponsored by the Canadian Department of National Defence. A configuration assessment is presented including processor selection, and a discussion of system architecture and configuration tradeoffs leading to a recommended configuration. Results of the system error analysis and the Kalman filter design are presented demonstrating integrated system performance.

Introduction

The roles of the military maritime helicopter include search and rescue, Anti-Surface Surveillance and Targeting (ASST), Anti-Submarine Warfare (ASW), and Anti-Ship Missile Defence (ASMD). Many of the missions must be carried out at ultra-low altitudes under all weather and visibility conditions. The increased range, speed and accuracy of modern weapon systems impose stringent accuracy and reliability requirements upon the aircraft navigation system. To enhance mission success in a hostile environment, the flight crew is required to operate weapon systems, target acquisition and designation systems, radar and ESM detection, night vision systems and perhaps engage in air-to-air combat. The traditional manual dead reckoning tasks can no longer provide the required performance accuracy and would unnecessarily distract the flight crew from performing mission-critical functions.

More specifically, the Canadian Forces Sea King helicopter will be nearing the end of its useful life by the beginning of the next decade. As a result, the Canadian Department of National Defence (DND) has begun studying options, including the update or replacement of the maritime helicopter fleet. A number of research and development projects have been initiated to develop certain avionic systems. One of these projects is to develop and test an integrated navigation system that is capable of satisfying the helicopter mission requirements within the cost limitations of the program. This project is called the Helicopter Integrated Navigation System (HINS). This paper describes the development and the basic software and hardware configuration of the system under study. Results of performance simulation analysis also are presented.

MISSION REQUIREMENTS

In the 1990s and beyond, the effort in Anti-Submarine Warfare will be directed toward extending the range of initial detection and maintaining contact with submarine targets. This may include ships towing sonar arrays and ASW helicopters working jointly with the ships. The steady improvement in the modern submarine's capabilities means that the CH-124A Sea King, which is currently deployed from Canadian ships, will eventually lack the range, endurance, detection and data-processing equipment necessary to localize and maintain these long-range submarine contacts. The two prime solutions for this problem are to update and life-extend the Sea King or replace it with a more modern maritime helicopter. A requirement exists for a number of new avionic systems for ASW helicopters, one of which is a new navigation system.

For the ASW mission the helicopter navigation system must maintain stable and accurate position over long periods of time. In the anti-surface ship targeting role high orders of absolute and relative navigational accuracy are vital to rapid and successful action. There are further complicating factors. Operations must often take place under radio silence and shore-based or satellite navigation aids may be destroyed or jammed during wartime. The small crew of the helicopter must not be burdened with monitoring the functioning of, or updating, the navigation system. Consideration of these factors has led to the following accuracy requirements:

1. Radial Position Error (95%):

- with external aids = 2.0 nautical miles (nm)
- without external aids = 1.5 nm/hr

2. Radial Velocity Error (95%):
   - with external aids = 3.0 ft/sec
   - without external aids = 4.0 ft/sec

3. Attitude Error (95%):
   - with or without external aids = 0.5 deg

4. Heading Error (95%):
   - with or without external aids = 0.5 deg

External aids are those systems such as Omega, Loran, and GPS which rely upon transmitters which are located external to the aircraft and may be unavailable during wartime. INS, Doppler, and radar altimeter are representative of internal or self-contained aids.

It is noted that the radial position error requirement with external aids can be exceeded by a large margin if GPS is available.

DEVELOPMENT PLANS

Modern avionics systems are becoming increasingly complex as the demands for better performance and higher reliability continue to escalate. These demands, however, are being pressed in an extremely cost-conscious environment. The HINS project addresses the development of the helicopter integration navigation system subsystems. This integration is the key to satisfying the HINS performance and reliability objectives in the most cost-effective manner.

With several navigation subsystems available for HINS - such as inertial, GPS (Global Positioning System), Doppler and Omega - a large number of equipment configurations are possible. The typical approach is to use previous experience in selecting two or three candidate configurations in an ad hoc manner. This has the potential danger of eliminating good alternatives early in the project and could eventually result in a suboptimal configuration.

DND has decided to spend a significant portion of the navigation system development time to simulate and study a number of potential configuration with the aim of identifying, developing and testing an integrated navigation system which best satisfies the requirements established for the project.

The HINS approach to achieving this aim is to first perform preliminary analysis and simulation to identify four or five candidate configurations that meet the mission requirements. From the detailed performance analysis of these configurations, one of them will be selected for advanced development. The product of this advanced development will be thoroughly tested. The completed navigation system will then be ready for incorporation in the maritime helicopter.

The HINS project has been divided into two phases:

Phase I: System Definition and Design

To define candidate integrated system configurations which may satisfy Sea King replacement mission requirements, evaluate candidate system performance by simulation and thereby identify the preferred configuration with which to proceed to advanced development.

Phase II: Development and Testing

To build an Advanced Development Model (ADM) of HINS, and conduct a series of ground and flight trials leading to a fully developed and flight-validated navigation system for incorporation in the maritime helicopter.

Phase I, completed in March of 1985, was carried out under contract to DND by Honeywell's Advanced Technology Centre, located in Toronto, supported by Honeywell's Systems and Research Centre (SRC) of Minneapolis.

A contract award for Phase II is planned for later this year for the delivery of a fully tested ADM to DND.

PHASE I ACTIVITIES

An extensive survey has been performed to collect relevant data on navigation subsystem and sensors. These data included information on candidate subsystem performance, weight, volume, power consumption, reliability, cost and Canadian content. Using Honeywell's Integrated Sensor Evaluation Program (ISEP), several hybrid system configurations were evaluated on the basis of these data leading to a short list of candidate integrated system configurations which might potentially satisfy the mission requirements. The results of this preliminary assessment were then used as the basis of the software development (left side of work flow chart, Figure 1) and detailed analysis and simulation work (right side) which followed.

Software development activities comprised the design and implementation of algorithms for integration of the HINS multiple sensors, and the development of extensive simulation tools for evaluation of candidate system performance.

Analytical work has focused on definition of HINS hardware, architecture, assessment of processor loading requirements, subsystem trade-off studies, and finally performance simulation of candidate configurations, including refinement of the integration algorithms.

These activities have culminated in the selection of a single recommended configuration for the HINS ADM. Comprehensive interface specifications have been prepared for this system.

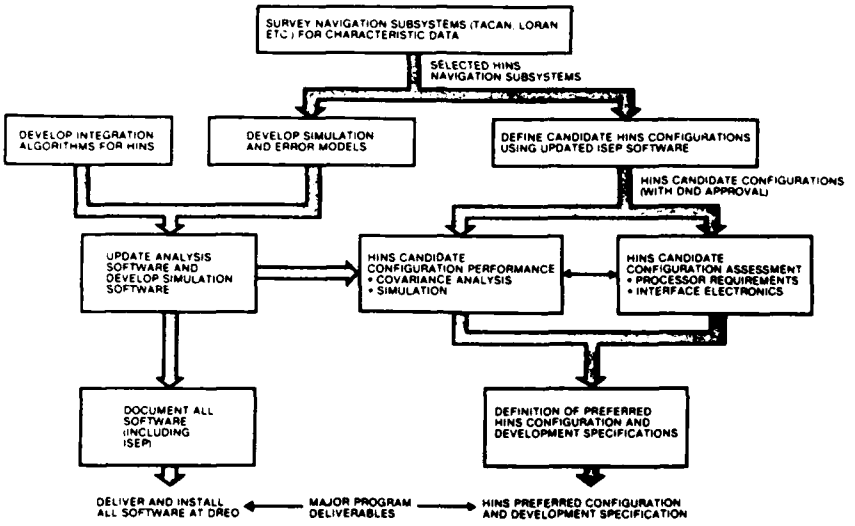

Figure 1: HINS Feasibility Study Tasks and Deliverable Items

RECOMMENDED CONFIGURATION

The recommended system shown in Figure 2 comprises an airborne processor to which four primary subsystem/sensors are interfaced by means of a MIL-STD-1553B serial multiplex data bus:

- o Inertial navigation system (INS).
- o NAVSTAR/GLOBAL Positioning System (GPS) receiver.
- o Doppler radar velocity sensor.
- o Magnetic heading reference.

Also interfaced to the processor are a radar altimeter, a TACAN receiver and an air data subsystem which supplies barometric altitude and true-air speed information.

The recommended processor - MIL-STD-1750A (500 KOPS) - implements a 23-state Kalman filter algorithm for integration of the data output by the HINS sensors, and algorithms for automatic failure detection, isolation and system reconfiguration. The Kalman filter blends the various sources of navigation data to perform three functions: Optimize overall HINS performance; calibrate sensor error sources (e.g. gyro drift rates); and enable both in-air and shipboard alignment of the INS.

Should a component subsystem/sensor fail, the system will reconfigure automatically, subject to operator override, to a degraded mode of operation. The high degree of system redundancy provides at least two levels of reversionary mode operation.

The recommended INS is a standard form-fit function (F3) inertial navigation employing ring laser gyros (RLGs). This is a completely self-contained, medium-accuracy system providing a full set of position, velocity and attitude outputs. Operating open loop (free inertial mode) following initial alignment, it offers accuracies of better than one nm/hr (RMS) in position, a few feet per second in velocity, one or two minutes of arc in roll and pitch, and a few minutes of arc in heading at moderate latitudes.

The GPS receiver, a five-channel Precise Position Service (PPS) model, provides highly accurate position and velocity data (nominally 50 ft (RMS) and 0.3 ft/s (RMS) respectively). These data are used by the Kalman filter to align the inertial sensors for enhanced free-inertial operation should GPS fail or be unavailable at some point in a mission.

The Doppler radar, an active radiating sensor, measures the velocity of the helicopter relative to the water surface. The Doppler performs two functions in HINS. First, as a back-up aid if GPS is not available, it provides redundant velocity information for

initial (in-air) alignment of the INS and for control of INS navigation errors during the mission. Also, as a back-up if both the GPS receiver and the INS are not available, the Doppler and the magnetometer are configured as a dead reckoning system providing degraded position, velocity and attitude data. The second Doppler function is to provide, in conjunction with the inertial system, information on helicopter motion relative to the water. This information is desireable for tactical navigation in which the position and velocity of the helicopter with respect to free-floating sonobuoys must be determined.

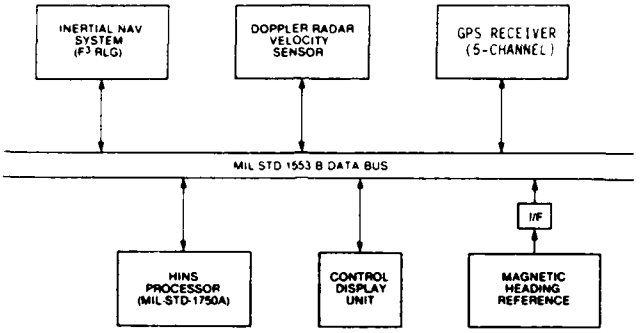

Figure 2: Recommended HINS Configuration

Kalman Filter

A comprehensive error model of the HINS is mechanized by the Kalman filter. The model defines the manner in which the system errors propagate in time and the geometry relating estimated error states to error observations constructed from the inertial and auxiliary sensor data. The model is of the form:

$$\mathbf{x}_k = \mathbf{F}_k \mathbf{x}_{k-1} + \mathbf{w}_k \qquad \text{dynamics model} \qquad (1)$$

$$\mathbf{z}_k = \mathbf{H}_k \mathbf{x}_k + \mathbf{v}_k \qquad \text{measurement model} \qquad (2)$$

where $\mathbf{x}$ is the n-element error state vector, $\mathbf{F}_k$ is the n x n state transition matrix for the interval t_{k-1} to t_k, $\mathbf{w}_k$ is an n-element vector white noise sequence with covariance $\mathbf{Q}_k$, and $\mathbf{z}_k$ is an m-element vector of error observations. The geometry relating the error state to the error observations at each time point tk is described by the m-vector measurement matrix $\mathbf{H}_k$; the observation noise is modeled as a discrete m-element vector white noise sequence $\mathbf{v}_k$ having covariance $\mathbf{R}_k$. $\mathbf{w}_k$, $\mathbf{v}_k$, and $\mathbf{x}_0$ are assumed to be normally distributed and mutually uncorrelated.

To improve computational efficiency by taking advantage of the structure of the model, the error state $\mathbf{x}$ is partitioned into three sub-vectors: $\mathbf{x}_n$, $\mathbf{x}_a$, and $\mathbf{x}_i$, where "n" represents the navigation error states (position, velocity, and attitude), "a" represents the navigation aiding error states (such as GPS, Doppler, magnetometer, sea currents, and wind), and "i" represents the inertial sensor error states (such as gyro and accelerometer biases, misalignments, and scale factors). The resulting partitioned system model is of the form:

$$\begin{bmatrix} \mathbf{x}_n \\ \mathbf{x}_a \\ \mathbf{x}_i \end{bmatrix}_{k+1} = \begin{bmatrix} \mathbf{F}_n & 0 & \mathbf{F}_{ni} \\ 0 & \mathbf{F}_a & 0 \\ 0 & 0 & \mathbf{F}_i \end{bmatrix} \begin{bmatrix} \mathbf{x}_n \\ \mathbf{x}_a \\ \mathbf{x} \end{bmatrix}_k + \begin{bmatrix} \mathbf{w}_n \\ \mathbf{w}_a \\ \mathbf{w}_i \end{bmatrix}_k \qquad (3)$$

Further advantage can be taken of the structure by noting that both $\mathbf{F}_a$ and $\mathbf{F}_i$ are diagonal.

A computationally efficient form of the Kalman filter which has been used in the HINS project is Bierman's UDU^T factorized filter [1]. This algorithm avoids explicit computation of the estimation error covariance matrix $\mathbf{P}$. Instead, $\mathbf{P}$ is propagated in terms of its factors $\mathbf{U}$ and $\mathbf{D}$:

$$\mathbf{P} = \mathbf{U}\mathbf{D}\mathbf{U}^T \qquad (4)$$

The UDU^T algorithm is efficient and provides significant advantages in numerical stability and precision. Specifically, this approach provides an effective doubling in computer word length in covariance-related calculations and avoids filter divergence

problems which can arise in more conventional filter mechanizations due to loss of the positive (semi) definite property of P through the accumulation of numerical roundoff and truncation errors.

Failure Reconfiguration

Figure 3 shows a failure reconfiguration diagram. Each branch of the failure tree will be addressed. The system models used in the Kalman filter are based on the inertial measurement unit. In any degraded mode which does not include the IMU, system integration is no longer performed by the HINS processor, and alternate modes of navigation are selected. If GPS is available, it is used. Without the IMU and GPS, dead reckoning is performed using Doppler velocities and magnetometer heading.

Two different IMUs are considered in the failure tree. One is an RLG medium accuracy strapdown INS, the other is a lower performance attitude and heading reference system (AHRS) employing dynamically tuned rotor gyros (DTGs).

The root of the tree indicates full system operation: IMU/GPS/Doppler. First consider Doppler radar failure. Obviously, under conditions of Doppler failure, relative (ocean surface-referenced) navigation accuracy will slowly degrade as the last sea current estimate becomes outdated. However, with the remaining IMU/GPS configuration we can expect high quality navigation data meeting any reasonable geographic (earth-referenced) navigation requirements.

If the second failure is the IMU then attitude information may be available from the DG/VG (directional-gyro/vertical-gyro) but it is lower quality than the primary IMU data. Magnetic heading is available, again of lower quality. If high quality attitude and heading data are necessary for mission completion, they are unavailable, and navigation provided by GPS will allow return to the ship. Otherwise navigation is provided by GPS to complete the mission.

If GPS is the second failure then the quality of the IMU is a factor. Assuming a well aligned IMU, and AHRS-quality unit will meet the performance goals for the short term (< 1 hour). An aligned INS will provide good geographic navigation accuracy for the duration of the mission.

Next consider the primary failure as GPS. The remaining IMU/Doppler combination performance is dependent on the quality of the IMU. For both the AHRS and INS, Doppler is used for attitude error damping. The Doppler provides velocities, however, the velocities are influenced by the sea state. With the AHRS/Doppler configuration the performance goals are again met for the short term. Also, a well aligned INS will perform will for the duration fo the mission. The quality of INS alignment will depend on the duration of GPS aiding prior to the GPS failure. The longer GPS is available, the better the INS will be aligned. Alignment time without GPS is dependent on initialization and trajectory parameters. For the RLG, initialization using GPS will require only 10-20 seconds of GPS data.

If the second failure is the IMU, then only Doppler velocities remain. This information combined with heading and attitude from the aircraft vertical gyro, directional gyro and magnetometer provides a rudimentary navigation capability not substantially different from many current helicopter navigation systems.

If the second failure is the Doppler, the situation is similar to the primary GPS failure scenario, the difference being an air-speed damped AHRS instead of Doppler damping. Again, an aligned INS performs well.

Finally, consider a primary IMU failure. GPS provides high quality geographic navigation data, but attitude and heading information must be provided by the DG/VG and magnetometer. Relative navigation accuracy is good due to the availability of the Doppler velocities.

If the second failure is Doppler, GPS and magnetometer data remain to provide position, velocity, and heading. DG/VG quality attitude data are available. If high quality attitude information is unnecessary this is considered to be a fail-operational degraded mode.

If the second failure is GPS, then Doppler/Magnetometer/VG dead reckoning provides degraded mode navigation.

Computation and Memory Requirements

The basic approach to deriving processing requirements for the HINS is to count the floating point operations necessary to implement the HINS integration algorithms. Then, since no simulation can implement 100% of the final software, an appropriately chosen safety factor is applied. The factored numbers then become the requirements for comparison to various processors.

A count of multiplications, additions, divisions, sine/cosines, exponentiation, square roots, arc-functions and other miscellaneous functions for one complete pass through the

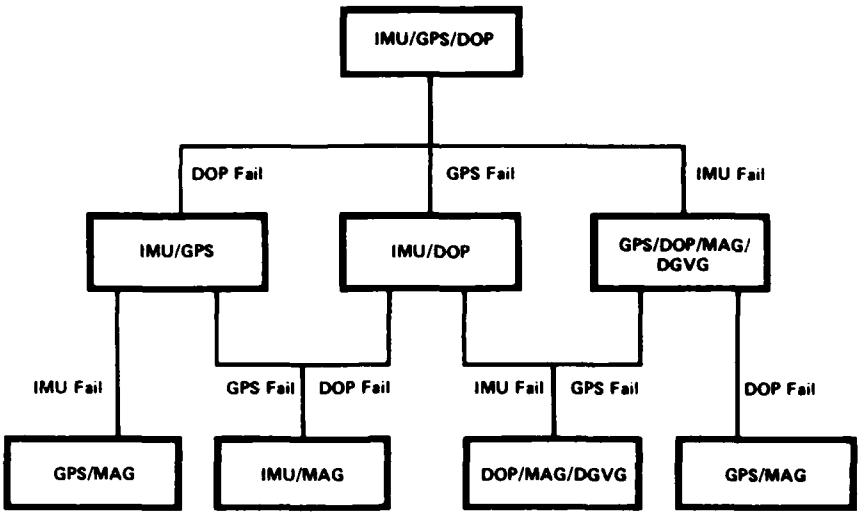

Figure 3: Failure Reconfiguration

filter was performed. A 26 state stabilized Kalman filter implementation was used to develop the requirements. This is the largest filter envisioned in the operational system. The stabilized Kalman filter used takes advantage of the partitioning of the HINS filter structure. If a UDUT algorithm optimised for the HINS structure is used, savings in computation can be made. However, for purposes of computer sizing, the estimated developed here are used.

Using memory-to-memory floating point operation times for the Fairchild 9450 (which implements the MIL-STD-1750a instruction set) and using rules of thumb for times not available from the literature a timing estimate was performed on the HINS Kalman filter. The times shown in Table 1 reveals that about 45% of the time is spent on add operations and 55% on multiplies. This indicates that the assumptions made on times such as trigonometric operations (which are compiler dependent) have negligible effect on processor selection. For purposes of this program, a safety factor of 5 was chosen. This was arrived at by allowing a factor of 2 for I/O and other non-floating point operations, a factor of 1.25 for compiler overhead and a factor of 2 for margin. These are in line with current practice. This provides the minimum margin, since compiler overhead can range from 1.15 to as high as 2 or 3.

The figures from Table 1 indicate that the Fairchild 9450 will execute the HINS algorithms in about 2.5 seconds (including the 5x factor). This is in line with studies which indicate that the filter can be cycled at about 0.1 to 0.2 Hz. (faster than the error dynamics of the problem) and satisfactory performance will be obtained.

Rough estimates indicate that the HINS algorithms can be implemented with memories in the 256K region. This estimate was arrived at by examining the object code for the appropriate modules as compiled on a VAX-11/750 running UNIX. The object code included various linkage, symbol table, debugging and other overhead, but does not include code resulting from system calls, I/O, and system functions.

Table 1: Computational Requirements

	ADD	MULT	DIV	SIN	EXP	SQRT	ATAN	AMOD	ASIN
SCALE IN	2	4	6	4					
INTEG	236	214	6	8					
TRANS	43	86	28	2	13	1			
PROP	19537	18713							
AIDHM	252	362	42	29		4	1		
CPM	8	20	4	6				4	4
GAIN	7104	7304	8						
UPDATE	13304	13296							
XFORM	1480	1517	10	8		40			
OUTPUT	25	43	2	1		5	3		
TOTAL	41991	41559	106	58	13	50	4	4	4
OP TIME	5.1	6.2	10.4	62	62	62	62	62	62
TIME (sec)	0.2141	0.2576	0.0011	0.0035	0.0008	0.0031	0.0002	0.0002	0.0002

Table 1 continued

TOTAL TIME = 0.4811 sec/iteration x 5	2.4058 sec/iteration
NUMBER OF STATES = 26	NUMBER OF MEASUREMENTS = 8

SIMULATION RESULTS

A detailed trade study - in which the suitability of a number of candidate configurations were assessed in terms of weight, power, cost and reliability - led to the selection of a short list of two alternative (but similar) candidates for performance simulation.

The purpose of the simulation effort was to determine the performance characteristics of the two remaining candidate systems for typical ASW helicopter flight profiles. This information was required to enable a final selection to be made, and to validate the operation of integration software (Kalman filter) which had been developed earlier in the project using analytical methods and software design tools (covariance analysis).

The two configurations subjected to simulation are similar, differing only in the type of inertial measurement unit employed. As described above, one is configured with an F3 ring laser gyro (RLG) medium - accuracy strapdown inertial navigation system; the other is configured with a lower performance strapdown attitude and heading reference system (AHRS) employing dynamically tuned rotor gyros (DTGs).

The following table compares approximate cost, weight, volume and mean time between failures (MTBF) estimates of the two configurations.

HINS CONFIGURATIONS COMPARISON
(as per Figure 2 without processor & CDU)

Configurations	Cost (k$U.S.)	Weight (lbs)	Volume (cu.ft.)	MTBF* (hrs)
F3 RLG	$235	95	1.6	2000
DTG AHRS	$165	65	1.4	1750

*for F3 RLG/DTG subsystem only

The estimated cost of the F3 RLG configuration does not reflect two factors which are expected to favourably influence the cost effectiveness of RLG systems in the future. First, recent trends indicate that pressure on RLG INS costs due to intense competition and continued U.S. government purchase of conventional platform technology inertial systems will lower the purchase price of this system substantially in the next few years. Second, RLG inertial systems have been demonstrating very impressive MTBFs in actual field applications. Reliability of systems in service have significantly exceeded the 2,000 hour specification. This characteristic is expected to persist in the future in both commercial and military applications. The effect of this will be to help drive total life-cycle costs down, improving the cost-competitiveness of RLG systems, from the standpoint of total cost of ownership, with respect to conventional inertial systems employing spinning-mass gyros (e.g. DTG's).

Simulation results indicate that, with all sensors/subsystems operational, the performance of the two configurations are essentially the same, both easily satisfying all HINS performance goals. This is because GPS dominates the navigation solution providing a highly accurate reference for control of system position, velocity and attitude errors.

Differences in performance between the two configurations occur when GPS is not available, either for the duration of the mission or when GPS is lost at some point into the mission. The most pronounced differences occur in the former case, in which both systems must rely on the Doppler radar for in-air alignment of the inertial measurement unit. As would be expected, the performance of the F3 RLG based system exceeds that of the DTG AHRS configuration due primarily to the superior performance characteristics of the ring laser gyros.

Figure 4 compares the position errors of the RLG and DTG configuration without GPS for the sonobuoy mission. Plotted in this figure are the predicted 95 precentile radial position error figures of merit (R 95) of the two systems. (The radial position errors of the systems should fall below these traces 95 percent of the time.) The performance of the F3 RLG based system is clearly superior to the DTG AHRS configuration, with an R 95 error rate limited to 0.8 nm/hr over the mission. The difference in performance of the two configurations is most pronounced in the first hour, in which the helicopter normally flies a constant heading while transiting to the area to be investigated. Here, the R 95 error rate of the AHRS based system is approximately 6.0 nm/hr. The position error is reduced dramatically, from 5 nm to about 3.2 nm, after completion of the transit leg following execution of a turn into the search area.

This turn, which changes the azimuth of the AHRS gyros with respect to the earth, enables the Kalman filter to gradually calibrate the relatively large biases of the gyros, trim the large heading error produced by these biases through gyrocompassing and remove a large portion of the position error build-up caused by heading error during the transit leg.

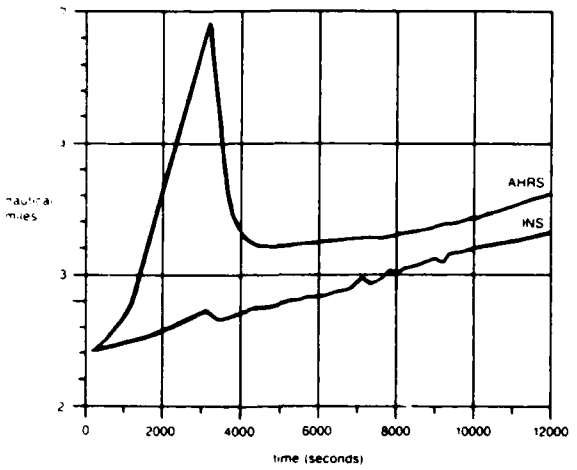

Figure 4: Comparison of AHRS and INS Performance Without GPS (Sonobuoy)

SENSITIVITY TO DESIGN PARAMETERS

A sensitivity analysis of various design parameters and error sources is useful to the designer in developing an error budget which will meet his performance goals. A graphic display of the sensitivity of the radial position error to the choice of gyro drift error is presented in Figure 5. The results are derived from the Sonobuoy Mission at about 3000 seconds into the mission and are shown for both the AHRS and the INS HINS configurations.

The interpretation that should be given to this type of plot is that it shows the change in the figure of merit (in this case R95) as a function of a scale factor applied to the level of the error source under consideration. For example, Figure 5(a) shows that increasing the magnitude of the gyro drift errors in the AHRS configuration by a factor of 3.5 will approximately double the 95% radial position error at 3000 seconds. The information shown at the top of the figure is interpreted as follows. "Nominal R95 = 4.7736 nm" indicates that the 95% radial position error using the nominal error budget is about 4.77 nm. "Nominal sgyrob = 0.2" indicates that the normalization coefficient (nominal value) of the 1-sigma gyro drift error is 0.2 deg/hour. The "sensitivity at nominal" shows the dependence of the figure of merit (in this case R95) on small variations of the error source in question. Figure 5(a) shows that a small change (D) in the one-sigma gyro drift error in the AHRS configuration will produce a change of about 0.27 times D in the 95% radial position error at 3000 seconds. Figure 5(b) indicates that a similar change in the one-sigma gyro drift error in the INS configuration will produce a change of about 0.006 times D in the 95% radial position error. Hence, the INS is much less sensitive to changes about the nominal gyro drift error.

CONCLUSION

The performance simulation results combined with the results of trade-off analysis has led Honeywell to conclude that the F3 RLG inertial system should be selected over the DTG AHRS for the HINS advanced development model. In balance, the relatively small cost and weight penalties incurred by choosing the F3 RLG have been judged to be outweighed by the advantages gained in reversionary-mode accuracy and system MTBF. The anticipated large size of the maritime helicopter (weight not very critical) and the expected downward trend in RLG inertial system cost are additional factors which further support this recommendation.

In summary, the extensive analysis and simulation work carried out in the first phase of the HINS program has concluded with the definition of an advanced hybrid navigation system design which will satisfy the mission requirements of any new maritime helicopter. A system prototype will be built and tested in the next program phase prior to production procurement.

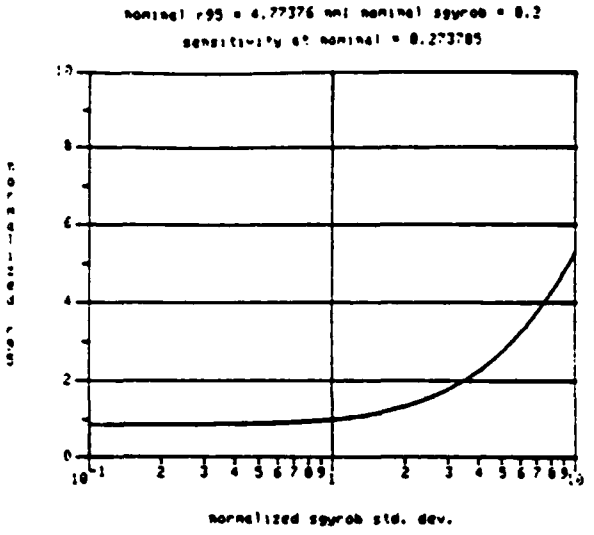

Figure 5a: Gyro Drift Error Sensitivity (AHRS)

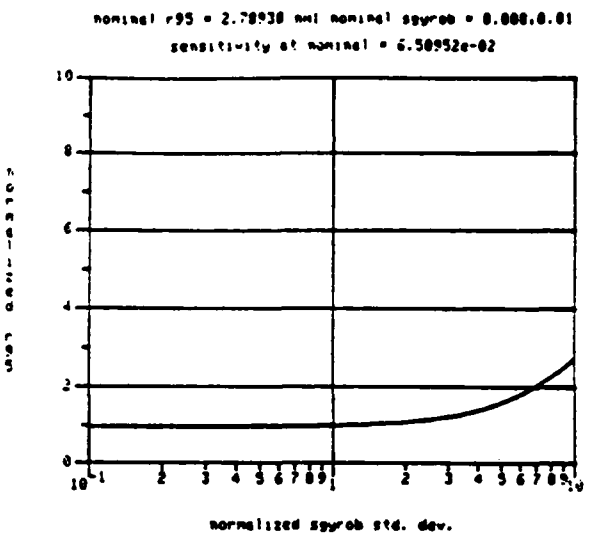

Figure 5b: Gyro Drift Eror Sensitivity (INS)

References and Bibliography

[1] Bierman, G.J. Factorization Methods for Discrete Sequential Estimation. New York: Academic Press, 1977.

[2] L.C. Vallot, J.K. Mahesh, S. Fingerote, W. Gesing, B. Reid, Helicopter Integrated Navigation System Feasibility Study, Report 005, Final Report. Submitted to Department of National Defence, 1985.

[3] W.S. Gesing, D.B. Reid, An Integrated Multisensor Aircraft Track Recovery System for Remote Sensing. IEEE Transactions on Automatic Control, Vol. AC-28, No. 3, 1983.

[4] D.B. Reid, W.S. Gesing, B.N. McWilliam, J.R. Gibson, An Optimally Integrated Track Recovery System for Aerial Bathymetry. IEEE Transactions on Aerospace and Electronic Systems, Vol. AES-19, No. 5, 1983.

Navigation Systems for the New Generation of Combat and Transport Helicopters and Associated Flight Tests

by

W. Hassenpflug, M. Bäumker

LITEF (Litton Technische Werke) der Hellige GmbH,
Lörracher Straße, D7800 Freiburg, Germany

1. Summary

The paper describes an integrated strapdown inertial helicopter navigator which is augmented by a doppler velocity sensor and a magnetometer. A radar altimeter is used to obtain height above ground. Accurate weapon delivery requirements and flight safety aspects while operating the helicopter under adverse weather conditions and at night demand the accurate determination of TAS throughout the entire speed regime.

Besides position, velocity and attitude, the strapdown system provides angular rates for stability augmentation and linear accelerations in bodyframe coordinates, inertial altitude and vertical speed from the doppler velocity sensor and the baro-inertial loop as well. The system communicates with the other avionics on board the helicopter through a dual MIL-STD 1553B bus and for redundancy purpose through an ARINC 429 interface with the AFCS directly.

Flight tests have been performed to demonstrate the navigation capability and performance of a doppler and flux valve augmented strapdown navigator, a new analytical true air speed system for the low speed regime and the performance of a strapdown magnetometer. The navigation performance has been verified in three different helicopters, a BO-105, a CH-53 and a Gazelle.

2. Introduction

Modern weapon systems such as the planned German-French PAH-2/HAP/HAC-3G and the NH-90/MH-90/SAR helicopters require an autonomous precise navigation system for enroute and highly dynamically NOE[1] flying.

The system architecture should allow the integration of GPS[2] as an option.

A cost effective solution to the autonomous 3D-navigation requirement for the motion envelope of a modern combat helicopter is the combination of a medium accurate velocity and heading augmented IRU[3] using a barometer and a radar altimeter for inertial vertical velocity and height above ground determination.

As weight is much more critical for helicopters than for any other airborne vehicle it is quite obvious that all the information required for stability augmentation and autopilot functions should be provided by the navigation system as well. The IRU must therefore be mechanized in strap down technology using small and lightweight two degree of freedom mechanical gyros and force balanced accelerometers. With a dual IRU installation a very high integrity for the flight safety critical portion of the system could be achieved.

Adverse weather, day and night operation and accurate weapon delivery requires the determination of TAS throughout the entire speed regime of the helicopter. As conventional pressure difference based methods are not applicable in the low speed regime (below 20 m/s) due to limited resolution of the available pressure differential measurement probes and the downwash, an analytical method[4] for the low speed regime has been

---

[1] Nap Of the Earth

[2] Global Positioning System

[3] Inertial Reference Unit

[4] patent applied

designed and flight tested[5].

A system beeing able to meet the requirements listed above includes the following equipments:

- ⊙ 2 Strap down IRU's
- ⊙ 1 Radar Altimeter (RAM)
- ⊙ 1 TAS system for the low speed regime
- ⊙ 1 Doppler Velocity Sensor DVS
- ⊙ 1 Magnetic Sensing Unit (MSU)
- ⊙ 1 TAS system for the high speed regime

The performance required by such a strapdown hybrid navigator is listed in table 2-1 below

Parameter		Range	Refresh-rate [Hz]	Accuracy (95 %) Requirement
Pitch	Θ	-30 ÷ 45°	50	.5°
Roll	Φ	± 90°	50	.5°
Heading	Ψ	360°	50	.5°
True Heading	Ψ^M	360°	50	.5°
Velocity along	v_x	-60÷+400km/h	50	.5%+.25kt
Velocity across	v_y	±50km/h	50	.5%+.25kt
Velocity vertical	v_z	±15m/s	50	.6%+.2 kt
geographic vertical	v_v	±15m/s	50	.6%+.2 kt
Ground speed	v_g	-60÷+400km/h	50	.5%+.25kt
Acceleration	a_x	±.5g	50	.01g
Acceleration	a_y	±.5g	50	.01g
Acceleration	a_z	-.5g÷+3.5g	50	.01g
Angu-	p	100°/s	50	.25°/s
lar	q	60°/s	50	.25°/s
rates	r	100°/s	50	.25°/s
Position(Enroute)	p.p		6.25	2%
Position(NOE)	p.p		6.25	300m/1/4 h
Drift	δ	±90°	6.25	1°
Wind	v_W	0÷+150km/h	6.25	1.2m/s
Direction	Ψ^W	±90°	6.25	1°
TAS	u^W	-25÷+100m/s	12.5	2m/s
	v	±14m/s	12.5	2m/s
	w	±15m/s	12.5	1m/s
Temperature static	T_o	-45÷+70°C	6.25	2°C+(T$_s$/100)
Static pressure	p_o	480÷1100mb	6.25	3mb
Height above ground	Z_{rs}	0÷2500ft	50	.5m o.5%
Target	WPT	±90°/±180°	12.5	0.5nm
Desired Track	DTK	0 ÷ 360°	6.25	1°
XTrack	XTK	±50km/h	6.25	1km
Track Angle Error	TKE	±100°	6.25	1°
Roll commanded	Φ_c	±30°	6.25	0.1°
Turnrate	$d\Psi/dt$	10°/s	12.5	0.6°/s

Table 2-1 Performance Requirements

Furthermore it is very much advisable to reduce the cost of ownership. This leads to highly reliable equipments and last but not least to a minimum use of special to type test equipment.

Normally magnetic sensors require a turntable for calibration and annual update of local magnetic variation. A calibration routine using a strapdown magnetometer has been designed[6] and flight tested which eliminates the need for calibration test equipment and logistic efforts for the annual update of magnetic variation.

An integrated helicopter navigator able to comply with the requirements listed above is described below. Its name is LHNS (Litef Helicopter Navigation System).

---

[5] LAASH (LITEF Analytical Air Data System for Helicopters)

[6] patent applied

3. LHNS Description

The LHNS is a heading- and velocity augmented SD-IRU, providing 3-D navigation information in conjunction with a radar altimeter and calculates the wind vector by means of a TAS system for the entire speed regime of the helicopter. The latitude range is ±80° (UTM range).

The on ground alignment time is

- ⊙ fixed base alignment time ≤ 2 min
- ⊙ moving base alignment time approx. 5 min

Angular rates and linear acceleration in the body frame coordinate system for flight control and weapon delivery purposes are supplied by the SD-IRU. The autopilot functions are supported by the following signals:

- Radar altitude	h_R	- Inertial altitude	h_i
- Doppler vertical velocity	v_{vD}	- Inertial vertical velocity	v_i
- Magnetic heading	Ψ_M	- True heading	Ψ
- Attitude	Φ, Θ	- Body velocities	v_x, v_y, v_z
- Velocities in the navigation frame	v_E, v_N, v_v		

Besides calculating the present position coordinates the following navigation functions are available:

- Bearing and Distance to the selected Waypoint
- Time to Go to this Waypoint based on the momentary speed
- Optimal steering information to the selected Waypoint
- Targets of Opportunity
- Position Update by flying over known landmarks whereby the position coordinates of these landmarks

- ⊙ are already stored
- ⊙ are read from the map and manually inserted after 'freezing' the position flown over
- ⊙ are gathered and inserted by means of a map-display after 'freezing' the position flown over

The position is calculated in geographical coordinates and will be distributed either in geographical or UTM coordinates depending on the crews request.

Coordinate insertion e.g. initial position coordinates and/or Waypoints could be accomplished in UTM or geographical coordinates as well.

Position coordinates calculated whilst landing are stored in an EEPROM and used as initial position coordinates prior to take off provided these coordinates

- ⊙ are not manually overwritten
- ⊙ are not automatically overwritten by GPS P-Code position
- ⊙ are not approximately identical with a stored waypoint

The LITEF designation of the SD-IRU is LHN-85, which uses two two degree of freedom DTG's[7] K-273 and three dry force balanced accelerometers B-280 together with the necessary instrument electronics and processing capacity to handle the strapdown and TAS algorithms, BITE, I/O handling, mode processing etc.

[7] Dry Tuned Gyroscope

With the two LHN-85 SD-IRU's in the LHNS the following features can be achieved:

- ⊙ triplex configuration for p and q
- ⊙ duplex configuration for r and a_1
- ⊙ probability of two flight critical axis simultaneously simplex below 10^{-5}
- ⊙ duplex navigation capability

The comprehensive BIT which takes care of the high failure detection rate has already been flight proven.

The programme proposed by LITEF to calculate true heading from magnetic heading measured through the proposed magnetometer is an improved version of the "MAG VAR" software already successfully in service with the close air support version of the ALPHA JET.

However the method to compensate for the rotation dependent and constant error sources which otherwise will very much reduce the accuracy of the heading determination differs considerably from the method used in the ALPHA JET programme. With this new method it is no longer necessary to centrally update for the annual change in magnetic variation (approximately 0.2° pa in middle europe).

The calibration method[8] proposed can be carried out by the average army/navy pilot in the field without any additional test equipment. Furthermore it is no longer necessary to carefully optically align the DVS and/or the MSU. This is valid for the initial installation and any subsequent installation required due to the exchange of units in the field.

This method is advantageous because

- there is no logistic effort for the annual update of the local magnetic variation
- there is no equipment required to optically align MSU and/or DVS
- there is no workload for the optical alignment of MSU and/or DVS

The land- and ship based operation of helicopters will require different calibration methods due to the larger iron masses aboard of ships. The calibration software in the LHNS could be made common for both versions.

In order to suppress high frequency emission which could cause premature detection both the RAM and the DVS will have the "RADAR SILENT" mode.[9]

The figures 3-1 ÷ 3-3 and the table 3-1 show the LHNS block diagram, the LHNS in- and output parameters, the LHNS interfaces and the most important installation parameters.

Figure 3-1 shows the basic LHNS for onboard autonomous navigation.

Figure 3-2 shows the modified LHNS with a GPS receiver and figure 3-3 shows a possible avionics architecture with the GPS receiver communicating with the helicopter avionics through the MIL-STD-1553B bus.

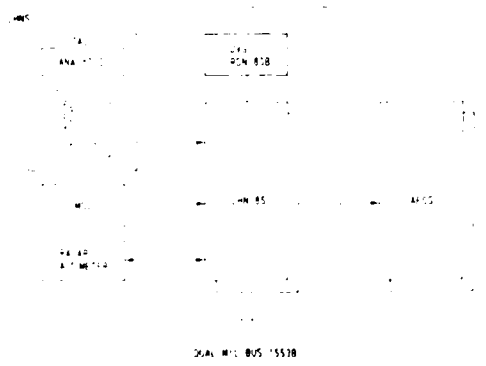

Figure 3-1 LHNS Block Diagram

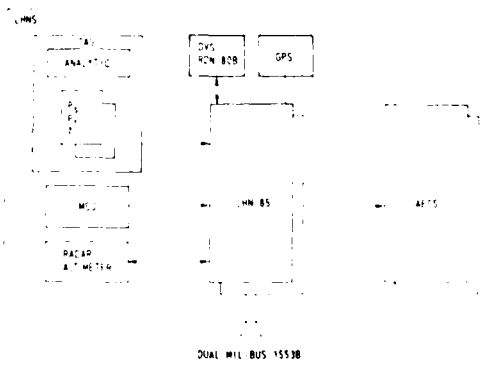

Figure 3-2 LHNS modified Block Diagram

[8] Patent applied

[9] this mode can be entered manually and/or automatically under software control

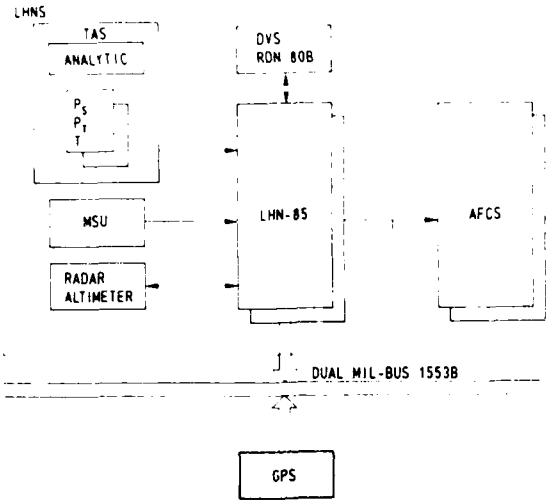

Figure 3-3 Block Diagram Avionics Architecture LHNS + GPS

Figure 3-4 displays the LHNS in- and output Parameters and figure 3-5 adds the GPS receiver as an input to the LHN-85 SD-IRU.

Map display and control- & display unit/functions are not part of the LHNS as to our understanding these functions are to be integrated into the multifunction display/keyboard equipment in the cockpit.

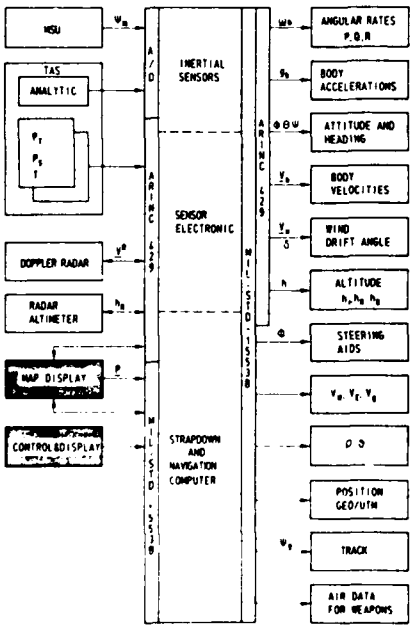

Figure 3-4 LHNS In- and Output Parameters

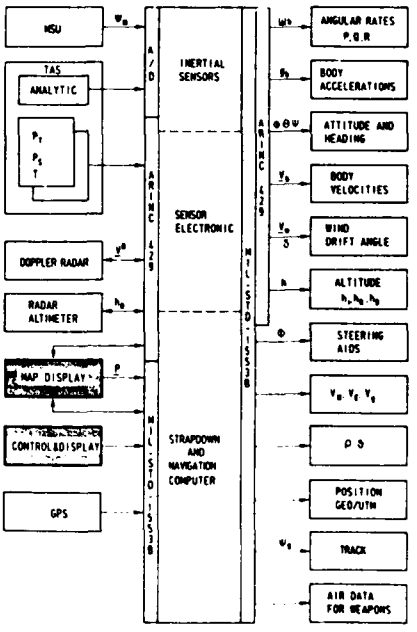

Figure 3-5 LHNS + GPS In- and Output Parameters

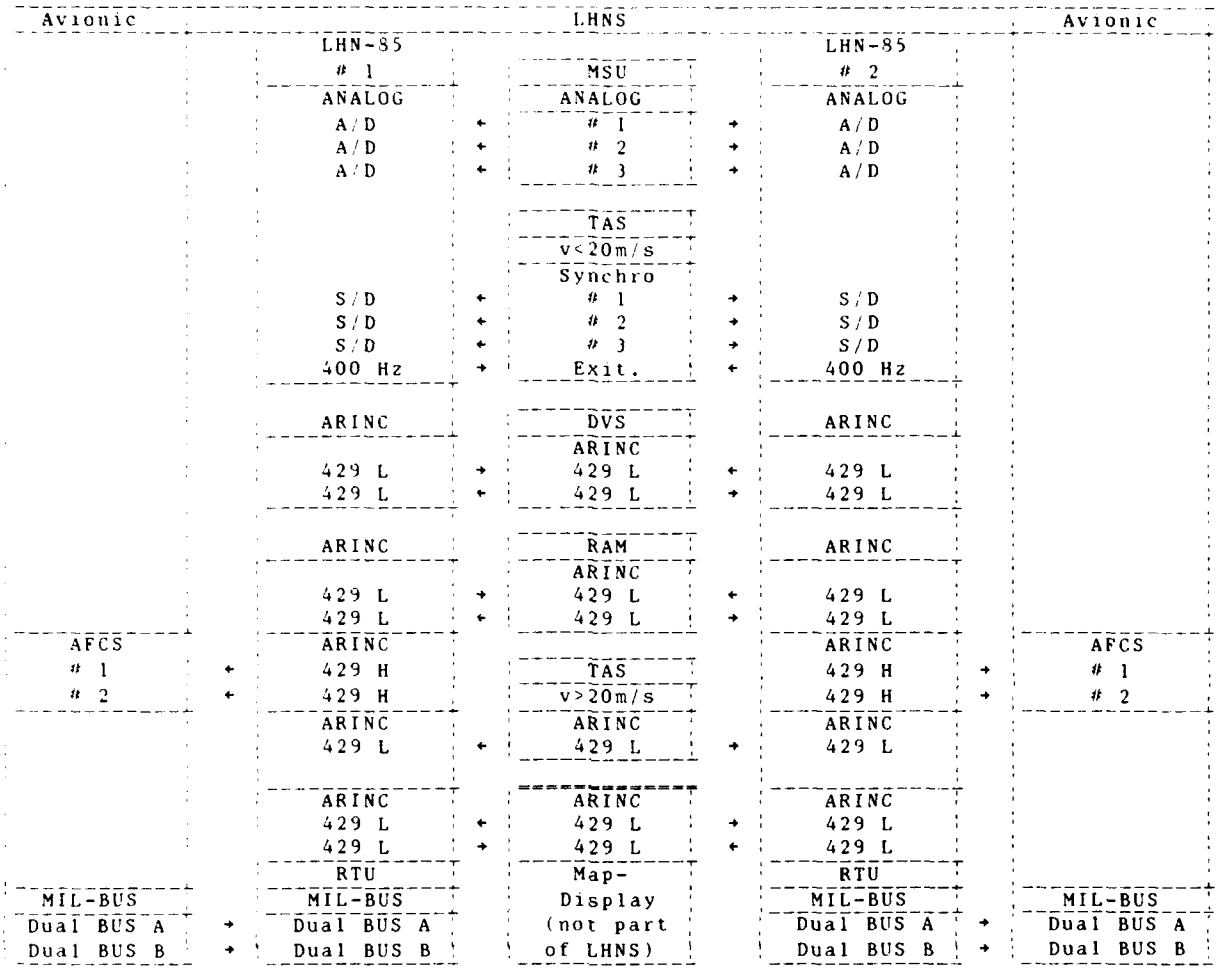

Figure 3-6 LHNS Interface Diagram

The interfaces of figure 3-6 show the flow of data, it is not an interwiring diagram.

Figure 3-6 does not show the interface to the GPS receiver which could be in accordance with MIL-STD-1553B or ARINC 429 or it could be fully integrated within the SD-IRU's.

Equipment/ Function	Designation	Housing (L,W,H)	Qty.	Mass [kg]	Power [W]
SD-IRU Mtg.prov.	LHN-85	4 MCU TBD	2 2	2x7.2 2x1.4	2x80
DVS	RDN 80 B	416x390x82	1	8.5	30
RAM	TBD	TBD	1	1.5	40
MSU	TBD	TBD	1	0.26	0.9
TAS v<20m/s	LAASH	na	1	0.16	≤ 1
TAS v>20m/s	TBD	2 MCU	1	3.2[10]	≤ 500[11]
Σ				30.82	

Table 3-1 LHNS Installation Parameters

[10] 2 Pitot-Static Tubes

[11] De icing Pitot-Static Tube

The housings of the LHN-85 and the conventional air data equipment are supposed to be in accordance with ARINC 600 using the relevant rear rack and panel connector.

The position of the LHN-85 in the helicopter is defined by the appropriate coding of four connector pins. This is necessary for the leverarm correction and the definition of the master IRU.

Reliability is very important and with the strap down technology a large and unexpected improvement was possible. Table 3-2 shows the reliability and the probability of failure for the individual equipments. These numbers are calculated in accordance with MIL-HDBK-217, but it should be mentioned, that the LTR-81 ARINC 705 strap down AHRS using the inertial instruments to be used in the LHN-85 SD-IRU has experienced a MTBF of more than 10.000 h within more than 400.000 equipment flying hours with the K-273 DTG's MTBF exceeding 139.000 hours.

Equipmment/ Function	Designation	QTY	Reliability	Probability of Failure
SD-IRU Mtg.prov.	LHN-85	2 2	.99999986 na	1.38×10^{-7} na
DVS	RDN 80 B	1	.99984	1.6×10^{-4}
RAM	TBD	1	.99972	2.85×10^{-4}
MSU	TBD	1	.99998	2×10^{-5}
TAS v<20m/s	LAASH	1	.999931	6.9×10^{-5}
TAS v>20m/s	TBD	1	.999875	1.25×10^{-4}

Table 3-2 LHNS Reliability Figures

Using the reliability figures listed above the probability of failure for the different modes of operation as navigation, stability augmentation and autopilot functions has been calculated and is listed in table 3-3 below.

Function	Param.	Probability of failure
Navigation	$pp(\phi,\lambda)$	1.8×10^{-4}
Stab.Augmentation	r	1.38×10^{-7}
	p,q	1×10^{-11}
Auto pilot	ϕ,θ	1.5×10^{-7}
	$\underline{a}$	1.4×10^{-7}
	h_i	7×10^{-5}
	v_i	7×10^{-5}
	Ψ	2×10^{-5}

Table 3-3 Probability of Failure

The navigation performance displayed in table 3.1-1 is based on the LHNS without GPS. Using GPS the position error will be limited to the GPS position accuracy depending on the code used.

3.1. Performance Parameters

Parameter		Range	Refresh-rate [Hz]	Accuracy (95 %) Requirement	LHNS
Pitch	Θ	-30 ÷ 45°	50	.5°	.25°
Roll	Φ	± 90°	50	.5°	.25°
Heading	Ψ_M	360°	50	.5°	.5°
True Heading	Ψ	360°	50	.5°	.5°
Velocity along	v_x	-60÷+400km/h	50	.5%+.25kt	.5%+.2kt
Velocity across	v_y	±50km/h	50	.5%+.25kt	.5%+.2kt
Velocity vertical	v_z	±15m/s	50	.6%+.2 kt	.2%+.1kt
geographik vertical	v_v	±15m/s	50	.6%+.2 kt	TBD
Ground speed	v_g	-60÷+400km/h	50	.5%+.25kt	.5%+.25kt
Acceleration	a_x	±.5g	50	.01g	.01g
Acceleration	a_y	±.5g	50	.01g	.01g
Acceleration	a_z	-.5g÷+3.5g	50	.01g	.01g
Angu-	p	100°/s	50	.25°/s	.2°/s
lar	q	60°/s	50	.25°/s	.2°/s
rates	r	100°/s	50	.25°/s	.2°/s
Position(Enroute)	p.p		6.25	2%	1.5%
Position(NOE)	p.p		6.25	300m/1/4 h	250m/1/4h
Drift	δ	±90°	6.25	1°	.5°
Wind	v_W	0÷+150km/h	6.25	1.2m/s	1.2m/s
Direction	Ψ_W	±90°	6.25	1°	1°
TAS	u	-25÷+100m/s	12.5	2m/s	2m/s
	v	±14m/s	12.5	2m/s	2m/s
	w	±15m/s	12.5	1m/s	1m/s
Temperature static	T_o	-45÷+70°C	6.25	2°C+|T_s/100|	2°C+|T_s/100|
Static pressure	p_o	480÷1100mb	6.25	3mb	3mb
Height above ground	Z_{rs}	0÷2500ft	50	.5m o.5%	.5m o.5%
Target	WPT	±90°/±180°	12.5	0.5nm	0.5nm
Desired Track	DTK	0 ÷ 360°	6.25	1°	1°
XTrack	XTK	±50km/h	6.25	1km	1km
Track Angle Error	TKE	±100°	6.25	1°	1°
Roll commanded	Φ_c	±30°	6.25	0.1°	0.1°
Turnrate	$d\psi/dt$	10°/s	12.5	0.6°/s	0.6°/s

Table 3.1-1 Performance Parameters

3.2. LHN-85

The LHN-85 SD-IRU uses two K-273 DTG's and three dry force rebalanced B-280 accelerometers. Figure 3.2-1 shows the LHN-85 Prototype

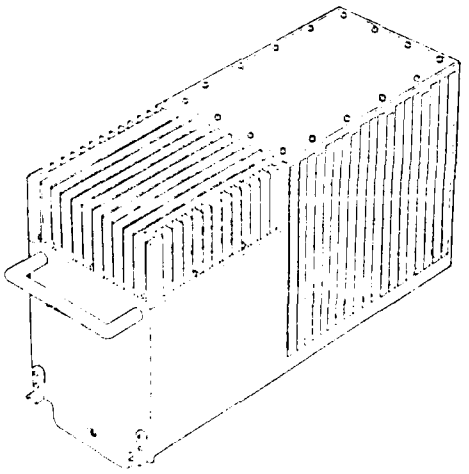

Figure 3.2-1 LHN-85

The main features of the LHN-85 are:

- 28 VDC input 80 Watts
- Arinc 429 I/O
- A/D converter to accept magnetometer- and aircraft controls input
- Duplex MIL-STD 1553B RTU
- MC 68000 family microprocessors
- 4 MCU housing with ARINC 600 mounting provisions

3.3. Control- & Display Unit

Modern combat & transport helicopters will have the control- and display functions required to operate the LHNS integrated into the MFD and MFK[12] of the cockpit. It is anticipated, that a map display is integrated as well.

3.4. LAASH

LAASH[13] is based on the experience that collective pitch represents the horizontal true airspeed of a helicopter in the low speed regime. This has been proven in many flight test hours with a BO-105[14]. Proper designed algorithms using along and across cyclic pitch information allow the determination of along and across TAS at an accuracy of approximately 2 m/s 95 % probability in the low speed regime up to 20 m/s.

To our knowledge these are worldwide the first flight tests with an analytical system of the accuracy class of 2 m/s 95 % probability. The VIMI system has not been designed to meet this accuracy requirement.

3.5. Doppler Velocity Sensor

The RDN 80 B is a three beam janus type FM/CW doppler velocity sensor manufactured by ESD. This DVS is widely used by the french armed forces[15] in most of their helicopters.

This DVS has already demonstrated an in service MTBF of more than 6.500 h in the military helicopter environment.

Figure 3.5-1 shows the RDN 80 B DVS

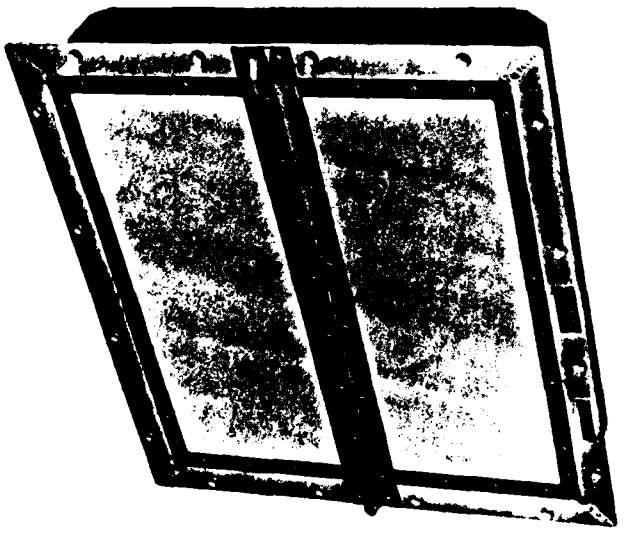

Figure 3.5-1 RDN 80 B Doppler Velocity Sensor

---

[12] MFD Multi Funktion Display / MFK Multi Funktion Keyboard

[13] patent applied

[14] These flight tests have been performed at the flight test center of the DFVLR (Deutsche Forschungs- und Versuchsanstalt für Luft- und Raumfahrt) in Braunschweig

[15] for navy application this DVS has a very high proven "false lock on" detection capability over calm water

3.6. Conventional Air Data System

At speeds above 20 m/s conventional air data sensors as pitot-static tubes and temperature probes can be used.

There are several manufacturers which have excellent experience in that field.

3.7. Radar Altimeter

Determination of "Height above Ground" requires the use of a radar altimeter. Frequency- and pulse modulated equipments are available on the market. These equipments operate in the C-band and the J-band as well. Generally the beam is a 40° cone.

Equipment selection will be based on price, performance and production experience.

3.8. Magnetometer

A three axis strapdown magnetometer[16] is proposed because the use of this device enables the customer to accomplish the instrument calibration without expensive test equipment and costly logistic provisions for the necessary annual update of the change in magnetic variation.

As there are many experienced suppliers available the best in price and quality can be selected.

4. Flight Tests

Flight tests have been performed to demonstrate

- ⊙ Navigation performance
- ⊙ Low air speed system performance (LAASH)
- ⊙ Strap down magnetometer inflight calibration procedures

In order to perform these flight tests, a LHN-81[17] was developed by modifying the software of the LTR-81 AHRU[18] (Attitude Heading Reference Unit) and subjected to three independent flight tests together with a DVS, a MSU and a Control- and Display Unit in accordance with ARINC 561. The tables 4-1 and 4-2 provides information about general flight test data and test results.

Helicopter		Location	Organisation	Test Purpose	Time Span
BO-105	(2.4t)	Braunschweig	DFVLR	Nav.	Sept.+Oct.1984
BO-105	(2.4t)	Braunschweig	DFVLR	LAASH	Feb.+March1985
BO-105	(2.4t)	Braunschweig	DFVLR	LAASH	Sept.+Oct.1985
BO-105	(2.4t)	Braunschweig	DFVLR	LAASH/ Magnetom.Nav.	May +June 1986
CH-53	(15t)	Manching	Erp.St.61	Nav.	Aug.+Sept.1985
Gazelle	(1.9t)	Brétigny	C.E.V.	Nav.	Oct.+ Nov.1985

Table 4-1 Flight Test Overview

---

[16] The required accuracy can be accomplished with a flux valve as well. See the flight test results.

[17] the LTR-81 hardware was kept unchanged

[18] designed for commercial airline use

Test Vehicle		BO-105	CH-53	Gazelle
Equipment under Test	SD-IRU	LHN-81 +	LHN-81 +	LHN-81 +
	DVS	AN/ASN 128 +	AN/ASN 128 +	RDN 80 B +
	MSU	Sperry P/N 658620	KEMS 802-1	KEMS 802-1
Testparameter				
Navigation	Enroute	1.3%[19]	1.01%[20]	1.58%[21]
	NOE	100m	299m	190m[22]
Attitude	Pitch	0.14°		
	Roll	0.29°		
Heading		1.05°	0.47°	0.89°
Velocity		1.18m/s		

Table 4-2 LHN-81 Navigation Flight Test Results[23]

As it could be seen the navigation requirements of table 3-1 are easily met by the equipment under test consisting out of the SD-IRU LHN-81 prototype, the DVS RDN 80 B or AN/ASN 128 and the MSU. During the entire flight test of more than 100 flight hours the equipment operated successfully without any complaints.

4.1. Navigation Performance

The navigation performance of the LHN-81 has been tested in three different helicopters at three test centres (see table 4-1). At the DFVLR in Braunschweig and at Erp.St.61 in Manching the navigation system under test consisted out of the LHN-81, a Doppler velocity sensor type AN/ASN 128 from Singer Kearfoot produced under license at SEL, and a flux valve. The tests at C.E.V. in Brétigny (France) were carried out using a Doppler velocity sensor RDN 80 B from E.S.D. Figure 4.1-1 demonstrates the interconnection of the individual devices including the control and display unit.

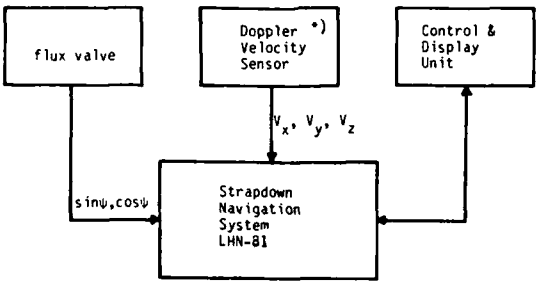

*) - at DFVLR and Erpr.St. 61: LDNS AN/ASN-128 (SEL)
- at C.E.V.: RDN 80 B (ESD)

Figure 4.1-1 System under Test Interconnection

The helicopters used are a BO-105, a CH-53, and a Gazelle. Figures 4.1-2, 4.1-3, 4.1-4, 4.1-5 and 4.1-6 are showing the different helicopters and the appropriate installations of the LHN-81 SD-IRU.

---

[19] calculated without assuming a normal distribution

[20] calculated according to STANAG 4278 (assuming a normal distribution)

[21] calculated without assuming a normal distribution

[22] related to 15 min duration

[23] all values 95 % probability

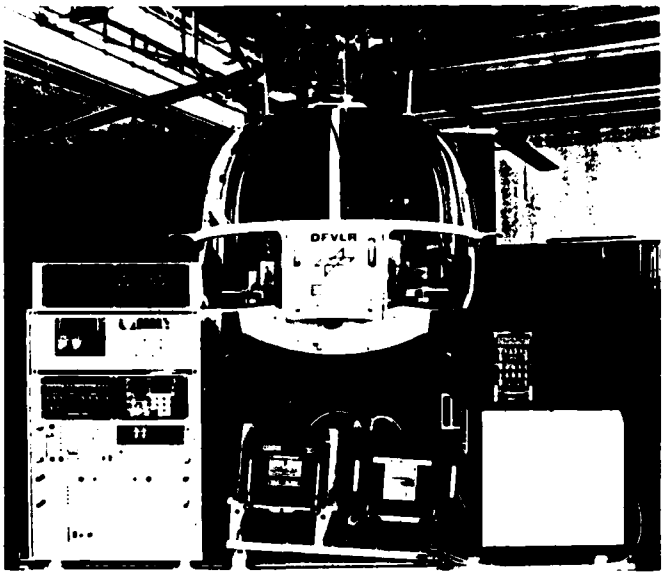

Figure 4.1-2 Flight Test Equipment in Front of the BO-105 used at DFVLR in Braunschweig

Figure 4.1-3 Helicopter CH-53 used at Erpr. St.61 in Manching

Figure 4.1-4 Installation of Flight Test Equipment in the CH-53

Figure 4.1-5 Helicopter Gazelle used at C.E.V. in Bretigny

Cockpit with CDU

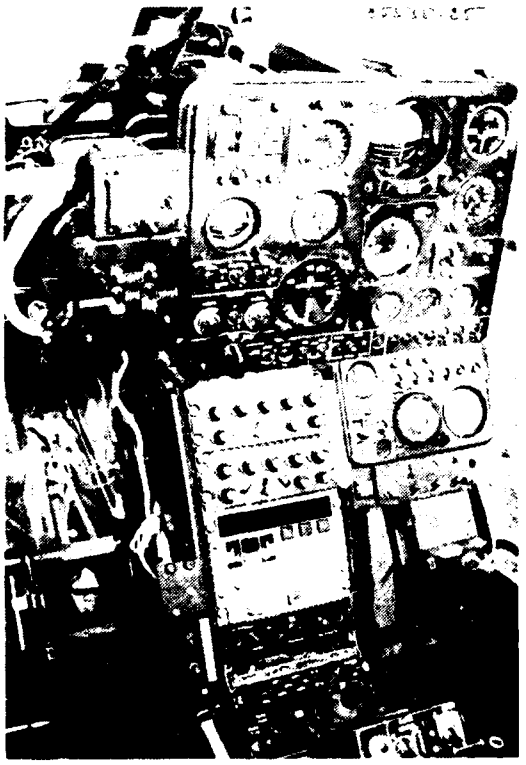

Installation Rack with LHN-81

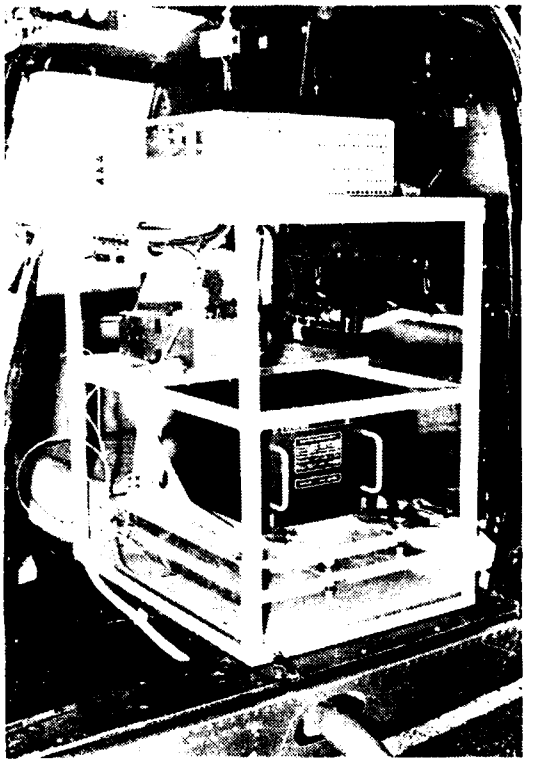

Figure 4.1-6 Installation of the Flight Test Equipment in the Gazelle

Due to the different helicopters in respect to their dynamic capabilities and their weights the LHN-81 had to be adapted to the various flight conditions. The necessary software changes mainly concerning the calibration, the cut-off-logic of the flux valve and the corresponding time constants. In Manching and in Brétigny a new flux valve calibration procedure, especially developed for an inflight calibration of a three axis strapdown magnetometer had been applied successfully. Most of the adaptation parameters have been derived from the results of a few test flights.

The purpose of the flight tests mentioned above was to demonstrate the navigation performance during cross country and high dynamic flights (NOE). The accuracies at Erp.St.61 and at C.E.V. were derived from the comparison of the position coordinates

provided from the hybrid navigator LHN-81 + DVS + MSU compared with the known coordinates of reference points flown over. The accuracies of the reference positions are declared to 20m up to 30m. At DFVLR the inertial laser gyro navigation system LTN-90 was used as a reference. At DFVLR the LHN-81 and the LTN-90 data were recorded with a frequency of 10 Hz by the MUDAS[24]. The accuracies of the LTN-90 position have been improved by post-flight filtering by a kalman filter algorithm using the velocities before take-off and after landing thus achieving a position accuracy of 50 m. Additionally the velocities, rates, heading and euler attitude angles have been recorded. The advantage of this data acquisition method is the large quantitiy of comparable data in contrast to the few values of the flight tests at Erp.St.61 and C.E.V., see table 4.1-1 below.

Therefore the statistical results particularly the result of the NOE-flights had to be treated very carefully.

Furthermore the statistical methods used by Erp.St.61 and by C.E.V. are quite different.

Thus the computation of the 95% values at Erp.St.61 are based upon a hypothetically assumed two dimensional normal distribution[25] of the postion errors whereas at DFVLR and at C.E.V. the overall results are independent of an a priori assumed error distribution. To get comparable results the values accomplished at Erp.St.61 and C.E.V. have been computed according to both methods.

test center	navigation		tactical flight	
	no. of flights	no. of comp. data	no. of flights	no. of comp. data
DFVLR	8	190800	1	8400
Erp.St.61	8	29	4	4
C.E.V.	5	37(44*)	4	8

*): including outliers

Table 4.1-1: Number of Test Flights and Comparable Data

4.1.1. Performance during Cross Country Flights

The navigation performance of the hybrid system is expressed in terms of position error relative to the distance travelled.

At DFVLR in Braunschweig additionally the accuracies of the heading and attitude angles as well as of the velocity could be computed. These values (95% probability) flown in 8 navigation flights are listed in table 4.1.1-1. Summarizing the individual results, relative navigation accuracies of 1.3% of the distance travelled, a heading accuracy of 1.05°, and a velocity accuracy of 1.18 m/s are observed. The corresponding graphs are displayed in figures 4.1.1-1, 4.1.1-2 and 4.1.1-3.

flight no.	heading accuracy [°]	pitch angle accuracy [°]	roll angle accuracy [°]	velocity accuracy [m/s]	rel. position accuracy [%]
21	0.64	0.14	0.33	1.07	0.85
22	1.49	0.13	0.28	1.16	1.74
23	1.09	0.13	0.26	1.08	0.91
24	1.30	0.11	0.27	1.58	0.79
26	0.75	0.13	0.25	1.05	0.84
27	0.89	0.15	0.29	1.19	1.40
28	[illegible]	0.13	0.29	1.36	1.03
30	0.74	0.17	0.3_	1.01	1.20
overall	1.05	0.14	0.29	1.18	1.30

Table 4.1.1-1: Accuracies (95% probability) of the Cross Country Flight Test at DFVLR

[24] Modular Data Aquisition System

[25] see STANAG 4278

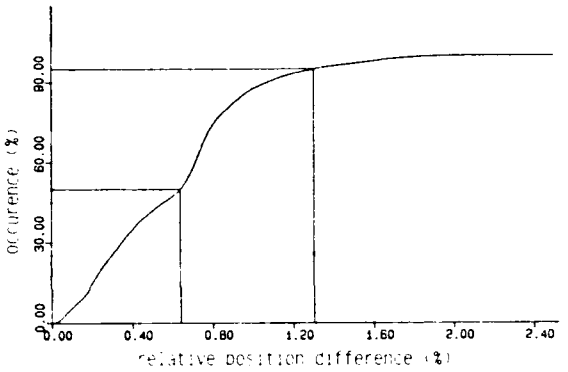

Figure 4.1.1-1 Distribution of the Relative Position Differences (Cross Country Flights at DFLVR)

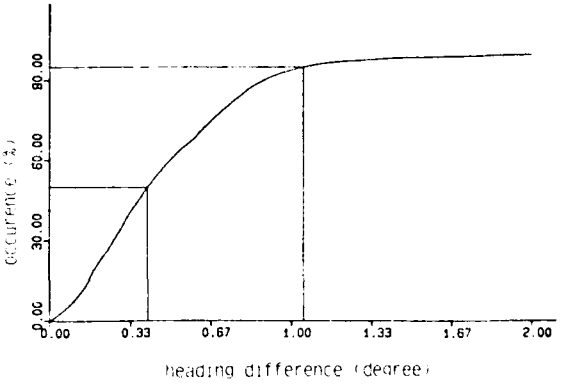

Figure 4.1.1-2 Distribution of the Heading Differences (Cross Country Flights at DFVLR)

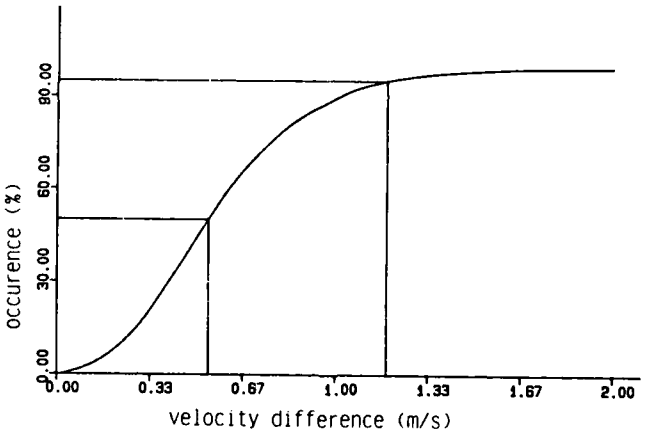

Figure 4.1.1-3 Distribution of the Velocity Differences (Cross Country Flights at DFVLR)

At Erp.St.61 in Manching the navigation accuracy of the LHN-81 has been demonstrated during 8 navigation flights. 4 of them are obtained flying a small triangle of approximately 150 km total length and 4 of them flying a large triangle of ~ 500 km total length.
The 29 individual results computed from the position differences at the reference points of the triangles are listed in table 4.1.1-2. The relative position differences are seperated in an along and an across track error.

Flight No. Date	Section	Distance [km]	Along Track Error [%]	Across Track Error [%]	Rel. [%]
11	1	57.8	0.034	-0.396	0.397
9.9.85	2	56.6	-0.190	-0.701	0.726
	3	32.9	-0.057	0.801	0.803
13	1	32.9	0.183	0.797	0.818
10.9.85	2	56.6	-0.074	-0.311	0.320
	3	57.8	-0.051	-0.462	0.465
15	1	57.8	-0.091	0.245	0.262
11.9.85	2	56.6	0.059	0.605	0.608
	3	32.9	0.088	0.343	0.354
17	1	32.9	0.070	0.696	0.699
11.9.85	2	56.6	-0.004	-0.269	0.269
	3	57.8	0.145	-0.280	0.315
21	1	57.8	0.027	-0.033	0.043
	2	115.5	-0.045	-0.138	0.146
16.9.85	3	106.5	0.042	0.060	0.073
	4	141.0	-0.078	-0.206	0.220
	5	57.7	0.008	-0.231	0.232
22	3	106.5	-0.035	-0.598	0.599
17.9.85	4	115.5	0.080	-0.700	0.705
	5	57.8	0.022	-1.067	1.068
24	1	57.8	0.102	-0.553	0.563
	2	115.5	0.006	-0.148	0.149
18.9.85	3	106.5	0.075	0.052	0.091
	4	141.0	-0.066	-0.285	0.292
	5	57.8	-0.038	-0.237	0.240
25	2	141.0	0.059	0.601	0.604
	3	106.5	0.177	-0.825	0.844
19.9.85	4	115.5	0.055	-0.287	0.293
	5	57.8	0.041	0.735	0.736

Table 4.1.1-2 Individual Results of the Cross Country Flights at Erp.St.61

The across track error can additionally be used for indirectly computing the heading error. As mentioned above the quantity of 29 individual results is quite a small number to compute statistical reliable values. Using the method of Erp.St.61 assuming a normal distribution, a relative position accuracy during cross country flights of 1.01% (95% probability) is obtained. With contrast to this method the individual results are summarized in figure 4.1.1-4. The application of this method free of a priori assumptions yields in a relative navigation accuracy of 0.83% thus showing the a priori assumption not beeing valid. The corresponding heading accuracy derived from the across track errors amounts to 0.47° (95% probability) including a systematic heading error of only -0.05°, and demonstrates the successfully employed flux valve calibration method. The accompanying graph is given in figure 4.1.1-5.

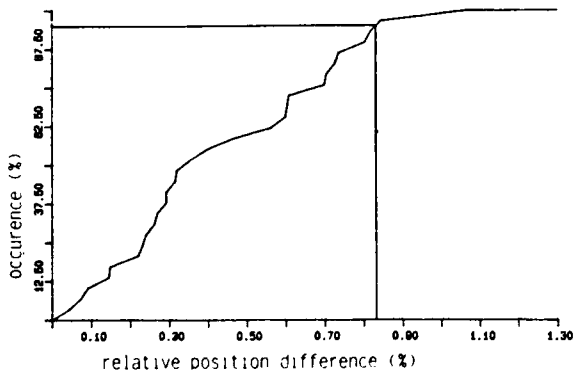

Figure 4.1.1-4 Distribution of the Relative Position Differences (Cross Country Flights at Erp.St.61)

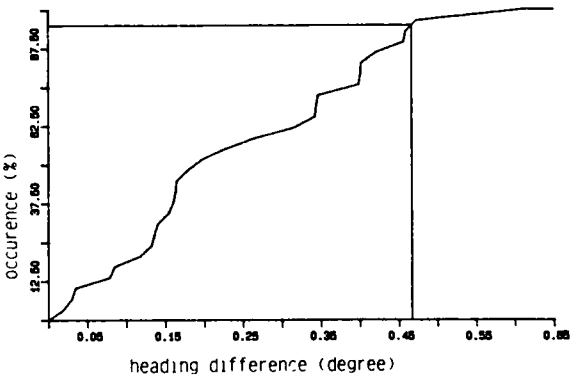

Figure 4.1.1-5 Distribution of the Heading Differences (Cross Country Flights at Erp.St.61)

The navigation accuracy of the LHN-81 was tested at C.E.V. in Brétigny using an east-west-profile consisting of 6 reference points (total length: 127 km), a north-south-profile consisting of 6 reference points (total length: 124 km) and a circle course including 5 reference points (total length: 126 km).

Due to light weight (1.9 t) and the high dynamic range of the helicopter used, the cut-out-logic and the filter constants of the flux valve disturbed evidently by the dynamics, had to be importantly modified.

Flight No. Date	Section and Direction	Distance	Along Track Error [%]	Across Track Error [%]	Rel. Error [%]
9	1 E -> W	26.0	-0.412	-0.477	0.628
13.11.85	2 E -> W	32.8	-0.186	0.210	0.282
East-	3 E -> W	24.8	-0.367	0.585	0.689
West-	4 E -> W	43.4	-0.445	0.394	0.594
East	4 W -> E	43.4	-0.433	0.864	0.965*
	3 W -> E	24.8	-0.294	1.560	1.585*
	2 W -> E	32.8	-0.262	1.552	1.573
	1 W -> E	26.0	-0.527	1.039	1.164
10	1 N -> S	33.9	-0.018	0.693	0.694
13.11.85	2 N -> S	33.5	-0.051	0.516	0.519
North-	3 N -> S	25.2	0.119	0.226	0.256
South-	4 N -> S	31.5	-0.248	1.168	1.196*
North	4 S -> N	31.5	0.016	1.737	1.738*
	3 S -> N	25.2	-0.230	2.333	2.347
	2 S -> N	33.5	0.069	1.012	1.014
	1 S -> N	33.9	-0.230	0.086	0.246
16	1 E -> W	26.0	-0.300	1.104	1.140
22.11.85	2 E -> W	32.8	-0.327	0.466	0.570
East-	3 E -> W	24.8	-0.145	-0.081	0.167
West-	4 E -> W	43.4	-0.394	0.138	0.417
East	4 W -> E	43.4	-0.150	0.813	0.827*
	3 W -> E	24.8	-0.226	0.891	0.917*
	2 W -> E	32.8	-0.198	1.482	1.494*
	1 W -> E	26.0	-0.538	1.262	1.368
11	1 ccw	24.7	-0.150	-0.798	0.813
14.11.85	2 ccw	33.0	-0.142	0.939	0.949
Rund-	3 ccw	22.0	-0.059	0.832	0.834
kurs	4 ccw	23.1	-0.420	0.545	0.689
	5 ccw	23.4	-0.145	-0.376	0.405
	5 cw	23.4	-0.013	0.603	0.603
	4 cw	23.1	-0.329	0.238	0.407
	3 cw	22.0	-0.123	-0 795	0.806
	2 cw	33.0	-0.161	0.255	0.300
	1 cw	24.7	-0.255	1.008	1.043
12	1 ccw	24.7	0.053	-0.073	0.091
14.11.85	2 ccw	33.0	-0.106	0.470	0.481
Rund-	3 ccw	22.0	0.377	-0.345	0.512
kurs	4 ccw	23.1	-0.294	0.134	0.324
	5 ccw	23.4	-0.239	-0.419	0.481
	5 cw	23.4	-0.141	-0.192	0.239
	4 cw	23.1	-0.238	-0.069	0.250
	3 cw	22.0	-0.023	-0.145	0.146
	2 cw	33.0	-0.106	1.185	1.190
	1 cw	24.7	-0.231	1.053	1.080

ccw: counter clockwise, cw: clockwise, *: outliers

Table 4.1.1-3 Individual Results of the Cross Country Flights at C.E.V.

The 44 individual results of the navigation flights at C.E.V. are listed in table 4.1.1-3. Assuming a normal error distribution relative navigation error of 1.38% to the mean and 1.75% to zero are obtained. The assumption free value amounts to 1.58%. The discrepancies between these values are cuased by systematic errors of the navigation system. Regarding the individual values a significant deterioration of the across track errors can be observed after the turns at the north-south and the east-west flights. A detailed examination has shown that the cut-out-logic of the flux valve was not active which leads to an important heading error. Due to the time constant in the flux valve augmented navigation system this error did not effect immediately the heading of the

navigation system.

By eliminating the so caused outliers, a navigation accuracy of 1.15% is obtained. This value corresponds to the value of 1.18% calculated by assuming a normal distribution. The heading accuracy amounts to 0.64° including a systematic heading error of only 0.15°. The graphs showing the navigation results at C.E.V. are displayed in Figure 4.1.1-6 and Figure 4.1.1-7.

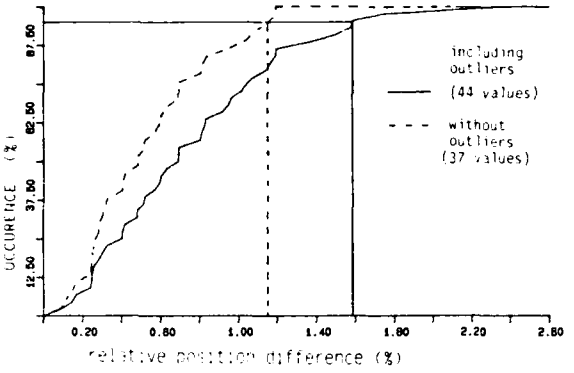

Figure 4.1.1-6 Distribution of the Relative Position Differences (Cross Country Flights at C.E.V.)

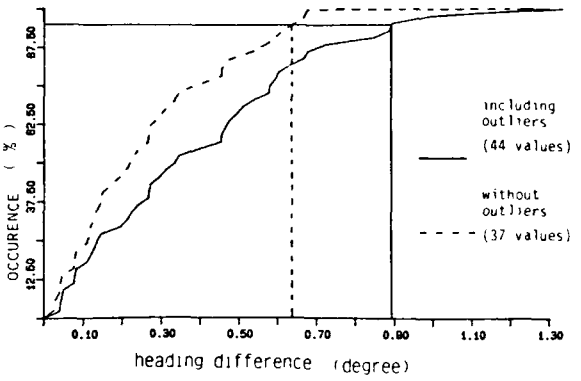

Figure 4.1.1-7 Distribution of the Heading Differences (Cross Country Flights at C.E.V.)

4.1.2. Tactical Flight

The 2nd purpose of the flight trials was to demonstrate the performance of the navigation system during a high dynamic tactical flight (NOE).

With contrast to the navigation flights, here the absolute position differences after a 15 min tactical flight was the essential evaluation criteria. At DFVLR and at Erp.St.61 the tactical flights exactly ended after 15 min while the tactical flights at C.E.V. differed in their duration. Each tactical flight at C.E.V. consisted of a tactical approach to a known waypoint from which the target point had been attacked.
The individual results of the tactical flights at DFVLR, at Erp.St.61 and at C.E.V. are listed in table 4.1.2-1. The time dependent values are summarized to a mean 15 min-value assuming a primary time dependent error model. The mean accuracies are 100m at DFVLR, 298m at Erp.St.61 and 190m at C.E.V. after a 15 min tactical flight.

	DFVLR Braunschweig	E61 Manching	C.E.V. Bretigny
individual results (after 15 min)	100 m	24 m 39 m 56 m 88 m (14^m06^s)	83 m (19^m30^s) 299 m 135 m (15^m00^s) 56m (29^m46^s) 124 m (28^m00^s) 61 m (15^m28^s) 312 m (35^m49^s)
CEP 95%	100 m	298 m	190 m [1]
1) related to 15 min duration			

Table 4.1.2-1: Results of the Tactical Flights

4.2. Low Air Speed System Performance

As conventional pressure and temperature based air data systems are not usable to the low speed regime of helicopters ($|v| < 20$ m/s), new measurement techniques had to be developed.

It was decided to investigate whether an analytical method based on the helicopter control signals collective and longitudinal and lateral cyclic pitch can be designed to comply with the accuracy requirement of 2 m/s 95 % probability.

In order to get a suitable data base to carry out the investigation in mind, an appropriate flight test was designed to collect the data shown in figure 4.2-1.

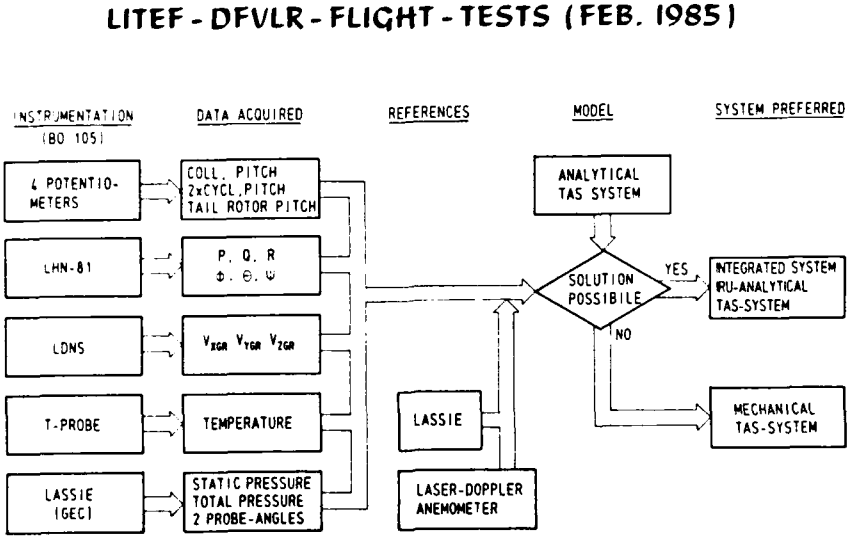

Figure 4.2-1 Block Diagram Data Collection

This flight test was performed during February/March 1985 at DFVLR in Braunschweig utilising their BO-105 with the data recording system already described.

After having analyzed the data gathered during this flight test, it was found that an analytical low air speed system could be mechanized to fulfill the accuracy requirements mentioned above. In order to verify the algorithms used a specific calibration procedure to the type of helicopter used had to be designed.

This calibration procedure was applied to the BO-105 of DFVLR in September/ October 1985.

The next step in the design of LAASH was the implementation of the LAASH algorithms into a LHN-81 SD-IRU and to perform appropriate flight tests for the necessary verification. This flight test was carried out during May/June 1986 at DFVLR using their BO-105 again. As of the time writing this paper the test data has not been fully analyzed. Preliminary analysis indicate satisfactory results.

4.3. Flux Valve Calibration

As the navigation flight test results of the hybrid navigator LHN-81 + DVS + MSU have shown the navigation accuracy mainly depends on the accuracy of the heading sensor used for augmentation.

During the flight tests at DFVLR, Erp.St.61 and C.E.V. a standard flux valve[26] was used. Like any magnetic field detector, the flux valve had to be compensated for magnetic materials in the airborne vehicle causing constant and cyclic heading errors.

Due to the sensitivity of the flux valve in respect to vibration and dynamics the compensation has to be made on ground.

The magnetic or geographic reference directions used were reference lines on the ground (at DFVLR and Erp.St.61) or a compass integrated in a theodolite (at C.E.V.).

---

[26] horizontal magnetic field only

The reference direction was transferred via plumbing or via a theodolite to the center line of the helicopter.

The flux valve corrections were carried out per software using the calibration function

$$\psi_{cor} = \psi + A + B \cdot \sin(\psi+\rho_1) + C \cdot \sin(2\psi+\rho_2).$$

The first flight test at DFVLR has shown that after such a compensation a constant heading error of about 1° remained in the navigation results. This effect is caused by mounting errors of the flux valve and of the doppler velocity sensor around the yaw axis of the helicopter.

As true north was required in the navigation equations, additional error sources are incorrect tables for magnetic variation or local and temporary anomalies of magnetic variation.

Therefore a new flux valve calibration procedure developed for a three axis strapdown magnetometer has been employed in the following flight tests at Erp.St.61 and at C.E.V.

In a first step the new procedure only compensates for the cyclic errors of the flux valve as usual. In a second step the constant heading error is calculated from the across track position differences measured during a calibration flight with the navigation system.

For optimal accuracy it is very much advisable to take redundant measurements by flying along a large enough triangle clockwise and counterclockwise to find the constant correction term from the differences at the corner points of that very reference triangle.

Using this procedure the constant heading errors could be reduced from about 1° to -0.054° at Erp.St.61 and to 0.15° at C.E.V.

In the same way the heading error (95% probability) has decreased from 1.05° to 0.47° at Erp.St.61 and 0.64° at C.E.V. The excellent result at Erp.St.61 is additionally influenced by the low dynamics of the CH-53 helicopter because the percentage augmentation time of the flux valve during the calibration and navigation flights was higher than in the highly dynamic helicopters Gazelle and BO-105.

4.4. Three Axis Strapdown Magnetometer

As can be seen on the results of the LHN-81 flight tests a well calibrated flux valve is able to reduce the heading errors to 0.5° (95% probability).

The disadvantages of the standard flux valve are:

- no inflight-calibration capability
- high noise
- requires specific adaptation to the type of helicopter
- highly sensitive to dynamics
- very little relative augmentation due to dynamics

A three axis strapdown magnetometer eliminating the a.m. disadvantages of a flux valve will be used in further applications.

Preliminary results with a three axis strapdown magnetometer have been obtained during laboratory and flight test in May 1986 at DFVLR in Braunschweig.

The goal of the magnetometer flight test was to develop a suitable inflight-calibration procedure and to test the accuracy of a magnetometer calibrated accordingly. The tests have been performed with two magnetometers which were installed at the tail of a BO. As reference a LTN-90 laser gyro inertial navigation system was used.

A three axis strapdown magnetometer measures the earth magnetic field in the vehicle coordinate frame of the vehicle. These components need to be transformed to attitude angles in the horizontal coordinate system so that an attitude determination yielding roll and pitch angles becomes necessary. The horizontal components then will be used for the heading computation.

Furthermore besides the cyclic heading-dependent errors, the roll and pitch errors need to be compensated for. This is done in accordance with the procedure by the calibration functions which eliminate the roll and pitch errors

AD-A191 464 ADVANCED IN GUIDANCE AND CONTROL SYSTEMS AND TECHNOLOGY 2/2
(U) ADVISORY GROUP FOR AEROSPACE RESEARCH AND
DEVELOPMENT NEUILLY-SUR-SEINE (FRAN CE) JUL 87
UNCLASSIFIED AGARD-CP-411 F/G 17/11 NL

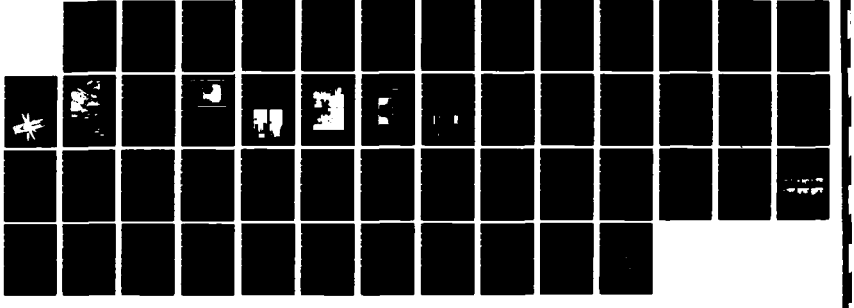

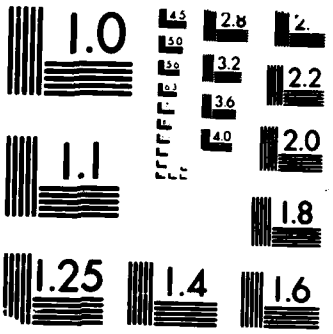

$$T_i^{cal} = T_i + A_i + B_i \cdot \sin\psi + C_i \cdot \cos\psi + D_i \cdot \phi + E_i \cdot \phi^2 + F_i \cdot \theta + G_i \cdot \theta^2$$

$$i = X, Y, Z.$$

where

ψ: Heading ϕ: roll angle θ: pitch angle

The calibration coefficients are calculated during a special calibration manoeuvre of the helicopter.

At the magnetometer flight test several calibration manoeuvres have been examined. For these purposes the magnetometer signals have been recorded via the MUDAS with a frequency of 20 Hz.

The necessary roll and pitch angles as well as the reference heading was provided in the same way from the LTN-90. First noise examinations of the magnetometer signals have shown that the inflight noise is mainly caused by the helicopter dynamics and vibrations:

Brand x: 70 n Tesla ($\hat{=}$ 0.2° in respect to heading)

Brand y: 100 n Tesla ($\hat{=}$ 0.4° in respect to heading)

(based upon a horizontal magnetic field intensity of 20.000 n Tesla).

The noise can be decreased to less than 35 n Tesla ($\hat{=}$ 0.1°) by appropriate filtering.

A suitable calibration function is a circular flight clockwise and counter clockwise with different bank angles and with additional pitch manoeuvres.

Due to dynamic effects and roll and pitch angle errors the measurement range of a magnetometer should not exceed 20° attitude angle respectively angular rates of 5°/s.

With the above mentioned manoeuvres the primarily uncompensated heading error (1σ) of the magnetometers could be reduced from 2.6° (brand x) and 1.3° (brand y) to 0.26° (brand x) and 0.39° (brand y). The corresponding 95% probability values are 0.41° (brand x) and 0.61° (brand y). The inflight calibration time was approximately 14 minutes.

In a second step the calculated calibration coefficients are used to correct the magnetometer signal during

- a navigation flight (enroute)
- a Nap of the Earth flight (NOE)
- a procedure turn clockwise and counter clockwise.

The results achieved with the calibrated magnetometers are listed in table 4.4-1. The cut-off limits of the magnetometer signals were set to angular rates of 5°/s. The important result is that the magnetometer augmentation can also be used during NOE-flight (percentage augmentation ~70%) and a procedure turn (~82%) where a conventional pendulous flux valve cannot be used for augmentation during these manoevres at all. The accuracy can be improved by additional filtering and a different setting of the cut-off limits. The preliminary analysis shows that a heading accuracy of 0.5° (95% probability) can easily be achieved with a properly calibrated magnetometer utilizing a suitable inflight calibration procedure.

	enroute flight	NOE flight	procedure turn
elapsed time	45 min	53 min	13.5 min
perc.augmentation	85%	70%	82%
$\delta\psi$ (brand x) 1σ bef.cal.	2.4°	2.1°	3.0°
$\delta\psi$ (brand x) 1σ after cal.	0.33°	0.47°	0.53°
$\delta\psi$ (brand x) 95% after cal.	0.55°	0.69°	0.84°
$\delta\psi$ (brand y) 1σ bef.cal.	1.15°	1.52°	1.3°
$\delta\psi$ (brand y) 1σ after cal.	0.33°	0.38°	0.36°
$\delta\psi$ (brand y) 95% after cal.	0.56°	0.59°	0.64°

Table 4.4-1: Heading Errors ($\delta\psi$) before and after Magnetometer Calibration

5. Acknowledgements

The autors wish to express their thanks to all participants of the various flight test campaigns and especially to the involved members of the Institut für Flugführung der DFVLR in Braunschweig, the Erprobungsstelle 61 der Bundeswehr in Manching, Dezernat 125 and AFB FE, the BWB[27] Referat FE V/5, and the C.E.V[28] Section Essais Equipments.

6. References

M.Bäumker[*]
W.Hassenpflug[*]
Autonomous Navigation Systems for the New Generation of Military Helicopters and Associated Flight Tests. Twelfth European Rotorcraft Forum Sept. 1986.

W.Hassenpflug[*]
R.Schwäble[÷]
A New Method of Analytical Evaluation of Helicopter True Airspeed. Twelfth European Rotorcraft Forum Sept. 1986.

Flugerprobung eines hybriden Navigationssystems für Hubschrauber LHN-81, LITEF Dokument 116198, März 1986

M.Kleinschmidt[*]
LHN-81 Strapdown Navigationssystem, Flug Test Report LITEF Doc.No. 115058-1 April 1985

H.-J.Hotop[α]
M.Kleinschmidt[*]
H.-P.Zens[α]
Flight Test of a Velocity Augmented Strapdown Navigation System LHN-81. DGON Symposium Gyro Technology 1985 Stuttgart, Germany.

[*] LITEF
[÷] Krupp Atlas Elektronik GmbH, formerly LITEF
[α] DFVLR Braunschweig, Institut für Flugführung

---

[27] Bundesamt für Wehrtechnik und Beschaffung Koblenz

[28] Centre des Essais en Vol Brétigny

JET REACTION CONTROL SYSTEM FOR AUTONOMOUS PRECISION MUNITION

by

Dr H.Peller and S.Büchele-Buecher
Guided Munition Department
Rheinmetall
4000 Düsseldorf, Ulmenstr. 125
Federal Republic of Germany

SUMMARY

This paper is presented as an introduction into actuation systems. The first part features the essential differences between missile and projectile application which are very important for actuation system designs. A following short trade study compares two methods of steering missiles and projectiles using aerodynamic or impulsive control, where the last mentioned one will be presented more exactly.

The described hot gas reaction jet control actuation block is mounted in a submunition called 'EPHRAM' which stands for terminal guided artillery munition. In this actuation system the gases produced by a gas generator are controlled by four individual thrusters. All these important and necessary components of a jet reaction control are explained and demonstrated by photographs and figures. Results of computer computation and simulation will finally verify that jet reaction control is the ideal application for such a cannon-launched guided projectile.

1. INTRODUCTION

We wish to present a concept of a jet reaction control system for a guided submunition. This submunition, which is a part of a 155 mm artillery projectile is capable of searching and detecting, tracking and destroying hard armour targets.

2. PROJECTILE SPECIFICATION AND DEMAND

In the first part of the presentation (figure 1) the essential differences between cannon launched projectiles and missiles are demonstrated. In order to provide a gun hardened projectile it is necessary to do some technical effort on the structure. This however will lift up mass of the projectile in contrast to missiles. The mechanical complexity of rocket systems is much lower than in artillery systems, because the wings must be unfolded just after leaving the tube. Moreover many other subsystems must be activated after the high acceleration phase.

We have to note three important accelerations during launch phase (figure 2):

- The axial acceleration of about 15.000 g
- The lateral acceleration of about ± 1.000 g
- The radial acceleration of about 300.000 rad/s²

The last one corresponds to a spin rate of 250 Hz at the muzzle. These specifications of cannon launched projectiles are contrary to the limited volume. Nevertheless the projectile has one big advantage in contrast to missiles and that is the very small dispersion.
The different possibilities of producing lateral forces are shown in figure 3.

3. ACTUATION SYSTEM TRADE STUDY

Figure 4 describes the trade study using the basic technology of impulsive and aerodynamic submunition concepts. The key feature of an impulsive, i.e. jet reaction control system is that it allows a very flexible submunition design and can be suitably adapted to the specific volume restrictions of a guided projectile. The positions and the diameter of the warhead and seeker can be optimally chosen and are not affected by wing and fin control actuating device volume. The low overall complexity of a jet reaction control system provides a high g survivability. The basic features of this system together with the potential of producing high thrust over a long duration indicate that only a jet reaction control system allows for an optimal submunition design, when the duration of the terminal guided flight is shorter than about 20 seconds. Concerning the cost of impulsive control systems in terminal guided projectiles, there are several low-cost impulsive control devices available, which depend on the wanted hit probability.

One viewgraph (figure 5) shows a pictorial representation of two basically different impulsive reaction control concepts: Controlled thruster devices and discrete charge arrangements. Within controlled thrust devices, a second decision must be made - whether to apply mechanical switching technology (figure 6) or a fluidic vortex amplifier arrangement (figure 7). There are two types of mechanical switching control systems applicable to an effective thrust control. One of them uses a solid propellant gas generator together with a double ended poppet valve for nozzle opening. Thrust control is performed by varying the switching frequency of the double ended poppet by pulse width modulation or bang-bang. This mentioned type belongs to the single stage systems, which is an ideal application as low cost device. The high electrical power consumption is one of the essential disadvantages. Two stage systems avoid just mentioned disadvantages but cause higher system costs due to the higher complexity. The second configuration has liquid propellant gas generators. It provides the ability to minimize fuel consumption by matching it to the duty cycle of the guided projectile.

Therefore it is an ideal application for a longer demonstration flight and end game. All these mechanical switching devices are showing off a very good efficiency of about 95 % and in connection with solid propellants better suited for gun applications than liquid propellants, they meet all requirements of high 'g' loading during launch.

Concerning actuation systems using fluidic elements, (see figure 7) the most devices use vortex valves to modulate the gas flow on the way to the thruster nozzles. An electro pneumatic converter is used to proportionally control the vortex valves by the pin movement in the control flow. The supply flow enters the vortex chamber radially through a relatively large port while the control flow enters tangentically.

With the control pressure approximately equal to the supply pressure, no tangential swirl is imported to the inlet flow; therefore, the inlet flow passes through the vortex chamber to the center exit hole without pressure loss. This is the maximum flow condition.
When control pressure exceeds supply pressure, the momentum of the interacting streams creates a vortex. Conservation of momentum results in a high velocity at the chamber exit causing a radial pressure gradient and a reduced flow. As the control pressure is further increased, the supply flow is continually reduced until the supply flow is completely shut off and all flow exiting from the vortex chamber is control flow. An inherent disadvantages of all vortex valve configurations is the high pressure loss in the main flow, the bad efficiency due to noise (turbulence) in the output flow and the fact that only about 40 % of the mass flow is available for production of thrust in one direction. This makes the device unsuited for high thrust and long time applications.

Discrete charge constellations (figure 8 and 9) can be implemented as high energy charges distributed around the circumference of the projectile or as short burn thrusters with miniaturized rocket motors and nozzles in and around the body of the projectile. The fixed combustion time of these devices is varying between 10 to 100 milliseconds for the short burn thrusters and about 50 microseconds for the high energy charges.

Common advantages of both charge constellations are the absence of movable parts, the availability of high thrust and the very low costs for such devices. However, end game simulations with discrete charge actuators showed that high miss distances are to be expected, particulary with moving targets, caused by the limited number of pulses. Both charge devices need a low spin rate during terminal guided flights and it is not confirmed that all modern activated seekers will survive the high 'g' loads during activation of discrete charges.

Once a thruster switching technology is chosen, the valves of an actuation system can be arranged in various configuration to provide an effective pitch, yaw and roll control (see figure 10). The effectiveness of a special valve configuration depends on the performance of the subsystems. An extensive analysis of the present subsystem design provides a four-thruster, pitch and yaw flight control to be the optimal choice, because roll control is only necessary for a projectile with preprogrammed flight.

4. GUIDED AMMUNITION 'EPHRAM'

In the next section of the presentation the Rheinmetall concept called EPHRAM (Endphasengelenkte Rohrartilleriemunition), see figure 11, which stands for terminally guided tube launched artillery ammunition, is demonstrated. The selected candidate concept is characterized by the following features (figure 12): A spin stabilized thin wall bus projectile, which has the same ballistic as the well known Rheinmetall RB 63, contains the submunition and a two stage dispensing system. After the seperation phase the terminal guided submunition (figure 13) will unfold 8 wings for lift production. An autopilot, which works according to the laws of proportional navigation controls the four lateral thrusters in front of center of gravity. Figure 14 shows the submunition during terminal guidance with one working thruster.

5. JET REACTION BLOCK DESIGN

The following part of the presentation gives a system overview of a jet reaction control actuation block using the two stage technology with four individual thrusters. The main parts are the gas generator and the block with four control units. The gas generator consists of the combustion chamber with a solid propellant, which is ignited by two diametrically mounted two stage igniters. The propellant (informations on figure 20) is designed to act as an end burning constant area type, which produces a clean hot gas at a comparatively low flame temperature of about 1500 K. Higher temperatures in the combustion chamber would lift up system cost because of temperature loading on the material enviroment specially for long duration applications. End burning solid propellants provide a rather high survivability during high 'g' launch and good storage capability at low cost. As above mentioned two igniters are used to ignite the gas generator propellant. The use of two igniters ensures uniform ignition and burning in an actuation block type with a boring for the shaped charge. The igniters consist of two stages in order to deliver the optimal igniting conditions for this special type of propellant. As the propellant starts burning, the pressure in the gas generator rises immediately until the relief valve crack pressure setting is reached. In addition, there is a mechanically operated safety disk. The hot gas is cleaned in a centrifugal filter before being delivered to the thrusters.

The filtering action ensures that no combustion debris will foul or clog the valves used to port the gas to the thrusters. Although it is not considered indispensable because of the clean gas the filter guarantees reliable functions.

One other important subsystem of the hot gas actuation block is the relief valve, which shall guarantee two functions: First of all the relief valve provides a constant pressure in the combustion chamber to ensure optimal propellant burning at a constant burning rate. The second reason for the installation of a relief valve is to avoid pressure peaks which would perhaps cause a bursting of the combustion chamber due to material stress. Normally mechanical relief valves, which are working as a spring-mass system do their job in such a hot gas generator. Another type of relief valve had been developed at Rheinmetall, called electronical relief valve, which is the ideal projectile application when only little volume is available. Figure 16 demonstrates the functional flow of this electronical relief valve. A pressure transducer senses gas pressure in the combustion chamber and sends an electrical signal to the microprocessor, which is incorporated in the autopilot electronic hardware. If the gas pressure is too high, the microprocessor issues a command to two opposite solenoids, so that surplus gas can escape with net force on the submunition of zero. The essential condition for such a system is the higher priority of the autopilot guidance signal, which initiates the solenoids to override the relief valve function. The principle operation of the solenoid activated valve arrangement in combination with the electronical relief valve is illustrated in the schematic diagramm of figure 17.

The actuation block with the hot gas control units consists of four individually controllable thrusters packaged in one common housing. Each thruster is a two stage solenoid operated, normally closed valve. Figure 18 and 19 show both a functional diagram and a picture of one single unit lifting up pilot and main stage. To open a thruster the solenoid must be energized. As the armature is attracted to the

solenoid housing by the electromagnetic force, its pushrod transfers a ball from 'vent' seat to 'pressure' seat. With the pressure source blocked, the chamber at the poppet head is connected to vent. The gas pressure available at the poppet seat chamber pushes the poppet to the valve open position and thrust force is developed at the valve nozzle. When the electrical signal to the solenoid is cut off, the reverse action takes place. The pressure acting on the ball transfers it to the 'vent' seat and pressurizes the head end of the poppet in the main stage causing valve closure. The poppet shuttles between the open and closed position by use of the control pressure action on the large and small diameter of the poppet.

The solenoid, pilot, main stage, pressure transducer and propellant were proven to work without failure when exposed to 16.000 g conditions. Subsequently functional and performance tests both with cold gas and hot gas showed that the components performed without failure (see figure 21 and 22).

6. SIMULATION RESULTS

The presentation is terminated by some results of computer computation and simulation.

Figure 23 which demonstrates the thermal analysis of the hot gas jet reaction control shows that the maximum temperature at the interface to other components does not exceed the permitted temperature limit of about 125°C after a burning time of 10 seconds.

The trajectory simulation results with implemented thruster block are shown in figure 24 and 25.
The simulation figure 24 demonstrates a presentation of the geodetical trajectory as side-view and as plan-view. The initial velocity is about 100 m/s in Xg-direction with an angle of 60 degrees.

The submunition will swing on a collision-heading according to the law of proportional navigation. The thrust-profile belonging to this trajectory is shown seperately for each thruster on figure 25. A black dark line stand for 8 milliseconds time of opening. According to the implemented logic it is only possible to open one single thruster.

Thruster control depends on the roll angle of the submunition, when a special trajectory is wanted. This is the reason for the wide black band of impulses in positive z-direction when the roll angle has a relatively constant value.

	PROJECTILE	MISSILE	REMARKS CONCERNING PROJECTILES
INITIAL VELOCITY	M > 2	↘	• HIGH STRESS ON STRUCTURE DURING LAUNCH PHASE
ACCELERATION DURING LAUNCH	10.000 - 40.000 g	↘	
SPIN RATE	0 - 16.000 RPM	↘	
RADIAL ACCELERATION	$\dot{\omega} > 10^5 RAD/S^2$	↘	
SPECIFIC WEIGHT	↗	↘	• GUN HARDENED COMPONENTS
MECHANICAL COMPLEXITY	↗	↘	• UNFOLDING MECHANISM FOR WINGS AND FINS IS NECESSARY • ACTIVATION OF NAVIGATION SYSTEMS AFTER LAUNCH PHASE
MANEUVRABILITY	↘	↗	• HIGH MASS AND SMALL WINGS
DIMENSIONS	LIMITED	MORE VOLUME	
TRAJECTORY	BALLISTIC FLIGHT AND TERMINAL GUIDANCE	GUIDED FLIGHT	
DISPERSION	↘	↗	

FIGURE 1 DIFFERENCES BETWEEN PROJECTILE AND MISSILE

O AXIAL ACCELERATION	MAX.	15.000 g
O LATERAL ACCELERATION	±	1.000 g
O RADIAL ACCELERATION	MAX.	$3 \cdot 10^5$ RAD/S^2
o SPIN RATE AT THE MUZZLE	MAX.	250 HZ
o MUZZLE VELOCITY	MAX.	850 M/S
o GAS PRESSURE	MAX.	4.365 BAR

FIGURE 2 LOADING DURING LAUNCH

- AERODYNAMICAL MEANS
  - o CANARDS
  - o WINGS
  - o FINS
- IMPULSIVE CONTROL
  - o THRUSTERS IN FRONT OF C.G.
  - o THRUSTERS IN BACK OF C.G.
  - o SHORT BURN THRUSTERS OR DISCRETE CHARGE DEVICES

FIGURE 3 GENERATION OF LATERAL FORCES

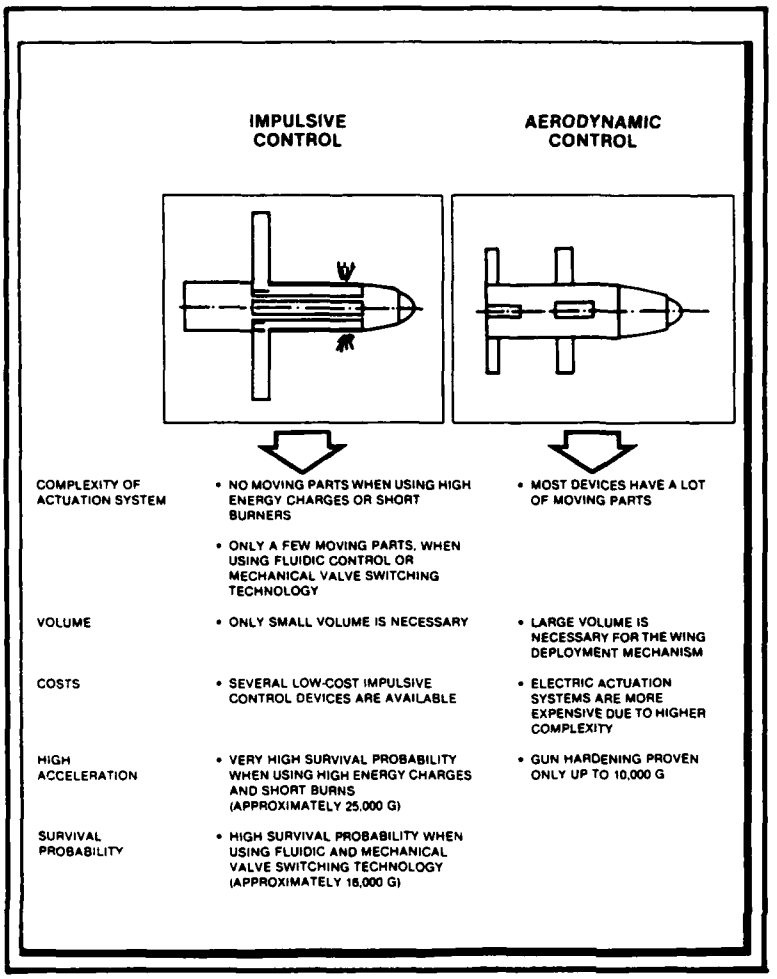

FIGURE 4 IMPULSIVE CONTROL VERSUS AERODYNAMIC CONTROL

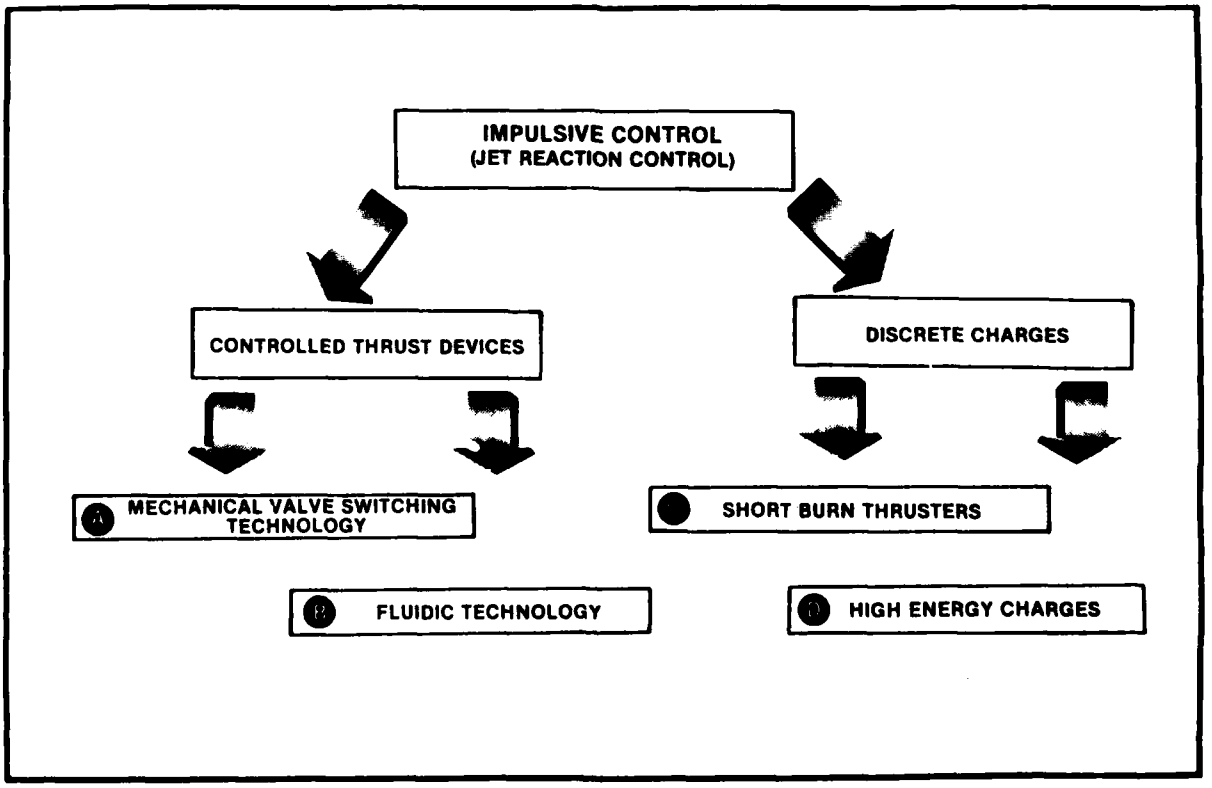

FIGURE 5 JET REACTION CONTROL SYSTEM TRADES

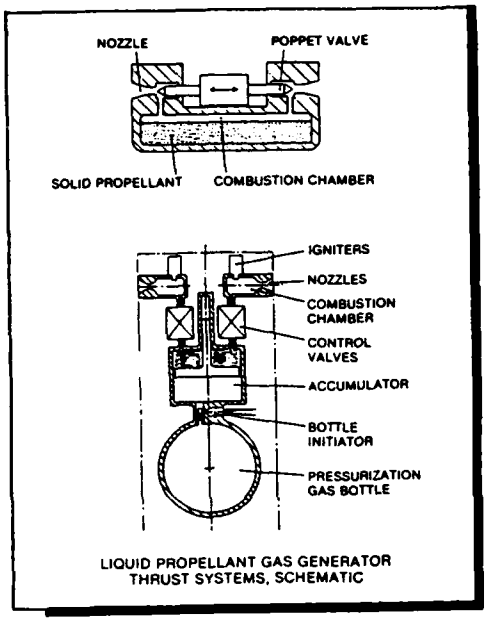

KEY FEATURES:

- FOR LIQUID PROPELLANT SYSTEMS: THRUST VECTOR CONTROL BY ALTERING THE FLOW RATE OF THE FLUID
- FOR SOLID PROPELLANT SYSTEMS: THRUST VECTOR CONTROL BY BANG-BANG OR PULSE WIDTH MODULATION

SINGLE STAGE SYSTEM:

ADVANTAGES:

- LOWER COST
- GOOD EFFICIENCY WHEN UTILIZING GAS (95%)

DISADVANTAGES:

- HIGH ELECTRIC POWER CONSUMPTION
- MOVING PARTS

TWO STAGE SYSTEM:

ADVANTAGES:

- LOW ELECTRIC POWER CONSUMPTION
- GOOD EFFICIENCY WHEN UTILIZING GAS (95%)

DISADVANTAGES:

- HIGHER COSTS
- MOVING PARTS

FIGURE 6 MECHANICAL VALVE SWITCHING TECHNOLOGY

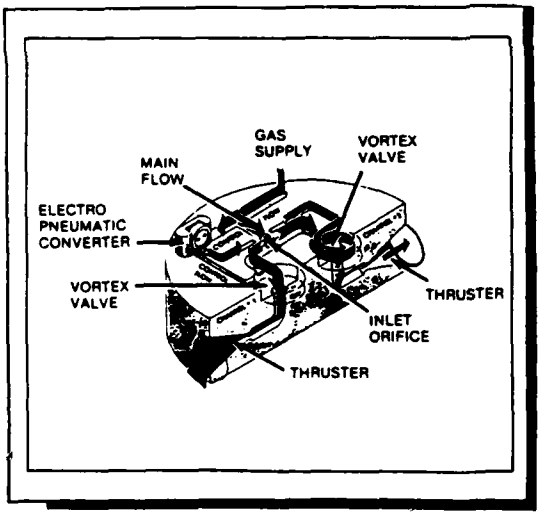

KEY FEATURES:

- FOR LIQUID PROPELLANT SYSTEMS: THRUST VECTOR CONTROL BY ALTERING THE FLOW RATE OF THE FLUID
- FOR SOLID PROPELLANT SYSTEMS: THRUST VECTOR CONTROL BY BANG-BANG OR PULSE WIDTH MODULATION

ADVANTAGES:

- ONLY ONE MOVING PART IS NECESSARY
- RELATIVELY SMALL SYSTEM SIZE

DISADVANTAGES:

- VERY HIGH PRESSURE LOSS IN MAIN FLOW
- HIGHER RESPONSE DUE TO VORTEX FORMING IN VORTEX CHAMBER
- 20% NOISE (TURBULENCE) IN FLOW (OUTPUT)

FIGURE 7 FLUIDIC TECHNOLOGY

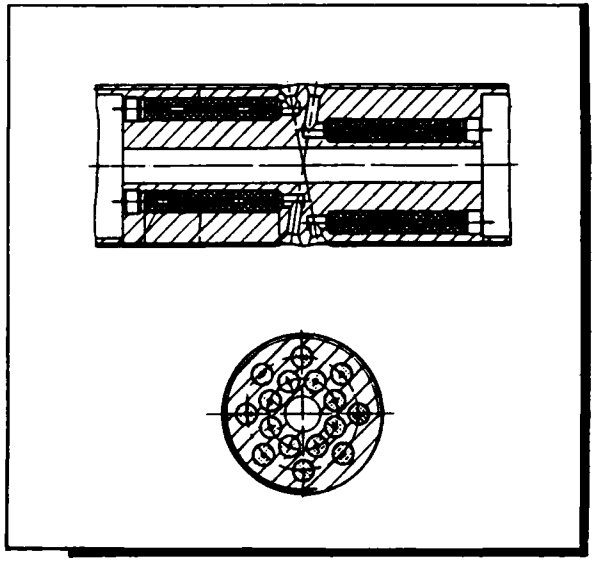

KEY FEATURES:

- FIXED COMBUSTION TIME BETWEEN 10 AND 100 MILLISEC
- MINIATURIZED ROCKET MOTORS WITH NOZZLES PROVIDE THRUST

ADVANTAGES:

- LARGE THRUSTS
- NO MOVING PARTS
- VERY INEXPENSIVE

DISADVANTAGES:

- NUMBER OF IMPULSES LIMITED
- SUITABLE ONLY FOR LATERAL CONTROL OF LOW SPIN RATE PROJECTILES
- REALIZATION OF PRECISE CONTROL IS DIFFICULT

FIGURE 8 SHORT BURN THRUSTERS

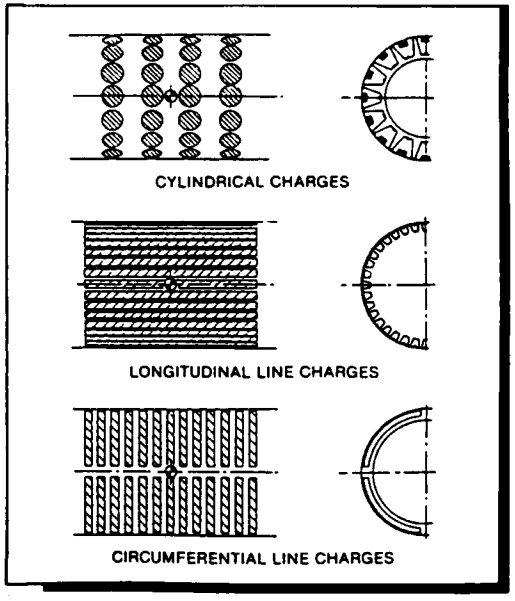

KEY FEATURES:

- SHORT BURN DURATION (≈ 50 MILLISECONDS)
- THESE DEVICES PRODUCE A THRUST IN THE CENTER OF GRAVITY WHICH ELIMINATES TORQUE MOMENT

ADVANTAGES:

- LARGE THRUSTS
- NO MOVING PARTS
- VERY INEXPENSIVE

DISADVANTAGES:

- NUMBER OF IMPULSES LIMITED
- DIFFICULTIES WITH THE IGNITION SYSTEM
- HIGH G-LOADS DURING ACTIVATION

FIGURE 9 HIGH ENERGY CHARGES

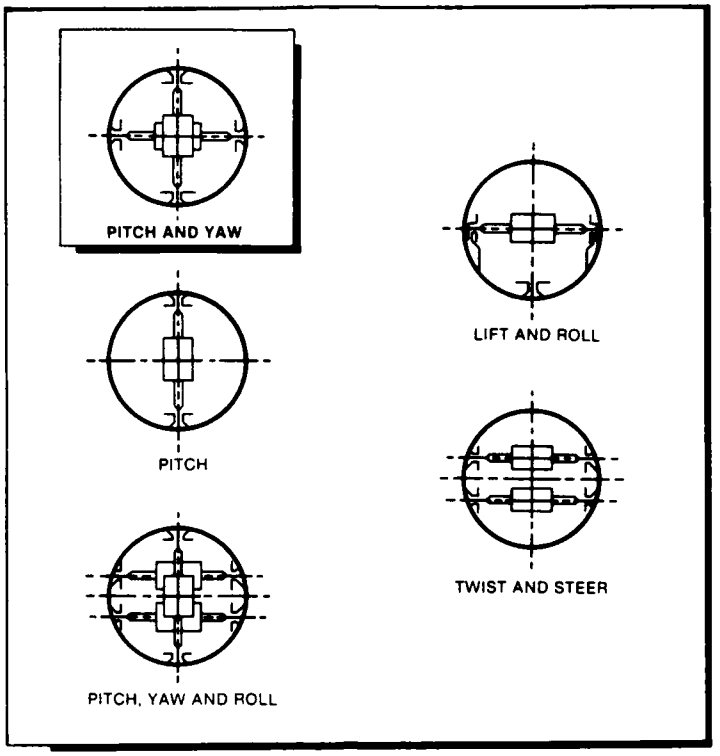

GENERAL FEATURES:

- THE VALVE CONFIGURATION DEPENDS ON THE SPIN RATE OF THE PROJECTILE
- TWO NOZZLES: HIGH SPIN RATE FOR FLIGHT CONTROL
- FOUR NOZZLES: LOWER SPIN RATE FOR FLIGHT CONTROL
- A ROLL CONTROL IS NECESSARY FOR A PROJECTILE WITH PREPROGRAMMED FLIGHT

FIGURE 10 POSSIBLE VALVE CONFIGURATIONS

EPHRAM

End-
PHasengelenkte
Rohr-
Artillerie
Munition

FIGURE 11 MEANING OF EPHRAM

THE SELECTED CANDIDATE CONCEPT IS CHARACTERIZED BY:

- SPIN STABILIZED, THIN WALL BUS PROJECTILE
  - SAME BALLISTIC AS RB 63
  - MAX. RANGE 22 KM
- TWO STAGE SUBMUNITION DISPENSING SYSTEM
- TERMINAL GUIDED SUBMUNITION
  - GUIDANCE
    - o PROPORTIONAL NAVIGATION
    - o AUTOPILOT
  - CONTROL/MANOEUVRE APPROACH
    - o LIFT FROM UNFOLDED WINGS
    - o CONTROL FORCE FROM 4 LATERAL THRUSTERS IN FRONT OF C.G.

FIGURE 12 GUIDANCE AND CONTROL

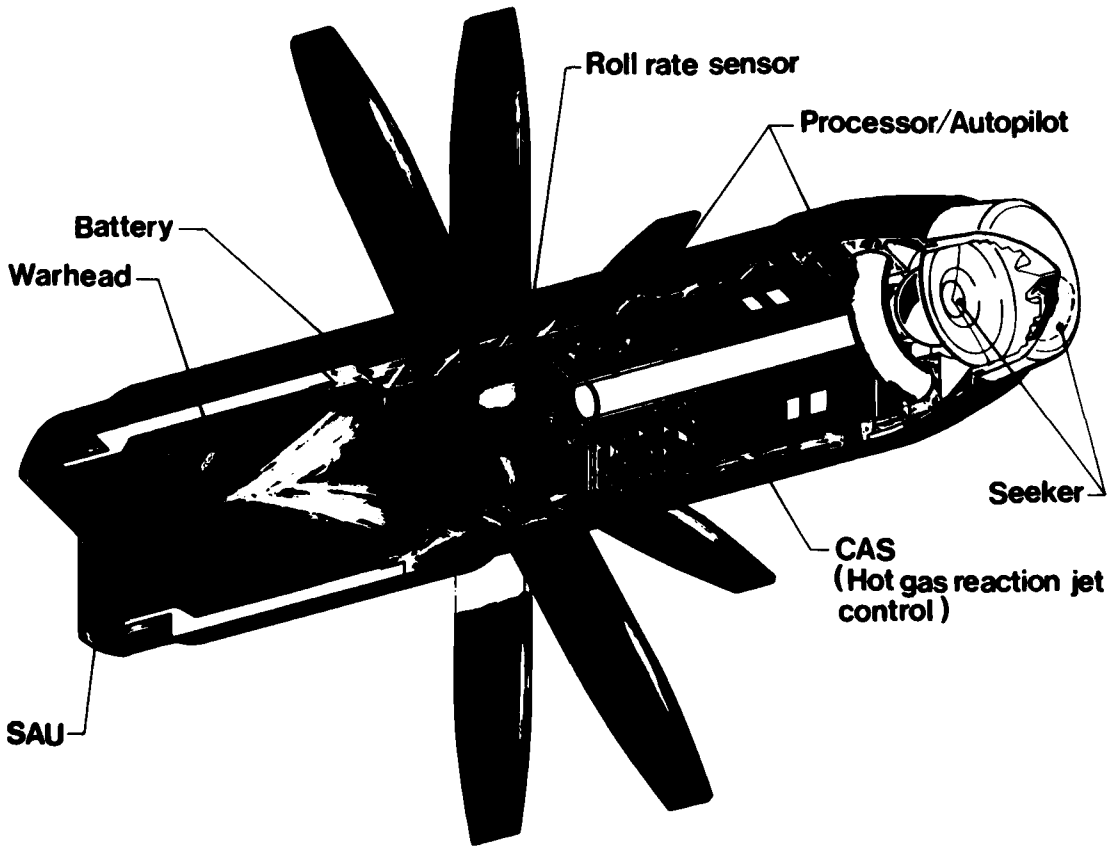

FIGURE 13 EPHRAM SUBMUNITION DESIGN

FIGURE 14 EPHRAM TERMINAL GUIDANCE

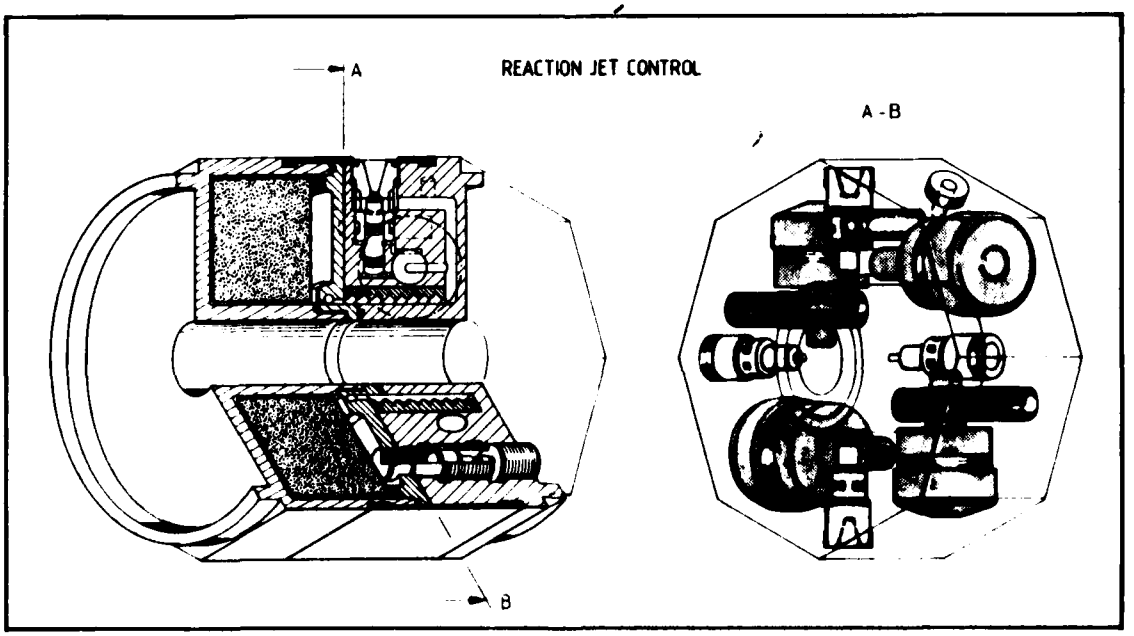

FIGURE 15 JET REACTION DESIGN

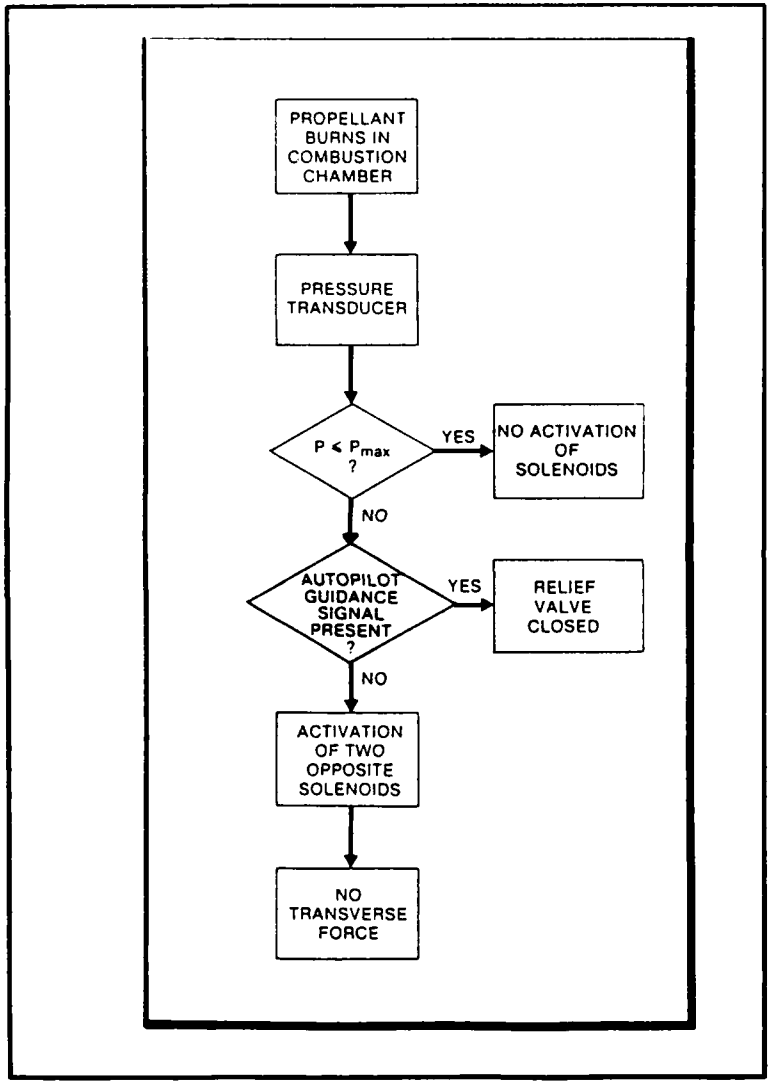

FIGURE 16 RELIEF VALVE FUNCTIONAL FLOW

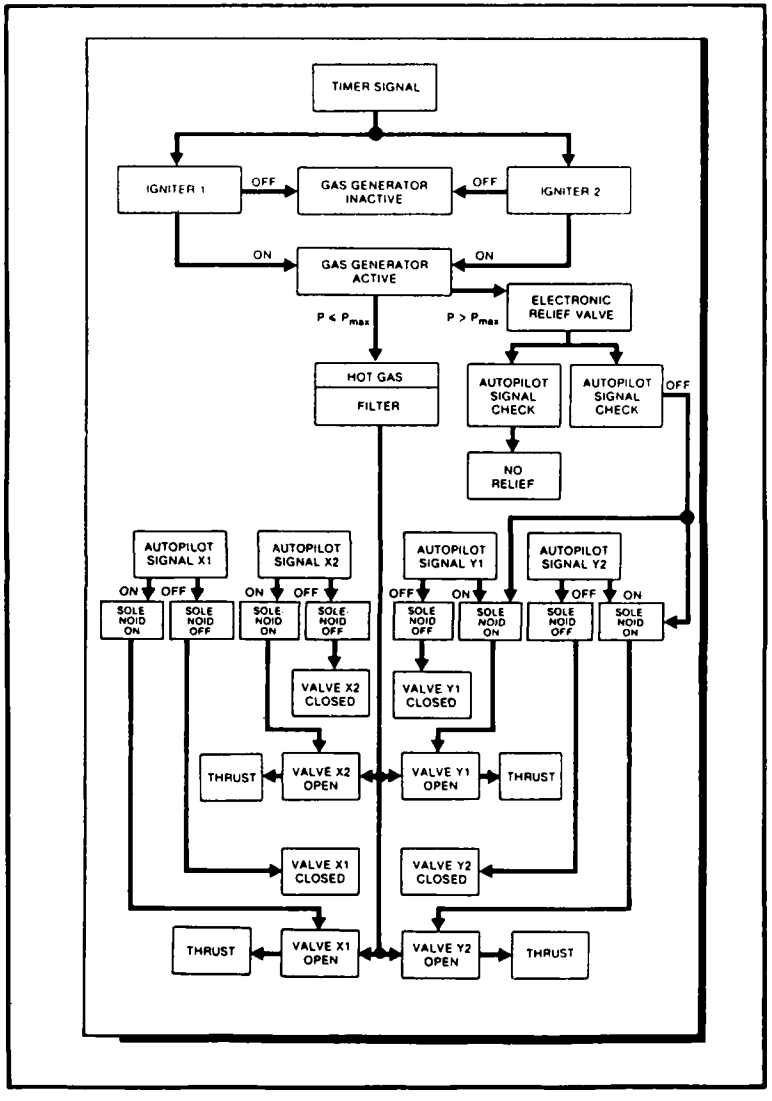

FIGURE 17 SOLENOIDS; RELIEF VALVE AND THRUSTER FUNCTIONAL FLOW DIAGRAM

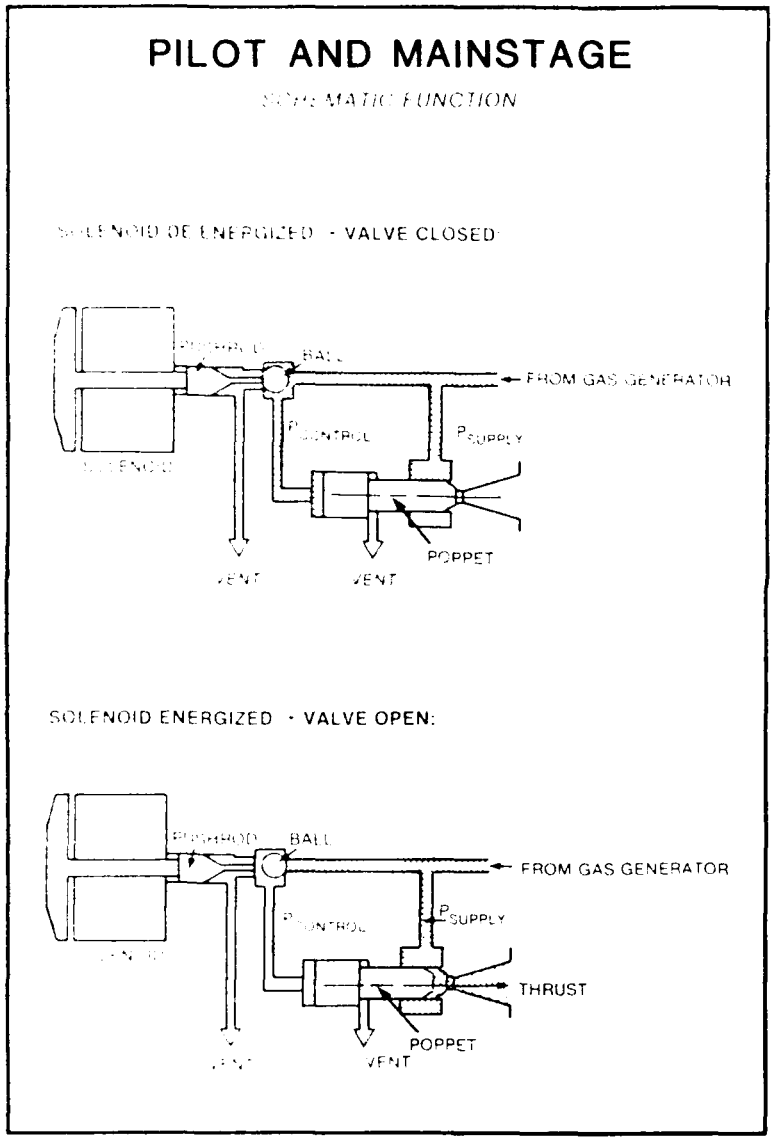

FIGURE 18 PILOT AND MAINSTAGE - SCHEMATIC

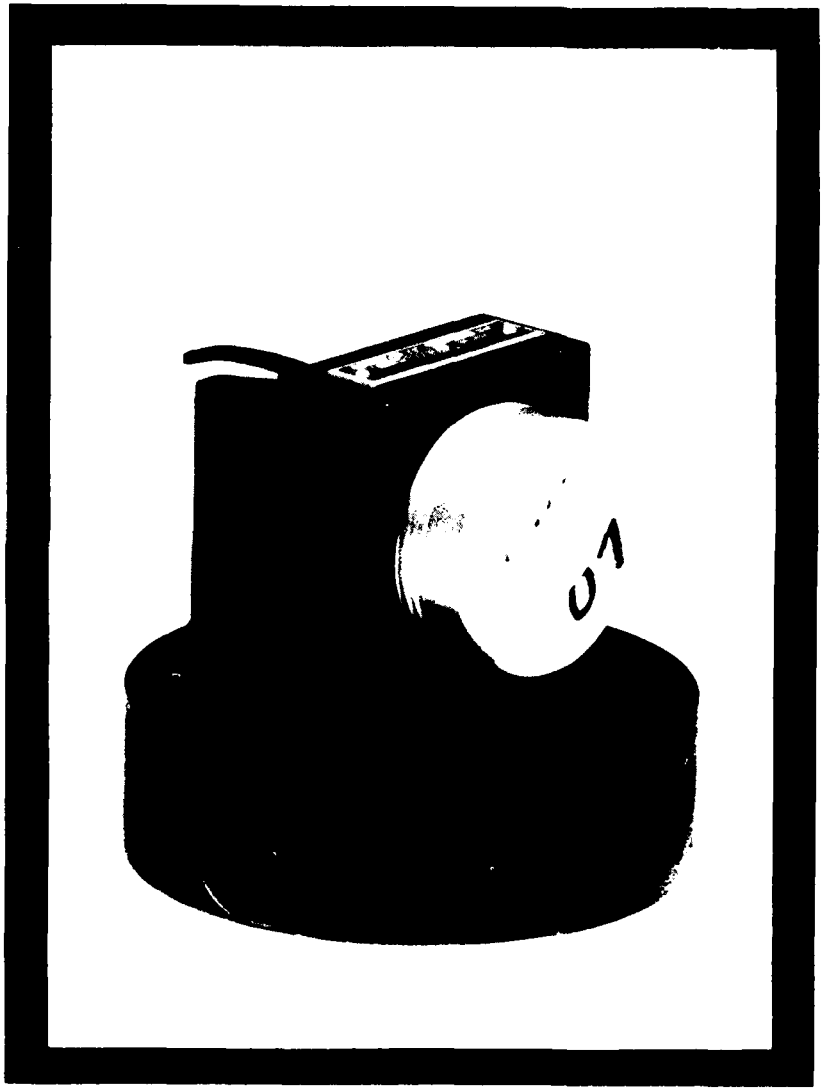

FIGURE 19 SINGLE THRUSTER HARDWARE

- ADVANTAGES OF SOLID PROPELLANT

  - HIGH ENERGY DENSITY
  - SIMPLICITY
  - SURVIVABILITY DURING HIGH 'g' LAUNCH
  - STORAGE CAPABILITY AND COST

- TYPES OF PROPELLANT FOR GAS GENERATOR APPLICATION

  - DOUBLE BASE (HIGH TEMPERATURE, ABOUT 2200 °C)
  - COMPOSITES (LOW TEMPERATURE, ABOUT 1200 °C)

DOUBLE BASES		COMPOSITE	
Advantage	Disadvantage	Advantage	Disadvantage
CLEAN GAS HIGHER LAUNCH SURVIVABILITY	HIGH TEMPERATURE (HIGH SYSTEM COST, BECAUSE OF TEMPERATURE LOADING ON THE MATERIAL ENVIRONMENT)	LITTLE SMOKE LOW TEMPERATURE (==> LOW SYSTEM COST)	STRESS CAPABILITIES OF 300 PSI ==> END BURNING PROPELLANT

FIGURE 20 PROPELLANT FOR PROJECTILE APPLICATION

FIGURE 21 GAS GENERATOR PERFORMANCE TEST

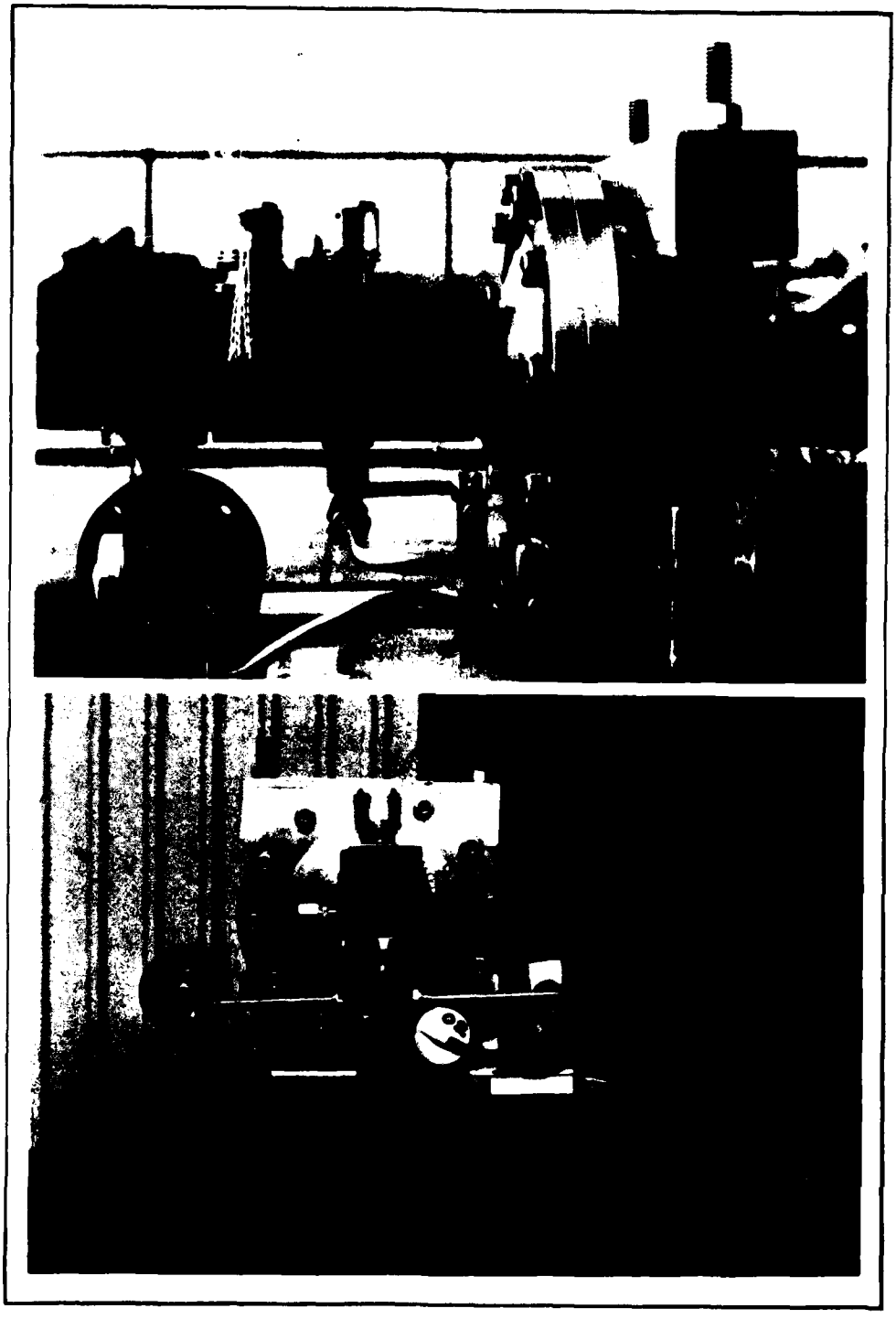

FIGURE 22 THRUSTER PERFORMANCE TEST

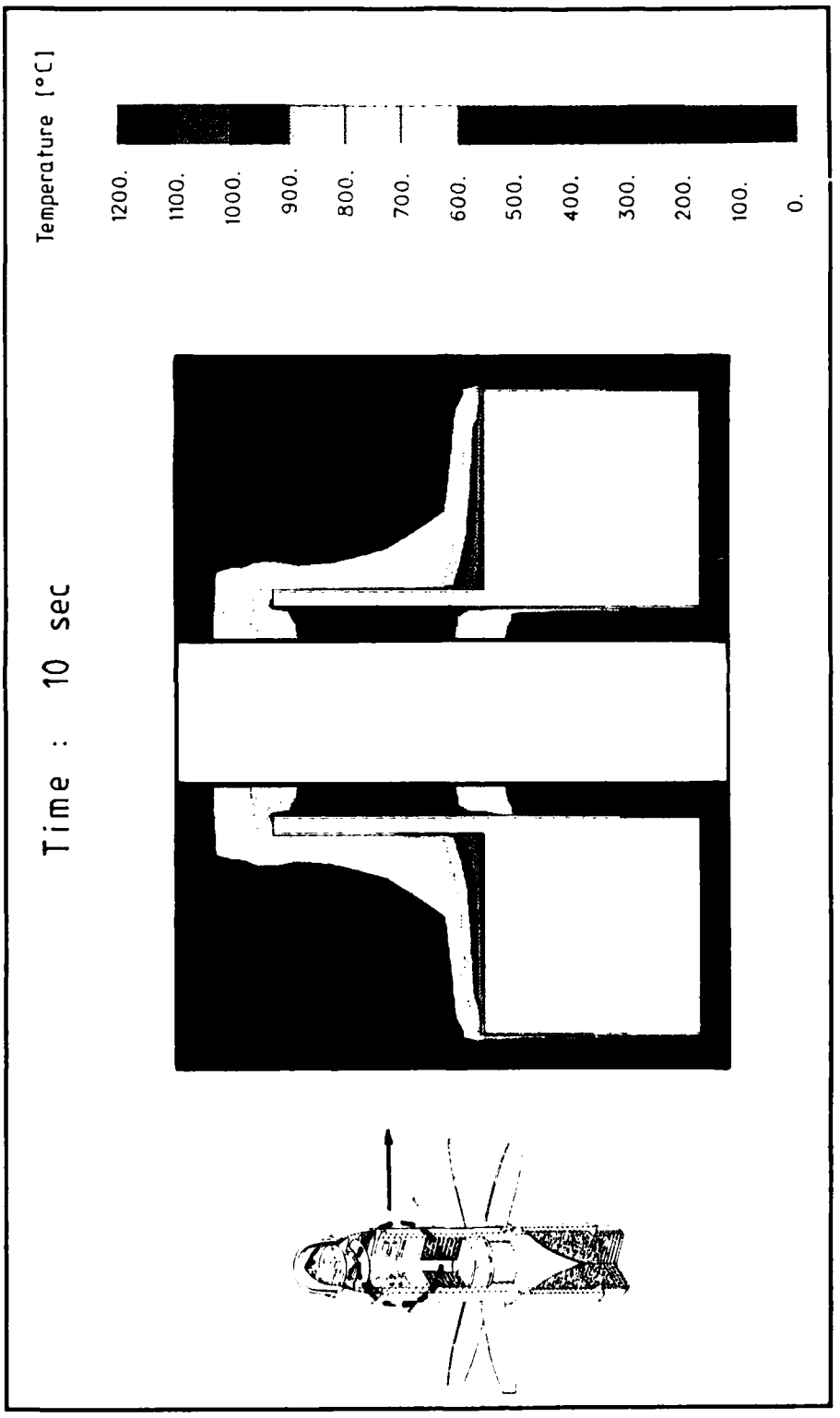

FIGURE 23 THERMAL ANALYSIS OF HOT GAS ACTUATION SYSTEM

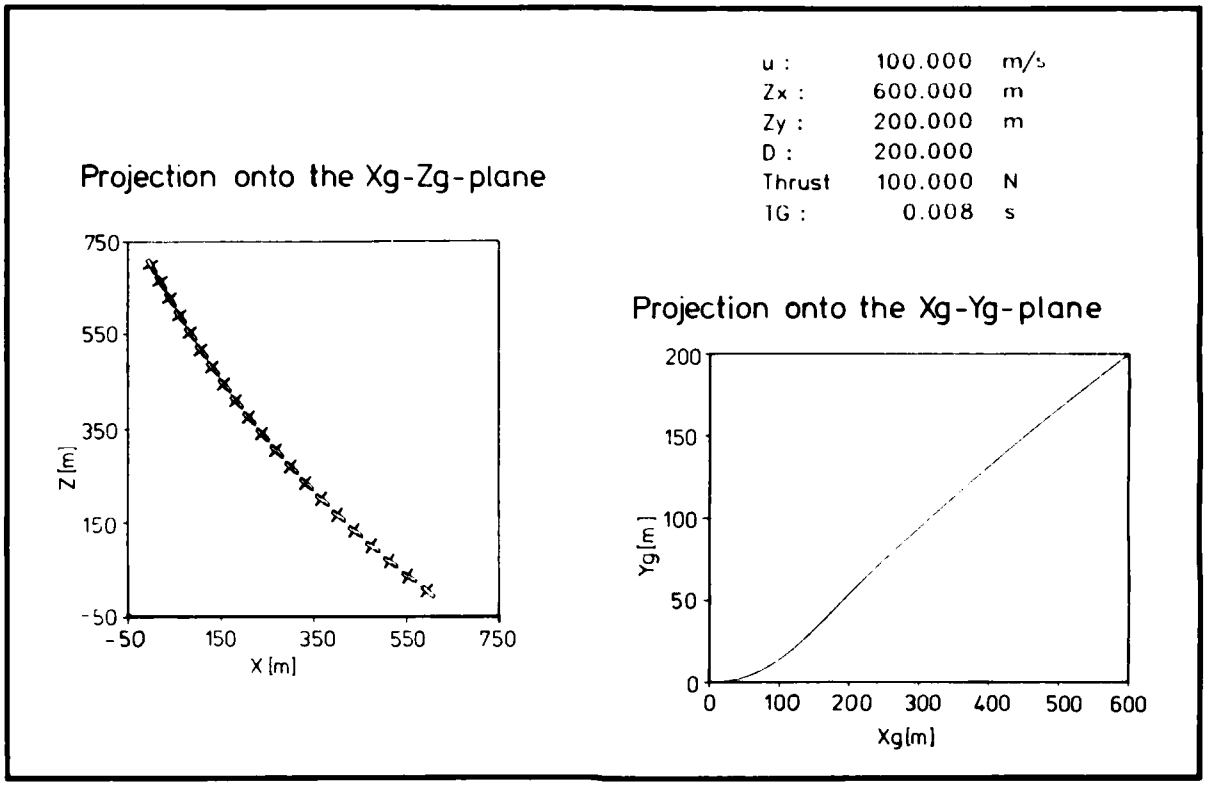

FIGURE 24 EPHRAM SIMULATION

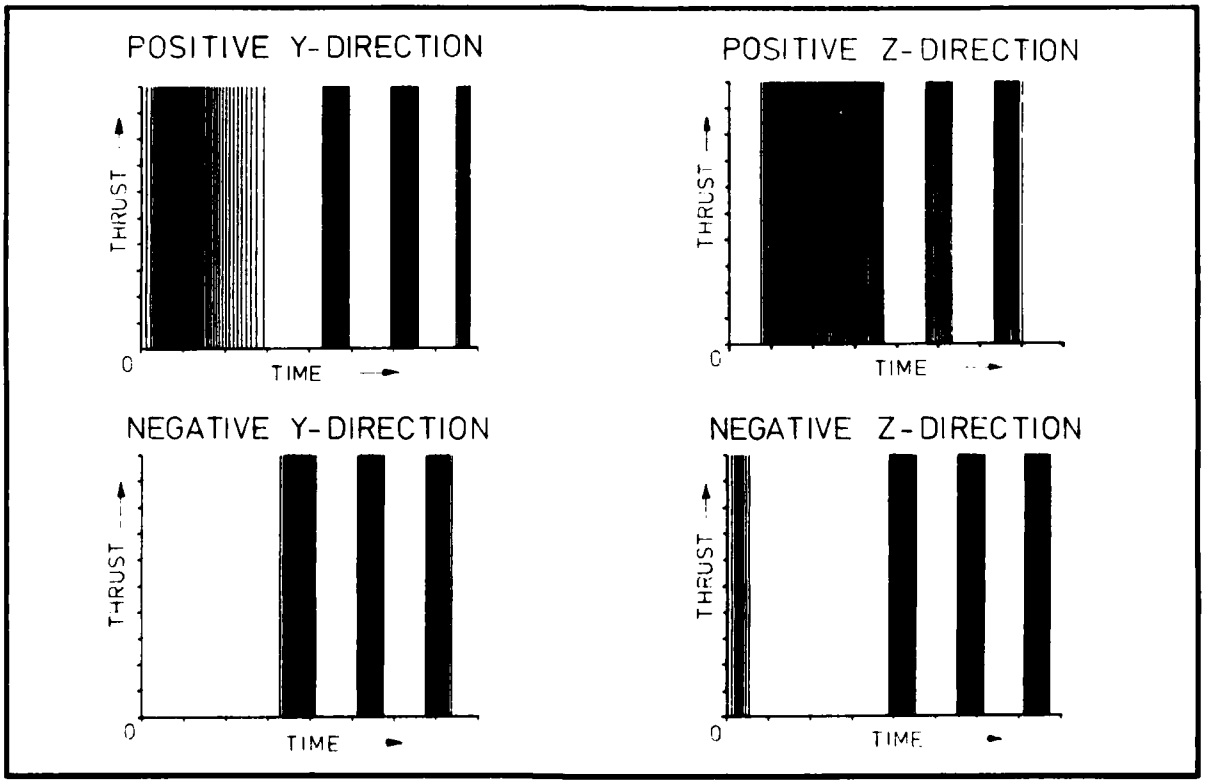

FIGURE 25 EPHRAM SIMULATION

APPLICATION OF OPTIMAL ESTIMATION AND CONTROL CONCEPTS TO A BANK-TO-TURN MISSILE

E. J. Ohlmeyer
Weapons Systems Department
Naval Surface Weapons Center
Dahlgren, Virginia 22448-5000, USA

SUMMARY

This paper addresses the design and evaluation of optimal estimators and optimal control laws for application to bank-to-turn missiles. Two guidance laws, one based on modern control theory and the other on an augmented form of proportional navigation, were compared to the classical implementation of proportional navigation. The former two control laws require the use of a state estimator, and an Extended Kalman Filter was devised for this purpose. Performance of the three guidance laws was compared on the basis of average miss distance achieved for a number of engagement scenarios.

INTRODUCTION

In recent years, the application of bank-to-turn guidance to tactical missiles has generated considerable interest.[1] This has been motivated by certain unique advantages that a bank-to-turn control configuration can offer. First, against high-performance threats, there is a need for defensive missiles to develop increasingly higher lift accelerations. High lift can be achieved in a single plane through wing-like aerodynamic surfaces as well as other means but requires a banking maneuver to properly direct the control vector.

Second, the need for greatly increased standoff ranges has led the design of tactical missiles towards airbreathing propulsion systems such as the ramjet. These designs generally have configuration geometries that are not cruciform, because of exposed inlets beneath the vehicle or other asymmetries. As a result, there are often stringent limits on the sideslip angle that can be developed during engine operation, and this also dictates some type of bank-to-turn control scheme.

In the present paper, a number of techniques for control of a bank-to-turn missile during terminal guidance are investigated.[2] Since, historically, proportional navigation has been the standard approach used to implement terminal homing, this control method was taken as a basis against which the performance of more advanced control laws could be compared.

Alternate control laws considered were augmented proportional navigation (APN)[3] and a control law based on modern linear quadratic optimal control theory.[4,5] For both of these, it was necessary to have available estimates of the complete states of the missile and target, and hence the utilization of a state estimator in conjunction with the control law was required. In the present work, an Extended Kalman Filter was employed to furnish the needed inputs.

The two advanced control laws were mechanized assuming that seeker measurements were available in the form of line-of-sight angles to the target, slant range, and range rate. These measured quantities were provided as input to the estimator, which in turn generated state estimates for use by the controller in computing guidance commands. The proportional navigation seeker was assumed to measure line-of-sight rates and closing velocity, and these were used to directly compute guidance commands without the need for a state estimator. In both cases, realistic levels of system noise were assigned to the basic measurements.

The objectives of the present work were first to evaluate the performance of the state estimator in terms of its ability to accurately estimate the system states from the available measurements in the presence of noise. Second, using the estimator in conjunction with the advanced control laws, it was desired to assess the relative merits of these control laws in comparison with proportional navigation. The control laws were evaluated using Monte Carlo sampling techniques and compared on the basis of average miss distance achieved for a number of engagement scenarios.

MISSILE EQUATIONS OF MOTION

The missile is modeled as a maneuvering point mass, with thrust equal to drag, and control acceleration applied normal to the velocity vector. The orientation of the missile in inertial space is described by Euler angles ψ_v, θ_v and Φ, when ψ_v and θ_v are horizontal and vertical flight path angles and ϕ is the roll or bank angle. With a_m and V_m denoting missile normal acceleration and velocity, the kinematic equations are

$$\dot{\theta}_v = (a_m \cos\phi - g\cos\theta_v)/V_m \tag{1}$$

$$\dot{\psi}_v = a_m \sin\phi / V_m \cos\theta_v \tag{2}$$

$$\dot{V}_m = -g\sin\theta_v \tag{3}$$

In addition, the missile is assumed to respond with first order lags to commands in normal acceleration and roll rate

$$\dot{a}_m = (a_c - a_m)/\tau_a \tag{4}$$

$$\dot{p} = (p_c - p)/\tau_p \tag{5}$$

$$\dot{\phi} = p \tag{6}$$

For the case where a roll position command is used rather than a roll rate command, Eq. (5) and (6) are replaced by

$$\dot{\phi} = (\phi_c - \phi)/\tau_\phi \tag{7}$$

MODERN CONTROL LAW

The optimum control law[4,5] generates the commands a_c and p_c so as to minimize a performance index of the form

$$J = \tfrac{1}{2}M_f^2 + \tfrac{1}{2}\int_o^t (b_1 a_c^2 + b_2 p_c^2)dt \tag{8}$$

when M_f is miss distance at final time and the integral term weights the expenditure of control energy.

Defining a missile body axis system with x along the velocity vector, y out the right wing, and k down, the resulting equations for a_c and p_c are

$$a_c = -3\, t_{go}\, M_{bz}/(3\, b_1 + t_{go}^3) \tag{9}$$

$$p_c = 7\, a_c^2\, t_{go}\, (3\, b_1 + t_{go}^3)\, \Delta\phi/(a_c^2\, t_{go}^5 + 63\, b_2) \tag{10}$$

$$\Delta\phi = -\tan^{-1}(M_{by}/M_{bz}) \tag{11}$$

In these equations, M_{by} and M_{bz} are the components of the projected zero effort miss distance (ZEM) along the body y and z axes, and t_{go} is time to go to intercept.

Define the relative position vector $\underline{S} = \underline{R}_T - \underline{R}_m$, the relative velocity $\underline{V}_R = \underline{V}_T - \underline{V}_m$, and a target acceleration model of the form

$$\underline{a}_T(t) = \underline{a}_T(t_o)\, e^{-\lambda(t - t_o)} \tag{12}$$

The ZEM in inertial axes may then be written

$$\underline{M} = \underline{S}(t_o) + t_{go}\underline{V}_R(t_o) + f\underline{a}_T(t_o) + \underline{M}_g \tag{13}$$

where

$$f = (\lambda t_{go} - 1 + e^{-\lambda t_{go}})/\lambda^2$$

$$\underline{M}_g = [0\ 0\ -\tfrac{1}{2}g t_{go}^2]^T$$

The ZEM in missile body axes is determined by transforming through the Euler angles ψ_v, θ_v, and Φ. Time to go is estimated as

$$t_{go} = -(\underline{S} \cdot \underline{V}_R)/(\underline{V}_R \cdot \underline{V}_R) \tag{14}$$

Thus, implementation of the control law requires that there be available estimates of $\underline{S}$, $\underline{V}_R$, and $\underline{a}_T$.

STATE ESTIMATOR

The nine-element state vector is defined to be

$$\underline{X} = [\underline{S} \mid \underline{V}_R \mid \underline{a}_T]^T \tag{15}$$

Target acceleration is modeled as an exponentially correlated random process with mean square value σ^2 and correlation time $1/\lambda$. Thus, along each of the inertial system axes, the acceleration is given by

$$\dot{a}_T(t) = -\lambda\, a_T(t) + w(t) \tag{16}$$

when w is zero mean white noise with spectral density $2\lambda\sigma^2$.

The system equations can be written in discrete form (with update interval T) as

$$\underline{X}(k+1) = \Phi\, \underline{X}(k) + \underline{b}(k) + \underline{u}(k) \tag{17}$$

where

$$\Phi = \left[\begin{array}{c|c|c} I & TI & [(\lambda T - 1 + e^{-\lambda T})/\lambda^2]I \\ \hline 0 & I & [(1 - e^{-\lambda T})/\lambda]I \\ \hline 0 & 0 & [e^{-\lambda T}]I \end{array}\right] \tag{18}$$

$$\underline{b}(k) = \left[-\int_{kT}^{(k+1)T}\int_{kT}^{t} a_m(\tau)\, d\tau\, dt \;\middle|\; -\int_{kT}^{(k+1)T} a_m(\tau) d\tau \;\middle|\; 0 \right]^T \tag{19}$$

when $\underline{u}(k)$ is a white noise sequence with covariance Q.

A detailed derivation[6] provides the elements of Q as functions of σ, λ, and T. The deterministic forcing term $\underline{b}(k)$ depends on missile acceleration, which is assumed to be known exactly.

A discrete measurement equation is assumed of the form

$$\underline{Z}(k) = \underline{h}(\underline{X}, k) + \underline{v}(k) \tag{20}$$

when $\underline{h}$ is a nonlinear function of the states and $\underline{v}$ is a white measurement noise with covariance R.

The missile seeker is assumed to provide measurements of line-of-sight angles, slant range, and range rate.[7] Thus the $\underline{h}$ vector is given by

$$\underline{h}(\underline{X}) = [\theta_s\ \Psi_s\ S\ \dot{S}]^T = [h_1\ h_2\ h_3\ h_4]^T$$

where

$$h_1 = -\tan^{-1}[x_3/(x_1^2 + x_2^2)^{\frac{1}{2}}] \tag{21}$$

$$h_2 = \tan^{-1}(x_2/x_1)$$

$$h_3 = (x_1^2 + x_2^2 + x_3^2)^{\frac{1}{2}}$$

$$h_4 = (x_1x_4 + x_2x_5 + x_3x_6)/(x_1^2 + x_2^2 + x_3^2)^{\frac{1}{2}}$$

The missile states are estimated by applying the standard Extended Kalman Filter algorithm [8, 9, 10] to the state and measurement equations given above. Since the measurement equation is nonlinear, it is necessary to form the Jacobian or matrix of partial deviations H

where

$$H_{ij} = \partial h_i/\partial x_j$$

ALTERNATE CONTROL LAWS

The performance of the modern guidance system (MGS), combined with the Kalman state estimator, was compared to two alternate bank-to-turn control schemes. These two control laws were conventional proportional navigation (PN) and APN.

The implementation of classical PN is as follows. The angular rate of the missile-target line-of-sight can be written

$$\underline{\omega} = (\underline{S} \times \underline{V}_R)/(\underline{S} \cdot \underline{S}) \tag{22}$$

If the components of $\underline{\omega}$ in the missile body frame are denoted by ω_{bx}, ω_{by}, ω_{bz}, then a roll error may be formed as

$$\Delta\phi = tan^{-1}(\omega_{bz}/\omega_{by}) \tag{23}$$

The bank-to-turn control commands are

$$\phi_c = \phi_o + \Delta\phi \tag{24}$$

$$a_c = N' V_c \omega_{by} \tag{25}$$

when ϕ_0 is current roll position, N' effective navigation gain, and V_c closing velocity along the line of sight.

Unlike PN, APN takes explicit account of target acceleration. Because of this, APN must be combined with a state estimator to furnish data needed for generating guidance commands. Using the estimator described previously, the ZEM components in body axes are formed, and the roll error computed as in Eq. (11). The roll angle command is given by Eq. (24) and the modified acceleration command by

$$a_c = -N' M_{bz}/t_{go}^2 \tag{26}$$

EVALUATION OF ESTIMATOR PERFORMANCE

The performance of the state estimator was evaluated during homing guidance using the engagement scenario shown in Figure 1. This scenario has the target and missile closing from an initial range of 4500 m. Missile speed is 600 m/sec and target speed is 300 m/sec. The target is 500 m below the missile and has a cross-range acceleration of 3 g's decaying exponentially with a time constant of 20 sec. In addition, the missile has an initial heading error of 10 deg in a direction opposite to the target acceleration. Time of flight for the engagement is 5 sec.

Figures 2 through 4 show time histories of the filter's estimates of relative position, relative velocity, and target acceleration in the cross-range direction, using the modern guidance system (MGS) and the nominal parameters of Table 1. In these figures, the symbols denote estimated quantities while the smooth curves denote the true values of the state variables.

The results indicate that the filter is able to track the system states in relative position and relative velocity quite well even though these are undergoing significant dynamic variations. The filter's estimates of target acceleration are fairly noisy, but correctly identify the mean target acceleration following an initial transient tracking period. The diagonal elements of the error covariance matrix appeared to be well-behaved functions of time that were decreasing in magnitude.

TABLE 1. NOMINAL PARAMETERS

Parameter	Symbol	Nominal Value	Applicable System*
Update interval	T	.05 sec	PN, APN, MGS
One sigma line-of-sight angle error	σ_θ	.15 deg	APN, MGS
One sigma slant range error	σ_s	3 m	APN, MGS
One sigma range rate error	σ_s^*	6 m/sec	APN, MGS
One sigma line-of-sight rate error	σ_ω	.5 deg/sec (low) 2 deg/sec (high)	PN
One sigma closing velocity error	σ_{v_c}	6 m/sec	PN
Missile maximum normal acceleration	a_{max}	20 g's	PN, APN, MGS
Missile maximum roll rate	p_{max}	1 Hz	MGS
Missile normal acceleration time constant	τ_a	5 sec	PN, APN, MGS
Missile roll rate time constant	τ_p	5 sec	MGS
Missile roll position time constant	τ_ϕ	5 sec	PN, APN
Effective navigation gain	N'	3	PN, APN
Filter process noise parameters Target RMS acceleration Correlation time	 σ $1/\lambda$	 5 g's 1 sec	 APN, MGS APN, MGS
Controller cost function parameters Weight on a_c Weight on p_c	 b_1 b_2	 .00578 sec 5 m^2 sec	 MGS MGS

*PN = Proportional Navigation
APN = Augmented PN
MGS = Modern Guidance System

Figure 5 shows histories of the missile's commanded normal acceleration and the achieved acceleration assuming a 0.5-sec autopilot time constant. The variation of the bank angle with time (also based on 0.5-sec roll response) is shown in Figure 6. The miss distance for this example was 5.7 m, indicating generally satisfactory estimator and control law performance.

COMPARISON OF THE CONTROL LAWS

The sensitivity of the three control laws to variations in missile maximum acceleration, roll and normal acceleration time constants, and sensor noise was evaluated based on miss-distance calculations for the scenario of Figure 1. The miss distance was computed based on an average of 30 Monte Carlo trajectories in which the sensor noise histories were varied from run to run. Table 1 is a list of nominal parameters used for each of the guidance laws.

In Figure 7, the variation of mean miss distance with missile maximum acceleration is indicated for the three control laws. For the PN control law, both high and low levels of sensor noise are considered. In terms of relative performance, the low-noise PN system and the APN system appear the best, giving nearly equivalent performance in terms of minimum required acceleration capability, with PN slightly better in terms of minimum achieved miss distance.

Of the advanced control laws considered, APN appears generally to outperform the MGS system. Assuming all the systems have sufficient maneuverability (say 20 g's), then the lowest miss distances are obtained by PN (1.7 m) followed by APN (3.1 m) and then by MGS (6.5 m). MGS also requires an additional margin of missile maneuverability (15 g's required) compared to the other two systems (13 g's required). The high-noise PN system yields the least satisfactory performance of all the systems considered.

Figure 8 indicates the effect of missile time constants on the three control laws. For PN and APN, nominal roll position time constants of 0.3 and 0.5 sec were assumed. For MGS, nominal roll rate time constants of 0.3 and 0.5 sec were assumed. The PN system achieves misses under the required 7 m out to fairly large values of the acceleration time constant. The APN system appears to perform better than the MGS system, but both require much smaller values of τ_a to stay within the miss distance tolerance.

The effect of sensor noise on the MGS system is shown in Figure 9. Results are presented as a function of line-of-sight angle measurement noise for missile maximum acceleration levels of 14 and 20 g's. The mean miss increases with increasing sensor noise, but the rate of increase is much lower for the higher acceleration capability.

One additional sensitivity investigated for the MGS system was that caused by missile maximum roll rate, p_{max}. Results are shown in Figure 10 for missile accelerations of 14 and 20 g's. Beyond a certain level, the miss distance is insensitive to further increases in p_{max}. This minimum roll rate occurs slightly below the nominal value of 6.28 rad/sec (1 Hz) assumed in the present study.

CONCLUSIONS

The Kalman Filter generally performed well in estimating the system states during dynamic engagements. Estimates of relative position and velocity were of better quality than estimates of target acceleration, which tended to be noisy.

Examination of the estimation errors revealed them to be consistently unbiased once steady tracking conditions were reached. This occurred almost immediately for all the state variables except the acceleration estimate in the direction of maximum target maneuver, where a small dynamic lag was noticed. The time histories of the error covariances showed smooth, well-behaved functions that decreased in magnitude as the engagement progressed.

While the performance of the filter appeared to be satisfactory overall, only a limited number of scenarios could be tested in the present study. An evaluation of the sensitivity of the filter to a wider range of initial conditions and engagement geometries is recommended in any future investigation.

It was observed during simulation runs that the guidance commands generated by the controller were fairly erratic as a result of noise propagating through the filter's state estimates. The fact that the missile could not respond instantaneously to jitter in the commands, however, produced generally smooth accelerations and roll rate histories for most trajectories.

The sensitivity of miss distance to missile maximum maneuverability, time constants, and sensor noise was also investigated. A threshold value was found on missile maneuverability below which the miss distance grew rapidly and above which the miss remained fairly constant. The trend, with regard to missile time constants, was that as the roll and normal acceleration responses were made faster, the miss distance decreased. For any given value of the roll time constant, there was a threshold value associated with the acceleration time constant beyond which the miss grew rapidly. The influence of sensor noise was such that increases in the noise levels produced corresponding increases in miss distance.

A comparison of the three control laws suggested the following general conclusions:

a) All of the control laws (with the exception of the high-noise PN system) achieved the required miss distance (<7 m) for their nominal parameter values.

b) In terms of absolute miss, PN achieved the lowest, followed by APN, then MGS.

c) The MGS system appeared to require an extra margin of maneuverability compared to the other two systems.

d) The PN system appeared more tolerant of increases in missile time constants than the other systems.

e) Of the advanced control laws considered, the APN implementation, employing roll-position commands, performed considerably better than the MGS implementation, employing roll-rate commands.

The effect of the filter's process noise parameters on average miss distance was also investigated for the MGS and APN systems. When target acceleration estimates were used in the computation of guidance commands, the miss distance was very sensitive to changes in the process noise parameters λ and σ, and it varied over a fairly wide range. It was suspected that this sensitivity might be caused by the amount of noise present in the target acceleration estimates. When target acceleration was not employed in the computation of guidance commands, the miss distance was shown to be much less sensitive to variations in the filter's process noise parameters. However, the minimum miss distances achieved were about the same in both cases, and were close to those obtained earlier using the nominal process noise values.

Based on results of the current study, it is believed that improvements are needed in the ability to accurately estimate target acceleration. Future investigations should examine alternate ways of characterizing the target acceleration model within the state estimator in the hope of obtaining more reliable real-time estimates of acceleration for use by advanced guidance laws.

REFERENCES

1. F. W. Riedel, National Aeronautics and Space Administration, *Bank-to-Turn Control Technology Survey for Homing Missiles*,1980, NASA Contractor Report 3325.

2. E. J. Ohlmeyer, Naval Surface Weapons Center, *Application of Optimal Estimation and Control Concepts to a Bank-to-Turn Missile*, 1985, NSWC TR 85-219.

3. F. W. Nesline and P. Zarchan, "A New Look at Classical Versus Modern Homing Missile Guidance," *AIAA Journal of Guidance and Control, Vol. 4, Jan-Feb 1981*.

4. D. V. Stallard, "An Approach to Optimal Guidance for a Bank-to-Turn Missile," Proceedings of AIAA Guidance and Control Conference, August 1980.

5. D. V. Stallard, "Biased Optimal Guidance for a Bank-to-Turn Missile," Proceedings of American Control Conference, June 1983.

6. R. A. Singer, "Estimating Optimal Tracking Filter Performance for Manned Maneuvering Targets," *IEEE Trans Aerosp Electron Sys*, Vol. AES-6, No. 4, July 1970.

7. P. H. Fiske, Air Force Armament Laboratory, *Advanced Estimation and Control Concepts for Air-to-Air Missile Guidance Systems*, 1979, AFATL-TR-79-29.

8. A. Gelb, *Applied Optimal Estimation*, MIT Press, Cambridge, MA, 1974.

9. A. H. Jazwinski, *Stochastic Processes and Filtering Theory*, Academic Press, New York and London, 1970.

10. B. D. O. Anderson and J. B. Moore, *Optimal Filtering*, Prentiss-Hall, Englewood Cliffs, NJ, 1979.

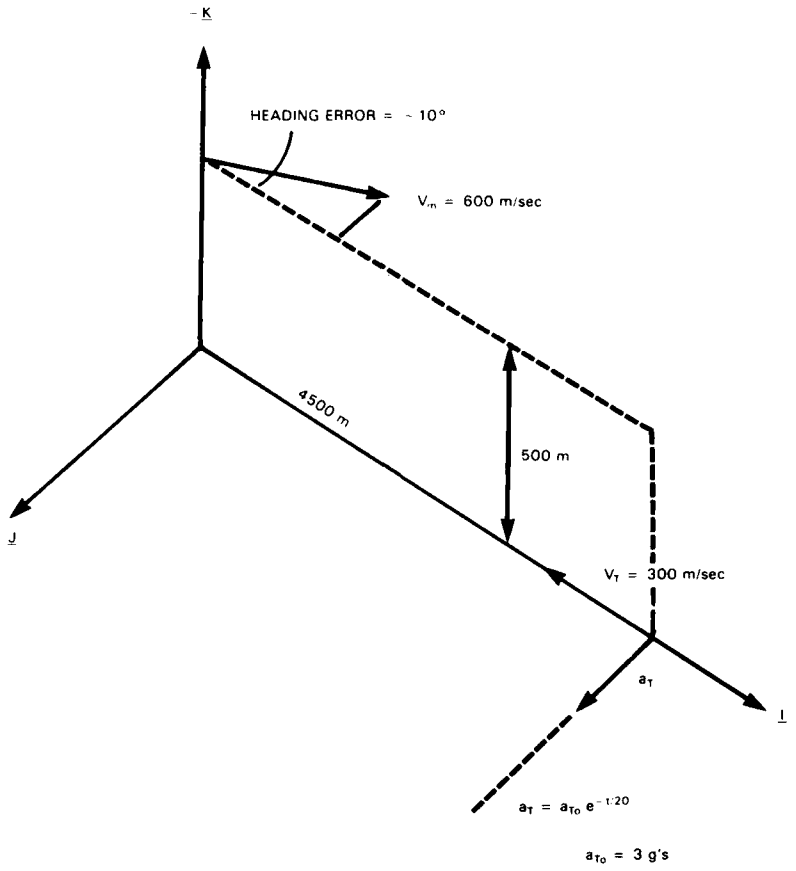

FIGURE 1. ENGAGEMENT SCENARIO

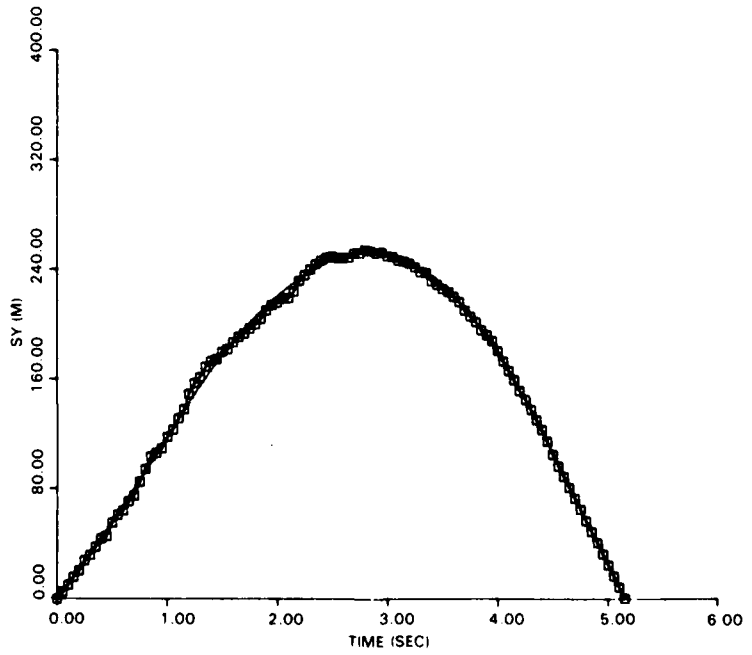

FIGURE 2. RELATIVE POSITION ESTIMATE VERSUS TIME

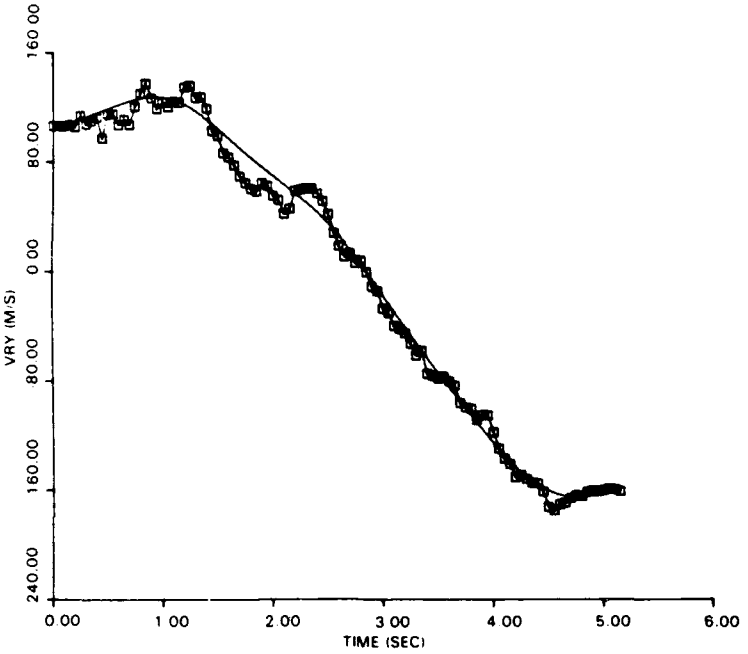

FIGURE 3. RELATIVE VELOCITY ESTIMATE VERSUS TIME

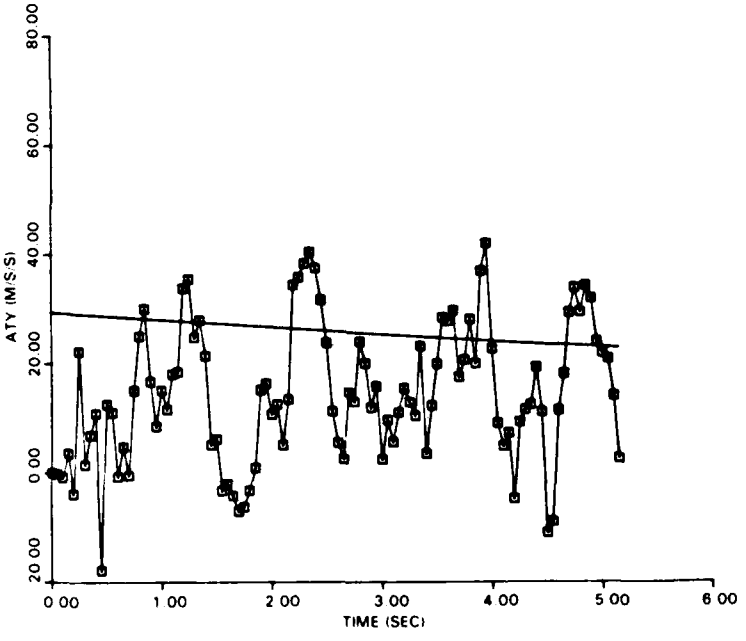

FIGURE 4. TARGET ACCELERATION ESTIMATE VERSUS TIME

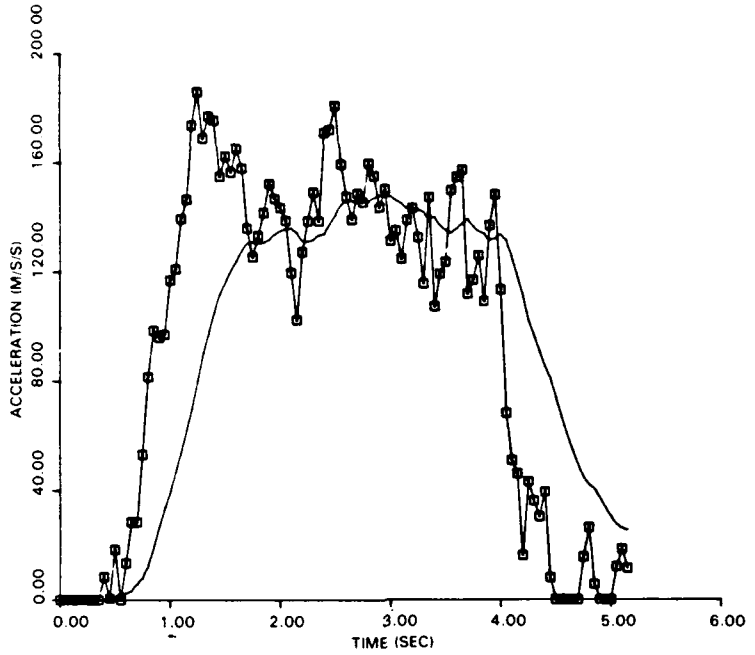

FIGURE 5. COMMANDED AND ACHIEVED NORMAL ACCELERATION VERSUS TIME

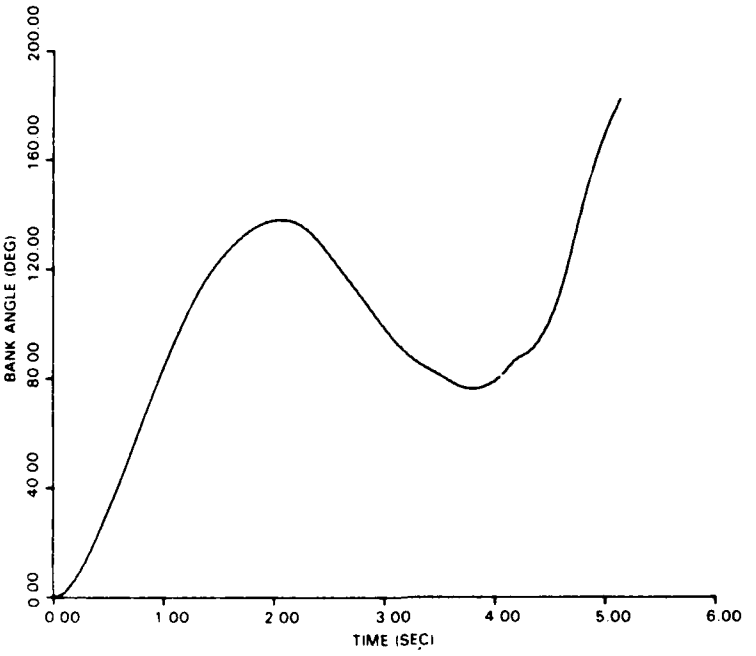

FIGURE 6. BANK ANGLE VERSUS TIME

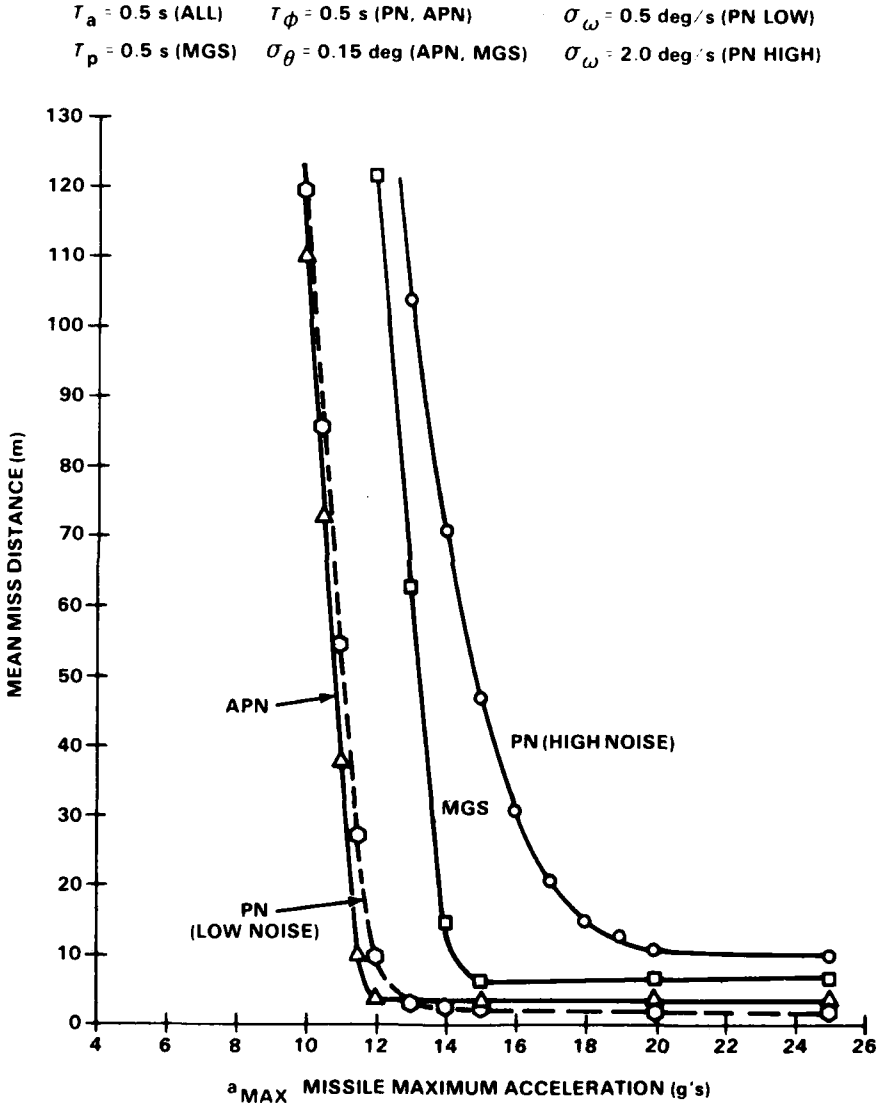

FIGURE 7. EFFECT OF MAXIMUM ACCELERATION ON GUIDANCE LAWS

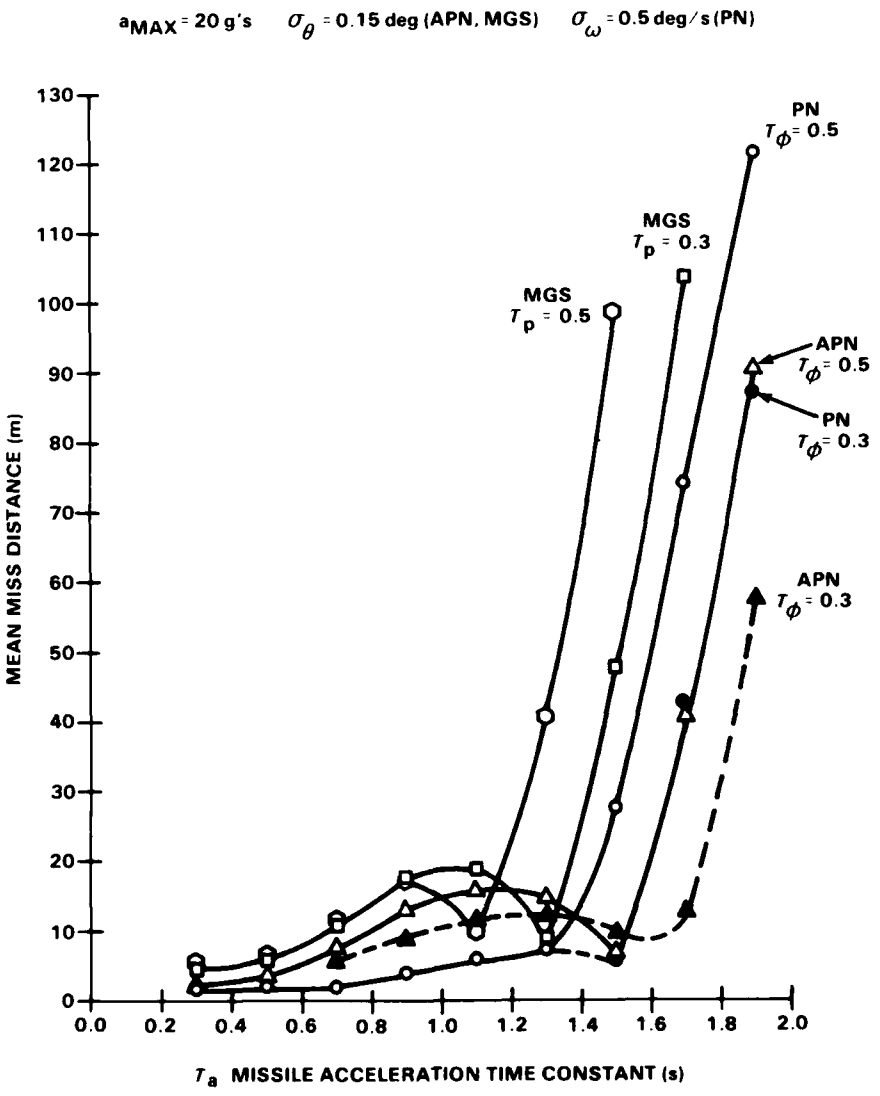

FIGURE 8. EFFECT OF TIME CONSTANTS ON GUIDANCE LAWS

MODERN GUIDANCE SYSTEM

$\tau_p = \tau_a = 0.5$ s $\lambda = 1$ $\sigma = 5$ g's $p_{MAX} = 6.28$
σ_s 3 m $\sigma_{\dot{s}} = 6$ m/s

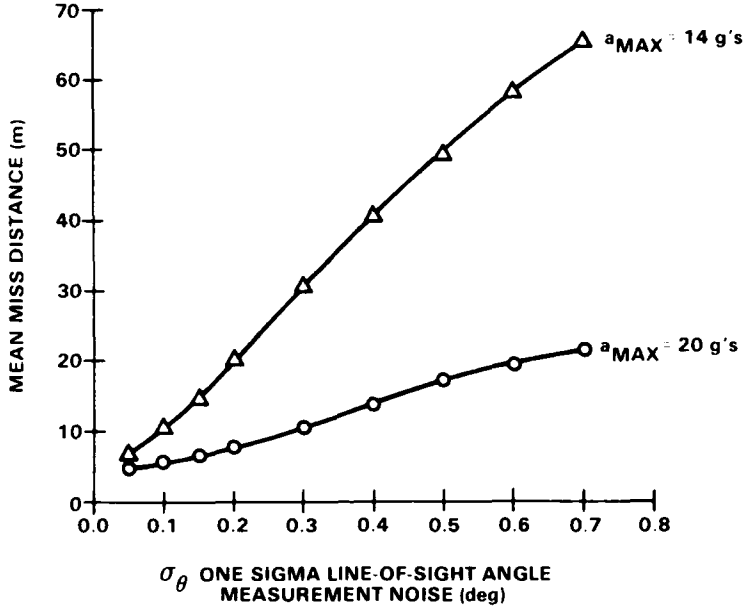

FIGURE 9. EFFECT OF SENSOR NOISE

MODERN GUIDANCE SYSTEM

$\tau_p = \tau_a = 0.5$ s $\lambda = 1$ $\sigma = 5$ g's $\sigma_\theta = 0.15$ deg

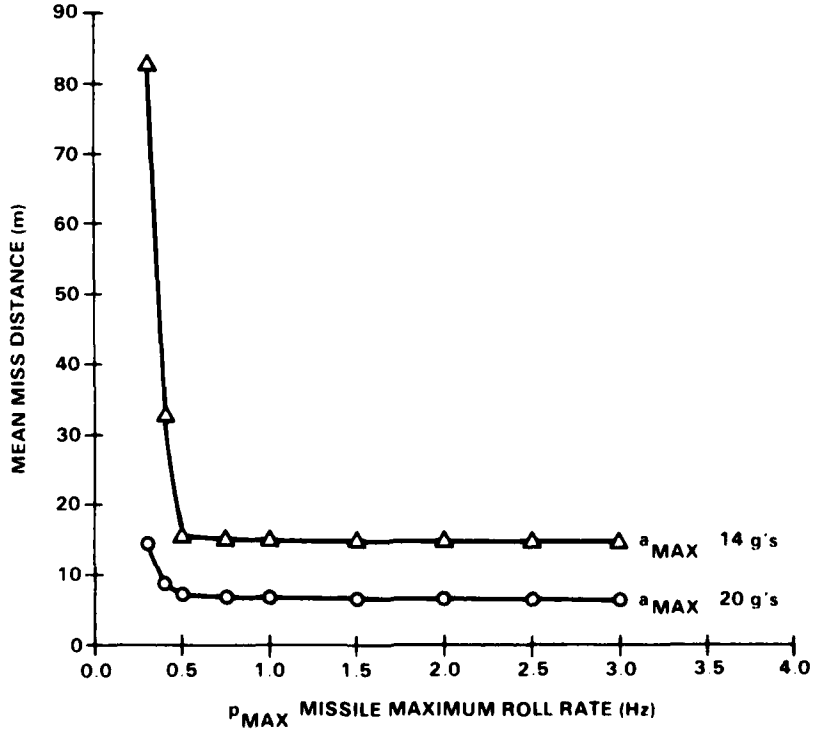

FIGURE 10. EFFECT OF MAXIMUM ROLL RATE

AN INTELLIGENT MULTI-TARGET TRACKING SYSTEM

by
E Heyerdahl
Norwegian Defence Research Establishement
N-2007 Kjeller
Norway

SUMMARY

An implementation of a general tracking system, integrating the target acquisition and tracking sub-systems, has been developed at NDRE. It is based on image analysis and extensive use of models. The system permits improvements compared to in-service trackers in the sense that it enables multi-target tracking, automatic acquisition also during tracking and tracking through obscurations. The system is an implementation of a general tracking system. This system produces alternative estimates of a target and projects the corresponding objects (subsets of $\mathbb{R}^3$) into the image plane. To do this estimates of the projecting function are used. The different projections are synthesized through a thresholding process. The implemented system uses parallel Kalman filters to produce the object estimates and estimates the sensor position through a model of sensor dynamics and measurements of sensor angle velocity. Results, produced by the implemented system from IR imagery of a moving target in field, are presented.

1. THE GENERAL TRACKING SYSTEM

Let us start with a general definition of a tracking system:

A frame sequence is a mapping from a subset of $\mathbb{R}$ and into a set of frames.
A segment is a mapping from $\mathbb{R}$ and into a set of subsets of $\mathbb{R}^2$.
A segmentation is a mapping from a subset of $\mathbb{R}$ and into a set of segments.
A tracking system TS is a mapping from a set of frame sequences and into a set of segmentations such that the domain of any frame sequence m equals the domain of TS(m).

We may now describe a multi-hypothesis tracking system as any tracking system characterized by the following:
Let FS be an element in the domain of the tracking system. To each element in the domain of FS (a time instant) there is defined a set of tracker banks. A tracker bank is a set of trackers. A tracker produces an estimate of an object (a subset of $\mathbb{R}^3$) and an estimate of a projection. The projection is the one associated with the actual frame and is a mapping from all subsets of $\mathbb{R}^3$ into subsets of $\mathbb{R}^2$. Let the trackers in a bank be denoted T_i for i = 1, . ., N. Let P_i be the projection estimate produced by T_i, and let O_i be the object given by the object estimate produced by T_i. T_i is said to track a target if $P_i(O_i)$ "almost equals" the (true) projection of the target. Let C_i be a "confidence" associated with the event that T_i tracks a target. Let F_i be the scalar field such that

$$F_i(r) = \begin{cases} C_i \text{ if } r \in P_i(O_i) \\ 0 \text{ if } r \in (\mathbb{R}^2 - P_i(O_i)) \end{cases}$$

Let the tracker bank be denoted TB_j and let F'_j be the scalar field such that

$$F'_j(r) = \sum_{T_i \, TB_j} F_i(r) \quad \text{for all} \quad r \in \mathbb{R}^2$$

Let t be a "threshold" and let S_j be the set such that

$$S_j = \{r \; r \in \mathbb{R}^2 \quad \text{and} \quad F'_j(r) \geq t\}$$

The tracking system, TS, is such that

$$TS(j) = \begin{cases} S_j \text{ if } j \text{ is a tracker bank index} \\ \emptyset \text{ otherwise} \end{cases}$$

The general properties of a multi-hypothesis tracking system are thus given.

An important feature of such a system is that the trackers produce estimates of a "physical" object (a subset of $\mathbb{R}^3$) and a projection. This implies that the system internally holds several scene descriptions. Another is that the system produces a segmentation which maps any time instant into a segment, which maps every tracker bank index into the part of $\mathbb{R}^2$ on which the total confidence of being a target projection exceeds a threshold.

We may define an "efficient" bank as one which contains a tracker which tracks a target. And so we may define an "intelligent tracking system" as a multi-hypothesis tracking system which at any time instant in the domain of any frame sequence in its domain contains only efficient banks, and which at a time instant in the domain a frame sequence in its domain contains a tracker bank.

Finally, we may define an "intelligent multi-target tracking system" as an intelligent tracking system which for a time instant in the domain of a frame sequence in its domain contains more than one tracker bank such that two trackers in different banks track different targets.

It is worth noticing that there is no guarantee for an intelligent multi-target tracking system to "track" any target even if the set of tracker banks is nonempty and no two trackers in any bank track different targets. This is due to the fact that the confidence and the threshold are free to choose. Even if the confidence is a reasonable measure such as the probability for the tracker to track a target given some image information, the system's ability to track is closely connected to the identifiability problem. Since this problem is unsolved, it would be very difficult to justify an implementation of an intelligent multi-target tracking system before running it, if it was required to track. So, when a tracking system is an intelligent multi-target tracking system this tells more about the internal structure of the system than of its performance.

In many cases a target in a scene and the projection are described by a veljunction of models. Each tracker in a bank may then produce estimates based on one of the models. If each model is "precise", such trackers, together with a rule for deciding confidence, constitute the heart of an implemented intelligent tracking system. In many cases it is possible to formulate a precise model as the conjuction of an a priori known and one which is derived from image data. This formulation of a model also opens for the possibility of implementing a multi-target tracking system as is done below.

2. IMPLEMENTATION

2.1 Introduction

Tracking depends on the ability to recognize imaged objects in succeeding frames. Prediction of the scene increases the probability for recognition. The prediction necessitates knowledge of the dynamics of the target and the image process. The (implemented) tracking system therefore tries to include a priori information about the targets and the image process by modelling the main elements involved. In the modelling it recognizes the fact that different targets may be described by different models, and it performs by running parallel estimators, "trackers", attached to each acquired object. This way the probability of track is not so sensitive to the accuracy in the acquisition data. Dynamic target models permit the system to track also during occlusion periods and it is able to classify an object dynamically. For the sake of clearity, it should be stated that the consepts "segment" and "segmentation" in the following will mean "part of an image plane" and "process which produces segments", respectively. For the same reason it should be stated that in the following a tracker is for convinience defined somewhat differently than the general concept. The connection between these consepts should, however, be intelligable from the text.

2.2 General description

The system consists of a set of tracker banks, an acquisition unit, an image registration unit, a target projection calculator and a system unit. A tracker is an estimator of a target state. Image segmentation and classification are used for acquiring targets and to make measurements necessary for the trackers. In the acquisition mode the segmentation is performed on picture areas outside predicted target projections whereas in the measuring mode it is performed inside target search areas.

As opposed to common correlation or contrast trackers the system recognizes the fact that frames in a tracking sequence are images of physical scenes. It is based on the assertion that knowlegde of the targets and the imaging process is the fundament for optimal tracking. The system therefore contains models for the targets and the sensor.

Each target is assumed to be a member of one class in a family of target classes. Members of the same class are described by the same models; a dynamic and a geometric. A tracker bank is assigned to each acquired target. Each tracker is based on a hypothesis. To ensure satisfactory tracking also with uncertain acquisition data, each tracker hypothesis is the conjunction of two, of which one is on initial target state, i e the target state when acquired. The tracker contains a measurement unit and a filter. The filter produces the target state estimate by processing the output from the measurement unit treating it as a measurement of the target state. The output from the measurement unit is obtained through image analysis. The measurement function is, however, dependent on the sensor position. To estimate the measurement function, the sensor position is estimated by the image registration unit. This unit therefore contains a model of the sensor dynamics.

The trackers are supervised by a bank controller; mis-adapted trackers are deleted from the bank. The banks are supervised by the system unit; banks with no trackers are deleted from the system. A bank produces target state- and class estimates based on information from all its trackers. Furthermore, using also the geometric models a target projection estimate is produced by the target projection calculator. This projection along with the target state- and class estimates produced by the bank are the tracking data describing a target. Tracking data describing all tracked targets and sensor data are stored in the system unit, and is available to all parts of the system.

If a segment is classified as a "target segment" by the acquisition unit, acquisition data is produced and sent to the system unit, which creates a tracker bank and provides it with the data.

The system was simulated on IR imagery containing operating military vehicles in field. Important features in the simulations are that a segmented image is determined as the union of the output from two independent segmentors. One segmentor is tuned to detect small, high contrast objects, i e hot spots, and the other tends to detect somewhat larger low-contrast objects. The filter in the trackers are continous-discrete extended Kalman filters.

2.3 Assumptions

Each target is assumed to be a self-radiative object in a flat terrain. The members of a target class have the same dynamic, geometric and radiative features. The first two are characterized by models.

A dynamic model describes the dynamic features of a target in a terrain fixed coordinate system. A geometric model describes the target surface and the center of mass in a target fixed coordinate system.

The imaging process is assumed to be performed by an analog, ground based thermovision camera with known characteristics. The camera panning- and tilting angles are time varying, and the system contains a model for this camera "motion". The initial camera angles are assumed known.

2.4 The trackers

Each tracker is a matched estimator for the target state. It contains a matched filter, i.e. a predictor and an updating unit based on a hypothesis on target class. The filter, which is a continous-discrete extended Kalman filter, is initiated by an initial estimate pair, i.e. an estimate of the initial state and a corresponding error covariance matrix. Thus, a tracker is an estimator matched to a hypothesis on target class and initial estimate pair. The individual tracker is illustrated in Figure 1.

The matched filter produces the predicted $\hat{\underline{X}}$ and Cov $\tilde{\underline{X}}$ and these are used by the tracker search area calculator to produce an area in the picture where the (imaged) target center of mass is likely to be found.

The main elements of $\hat{\underline{X}}$ are target center of mass position and orientation in the terrain, and the search area is found by first calculating a confidence area in the terrain space with central coordinates given by the position elements of $\hat{\underline{X}}$ and the geometric model. This area is then projected onto the picture plane. It is sent to the matched segmentor/measurement unit which segments the area minus other target projections. The resulting segment is classified with respect to target center of mass picture position and aspect angle.

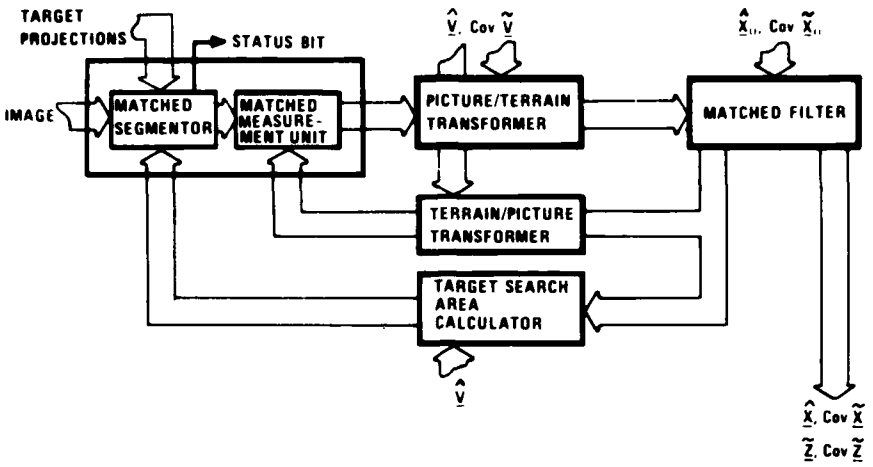

Figure 1 The individual tracker
$\hat{X}_o$, Cov $\tilde{X}_o$ is an initial estimate pair. $\hat{X}$ and Cov $\tilde{X}$ are the state estimate and estimate error covariance matrix respectively, produced by the tracker. $\tilde{Z}$ and Cov $\tilde{Z}$ are measurement deviation and the deviation covariance matrix respectively. $\hat{V}$ and Cov $\tilde{V}$ are the camera angles state estimate and estimate error covariance matrix repectively, provided by a registration unit.

According to the description of a tracker given in section 2.2 the picture/terrain-transformer and the target search area calculator should be regarded as a part of the segmentor/measurement unit. The picture/terrain transformer should be regarded as a part of the filter. These units have been lifted out to highlight the measurement process. The segmentor/measurement unit is what in section 2.2 is called the measurement unit.

The segmentor/measurement unit is matched in the sense that it is based on the tracker class hypothesis and guided by the filter output. The guidance represents a feedback problem and is discussed in some detail in (1). The measurement unit also produces a measurement error covariance matrix. The picture based measurement and error covariance matrix are transformed by the picture/terrain transformer into corresponding terrain based quantities, which are used by the filter to update $\hat{X}$ and Cov $\tilde{X}$. To perform this transformation the camera angle estimate and linearization are used. The measurement unit performs all picture processing in the tracker. Details about the processing are given in (2).

A tracker also returns with a status bit telling if the measurment process has failed, i.e. if the segmentor returns with no segment. This happens when no "segment candidate" is classified into the hypothesized tracker class. Segment candidates and the classification result are produced by internal segmentor processes.

2.5 The tracker bank

The tracker bank is an adaptive estimator for a target state and class. A block diagram is given in Figure 2.

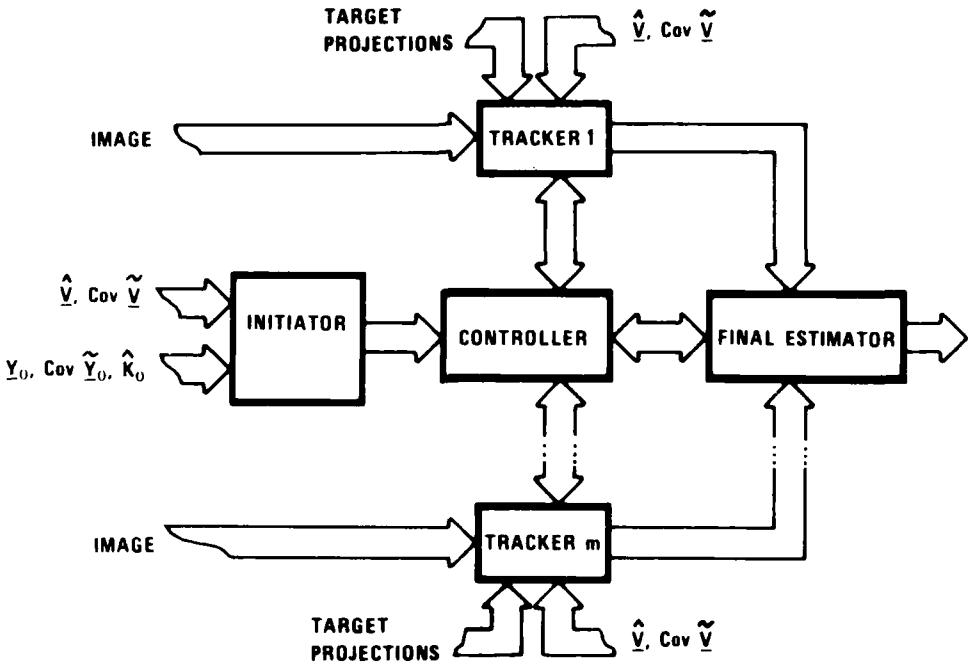

Figure 2 The tracker bank
$\underline{Y}_0$ = Initial target measurement
Cov $\tilde{\underline{Y}}_0$ = Error covariance matrix for $\underline{Y}_0$
$\hat{K}_0$ = Initial target class estimate

$\underline{Y}_0$, Cov $\tilde{\underline{Y}}_0$ and $\hat{K}_0$ are provided by the acquisition unit. Based on $\underline{Y}_0$ and Cov $\tilde{\underline{Y}}_0$ the initiator generates initial estimate pairs and sends them to the controller, which provides each tracker with one pair and labels the tracker "active". Trackers with hypothesized class $\hat{K}_0$ are given high initial probabilities. The controller contains a performance test and deletes mis-adpated trackers from a list of active trackers. The test is a modified χ^2-test on measurement deviation (see (1)) and a probability test. The final estimator calculates the tracker hypothesis probabilities by using essentially Baye's law.

The status bits from the measurement units in the trackers have an important impact on the tracker hypothesis probabilities. One could say that even if several trackers are equally adapted with respect to measurement deviation, the tracker which contains a measurement unit which returns with a measurement, will tend to have a high probability. Details about this are given in (1). The tracker hypothesis probabilities are the confidences defined in section 1.

The hypothesized class of the tracker with the highest probability is taken as the final target class estimate. The output from the tracker bank also contains the state estimate, hypothesis probability and target class from each active tracker and a status bit which tells if the bank is empty. A tracker bank is empty when it contains no active tracker.

2.6 The complete system

The acquisition process which is necessary for tracking is a part of the tracking system. The system is illustrated in Figure 3.

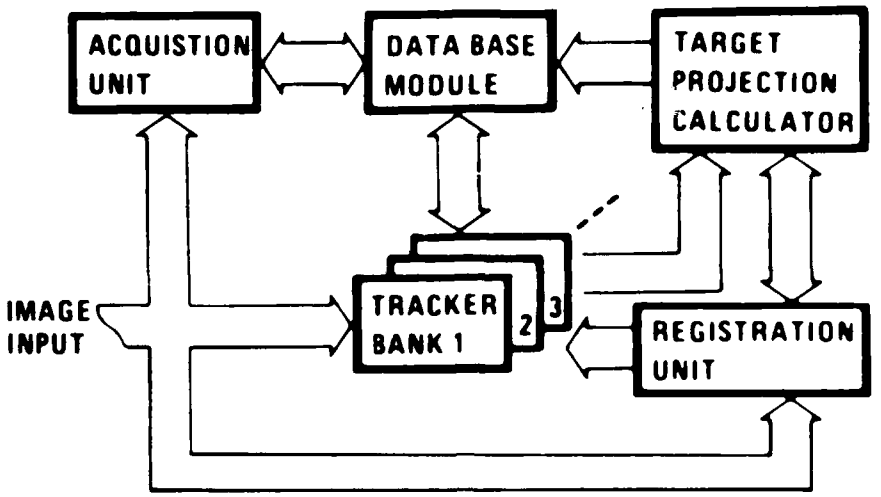

Figure 3 The intelligent multi-target tracking system

Based on the state estimate and hypothesis probabilities from the trackers in a bank and the camera position estimate from the registration unit the target projection calculator produces estimates of the target projections. To do this the geometrical models associated to the hypothesized target class of the different trackers are used. The estimated target projections are labeled with the tracker bank labels and are the main tracking data, stored in the data base module. The image registration unit estimates the camera angles through a constant angle velocity model and measurements of camera angle velocities. The measurements are obtained by finding the displacement between "profiles" from succeeding frames which minimizes the square deviation between them. A profile is essentially the column- or line integrated image function in a frame. The frame is a frame in the sequence, where the estimated target projections are masked out. Column- and line integrated profiles are treated separately. See (1) and (2) for futher details.

The acquisition unit searches picture areas outside the estimated target projections for segments containing non tracked, imaged targets. If such a segment is found, it is classified, and center of mass position and aspect angle are measured. The results are sent to the data base module which distributes them to an empty tracker bank. This way the system is able to detect and track new targets in the field of view.

2.7 Comments

Since the tracking system produces the (unequely) labeled target projection estimates it is easily realized that the implemented system is in all essence a tracking system. The target projection estimates are produced such that the system is a multi-hypothesis tracking system. The system being an intelligent tracking system is closely tied to the performance test in the tracker banks. If this test is effective, the system is an intelligent tracking system. From simulation results (see (2)) one could say that it is to a fairly large extent. Simulations show that if the system is regarded as an intelligent tracking system, it is a multi-target tracking system.

The implementation has some deficiencies:
The matched segmentors segment the images using little tracker information (see (2)). This results in unstable segments which, in turn, result in missing or unreliable measurements. The calculations of the terrain based measurement error covariance matrices are done numerically and show considerable instabilities.

2.8 Results

The system has been simulated on several sequences containing IR images of military targets in field. The presented results are from a simulation on a sequence of 32 frames with interframe periode equal to 0.3 s containing a tank moving on an airfield. The scenes also contain some vegetation and a fire, which both cause partial occlusions of the target. Some of the images from the sequence are shown in Figure 4.

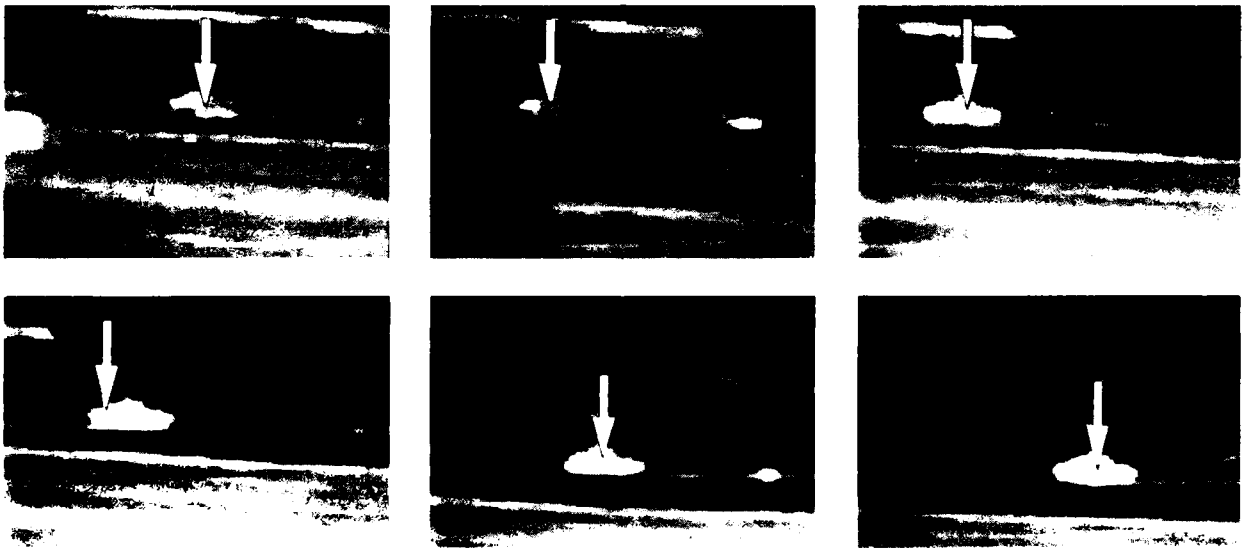

Figure 4 Images 1, 7, 13, 19, 25 and 31 of the simulation sequence. The estimated center of mass position is indicated.

The tracker bank initially contained 8 trackers, four based on a "tank-hypothesis" and four on a "jeep-hypothesis". For each target class hypothesis there were generated four trackers with initial orientation corresponding to aspect angles, 0^{o} (front view), 90^{o} (right side view), 180^{o} (rear view), and 270^{o} (left side view).

All velocity components in the initial state estimates were zero. Figure 5 shows the time evolution of the tracker hypothesis probabilities.

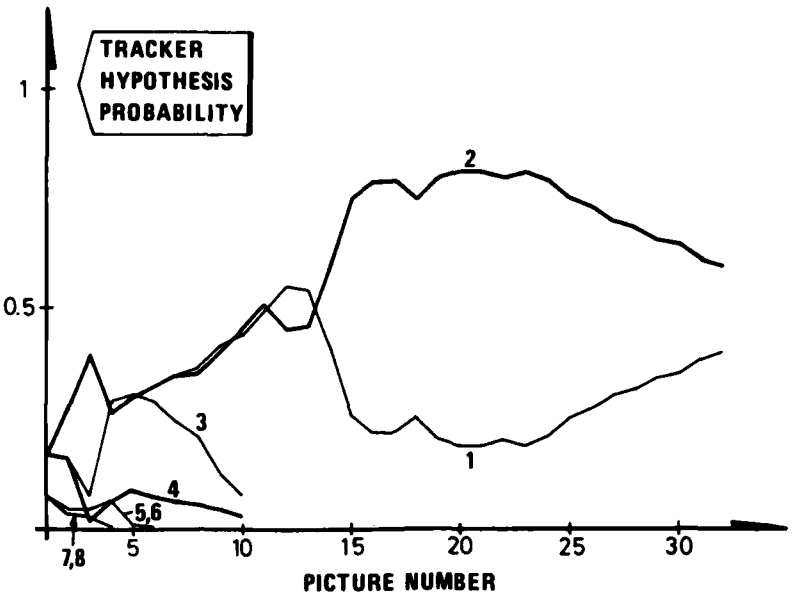

Figure 5 Time evolution of the tracker hypothesis probabilities. Traces 1-4 are "tank-tracker" probabilities. Traces 5-8 are "jeep-tracker" probabilities.

The two trackers with initial estimated orientation corresponding to aspect angles 90° and 270° remain in the bank because the matched measurement unit in a tracker does not distinguish between aspect angles corresponding to left and right side view of a target. The estimated orientations (angles) from the two trackers differ by approximately 180°, and the estimated speed values are approximately equal and show realistic values.

3. CONCLUSION

Despite deficiencies in the implementation, the tracking system produces some fairly good results. It therefore seems reasonable to assume that the intelligent multi-target tracking system has a high potential ability to acquire and track military vehicles in complex scenarios.

4. REFERENCES

1. Heyerdahl E, A Multi Hypothesis Single Target Tracking System, In preparation, Norwegian Defence Research Establishment.

2. Heyderdahl E, Dyrdal I, Grinaker S, An Intelligent Multi-target Tracking System based on Image Analysis, 1984, FFI/RAPPORT-84/4008, Norwegian Defence Research Establishment.

GUIDANCE AND CONTROL PANEL 43RD SYMPOSIUM
ROUND TABLE DISCUSSION

The final session of the symposium was a round table consisting of some speakers, some audience members, and some session chairmen. The following summary of the round table discussion is drawn from a tape of the session. Because this is a summary prepared by the symposium chairman (who also chaired the round table) and not a verbatim transcript, the names of the speakers have not been included. The intent of this summary is to give the flavor of discussions which were at times more heated than this summary reflects.

PANEL CHAIRMAN

The first topic that I would like the panel to address is practical issues in applying imaging systems.

PANEL SPEAKER

The topic of imaging systems in my view is getting more and more interesting because we are constantly seeing a dichotomy between the needs of the human operator and the needs of the computer. The human operator likes to see detail, we have an eye for detail and we've evolved it over a few million years, and the human operator will be able to pick out objects in a very rich field. The computer isn't quite so good at doing that. Ideally what the computer would like to have is just the targets, eliminating everything else. But because of this dichotomy we have a problem: if we give the operator what he wants we present the computer with a much more difficult task in recognition. The same thing is true in the topic which was discussed in the first paper, Synthetic Aperture Radars. We like to see synthetic aperture radar pictures; they look very realistic. It is incredible the amount of detail we get when we reach down below 3 meter resolution, but the transmitted power required to increase radar resolution from 30 meter transmitted to 3 meter resolution is much larger and that increases the size, the weight, and the cost of the system. The power requirements on the system goes up and again we get into a vicious circle of having high cost systems.

There is another dichotomy because we have to get more and more precise identification of the target because we want to hit only high value targets. The reason we want to hit high value targets is that the weapon is extremely expensive and therefore we can't afford to use this weapon on a small jeep or something of this nature. But as we try and do more and more precise identification of targets complexity goes up therefore the price of the whole system goes up so we increase the cost of our weapons to be used against high value targets.

ANOTHER PANEL SPEAKER

I have to take a little different approach to developing sensors for aircraft. He's right in saying that long range sensors on an aircraft, to find their own target, run up the expense of the aircraft and you are going to run up the probability of losing aircraft. I think we need to put missiles in there that will find the target without having to put the pilot and the airplane over the target. The technology of finding high value targets is here today. The technology of finding tanks in mass mobile targets is here today. The technology issue is not if we can find high value targets, but can we find mass mobile targets; can we build seekers that are cheap enough to go into missiles; that we can use a lot of them and still keep the aircraft out of range of the target. In ten years we are going to find that autonomous missiles, that are going to be launched from aircraft outside the target area, are cheap.

We have to use data bases that are available in the field as a tactical system. We are limited in funds. We cannot go out and build new data bases for all these targets. We have to use what is available. We are trying to develop reference systems for our missiles, and for our seekers which use available data at the squadron level, use whatever pictures and information that is available there. Some of it's not real good, but for high grade targets I think we can accomplish the objective with that information. For the tank type target, we're going to have to build seekers to pick out the tanks from the jeeps and from the other targets.

Those days are here and the objective now is to do it cheaply. So, my comment on this question is the sensors and imaging systems we need are here for missiles. That should be separate from the final target end game, the structure of the target, and from the pilot and the airplane.

PANEL CHAIRMAN

You say we can't afford the additional cost of the data base systems. Do you think that we have sufficient data for mapping or such kinds of data for autonomous target recognition without sending, for example, high value airplanes into the target on special reconnaissance missions, and do you believe we have enough aspect dependent data to make robust target identifiers in an autonomous missile?

PANEL SPEAKER

We are always going to need reconnaissance. When we start building radar guided missiles and IR guided missiles without a data base we are going to have to do bomb damage assessments by sending in reconnaissance aircraft. Those aircraft are still going to fly out there and do the dirty work, but they also don't have to fly right over the target, they can fly standoff. Maybe there are other techniques which can be accomplished to get an image of the target, but we are always going to need that.

ANOTHER SPEAKER

I believe the situation to be a bit worse than what has been described. In fact, the decisions made about some avionics and avionics research programs are at the moment almost entirely devoid of confidence that the results of the programs are actually going to be used. There are several reasons for these, one is that the Air Force is finding the aircraft more expensive to operate and none of us have the confidence that we used to have with procurement programs we're actually going to wind up with. We can effect a balance between missiles and aircraft and have an enormous effect on the actual survivability of the aircraft. The part of the equation I see missing at the moment is stabilizing the whole procurement situation so that when we get a much more stable idea which of all of these options we are going to have. We may be our own worst enemies in producing so many different options and so many different sorts of targets to be attacked in so many different ways and so many devices all claiming to reduce costs, I'm not sure the people in procurement have the foggiest clue how they ought to be moving in the future.

SPEAKER FROM THE FLOOR

The remarks about imaging raise, I think, a fundamental issue for the technical community. The fundamental issue is, as one of the panel members mentioned, the amount of details and the need for more details. Engineers tend to think of processing signals rather than information. In using imaging systems to recognize targets more attention needs to be given to the fundamental information and the exterior information, for example, you are not likely to find a tank depot inside a monastery. And therefore, some of that type of information needs to be incorporated in these missiles systems. I think that you could reduce these requirements if that was done.

PANEL CHAIRMAN

The next topic that seems to draw some interest is the entire concept of multifunction systems. The kinds of comments that I've had in writing question the direction in which we were moving in the sense that there might be several counter-currents concerning multifunction systems. For example in order to avoid cost, we are trying to do lots of things in a single package, but the question arises thereby are we suffering from the probability of point failure in reliability problems internal to the equipment or survivability under fire outside the platform.

PANEL SPEAKER

I don't necessarily think that the development issue of multifunction systems is cost. As an example, the U.S. Army is about to embark on the development of a one-man combat helicopter. If we are going to develop a system to be operated by one man in combat, its going to be a very sophisticated system and its going to have to be "full up" for him to carry out his mission. The one way to achieve this "full up" cabability is through the use of multifunction systems. The most obvious example is communications; if you have three communications channels available, you want different ones in different phases in the mission. If you have a multifunction system you can do that. This of course leads to tremendous integration problems in that it leads to all sorts of man/machine interface issues, this image question is just one of them. But I really see us continuing to move in the direction of multifunction systems because of that problem.

ANOTHER PANEL SPEAKER

I became a little confused thinking about this and I concluded that we are really using the term multifunction to cover too many different cases; I believe there are at least three. The first is where there is ingenious design to minimize the number of sensors such as the gyroscopes in the aircraft, I think that is one discipline, and the question there is really about safety. Then there is a second one which I think is important, and that is that many sensors actually can acquire and do acquire information which isn't used. It is probably most pronounced in the case of radar where we have to get a lot of information out of it. A good question is whether that information can be used elsewhere in the system where it hasn't been used so far. And the third one, I think, is that it may be possible to realize multiple or new functions by some of the other techniques that have been discussed here, e.g., analylitic redundance and confusing data. I believe those should all be seen separately. They've all got different sorts of cost implications and all have different sorts of operational benefits.

PANEL CHAIRMAN

Let me pursue that for just a moment. I think we had several papers more of the third type of function. But in your first two cases I think one might reasonably ask, "Do you see the proper architectural considerations evolving to answer the questions as to

whether survivability and utility are there? I simply lay that as a question. Are you all comfortable with the architectural considerations in multifunction systems that they are addressing problems of reliability, verifiability, and survivability as well as functionality?

PANEL SPEAKER

Well, my experience with flight control goes back a long way but I seem to remember that the nightmare the whole time was whether all the bugs were visible or whether they were working underneath the rug and might crawl out later. I think if I were confronted with the architecture I would still want to know that all the problem areas are visible.

PANEL CHAIRMAN

Anybody in the audience see any lumps under this rug that concern you? No? Then I take it that you're comfortable that the right architectural issues are being addressed and that the utility of functionality can proceed.

PANEL SPEAKER

Except its a new problem for everyone who embarks on a new system you better not assume you'll carry all wisdom over.

ANOTHER PANEL SPEAKER

One of the things which concerns me is that as we go for systems with all these multifunction elements onboard, we are in grave danger of taking more and more of our sensors and our displays and so on from a mission critical role to a safety role. As soon as we do that then we get into the question of integrity and redundancy and all the other aspects which impacts on flight control. There is a bump under the rug.

This could then mean that it actually costs us more to come up with less and less so we need to ensure that we don't get ourselves into a danger of putting the cockpit multifunction displays into flight critical roles. We have to be very very careful to ensure that the pilot can still fly the airplane despite the fact that his display is out.

The maintenance problems on the multifunction system may not be as easy to deal with as they have been in the past. It might be more and more difficult to keep them flying when they're being maintained in a tent with the operator or the maintainer up to his ankles in mud wearing a flak suit, with people trying very hard to find him to drop a bomb on him. So we have to bear in mind that while we integrate more and more systems this may make the maintainers' task much more difficult.

ANOTHER SPEAKER

I too agree with the fact that flight control is the most critical issue for multifunction systems for the reason of safety. People in the field of flight control are very reluctant to depend on any other type of equipment.

SPEAKER FROM THE FLOOR

I want to put some emphasis on the increasing amount of software with these highly integrated or multimode, multifunction systems. As we have more software in flight critical functions, the more the effort is to verify, and validate these kind of software. There has been an explosion in the amount of time, engineering effort, creativity and money to deal with this. We have dealt with dormant failure, double-dormant failures and all these things, and it gets even worse when you go to modern aircraft like the controlled configured vehicles.

PANEL CHAIRMAN

Well, we've heard from the beginning of the discussion on this topic there were no problems. But we've heard some very clear warnings produced, I guess that reflects my own feelings if I were asked the question as a technologist I'd say, "Yes the technology is here," but if I were asked to be the systems engineer on a program I would advise a great deal of caution.

Let's move to the third and last topic. That is the question of precision in guidance and control versus the stipulated need from the user and the totally independent aspect of what we can afford to buy balancing those two things.

PANEL SPEAKER

I say the issue is overmanagement versus need versus cost. Let me take a little poll here; first, I assume everybody in this room is primarily interested in these three phases of the program, regardless of what your function is, either the early proposal stage or advanced development or engineering development, not necessarily after we've got it all done, and then the users stage. Okay, who are the players? There are three as I see it. Its a three-legged stool; there's the prime contractor, that's me. It's many of you; how many of you are representing the vendor and prime contractor? Lets see a show of hands, come on, higher. Okay. Then there's next those wonderful civil servants who are working in the government laboratory, the government agency, the watchdog

of our liberty. How many of those? Its you guys I'm going to be after. And then, finally, how many users do we have; how many pilots or soldiers or these sort? How many of those? Ah, now there you go. One thing I've got to say for both of us first two, we don't get that third guy involved enough.

The first thing we're doing, I say, is we're over-specifying this thing; we're making it easy for you guys in that No. 2 slot to say "Hey I've done this before; its easy, its safe, I'm going to protect my you know what." What happens? The good old vendor says: "Huh, I'm going to the cash register and I'm going to ring it up, bing, bing, more money". More importantly is this, there's too much overmanagement for every piece of hardware we have.

Why do we generate all this paper? Because for everyone of us working doing this job, there's two or three of you watchdogs looking over our shoulders saying, "Hey, I want to know what you're doing. Give me this report; give me that piece of paper; I've got to justify my existence too." How about that, can we cut that down? That's enough. How about some action? Tell me where I'm wrong; tell me where I'm right.

SPEAKER FROM THE FLOOR

Well if you guys weren't such crooks, we wouldn't have to have so much paper. Well, I think a lot of the points that you have made here are good. We left out the production people. You said most of the people from the audience are from the development end. That's a big problem because one of the reasons that we have high cost systems is because no one at the technology end considers how you're going to make the thing. We had one good example in a paper here: The people with the lost cost gyro who are working the technology at one end and the production at the other end. That's the way you should do it. We've had some other papers here which in one case was a very simple system that would require many machine operations to make, and other systems with multiple, complicated optical systems. Systems which require terrain data bases tend to make operational people go up the wall.

PANEL CHAIRMAN

I'd like to hear from one of the operators back there. Its hard to tell that you have operators present unless they are in uniform, but I've got you now. Two of you raised your hands. I'd like to hear from each of you in turn if I may, and not necessarily on the topic we're discussing here. Our hunger for words from operators is so great that we'd like to hear any comments you'd like to make on any aspect of what we've discussed for the entire week.

SPEAKER FROM THE FLOOR

Most of my experience has been in flight testing so the topic I was most interested in was the last day, specifically the weapons systems. I would have liked to see this conference place more stress on how you are going to test the systems once you've obtained the ones you have built. The other problem is as has already been said, once its been built, how are you going to validate and test the software? These problems I would like to see more stressed.

PANEL SPEAKER

I would like to make a comment just to stir things up even more. The cost of airplanes rises at around eight percent per annum. Before you missile guys can place them, the cost of target missiles is rising about 9.5 percent per annum. That means an airplane is going to double its price in nine years; a missile is going to double its price in eight. One thing I'm certain of is the equipment budget isn't going to double in that period of time. I estimate that within 10 years the UK defense budget, due to the current rate of escalation, will be short by 10 billion pounds in terms of equipment procurement capability. In other countries they're in worse state still, as they buy more. And their costs rise just like everyone elses. And don't assume that we'll be able to buy elsewhere. So how are we going to get these prices down? The only way is to take this topic of precision versus need versus cost seriously. So let me throw a challenge out to the floor. You're going to be 10 billion, you UK guys, you're going to be 10 billion short in the next 10 years. What are you gong to do about it? Resign; go out to find another job. You U.S. guys, you're going to be 100 billion short in the next 10 years, the French will be short as well; Germans, you're in the same state. What are you going to do about it? Bleed the industry or start designing cheap systems. If we're going to design cheap systems, how are we going to do it?

SPEAKER FROM THE FLOOR

In Europe you probably have the same problem we have in the United States. A good deal of our expense, perhaps most of it, is not what you buy, but how you buy it. And saying we should have simple systems is not enough; simple systems can cost 10 times more than the complex system if your acquisition policies and strategies are wrong. So one of the things we have to bring under control is how we acquire things, how we go about it, what do we buy, who do we buy it from, and when do we buy it.

AUDIENCE IN GENERAL

Here, here.

ANOTHER PANEL SPEAKER

We do try to build a bridge. The efforts of the industry and of the operators themselves, and in our case in the UK, that most important group of people that we call aircraft establishments. The thing that we did not generally appreciate is the fact that we cannot resolve the compromise between the pilot needs and technology. How do we get the requirements derived from the threat forward through the technical network in the system, and how do we get all the implications of doing that back up again to the procurement decision.

PANEL CHAIRMAN

Admitting that the cost estimates are a little chancy at the technology stage, and given the complexity of combinations of systems that we are proposing now, do you think that we have or use the right tools to show the procurement executives which systems should be used? Do you see people producing sortie rate tradeoffs, or number of missiles to be delivered for a given Pk to evaluate the complex systems alternatives. I don't see very much of that. I'm wondering if anyone else does. Are we technologists giving the procurement executives the right decision data at a level they can make sense out of?

PANEL SPEAKER

I think a lot of that data is about, and one has to give credit where it's due. There are studies in the right place and very often well put together.

SPEAKER FROM THE FLOOR

I think one of the issues that's been brought up is really significant and I'd like to give you an example that I see in our company, and it's applying the navigation systems to the U.S. Air Force, Navy and Army. We have a parallel division that supplies navigation systems to the commercial airlines industry. The technology which is used in these systems is identical; you can take a platform or laser gyro triad from a military system and put it into the commercial system and vice-versa. There's no difference between the components or the way they are used. And yet the infrastructure in the military divisions, the requirements of the customer, make the cost a factor of at least two and a half times the manufacturing cost of hardware. And it's very hard to understand how that happens. Let me stress that the commercial end of the business is just as precise, just as well documented, just as well tested as is the military hardware. Actually, in my company, and in other companies, they've taken commercial equipment, put it in fighter aircraft and flown it and used it in maneuvering environments and it performs as well as the best of the military equipment. So it's an infrastructure problem that produces a lot of these problems and I think the inertial business is a very revealing one because we do use the same hardware in both product lines.

ANOTHER SPEAKER FROM THE FLOOR

I would like an exchange of information, please. I would like to ask if he has noticed any modifications in the balance between civil and military market, either market leading.

PANEL CHAIRMAN

When you answer that question would you do it in a timeframe sense -- not only what the answer is today, but can you trace that question back to 10 years ago and give the 10 year old answer as well as the answer for 1987?

PREVIOUS SPEAKER FROM THE FLOOR

The commercial airline market inertial navigation systems was one of the largest, most wonderful bon anzas in marketing that you can imagine. The reason for that was that there were on the order of 3,000 long-range aircraft. Starting with 707's and DC8's, they were flying an inventory with human navigators using Lorans and Dopler navigators, etc. So 3,000 airplanes times three systems per airplane, gives you a whole worldwide marketplace in the order of 9,000 to 10,000 systems. There is no place in the military environment that you can look today and have a market forecast that showed you that you would have something in the order of 10,000 systems. So the commercial world started off with an inability to produce the hardware fast enough to fill the holes in the airplanes.

The military airplane application has always started out with a purchase of 10, then a purchase of 50, then they buy them in lots of 100 and deliver them in the order of 10 to 20 a month; and so, it's an entirely different kind of a marketplace. The military marketplace is characterized by the tight specifications that everybody writes, not only do they write tight specifications but they always use the specifications from the last systems that you built that don't apply to the one that you are building today, but they write very tight specifications and then when it comes time to deliver and you don't meet the performance requirements that's called out in the specifications, you point out to them that you can either give me a waiver to the performance requirements or I can't deliver the hardware. You always get a waiver to the performance requirements so you can deliver the hardware, so you can put the equipment in the airplane and proceed with the flight-test program. That characterizes the military side.

On the commercial side, when you sign a contract for a commercial plane such as the 707 or 767 or some airplane complete like that, you don't get a contract for 10 systems, you get a contract for 2,000 systems. And for the 2,000 systems the price is fixed, and the performance specification is fixed and you must meet the performance specifications. I've seen many of the Vice Presidents squirm on the carpet in front of the Boeing Corporation trying to get out of performance characteristic requirements for their systems and it just doesn't work. You sign a contract to a specification and you meet the specification before you deliver the first piece of hardware. So the characteristics of the marketplace are markedly different. I'm not saying that one is better than the other; they are just different and there are opportunities for new pieces of equipment in the commercial world, commercial airlines world, that are just fantastic. It is very hard to do the same kind of thing in the military.

PANEL CHAIRMAN

Ten years ago in the kinds of estimates that he was talking about, the total inertial military market was estimated at 1500 systems.

PANEL CHAIRMAN

I would like to open the microphone to questions from the floor on any issue that you care to raise that has not been addressed.

SPEAKER FROM THE FLOOR

I'd like to continue on the question raised concerning the market that exists. I think we need to start to consider apples for apples. If you look at the cost that we've been considering, I think you've been talking about procurement costs. On military aircraft you've got the operating costs, which go on year upon year. The use of the aircraft eventually will be restricted to perhaps two or three days intensive use, with very high attrition rate. One wonders the number of sorties that aircraft (for which one's paid the year upon year) will actually achieve. The projected costs of these high technology standoff weapons and multifunction systems in fact is low, and I think when that consideration is made and the actual cost estimate is made, the sort of market that we're talking about will be revealed.

PANEL CHAIRMAN

Thank you for that comment, and on that note which I think is an appropriate one, I'd like to close this panel discussion. I want to thank the panel, who have braved some opinions; I want to tell you that these opinions don't represent the international points of view, corporate points of view, and even, in some cases, their personal points of view. The panel were merely presenting issues which they thought should be heard and discussed, and I thank them for that and I thank you for your participation.

REPORT DOCUMENTATION PAGE

1. Recipient's Reference	2. Originator's Reference	3. Further Reference	4. Security Classification of Document
	AGARD-CP-411	ISBN 92-835-0421-6	UNCLASSIFIED

5. Originator Advisory Group for Aerospace Research and Development
North Atlantic Treaty Organization
7 rue Ancelle, 92200 Neuilly sur Seine, France

6. Title

ADVANCES IN GUIDANCE AND CONTROL SYSTEMS AND TECHNOLOGY

7. Presented at

the Guidance and Control Panel 43rd Symposium held in London, UK from 7 to 10 October 1986.

8. Author(s)/Editor(s)	9. Date
Various	July 1987
10. Author's/Editor's Address	**11. Pages**
Various	150

12. Distribution Statement This document is distributed in accordance with AGARD policies and regulations, which are outlined on the Outside Back Covers of all AGARD publications.

13. Keywords/Descriptors

Target and terrain sensors
Aircraft state sensors
Force and moment generators
Guidance and control algorithms
Integrated systems

14. Abstract

This volume contains the Keynote Address, 10 out of 11 unclassified papers presented at the Guidance and Control Panel 43rd Symposium held in London, UK from 7 to 10 October 1986 and the Round Table Discussions. The remainder is published in the classified volume CP 411 (Supplement).

The papers were presented under the following headings: Target and terrain sensors; Aircraft state sensors; Force and moment generators; Guidance and control algorithms; Integrated systems.

The symposium concluded with a Round Table Discussion under the chairmanship of the Programme Chairman, Mr R.S.Vaughn, USA. It covered the following topics: Practical issues in applying imaging systems; Multifunction systems; more or less? Precision vs need vs cost.

AGARD Conference Proceedings No.411 Advisory Group for Aerospace Research and Development, NATO ADVANCES IN GUIDANCE AND CONTROL SYSTEMS AND TECHNOLOGY Published July 1987 150 pages This volume contains the Keynote Address, 10 out of 11 unclassified papers presented at the Guidance and Control Panel 43rd Symposium held in London, UK from 7 to 10 October 1986 and the Round Table Discussions. The remainder is published in the classified volume CP 411 (Supplement). The papers were presented under the following headings: P.T.O	AGARD-CP-411 Target and terrain sensors Aircraft state sensors Force and moment generators Guidance and control algorithms Integrated systems	AGARD Conference Proceedings No.411 Advisory Group for Aerospace Research and Development, NATO ADVANCES IN GUIDANCE AND CONTROL SYSTEMS AND TECHNOLOGY Published July 1987 150 pages This volume contains the Keynote Address, 10 out of 11 unclassified papers presented at the Guidance and Control Panel 43rd Symposium held in London, UK from 7 to 10 October 1986 and the Round Table Discussions. The remainder is published in the classified volume CP 411 (Supplement). The papers were presented under the following headings: P.T.O	AGARD-CP-411 Target and terrain sensors Aircraft state sensors Force and moment generators Guidance and control algorithms Integrated systems
AGARD Conference Proceedings No.411 Advisory Group for Aerospace Research and Development, NATO ADVANCES IN GUIDANCE AND CONTROL SYSTEMS AND TECHNOLOGY Published July 1987 150 pages This volume contains the Keynote Address, 10 out of 11 unclassified papers presented at the Guidance and Control Panel 43rd Symposium held in London, UK from 7 to 10 October 1986 and the Round Table Discussions. The remainder is published in the classified volume CP 411 (Supplement). The papers were presented under the following headings: P.T.O	AGARD-CP-411 Target and terrain sensors Aircraft state sensors Force and moment generators Guidance and control algorithms Integrated systems	AGARD Conference Proceedings No.411 Advisory Group for Aerospace Research and Development, NATO ADVANCES IN GUIDANCE AND CONTROL SYSTEMS AND TECHNOLOGY Published July 1987 150 pages This volume contains the Keynote Address, 10 out of 11 unclassified papers presented at the Guidance and Control Panel 43rd Symposium held in London, UK from 7 to 10 October 1986 and the Round Table Discussions. The remainder is published in the classified volume CP 411 (Supplement). The papers were presented under the following headings: P.T.O	AGARD-CP-411 Target and terrain sensors Aircraft state sensors Force and moment generators Guidance and control algorithms Integrated systems

Target and terrain sensors; Aircraft state sensors; Force and moment generators; Guidance and control algorithms; Integrated systems.

The symposium concluded with a Round Table Discussion under the chairmanship of the Programme Chairman, Mr R.S.Vaughn, USA. It covered the following topics: Practical issues in applying imaging systems; Multifunction systems; more or less? Precision vs need vs cost.

ISBN 92-835-0421-6

Target and terrain sensors; Aircraft state sensors; Force and moment generators; Guidance and control algorithms; Integrated systems.

The symposium concluded with a Round Table Discussion under the chairmanship of the Programme Chairman, Mr R.S.Vaughn, USA. It covered the following topics: Practical issues in applying imaging systems; Multifunction systems; more or less? Precision vs need vs cost.

ISBN 92-835-0421-6

Target and terrain sensors; Aircraft state sensors; Force and moment generators; Guidance and control algorithms; Integrated systems.

The symposium concluded with a Round Table Discussion under the chairmanship of the Programme Chairman, Mr R.S.Vaughn, USA. It covered the following topics: Practical issues in applying imaging systems; Multifunction systems; more or less? Precision vs need vs cost.

ISBN 92-835-0421-6

Target and terrain sensors; Aircraft state sensors; Force and moment generators; Guidance and control algorithms; Integrated systems.

The symposium concluded with a Round Table Discussion under the chairmanship of the Programme Chairman, Mr R.S.Vaughn, USA. It covered the following topics: Practical issues in applying imaging systems; Multifunction systems; more or less? Precision vs need vs cost.

ISBN 92-835-0421-6

END

DATE

FILMED

5-88

DTIC